Doctorate Research Program in Plant Biology
Dipartimento di Ecologia – Università della Calabria
XX Cycle (2004-2007) – Coordinator Prof. A. Musacchio

DEVELOPING LARGE-SCALE MOLECULAR TOOLS TO INVESTIGATE GENES RELATED TO QUALITY AND QUANTITY TRAITS IN CROP PLANTS

BIO/11

Coordinator
(Prof. Aldo Musacchio)

Supervisor
(Dr. Gaetano Perrotta)

Doctoral student
(Dr. Fabrizio Carbone)

CONTENTS

1. INTRODUCTION

Typical approaches to gene identification and functional characterization have and continue to involve protein characterization, peptide sequence determination, and identification of the corresponding DNA sequence. More recently, expressed sequence tags (ESTs), microarrays, large-scale gene expression (transcriptome) profiling, and associated informatics technologies are rapidly becoming commonplace in the plant sciences. These genomic approaches typically take advantage of technologies for characterizing large numbers of nucleic acid sequences, bioinformatics, and the expanding collection of nucleic acid sequence data from diverse taxa. Systems biology attempts to combine large-scale DNA sequence, gene expression, protein, metabolite, genotype, and/or phenotype data to develop a comprehensive understanding of biological process. Combination of these approaches also makes it possible to extract more meaningful functional information as new DNA sequence data are generated (Alba et al., 2004). While the potential of this technology is enormous, the utility of large-scale expression data is not always well understood, nor are the limitations in analysis and interpretation. Comprehensive transcriptome analysis should make it possible to identify and dissect complex genetic networks that underlie processes critical to physiology, development, and response. For example, gene regulatory networks have been inferred using microarray data obtained from a variety of organisms (de Hoon et al., 2003; Shmulevich et al., 2003; Hashimoto et al., 2004), and it is also possible to correlate these genetic networks with metabolic processes (Mendes, 2001; de la Fuente et al., 2002). Gene networks are also being dissected in plants for processes ranging from seed filling to cold tolerance (Fowler and Thomashow, 2002; Ruuska et al., 2002). Further characterization of gene networks in plants will help us to understand the molecular basis of plant processes and identify new targets for manipulating biochemical, physiological, and developmental processes in crop species.

1.1 Expressed sequence tags: tools for gene discovery and expression analysis

Gene expression in most eukaryotes is studied by starting with complementary DNA (cDNA) clones. DNA cloning involves the selective amplification of a desired fragment of DNA. This method creates an abundance of the selected DNA sequence so further genetic work can be carried out with it. If a short nucleotide sequence of a particular clone is available then oligonucleotide primers can be designed for amplification of this clone by PCR. The site of this clone can then be compared to a tag for this clone and it is called a sequence-tagged site (STS). The expressed component of eukaryote genomes represent only a fraction of the total genome. cDNA clones are created and short sequences of about 200bp are used as tags so sequence-specific primers can be designed for a PCR assay. This implicates that an STS is available for an expressed sequence. The tag is called an expressed sequence tag (EST), in other words, ESTs are single pass, partial sequences of cDNA clones.

ESTs are created by sequencing the 5' and/or 3' ends of randomly isolated gene transcripts that have been converted into cDNA (Adams et al., 1991). Despite the fact that a typical EST represents only a portion (approximately 200–900 nucleotides) of a coding sequence, en masse this partial sequence data is of substantial utility. For example, EST collections are a relatively quick and inexpensive route for discovering new genes (Bourdon et al., 2002; Rogaev et al., 1995), confirm coding regions in genomic sequence (Adams et al., 1991), create opportunities to elucidate phylogenetic relationships (Nishiyama et al., 2003), facilitate the construction of genome maps (Paterson et al., 2000), can sometimes be interpreted directly for transcriptome activity (Ewing et al., 1999; Ogihara et al., 2003; Ronning et al., 2003), and provide the basis for development of expression arrays also known as DNA chips (Chen et al., 1998; DeRisi et al., 1996; Shalon et al., 1996; Shena et al., 1995). In addition, high-throughput technology and EST sequencing projects can result in identification of significant portions of an organism's gene content and thus can serve as a foundation for initiating genome sequencing projects (van der Hoeven et al., 2002). With many large-scale EST sequencing projects in progress and new projects being initiated,

the number of ESTs in the public domain will continue to increase in the coming years. The sheer volume of this sequence data has and will continue to require new computer-based tools for systematic collection, organization, storage, access, analysis, and visualization of this data. Not surprisingly, despite the relative youth of this field, an impressive diversity of bioinformatics resources exists for these purposes.

As sequence and annotation data continue to accumulate, public databases for genomic analysis will become increasingly valuable to the plant science community. The *Arabidopsis* Information Resource (TAIR; http://www.arabidopsis.org/home.html), the Salk Institute Genomic Analysis Laboratory (SIGnAL; http://signal.salk.edu/), the *Solanaceae* Genomics Network (SGN; http://sgn.cornell.edu/), and GRAMENE (http://www.gramene.org/) serve well as examples of these on-line resources.

With databases such as these, and advances in computational molecular biology and biostatistics, it is possible to mine and analyze large EST datasets efficiently and exhaustively (i.e. digital expression profiling; Ewing et al., 1999; Ogihara et al., 2003; Ronning et al., 2003).

By clustering genes according to their relative abundance in the various EST libraries, expression patterns of genes across various tissues were generated and genes with similar patterns were grouped. In addition, tissues themselves were clustered for relatedness based on relative gene expression as a means of validating the integrity of the EST data as representative of relative gene expression.

1.2 Gene expression profiling

One of the biggest challenges in studying global gene regulation in multicellular organisms is the heterogeneity of gene expression. Each organ is unique at the level of its tissues, cells, and gene expression profiles. In addition, there is growing evidence that responses to environmental stimuli or developmental signals occur differentially at the cell or tissue level. Thus, to better understand gene regulatory circuits, gene expression should be analyzed at a single cell or tissue type.

Various methods are available for detecting and quantitating gene expression levels, including northern blots (Alwine et al., 1977), S1 nuclease protection (Berk and Sharp, 1977), differential display (Liang and Pardee, 1992), Real Time quantitative PCR (Higuchi et al., 1992, 1993; Heid et al., 1996; Wittwer et al., 1997a), sequencing of cDNA libraries (Adams et al., 1991; Okubo et al, 1992), serial analysis of gene expression (SAGE) (Velculescu et al., 1995) and cDNA and oligonucleotide microarrays (Shena et al, 1995). Although the established and reliable method of RNA gel-blot analysis can be quite sensitive and allows for the accurate quantification of specific transcripts (Hauser et al., 1997), this method is not readily adapted to genome-scale analysis. Differential display uses low-stringency PCR, a combinatorial primer set, and gel electrophoresis to amplify and visualize larger populations of cDNAs representing mRNA populations of interest. Differential display has important advantages when compared with scale-limited approaches such as RNA-blot analysis (e.g. minimal mRNA is required, parallel profiling of mRNA populations is feasible), yet this technique suffers from output that is not quantitative and positives are often difficult to clone and confirm (Debouck, 1995; Ding and Cantor, 2004). More recently the principles of AFLP® have been applied to cDNA templates (i.e. cDNA-AFLP; Bachem et al., 1996, 1998) and this approach has been used to identify differentially expressed genes involved in a variety of plant processes (Bachem et al., 2001; Dellaqi et al., 2000; Durrant et al., 2000; Qin et al., 2000). This technique offers several advantages over more traditional approaches. Of particular importance is the fact that poorly characterized genomes can be investigated in a high-throughput manner. Because the stringency of cDNA-AFLP PCR reactions is quite high (which is not the case with differential display) the fidelity of the cDNA-AFLP system allows much greater confidence in acquired data and differences in the intensities of amplified products can be informative (Bachem et al., 1996). In addition, this technique allows a wide variety of tissue types, developmental stages, or time points to be compared concurrently. As with the other profiling methods described here, the sensitivity of cDNA-AFLP is only limited by the ability of cDNA libraries to capture low-abundance transcripts. Sequencing of cDNA libraries is a more direct and comprehensive approach to

gene expression profiling (Adams et al., 1991; Okubo et al., 1992), but this method requires substantial resources for cloning and sequencing, and is less sensitive to low-abundance transcripts as mentioned above. Serial analysis of gene expression (i.e. SAGE; Velculescu et al., 1995) is an elegant technique that combines differential display and cDNA sequencing approaches, and it has the advantage of being quantitative. Unfortunately, SAGE is laborious, requires an extensive foundation of sequence information, and suffers from some of the same concerns regarding low-abundance transcripts.

Since its establishment in the 1990s (Higuchi et al., 1992, 1993; Heid et al., 1996; Wittwer et al., 1997), quantitative real-time RT-PCR (qPCR) has been widely used, allowing fast, accurate and sensitive mRNA quantification with a high throughput of samples. Unfortunately, the issue of real-time PCR data analysis is often underestimated by researchers. In the past years several authors have published approaches for enhanced qPCR data analysis (Pfaffl, 2001; Peirson, 2003; Ramakers, 2003; Wong and Medrano, 2005). qPCR offers the opportunity to observe the amplification kinetics of a PCR in “real time” via accumulation and measurement of specific fluorescence signals with each cycle (Higuchi et al., 1992; Heid et al., 1996; Wittwer et al., 1997) and was widely used for gene-specific mRNA quantification.

Microarrays take advantage of existing EST collections and genome sequence data (and are thus limited by the availability of the same), robotic instrumentation for miniaturization, and fluorescent dyes for simultaneously detecting nucleic acid abundance in RNA populations derived from multiple samples. Populations of fluorescent cDNA targets representing the mRNA populations of interest are queried via hybridization with a large number of probes that have been immobilized on a suitable substrate (Chen et al., 1998; DeRisi et al., 1996; Shalon et al., 1996; Shena et al., 1995). The arrays themselves are composed of collections of DNA sequences (typically PCR products, cDNAs, or oligonucleotides) that have been printed as a microscopic grid of catalogued features by a high-fidelity robotic system. This technique for gene expression profiling has important advantages when compared with RNA-blot analysis, cDNA sequencing, real time RT-qPCR, differential display, AFLP analysis, and

SAGE. Most importantly, it can measure tens-of-thousands of different mRNA transcripts in parallel, it is semi-quantitative, and it is sensitive to low-abundance transcripts that are represented on a given array. This last point is worth emphasizing in that microarrays are inherently limited to their contained sequences, while so-called 'open architecture' systems such as differential display and SAGE can capture information for any sequence that is expressed at a level sufficiently above the level of detection. In those instances where complete genome sequence is available, microarrays make it possible to monitor the expression of an entire genome in a single experiment (Gill et al., 2002; Jiang et al., 2001; Wang et al., 2003). Despite this potential, predominant uses of microarrays facilitate analysis of significant, yet limited, subsets of the target genome. When used for time-course analyses, analyses of transcriptome alterations caused by genetic lesions, or comparison of transcript accumulation in similar tissues from closely related species, the potential of microarrays for gene expression profiling is not only enormous, but is also just beginning to be realized.

1.3 Real Time RT-qPCR

Real time RT-qPCR (sometimes called kinetic PCR) is used in research laboratories to quantify gene expression and to confirm differential expression of genes detected by array technology. In analytical laboratories, real time RT-qPCR is used to measure the abundance of particular DNA or RNA sequences in clinical and industrial samples and, in both types of laboratories, to screen for mutations and single nucleotide polymorphisms. Real time RT-qPCR uses commercially available fluorescence-detecting thermocyclers to amplify specific nucleic acid sequences and measure their concentration simultaneously. Because the target sequences are amplified and detected in the same instrument plots the rate of accumulation of amplified DNA over the course of an entire PCR. The grater the initial concentration of target sequences in the reaction mixture, the fewer the number of cycles required to achieve a particular yield of amplified product (Becker et al., 1996; Gibson et al., 1996; Heid et al., 1996; Freeman et al., 1999). In the initial cycles of PCR, there is no significant change in fluorescence signal.

This predefined range of PCR cycles is called the baseline. First, the instrument softwares generate a baseline subtracted amplification plot by calculating a mathematical trend using R_n values (the ratio of the fluorescence emission intensity of the reporter dye to the fluorescence emission intensity of the passive reference dye) corresponding to the baseline cycles. Then, an algorithm searches for the point on the amplification plot at which the ΔR_n ($R_n - baseline$) value crosses the threshold. The initial concentration of target sequences can therefore be expressed as the fractional cycle number (C_T) required to achieve a present threshold of amplification. The target sequences in an unknown sample may be easily quantified by interpolation into this standard curve. Unlike other forms of quantitative PCR, internal standards are not required in real time RT-qPCR.

The ability to quantify the amplified DNA during the exponential phase of the PCR, when none of the components of the reaction are limiting, results in an improved precision in the quantitation of target sequences. By contrast to methods that measure the amount of product at the end of the reaction, real time RT-qPCR is not affected to a significant extent by slight variations in the components of the reaction and is less sensitive to differences in the efficiency of amplification.

The earliest of the real time RT-qPCR instruments used a fluorometer coupled to a thermal cycler to measure the enhanced fluorescence by dies that intercalate into, or bind to the grooves of, double-stranded DNA. During the exponential phase of a PCR, the amount of amplified product synthesized in each cycle increases in a quasi-geometric fashion. The yield of amplified DNA may therefore be estimated at any point from the amount of fluorescence emitted by dies such as ethidium bromide (Higuchi et al., 1992, 1993), SYBR Green I (Wittwer et al., 1997a), or certain oxazole yellow derivatives (Ishiguro et al., 1995).

Because of the high sensitivity of fluorometric detection, real time RT-qPCR is capable of measuring the initial concentration of target DNA over a range of five or six orders of magnitude (Heid et al., 1996). Currently, the limit of detection when fluorescent dyes such as SYBR Green I are used is ~10-100 copies of template DNA in the starting specimen (Higuchi et al., 1993; Wittwer et al., 1997b).

Generic DNA-binding dyes such as ethidium bromide and SYBR Green I are universal probes that detect any double-stranded DNA generated during PCR, independent of the template and primers used in the reaction. Because many molecules of the dyes can bind to each DNA product, the intensity of signal generated is high and is proportional to the total mass of DNA generated during the PCR and is independent of the number of types of molecules produced. High levels of sensitivity are achieved only in real time PCRs that generate a single amplification product. Nonspecific amplification or the formation of primer-dimers can generate significant errors in quantifying small numbers of target molecules when universal dyes are used as reporters. In the worst cases, the emitted fluorescence may bear little or no relationship to the amount of starting target DNA or the amount of full-length product produced. Several methods have been developed to confirm the specificity of the amplified product produced. Several methods have been developed to confirm the specificity of the amplified products of real time RT-qPCRs:

- Melting temperatures. As the end of the PCR, the thermocycler/fluorometer can be programmed to generate a thermal denaturation curve of the amplified DNA and to measure the melting temperature (T_m) of the PCR product(s). The shape of the melting curve indicates whether the amplified products are homogeneous and the T_m provides reassurance that the correct product has been specifically amplified. Primer-dimers, which generate much of the background noise in real time RT-qPCR, because of their short length, generally denature at much lower temperatures and can easily be distinguished from the amplified target DNA (Ririe et al., 1997).
- Fluorescently labelled oligonucleotide probes. Two methods have been developed in which fluorescently labelled oligonucleotide probes are used to quantify the amount of the target sequences generated by real time RT-qPCR. In each case, the fluorescent signal in generated after extension of the oligonucleotide by Taq polymerase. The strength of the signal is therefore proportional to the amount of the target DNA and is not influenced by the accumulation of non specific products such as primer-dimers, which do not hybridize to the labelled oligonucleotide probe.

- The TaqMan method of real time RT-qPCR (Holland et al., 1991; Livak et al., 1995), uses an oligonucleotide that anneals to an internal sequence within the amplified DNA fragment. The oligonucleotide, usually 20-24 bases in length, is labelled at one end with a fluorescent group (Fam<Hex or Tet) at its 5' end and a quenching group (usually Tamra) at its 3' end, which is blocked with PO_4, NH_2, or a blocked base. The labelled oligonucleotide is added to the PCR together with primers required to drive the amplification of the target sequence. When both the fluorescent and quenching groups are present in close apposition on the intact hybridization probe, any emission from the reporter dye during the course of real time RT-qPCR is absorbed by the quenching dye, and the fluorescent emission is low. As the reaction progresses, and the amount of target DNA increases, progressively greater quantities of oligonucleotide probe hybridize to the denatured target DNA. However, during the extension phase of the PCR cycle, the 5'→3' exonuclease activity of the thermostable polymerase cleaves the fluorophore from the probe. Because the fluorophore is no longer in close proximity to the quencher, it begins to fluoresce. The intensity of fluorescence is in direct proportion to the amount of target DNA synthesized during the course of the PCR.
- Binary hybridization probes labelled with different fluorescent dyes can also be used to differentiate the products of real time RT-qPCRs (Wittwer et al., 1997b). By themselves, these probes emit only low levels of fluorescence. However, when brought into close proximity by hybridization to adjacent sequences in a target DNA during the course of real time RT-qPCR, the fluorescent dyes act in synergy to generate a powerful fluorescent emission. Oligonucleotides that form a mismatched hybrid with the target DNA melt at a lower temperature than the corresponding perfectly matched hybrid. The resulting differences in melting temperature are sufficient to distinguish between target DNAs carrying wild-type or mutant sequences (Lay and Wittwer, 1997; Bernard et al., 1998).

1.3.1 Quantification assay chemistry

RT-PCR is usually used to quantify RNA. RT-PCR can be performed as a one-step or two step procedure.

The one-step RT-PCR performs RT as well as PCR in a single buffer system. The reaction proceeds without the addition of reagent between the RT and PCR steps. This offers the convenience of a single-tube preparation for RT and PCR amplification. However, the carryover prevention enzyme, uracil-N-glycosylase, cannot be used with one-step RT-PCR, because it would destroy the cDNA as it is being made. Two-step RT-PCR is performed in two separate reactions. This is useful when detecting multiple transcripts from a single cDNA reaction, or when storing a portion of the cDNA for later use. When performing PCR, if dUTP is not used as a base in the RT step, uracil-N-glycosylase enzyme can be used to prevent carryover contamination.

Both TaqMan and SYBR Green I dye chemistries, the most chemistries emploied, can be used for either one-step or two-step RT-PCR. For two-step RT-PCR, the Oligo $d(T)_{16}$, random hexamers or sequence-specific reverse primers can be used for cDNA synthesis. For short RNA sequences containing no hairpin loops, any of the three priming systems works equally well. For longer RNA transcripts or sequences containing hairpin loops there are some differences. Usually, oligo $d(T)_{16}$ primers are used to reverse transcribe eukaryotic mRNAs and retroviruses with poly-A tails and are avoided with long mRNA transcripts or amplicons greater than 2 kilobases upstream. Random hexamers are used with long reverse transcripts or reverse transcripts containing hairpin loops and to transcribe all RNA (rRNA, mRNA, and tRNA). Finally, sequence-specific reverse primers are used to reverse transcribe RNA-containing complementary sequences only.

Moreover, selecting a good amplicon site ensures amplification of the target mRNA/cDNA without co-amplifying the genomic sequence, pseudogenes, and other related genes. The amplicon should span one or more introns to avoid amplification of the target gene in genomic DNA. The primer pair should be specific to the target gene to avoid amplification of pseudogenes or other related genes.

An important parameter is the selection of amplicons in the 50- to 150-basepair range. Small amplicons are favoured because they promote high-efficiency amplification. In addition, hight-efficiency assays enable relative quantification to be performed using the comparative C_T method ($\Delta\Delta C_T$) (Livak and Schmittgen, 2001). This method increases sample throughput by eliminating the need for standard curves when looking at expression levels of a target relative to a reference control. (For more information on the comparative C_T method, see next paragraph).

Whenever possible, primers and probes should be selected in a region with a G/C content of 30 to 80%. Regions with a G/C content in excess of this may not denature well during thermal cycling, leading to a less efficient reaction. In addition, G/C-rich sequences are susceptible to nonspecific interactions that may reduce reaction efficiency and produce non specific signal in SYBR Green I dye assays.Selecting primers and probes with the recommended melting temperature (T_m) allows the use of universal thermal cycling parameters. Having the probe T_m be 8 to 10 °C higher than that of the primers is recommended.

1.3.2 Data Analysis

Data analysis varies depending on the product, assay, and instrument. The general process for analyzing the data from gene expression assays involves three procedures: (1) viewing the amplification plot, (2) setting the baseline and threshold values, (3) using the appropriate quantification method to determine results.

It is possible to use relative or absolute quantification. Relative quantification describes the change in expression of the target gene in a test sample relative to a calibrator sample. The calibrator sample can be an untreated control or a simple at time zero in a time-course study. Relative quantification provides accurate comparison between the initial level of template in each sample (Livak and Schmittgen, 2001). Absolute quantification determines the input copy number of the transcript of interest, usually by relating the PCR signal to a standard curve (Livak and Schmittgen, 2001).

1.3.2.1 Calculation methods for Quantification

The calculation methods used for relative quantification are relative standard curve method and comparative C_T method ($\Delta\Delta C_T$), while the calculation method used for absolute quantification is only the standard curve method.

In the relative standard curve method quantity is expressed relative to some basis sample, such as the calibrator. For all experimental samples, target quantity is determined from the standard curve and divided by the target quantity of the calibrator. Thus, the calibrator becomes the 1xsample, and all other quantities are expressed as an n-fold difference relative to the calibrator. Some requirements are critical for proper use of this quantification method: (1) it is important that the stock RNA or DNA be accurately deluited, but the units used to express this diluition are irrelevant. If two-fold diluitions of a total RNA preparation from a control cell line are used to construct a standard curve, the units could be the diluition values 1, 0.5, 0.25, 0.125, and so on. By using the same stock RNA or DNA to prepare standard curves for multiple experiments, the relative quantities determined can be compared across the experiments. (2) For quantification normalized to an endogenous control, standard curves are prepared for both the target and the endogenous control is determined from the appropriate standard curve. Then, the target amount is divided by the endogenous control amount to obtain a normalized target value. Amplification of an endogenous control can be performed to standardize the amount of sample RNA or DNA added to a reaction. For the quantification of gene expression, are used hosekeeping genes as β-actin, GAPDH, ribosomal RNA, or other RNAs. Another approach is to normalize to a measurement external to the PCR experiment. For example, it is possible to use UV absorption to determine the amount of RNA added to a cDNA reaction, to run a PCR using cDNA derived from the same amount of input RNA (Livak and Schmittgen, 2001).

The comparative C_T method is similar to the relative standard curve method, except it uses an arithmetic formula rather than a standard curve to achieve the same result for relative quantification. The amount of target, normalized to an endogenous control and relative to a calibrator, is given by:

$$2^{-\Delta\Delta C_T}$$

The derivation of the formula is obtained by Livak and Schmittgen (2001) and is described as follow:

the equation that describes the exponential amplification of PCR is:

$$X_n = X_0 \times (1 + E_X)^n$$

where X_n is the number of target molecules at cycle n of the reaction, X_0 is the initial number of target molecules. E_X is the efficiency of target amplification, and n is the number of cycles (Murphy et al., 1990).

The threshold cycle (CT) indicates the fractional cycle number at which the amount of amplified target reaches a fixed threshold. Thus,

$$X_T = X_0 \times (1 + E_X)^{C_{T,X}} = K_X$$

Where X_T is the threshold number of target molecules, $C_{T,X}$ is the threshold cycle for target amplification, and K_X is a constant (Noonan et al., 1990).

A similar equation for the endogenous reference (internal control gene) reaction is:

$$R_T = R_0 \times (1 + E_R)^{C_{T,R}} = K_R$$

whereR_T is the threshold number of reference molecules, R_0 is the initial number of reference molecules, E_R is the efficiency of reference amplification, $C_{T,R}$ is the threshold cycle for reference amplification, and K_R is a constant (Horikoshi, 1992).

Dividing X_T by R_T gives the expression (Heid et al., 1996):

$$\frac{X_T}{R_T} = \frac{X_0 \times (1 + E_X)^{C_{T,X}}}{R_0 \times (1 + E_R)^{C_{T,R}}} = \frac{K_X}{K_R}$$

For real-time amplification using TaqMan probes, the exact values of X_T and R_T depend on a number of factors including the reporter dye used in the probe, the sequence context effects on the fluorescence properties of the probe, the efficiency of probe cleavage, purity of the probe, and setting of the fluorescence threshold. Therefore, the constant K does not have to be equal to one. Assuming efficiencies of the target and the reference are the same:

$$\frac{X_0}{R_0} \times (1 + E)^{C_{T,X} - C_{T,R}} = K$$

Or

$$X_N \times (1 + E)^{\Delta C_T} = K$$

Where X_N is equal to the normalized amount of target (X_0 / R_0) and ΔC_T is equal to the difference in threshold cycles for target and reference ($C_{T,X} - C_{T,R}$) (Winer et al., 1996; Schmittgen et al., 2000).

Rearranging gives the expression (Schmittgen and Zakrajsek, 2000):

$$X_N = K \times (1 + E)^{-\Delta C_T}$$

The final step is to divide the X_N for any sample (q) by the X_N for the calibrator (cb):

$$\frac{X_{N,q}}{X_{N,cb}} = \frac{K \times (1 + E)^{-\Delta C_{T,q}}}{K \times (1 + E)^{-\Delta C_{T,cb}}} = (1 + E)^{-\Delta\Delta C_T}$$

Where $\Delta\Delta C_T = \Delta C_{T,q} - \Delta C_{T,cb}$ (Chen and Shyu, 1999).

For amplicons designed to be less than 150 bp and for which the primer and Mg2+ concentrations have been properly optimized, the efficiency is close to one. Therefore, the amount of target, normalized to an endogenous reference and relative to a calibrator, is given by (Iyer et al., 1999):

$$\text{amount of target} = 2^{\Delta\Delta C_T}$$

1.4 Microarray technology

1.4.1 Microarray fabrication

Two main approaches are used for microarray fabrication: deposition of DNA fragments and *in situ* synthesis (Gao et al., 2004). The first type of fabrication involves two methods: deposition of PCR-amplified cDNA clones (long DNA sequences, over one hundred bases) and printing of already synthesized oligonucleotides. In situ manufacturing can be divided into photolithography, ink jet printing and electrochemical synthesis.

1.4.1.1 Deposition of DNA fragments

In the deposition based fabrication, the DNA is prepared away from the chip. Robots dip thin pins into the solutions containing the desired DNA material and then touch the pins onto the surface of the arrays. Small quantities of DNA are deposited on the array in the form of spots. Spotting methods for DNA microarrays (Chrisey et al., 1996; Steel et al., 1999; Okamoto et al., 2000;

Ramakrishnan, 2002) typically use noncontact or contact printing technologies, such as those by robotic pin or piezoelectric ink-jet instruments, to deposit DNA on a surface according to a predetermined pattern (layout) containing one sequence per site (fig. 1). In most cases, these sequences are subsequently immobilized on the surface by chemical attachment of a functional group, like as amine, poly-L-lysine, aldehyde, epoxy, succinimide and carbodiimite.

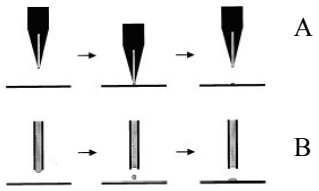

Figure 1: A. contact printing; B. noncontact printing

Amine and poly-L-lysine substrates are used to immobilize unmodified DNA. The printed sample dehydrates causing a loss of water and an large increase in the DNA concentration, resulting in attachment of the DNA to the amine surface via the formation of electrostatic bonds (step 1) between the positively charged (+) amine or lysine groups and the negatively charged (-) DNA. The attachment of the DNA can be enhanced by the formation of covalent bonds (step 2) by baking at elevated temperature or treatment with ultraviolet light (Genetix, Corning, Nunc Brand Products, Arrayit, Sigma-Aldrich).

Aldehyde substrates are used to immobilize amino modified DNA. Primary amino linkers (NH2) on the DNA attack the aldehyde groups forming covalent bonds. Attachment is stabilized by a dehydration reaction (drying in low humidity) which leads to Schiff base formation. Specific and covalent end attachment provide highly stable and accessible attachment of DNA (Genetix, Nunc Brand Products, Arrayit).

Epoxy substrates are used to immobilize both amino modified and unmodified DNA. DNA contain primary amine groups on the A, G, and C residues. The lone electron pair (double dots) attack the electrophilic carbon on the epoxide group, forming a covalent bond between the DNA and the substrate (Genetix, Corning, Nunc Brand Products, Arrayit). Succinimide and carbodiimite surfaces are able to bind covalently amino modified DNA (GE Healthcare, LifeLineLab, Nunc Brand Products).

1.4.1.1.1 cDNA microarrays

Unlike in situ manufacturing where the length of the DNA sequence is limited, spotted arrays can use small sequences, whole genes or even arbitrary PCR products. The cDNA cloned inserts are amplified by PCR from plasmid DNA, and the purified PCR products are then printed on solid support. cDNA microarrays (Shena et al., 1996) were quickly accepted since it is simpler to prepare these based on publicly accessible information (Ferea and Brown, 1999) and the DNA sequences are available in many biology laboratories. The applications of cDNA microarrays in unknown gene identification (Shena et al., 1996) and gene expression profiling of human, yeast, mouse, or other systems have provided valuable insights into the relationships of gene regulation and functions (Ferea and Brown, 1999). However, in recent years, as oligonucleotide microarrays have gradually gained popularity, it has been realized that the applications of cDNA arrays are mostly limited to gene expression. The reproducible production of long DNA of correct sequences is more difficult, and thus reproducible microarray preparation and the implementation of a unified standard for microarray experiments are unlikely. Long DNA sequences also tend to cross-hybridize with undesirable target DNA due to their sufficiently long overlapping regions that form stable duplexes between a probe and a target. It is therefore not possible to use cDNA to discriminate homolog genes of the same family. On the contrary, oligonucleotide probes by design can be highly specific in sequence and flexible to allow variations in sequences lengths.

1.4.1.1.2 Oligonucleotide Microarrays

DNA microarrays consisting of oligonucleotides are made using any methods. Oligonucleotides are prepared by well-controlled automated chemical synthesis processes. Oligonucleotide probes have been placed within a microarray for gene expression profiling, mutation detection, resequencing, and various other applications (Lipshutz et al., 1999). In the foreseeable future, oligonucleotide microarrays will largely replace cDNA microarrays in DNA microarray applications. The main limitations in development of oligonucleotide arrays are the costs associated with sequence selection and oligonucleotide synthesis. As

these costs continue to decline oligo-based arrays are likely to become more predominant in the near future because they offer a number of important advantages over cDNA arrays.

The chemical moieties allowing oligonucleotides to extend from surface are spacers, which are anchored to linkers, which are directly attached to the surface. Routine oligonucleotide synthesis requires cleavage and recovery of the 3-OH products. For microarray oligonucleotides it is desirable to use noncleavable linkers that will be stable under their assay conditions such as physiological aqueous buffer solutions. In addition to mediating extension, linkers and spacers serve other purposes as well. They can be used to adjust sequence surface density if the surface-coupled linker or spacer molecules used do not undergo further chain extension reactions (Leproust et al., 2001). They are also moieties for introducing functional groups for modifying surface properties, such as charge, adhesion, or hydrophobicity/hydrophilicity, and autofluorescence.

In most cases, these sequences are subsequently immobilized on the surface by chemical attachment of a functional group, linked through a few rotational bonds to the 5-end of oligonucleotides, to the surface. There are usually no special spacers but the first few residues close to surface function as spacers rather than as specific probes. Several advantages are associated with the spotted oligonucleotide microarrays. Since the 5-functional group is attached at the last step of synthesis and the failure sequences from synthesis in theory do not react at this step, the attachment step is thus a purification filter for removing impurity sequences. The 5-attachment results in 3-OH of oligonucleotides away from the surface, which are thereby available for enzymatic reactions such as primer extension by a DNA polymerase, and hence enzymatic assays. Furthermore, the presynthesized oligonucleotides may be purified by a conventional means before spotting, which would result in high-quality spotting materials. Conceivably, it is economical to massively produce spotted DNA microarrays since each oligonucleotide can be used for thousands of spots. But this method requires significant up-front investment for the synthesis, lacks flexibility in fast sequence substitutions, and is limited in spot feature size of larger than 100 μm. The quality of the spotted microarrays varies greatly due to fluctuation in oligonucleotide

supplies, environmental factors such as humidity, and many other operational factors such as spotter pin wear-and-tear and changes in surface properties. Other special methods for preparation of DNA microarrays using presynthesized oligonucleotides include stamping simultaneously multiple spots of oligonucleotides on a surface, immobilizing them on the inner wall of flow-through glass microchannels, which are fused together to form a rigid matrix or glass capillary microarrays (Steel et al., 1999; Cheek et al., 2001; Benoit et al., 2001). or immobilizing oligonucleotides on beads to form random massive bead microarrays whose hybridization signals are detectable through adhering of the beads to the etched tip of fiber-optic bundles (Walt, 2000; Yeakley, 2002). The random bead array requires signature coding of each bead using an oligonucleotide sequence and the bead identity is revealed through a second hybridization to the decoding sequences.

1.4.1.2 In situ synthesis

A number of methods of in situ synthesis of oligonucleotide microarrays have been reported (McBride and Caruthers, 1983; Caruthers, 1991; Fodor et al., 1991; Maskos and Southern, 1992; Case-Green, 1998; Gao et al., 2004), among which the method of mask directed in situ parallel synthesis using the photolabile-protecting group (PLPG) (Fodor et al., 1991) has been successfully used to manufacture high-density gene chips. A variety of DNA microarrays fabricated by other methods have since become available for the study of diverse living species and the applications requiring flexibility in sequence design and longer oligonucleotides of higher quality. In situ parallel synthesis has distinct advantages, which include standardized automated production processes, suitable for spot and thus array miniaturization, regularity in spot alignment (thus faster signal reading and greater ease of signal processing automation), and high spot quality. It is possible to obtain oligonucleotide microarrays of one's own design in a short amount of time and low cost using the in situ synthesis approach. The foundation for the synthesis of DNA microarrays is nucleophosphoramidite chemistry, which was developed from decades of efforts for optimization of oligonucleotide synthesis and routinely achieves better than 98.5% stepwise yield

on a DNA synthesizer (McBride and Caruthers, 1983; Caruthers, 1991). Conventional oligonucleotide synthesis usually is carried out on solid support such as controlled porous glass (CPG) or functionalized polymeric beads and involves multicycles with each cycle containing four reaction steps: deprotection to release terminus OH group, coupling of a 5-O-4,4-dimethoxytrityl (DMT) protected nucleophosphoramidite monomer, capping of the free OH groups that failed to couple, and oxidation of the internucleotide phosphite to phosphate triester. In the end of synthesis, the protecting groups on nucleobases and phosphotriester are removed by treatment with concentrated aqueous ammonia and at the same time the sequences are cleaved from the support) (fig. 2). A key step in performing a large number of these reactions in parallel in a small area, e.g., 1 cm2, is to control at each site whether the reaction occurs or does not occur in each reaction cycle (referred to as gating on and off of the reactions). In each of the following methods described, a different gating mechanism is used during the deprotection step. The fundamentals of these methods determine the characteristics of the DNA microarrays synthesized and their suitability in serving the various application needs.

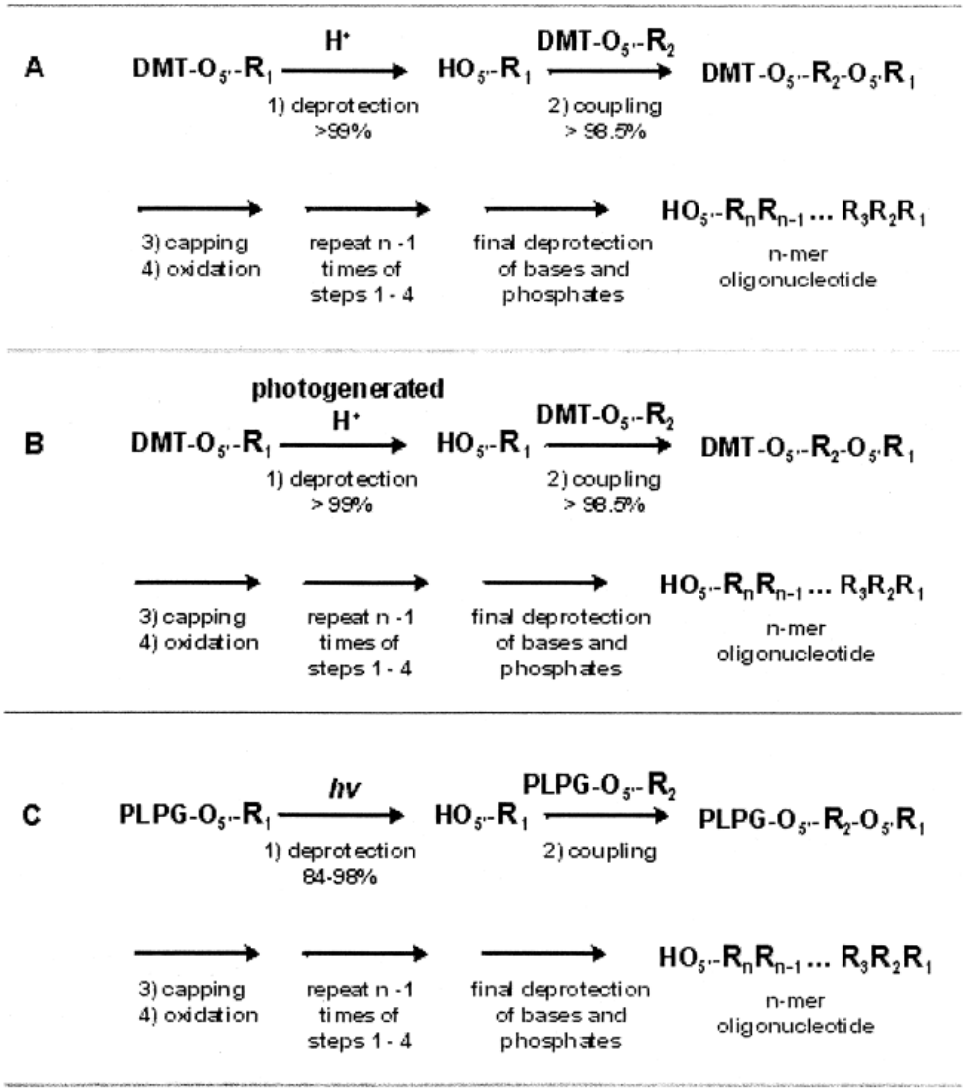

Figure 2: Schematics showing major steps of chemical synthesis of n-mer oligonucleotides. R_1, R_2, etc., represent arbitrary A, C, G, or T nucleotides. Stepwise yields in percent are indicated when available. (A) Conventional phosphoramidite chemistry using electrogenerated acid as deprotecting agent (H^+) for removal of the DMT group. (B) Synthesis using digital photolithography (H^+) as deprotecting agent and phosphoramidite chemistry. (C) Synthesis using PLPG-protected monomers and deprotection is a photolytic reaction involving 5'O terminal. PLPG may be (a-methyl-2-nitropiperonyl)oxycarbonyl (MeNPOC) or 2-(2-nitrophenyl)propoxcarbonyl) (NPPOC) (Gao et al., 2004).

The method most used is photolithographic (Affymetrix, Santa Clara, CA), and is similar to the technology used to build very large scale integrated (VLSI) circuits used in modern computers. This fabrication process uses photolithographic masks for each base. If a probe should have a given base, the corresponding mask will have a hole allowing the base to be deposited at that location. Subsequent masks

will construct the sequences base by base. This technology allow the fabrication of very high density arrays but the length of the DNA sequence constructed is limited. This is because the probability of introducing an error at each step is very small but different from zero. In order to limit the overall probability of an error, one needs to limit the length of the sequences. The particular sequences must be chosen carefully to avoid cross-hybridization between genes.

The second approach is the ink jet technology (Agilent, Protogene, etc.) and it employs the technology used in ink jet color printers. Four cartridges are loaded with different nucleotides (A, C, G, and T). As the print head moves across the array substrate, specific nucleotides are deposited where they are needed.

Finally, the electrochemical synthesis approach (CombiMatrix, Bothel, WA) uses small electrodes embedded into the substrate to manage individual reaction sites. Solutions containing specific bases are washed over the surface and the electrodes are activated in the necessary positions in a predetermined sequence that allows the sequences to be constructed base by base.

1.4.2 Target labelling and hybridization

The targets for arrays are labelled representations of cellular mRNA pools. Typically, reverse transcription from an oligo−dT primer is used. This has the virtue of producing a labelled product from the 3′ end of the gene, directly complementary to immobilized probes synthesized. Frequently, total RNA pools (rather than mRNA selected on oligo−dT) are labelled, to maximize the amount of message that can be obtained from a given amount of tissue. The purity of RNA is a critical factor in hybridization performance, particularly when using fluorescence, as cellular protein, lipid and carbohydrate can mediate significant non−specific binding of fluorescently labelled cDNAs to slide surfaces. For radioactive detection, ^{33}P-dCTP is preferred to more energetic emitters, as array elements are physically close to each other and strong hybridization with a radioactive target can easily interfere with detection of weak hybridization in surrounding targets. As fluorescent labels, Cy3−dUTP and Cy5−dUTP are frequently paired, as they have relatively high incorporation efficiencies with reverse transcriptase, good photostability and yield, and are widely separated in

their excitation and emission spectra, allowing highly discriminating optical filtration.

The two most common methods for labeling cDNA targets are direct incorporation of fluorescent nucleotides during reverse transcription, and a two-step incorporation method often referred to as indirect incorporation or amino-allyl labeling. Direct incorporation was initially the method of choice, but persistent problems with this method have been reported (Hegde et al., 2000; Payton et al., 2003; Smyth et al., 2002; Yang et al., 2002b). For example, the rate of incorporation for nucleotides labeled with cyanine3 (Cy3^{TM}) and cyanine5 (Cy5^{TM}) (GE Healthcare), is typically low, can be influenced by cDNA sequence, and can have negative effects on cDNA yield – all leading to inaccurate representations of expression. Indirect incorporation is the emerging method of choice for labeling cDNA prior to microarray hybridization (DeRisi et al., 1996, 1997; Shena et al., 1995). This method utilizes dUTP nucleotides that are modified with an amino-allyl group [e.g. 5-(3-aminoallyl)-2'-dUTP]. After incorporation of these nucleotides during cDNA synthesis, the modified cDNA is labeled using an N-hydroxy-succinimide ester form of Cy3^{TM} or Cy5^{TM} and a carbonate-based coupling buffer. This approach circumvents low incorporation rates and incorporation bias that are likely due to the size of the dye molecules.

A clear limitation to the application of this technology is the large amount of RNA required per hybridization. For adequate fluorescence, the total RNA required per target, per array, is 20−200 μg (2−5 μg are required when using poly(A) mRNA). For mRNA present as a single transcript per cell (approximately 1 transcript per 100,000), application of target derived from 100 μg of total RNA over an 800 mm^2 hybridization area containing 200 μm diameter probes will result in approximately 300 transcripts being sufficiently close to the target to have a chance to hybridize. Thus, if the fluorescently tagged transcripts are, on average, 600 bp, have an average of 2 fluor tags per 100 bp and hybridize, all of them, to their probe, approximately 12 fluors will be present in a 100 μm^2 scanned pixel from that probe. Such low levels of signal are at the lower limit of fluorescence detection, and could easily be rendered undetectable by assay noise. Although radioactive targets may have a higher intrinsic detect ability, they too reach a level

of dilution that prohibits effective detection, thus precluding experimentation on very small numbers of cells. A variety of means by which to improve signal from limited RNA has been proposed. These are being evaluated by our laboratory and many others. Efficient mixing of the hybridization fluid should bring more molecules into contact with their cognate probe, increasing the number of productive events. This entails, however, a larger 'mixing' volume, which might offset the potential gain. Methods that produce multiple copies of mRNA using highly efficient phage RNA polymerases have been developed (Phillips and Eberwine, 1996). A version of this approach, in which labelled target (cRNA) is made directly from a cDNA pool, having a T7 RNA polymerase promoter site at one end via in vitro transcription, has been applied to arrays (Lockart et al., 1996). Posthybridization amplification methods have also been reported in which detectable molecules are precipitated at the target by the action of enzymes 'sandwiched' to the cDNA target (Chen et al., 1998). Detection of hybridized species using mass spectroscopy or local changes in electronic properties can also be imagined (Thorp, 1998; Marshall and Hodgson, 1998).

1.4.3 Image analysis and data extraction

Once the fluorescent sample is reacted with the microarray, the unbound material is washed away and the sample bound to each element on the chip is visualized by fluorescence detection. Confocal scanning devices (Fodor et al., 1991; Schena and Davis, 1998; Schena et al., 1995; Chee et al., 1996; Schena, 1996; Schena et al., 1996; Lockart et al., 1996; DeRisi et al., 1996; Shalon et al., 1996; Heller et al., 1997; DeRisi et al., 1997; Lanshkari et al., 1997; Wodicka et al., 1997; de Saizieuet al., 1998; Lemieux et al., 1998; Schena et al., 1998) and CCD cameras (Schena and Davis, 1998) have both been used successfully for microarray detection. The most common configuration of a confocal scanner utilizes laser excitation of a small region of the glass substrate (~100μm^2), such that the entire image is gathered by moving the substrate or the confocal lens (or both) across the substrate in two dimensions. Light emitted from the fluorescent sample at each location is separated from unwanted light using a series of mirrors, filter, and lenses, and the light is converted to an electrical signal with a photomultiplier tube

(PMT) or an equivalent detector. The speed of data gathering with a confocal scanner (1-5 min) is orders of magnitude faster than autoradiography with radioactive filters used in conventional experiments (one to ten days). Rapid fluorescent detection technology is a revolutionary aspect of microarray technology. Fluorescent imaging with a CCD camera uses many of the same principles as a confocal scanner, though key details are different in both excitation and detection technology. One difference is that CCD-based imaging often involves illumination and detection of a large portion of the substrate (1 cm^2) simultaneously. The ability to capture a relatively large field has the advantage of obviating the requirement for movable stages and optics, which reduces cost and simplifies instrument design. Another key difference between confocal scanners and CCD-based detection systems is that the latter often use continuous wavelength light sources such as arc lamps thereby obviating the need for multiple lasers. Fastidious filtering of emission spectra in CCD-based systems minimizes optical cross-talk between different channels.

Microarray scanners can take many forms, whether confocal or not, but any of these instruments must provide the following functions: excitation, emission light collection, spatial addressing, excitation/emission discrimination and detection.

Once the fluorescent emission from the microarrays is converted into a digital output by the detection system, the data files (usually 16-bit TIFF) are quantitated and interpreted. Quantitation is usually accomplished an average intensity value for each microarray element with automated software. Intensity values can then be converted into biologically relevant outputs such as the elements present in a given microarray. Quantitative gene expression, genotyping, and other outputs are then correlated with the gene sequences represented in the microarray and higher order relationships such as co-regulation and gene regulatory networks can be identified.

1.4.4 Normalization

The process by which data from different channels or different chips are equalized before analysis is known as normalization, and the value that is used to normalize different datasets is known as a normalization factor. If performed properly, the

normalization process does not alter the content of the data but rather corrects for minor imbalances that arise during the imaging process owing to differences in labeling and hybridization efficiency, washes, differential quantum yield of dyes, variations in laser power and detector sensitivity, and many other causes of slight disparities between different chips or channels. Normalization enables precise ratio calculations and other valuable comparisons that would be ill-advised with nonnormalized images. As a prerequisite to normalization, hardware settings on the detection instrument should be adjusted before imaging to produce images that are as closely matched as possible. With matched images in hand, data normalization is a relatively straightforward process. Normalization can be accomplished using a variety of different criteria, including global intensities, housekeeping genes, and internal standards.

Global intensity normalization uses the sum of signals in multiple images to provide equalized signals. Images that have slightly different signal ratios can be adjusted computationally using a normalization factor to balance the data globally. Global intensity matching works extremely well for samples that share many common signal intensities, such as differential gene expression experiments that compare a test and reference sample prepared from a common biological source. Global methods assume that the cy3 (green, G) and cy5 (red, R) intensities are related by a constant factor. That is, $R = k \cdot G$, and in practice, the center of the distribution of log-ratios is shifted to zero:

$$Log_2\ R/G \rightarrow Log_2\ R/G - c = Log_2\ R/(kG)$$

A common choice for the location parameter $c = Log_2\ k$ is the median or mean of the log-intensity ratios for a particular gene set.

In many cases, the dye bias appears to be dependent on spot intensity, as revealed by plots of the log-ratio $M = Log_2\ R/G$ vs. overall spot intensity $A = Log_2\ \sqrt{RG}$. An intensity or A-dependent dye normalization method may thus be preferable to global methods. A more flexible normalization method uses the robust scatter-plot smoother lowess from the statistical software package R (Cleveland, 1979) to perform a local A-dependent normalization:

$$Log_2\ R/G \rightarrow Log_2\ R/G - c(A) = Log_2\ R/(k(A)G)$$

Where $c(A)$ is the lowess fit to the $M\ vs.\ A$ plot. The lowess () function is a scatter-plot smoother which performs robust locally linear fits. In particular, the lowess () function will not be affected by a small percentage of differentially expressed genes which will appear as outliers in the $M\ vs.\ A$ plot. The user defined parameter f is the fraction of the data used for smoothing at each point; the larger the f value, the smoother the fit.

Furthermore, normalizing or equalizing signals to a set of a cellular genes known as housekeeping genes, which are expressed at approximately the same level in many tissues, is one approach to normalizing data derived from different tissue or chips.

Another approach is to dope in small quantities of control samples from a foreign source into each labeling reaction, and normalize the images using the signal intensities obtained from the control spots

1.4.5 Data management and mining

The final step in microarray analysis is data mining and modeling. Once microarray data are quantified and normalized, it is necessary to interpret the meaning of the data vis-à-vis the vast amount of scientific information available on the genes, gene products, tissues, cells, and organisms used in the experiments. Data transformation, scatter plots, principle component analysis, expression maps, pathway analysis, cluster analysis, self-organizing maps, and workflow management are among the mining and modeling methods and tools most used.

This type of analysis, with large data sets, can provide novel perspectives on cellular regulatory mechanisms and can associate expression of unknown genes with a putative function. Hierarchical clustering of gene expression data in combination with false colour coding of the expression levels has become a popular way of data analysis and presentation (Eisen et al., 1998). With this technique genes are grouped in clusters based on the similarity between their expression profiles. In a bottom-up approach genes are joined to form nodes, which in turn are then further joined. Joining proceeds until all genes are combined in a single hierarchical tree. Although nice figures seem to be guaranteed, one should be careful when drawing conclusions from them. As many

similarity measures and clustering algorithms are available different outcomes are possible, depending on the method chosen. For example, when using Euclidean distance or Pearson correlation as a similarity measure, different relationships between the studied genes are explored. In the latter case clusters are formed based on the 'shape' of the expression profiles and not on the absolute expression values. Also, the presence of genes showing no apparent behavior might obscure the formation of discrete clusters; a problem that can be overcome by first filtering out the non-responsive genes. A self-organizing map has a pre-defined number of partitions in a two-dimensional grid. Via an iterative procedure the algorithm produces a reference expression profile for each partition in such a way that related profiles are neighboring. In a final step each gene is assigned to a partition depending on which reference profile its expression most closely resembles. The advantages of this procedure are the absence of any hierarchy and also a clear delimitation of the clusters obtained. An apparent drawback is the need for the number of partitions to be defined beforehand. PCA is a standard statistical method that helps to visualize multi-dimensional data sets in two- or three dimensional space. When considering genes, the dimensions (experiments) are redefined as components in such a way that as much of the original variation as possible is retained. In this way a scatter plot of the genes in principal component (PC) space can be made with as little loss of information as possible. This is a valuable way of analysing data, especially in cases where biological meaning can be given to the PC axes.

1.4.6 Verification of microarray

Verification of microarray data can be accomplished in a variety of ways, including RNA-blot analysis, RT PCR, real-time quantitative PCR, and/or comparison with EST expression databases (e.g. http://ted.bti.cornell.edu/). The latter being the only approach that has potential for genome-scale verification. The continued expansion of EST collections will only increase the feasibility of this approach for large-scale verification of transcriptome data.

Differential expression of genes identified via comparative expression profiling can also be used in conjunction with large-scale proteome analysis (Alba et al.,

2004) to dissect regulatory processes. Comparisons that combine expression and proteome profiling should allow one to distinguish transcriptional versus post-transcriptional regulation. To date, however, the potential for using comparative genomics/proteomics for this type of molecular analysis in plants remains largely untapped.

Sufficient replication is an important issue in meaningful transcriptome profiling and decisions in this regard should be based on (1) the extent of biological and technical variation in one's experimental system, (2) the experimental question, (3) desired resolution, (4) available resources, (5) available time, and (6) opportunities for downstream validation. In most cases biological replication is superior to technical replication, and technical replication is far better than none (Callow et al., 2000; Churchill, 2002; Kerr et al., 2000a; Lee et al., 2000). Consistent with the proposal of Lee et al. (2000), for time-course experiments it's useful a minimum of three to four biological replicates for each time point with a dye-swap technical replicate for each biological replicate (Cochran and Cox, 1992; Kerr et al., 2000a). This approach minimizes dye-specific artifacts and makes statistical analyses possible. Dye-swap replicates, which involve repeating the hybridization conditions with dye reversal in the second hybridization, are useful for reducing systematic dye bias (Tseng et al., 2001; Yang et al., 2001). Presumably this dye bias derives from differences in mean brightness and background noise, dye-specific incorporation efficiency, different extinction coefficients, differences in quantum fluorescence yield, and other physical properties of the dyes (e.g. molecular size, sensitivity to light and heat, relative half-life). For experiments comparing only two or three different samples (e.g. wild-type versus mutant), it's suggested a minimum of three to six biological replicates to make statistical analysis possible while minimizing resource depletion. Dye-swap replicates should be used in this situation as well. It is also important to point out that we are not implying that the 'law of diminishing returns' has firmly set in after three to six replicates. In some cases, particularly scenarios where more precision is required or greater systemic variance has been documented, greater replication (i.e. more than three to six replicates) is likely to be worth the additional resource investment. Thus, three to six replicates should

be considered only as an initial guideline during experimental design. Although biological replication is most desirable, in some cases such replication is not possible. In these instances, consistent with the hypothesis of Peng et al. (2003), a single RNA extraction from a homogenous pool of replicate tissue is superior to a single RNA extraction from an individual tissue sample. This being said it is important to point out that direct comparisons to test this hypothesis have not been reported in the literature. It should also be noted that replicate measurements from a pool of tissue only provides information about variability stemming from measurement error, and provides no information about variability that stems from population heterogeneity.

1.4.7 Experimental design

A variety of experimental designs are possible for microarray analysis, most of which have been discussed in detail (Churchill, 2002; Dobbin and Simon, 2002; Dobbin et al., 2003; Kerr and Churchill, 2001; Yang and Speed, 2002a). For profiling gene expression during time-course studies or analyses of developmental transitions it has found the direct-sequential linear design and the direct-sequential loop design (Kerr and Churchill, 2001; Yang and Speed, 2002a) to be well suited for this purpose. For example, because expression profiles obtained with these designs derive from pair-wise comparisons of adjacent time points, direct comparison of expression differences between time points is possible. Such comparisons can only be made indirectly when designs utilizing a common reference are employed, which may make subtle differences from one time point to another difficult to detect. Equally important, the direct-sequential loop design increases precision for some of the pair-wise comparisons in the time course, which reduces the mean variance for data collected in this way (Yang and Speed, 2003). More recently, experimental designs for microarray analyses have begun to incorporate interspecies comparisons using arrays that originate from one of the genomes being investigated (Dong et al., 2001; Horvath et al., 2003; Ventelon-Debout et al., 2003). Toward this objective, comparison of closely related species is most informative because artifacts stemming from sequence divergence are minimized.

1.4.8 Current applications of microarrays in plant

As in other biological disciplines, plant microarrays will prove an indispensable tool for research in the field of molecular plant science. The systematic, nonbiased, accurate and large-scale acquisition of data using microarray technology enables new experimental approaches for plant molecular biologists. Essentially, microarrays may be used to analyze any kind of variability in gene expression between given samples. These differences can be either naturally occurring or induced. Natural variation may occur between different plant cultivars, tissues, developmental stages, environmental conditions or during circadian rhythm in both reference and crop species.

1.4.8.1 *Arabidopsis* and rice: reference species and reference microarray expression data

The *Arabidopsis* community adopted microarrays as a tool when they were first developed. The initial AG Affymetrix array represented only ~8000 unique genes (Zhu and Wang; 2000), whereas the more recent ATH1 array represents ~23750 unique genes (Redman et al., 2004). It has been shown that expression data obtained with both array versions are largely similar and comparable (Hennig et al., 2003). In addition to the Affymetrix platform, long oligonucleotide arrays for *Arabidopsis* are available as well as spotted arrays with gene-specific sequence tags (Allemeersch et al., 2005). However, based on the predominance of literature reports and available datasets, the ATH1 array now appears to be the platform of choice for the *Arabidopsis* community. Together with ArrayExpress (Parkinson et al., 2005), The Nottingham *Arabidopsis* Stock Center (NASC) now provides the largest resource for *Arabidopsis* expression data because The *Arabidopsis* Information Resource (Rhee et al., 2003) recently stopped collecting expression data. Large quantities of expression data have been generated using the ATH1 array in individual studies and as part of the expression profiling service at NASC (Craigon et al., 2004). All hybridizations and data processing are performed at NASC using user-supplied RNA. Another large *Arabidopsis* expression dataset is provided through the AtgenExpress project, which is also available through

NASC. This dataset includes a gene expression map of *Arabidopsis* covering samples of many stages of development (Schimid et al., 2005). A detailed gene expression map of the *Arabidopsis* root is also available (Birnbaum et al., 2003).

Currently, only limited amounts of expression data are available for rice. Several published studies have used relatively small-scale spotted cDNA microarrays addressing rice pollination and fertilization (Lan et al., 2004), responses to elicitors (Akimoto-Romiyana et al., 2003), and salt stress (Kawasaki et al., 2001). Two studies have been published that used a proprietary rice Affymetrix array to study grain filling of rice (Zhu et al., 2003) and drought tolerance (Hazen et al., 2005). No whole genome expression data providing a comprehensive expression map for rice are available to date but work is in progress at the Virtual Center for Cellular Expression Profiling of Rice in which laser capture microdissection is being used for whole genome expression profiling of rice cell types. Several public array platforms are now available for rice. Coupled with the public availability of genome-scale rice arrays, expression databases dedicated to housing rice expression data have also been developed.

1.4.8.2 Microarray expression profiling of crop species

Microarray platforms for crop species have been developed as well. Because the research communities for some of these species are smaller, several projects have been organized as consortia to provide a microarray expression platform for these species, either from Affymetrix or as synthesized long oligonucleotide sets. Because most of these microarrays have become available only recently, little data are publicly available. However, studies using arrays with crop species has been reported for barley (Oztur et al., 2002; Close et al., 2004), grape (Waters et al., 2005), maize (Fernandes et al., 2002; Cho et al., 2002; Wang et al., 2003; Yu et al., 2003), pine (Watkinson et al., 2003), poplar (Moreau et al., 2005), potato (Ducreux et al., 2005; Restrepo et al., 2005; Rensink et al., 2005), tomato (Erixsson et al., 2004; Baxter et al., 2005), soybean (Thibaud-Nissen et al., 2003; Moy et al., 2004; Vodkin et al., 2004) and wheat (Clarke and Rahman, 2005).

Crop species-specific gene expression databases are publicly accessible. Several reference experiments using the barley 22K GeneChip (Close et al., 2004) are available through BarleyBase (Shen et al., 2005). In addition to the barley

expression data, BarleyBase is expanding to PLEXdb, which is pursuing collection of expression data for several plant species. In addition, a tool is available for linking probes between the different species and platforms within PLEXdb. Expression data for soybean generated using a spotted cDNA array are available through the Soybean Genomics and Microarray Database (SGMD) (Alkharouf and Matthews, 2004). Large quantities of expression data for the *Solanaceae*, including potato and tomato, are available through the *Solanaceae* Gene Expression Database, and tomato gene expression data are available through a tomato expression database (http://sgn.cornell.edu). Maize gene expression data are available through the Zeamage database (Gardiner et al., 2006). In the near future, it can be assumed that large amounts of expression data will be generated; for data integration and cross-species comparisons, special care should be given to the identification of homologous genes and probes representing these genes.

Using a strawberry cDNA microarray, Aharoni et al. (2000) identified an acyl transferase that contributes to flavor development in one of the first demonstrations of large-scale expression analysis in fruit.

1.5 Tomato

Solanum lycopersicum is the common tomato. It has a modest sized diploid genome with 12 chromosomes with a total of 950MB of sequence and tolerance to inbreeding, making it the genetic centerpiece of the *Solanaceae* family. Tomato originated in the New World in the Andean region.

Tomato has long served as a model system for plant genetics, development, pathology, and physiology, resulting in the accumulation of substantial information regarding the biology of this economically important organism. In recent years the most widely studied aspects of tomato biology include the development and ripening of their fleshy fruits and characterization of responses to infection by microbial pathogens. Although *Arabidopsis* has surpassed some plant systems as a model for basic plant biology research, the areas of fruit ripening and pathogen response continue to thrive using tomato as the system of choice. In the case of fruit development this is simply due to the fact that the developmental program which results in the dramatic expansion of ripening of carpels in tomato (and in many other economically and nutrionally important species) does not occur in *Arabidopsis*. With regard to plant defense, decades of applied and basic research on tomato have resulted in characterization of responses to numerous disease agents including bacteria, fungi, viruses, nematodes, and chewing insects. In many cases this research has led to the identification and genetic characterization of loci which confer general or pathogen-specific resistance. In addition, many experimental tools and features of tomato make it an excellent model system in its own right. These include: extensive germplasm collections, numerous natural, induced, and transgenic mutants and genetic variants, routine transformation technology, a dense RFLP map, numerous cDNA and genomic libraries, a small genome, relatively short life-cycle, and ease of growth and maintenace. The intense research effort in fruit biology and disease responses and the tools which make tomato an especially attractive model system have resulted in many important recent discoveries. Specific highlights which have a broad impact on the field of plant biology include control of gene expression by antisense/sense technology, functional characterization of numerous genes influencing fruit development and ripening,

transgenic analysis of genes which impact susceptibility of responses to pathogen attack, and isolation of more disease resistance (R) genes than in any other plant species.

Tomato genome sequencing has been taking place through an international, 10-year initiative entitled the "International *Solanaceae* Genome Project" (SOL). The strategy proposed by the SOL consortium is to sequence the approximately 220 Mb of euchromatin that contains the majority of genes, rather than the entire tomato genome. Divergent phenotypes and habitats of the *Solanaceae* also make the family an ideal model to explore the bases of diversification and adaptation (Shibata et al., 2005).

1.6 Strawberry

Strawberries include a small group of soft-fruited species that belong to the genus *Fragaria*, in the *Rosaceae* family. Phylogenetic relationship among these species is supposed to have its origin in the successive genome duplication of the original diploid ancestor (Bringhurst, 1990), rendering the variable ploidy level which is now found amongst them. This level ranges from diploidy, in *Fragaria vesca*, with two sets of seven cromosomes, to the colchicine-induced hybrid decaploid, *Fragaria x vescana* (Bauer, 1993). In the octoploid level, a number of interesting species is found. The relevance of the most important one, *Fragaria x ananassa,* resides on its extensive cultivation, carried out all over the world, being the most important strawberry in terms of acreage and production. This species was originated in Europe in the early 1700's, when plants of other two octoploid species were spontaneously hybridized (Hancock, 1999). These parental species were *Fragaria virginiana* from North America and *Fragaria chiloensis* from Chile. Despite, what nowadays is known as commercial strawberry is the result of many decades of breeding effort, and many important traits, as day neutrality (Bringhurst and Voth, 1984), have been introgressed from wild relatives to commercial cultivars. Nevertheless, strategic reconstruction of *Fragaria x ananassa*, through the utilization of elite clones of the parental species, is something that has been proposed as an efficient way to obtain high-quality,

heavy-yielding, stress-tolerant new cultivars for modern agriculture (Hancock et al., 1993).

Genetic research on strawberry has been mainly focused on fruit quality. Fruit firmness, flavor and aroma are key aspects that have attracted the interest of scientific community, in search of biotechnological approaches to understand the ripening process and exploit its manipulation. Lately, nutritional facts, primarily related to antioxidant compounds, have also become an important matter of study. However, fruit ripening is a complex process in which several metabolic pathways must be spatially and timely coordinated to allow the successful development of this plant organ, involving the interaction of a vast number of genes and delicate regulatory mechanisms.

1.7 Ripening

The ripening of fruit organs represents the terminal stage of development in which the matured seeds are released. In the dehiscent fruit of the *Arabidopsis* silique, this process is facilitated by senescence of the mature carpel tissue followed by separation of the valves at an abscission cell layer (termed the dehiscence zone) that is formed between the valve-replum boundary. The MADS box SHP1 and SHP2 genes were shown originally to regulate the formation of the dehiscence zone (Liljegren et al., 2000) under the negative regulation of the FRUITFUL (FUL) and REPLUMLESS gene products, which together limit SHP expression to the dehiscence zone (Ferrandiz et al., 2000; Roeder et al., 2003). The SEEDSTICK MADS box gene was demonstrated recently to be required for the formation of the funiculus/seed abscission zone that allows separation of the seed from the carpel to facilitate seed dispersal at dehiscence (Pinyopich et al., 2003). In contrast to *Arabidopsis*, fleshy fruits such as tomato undergo a ripening process in which the biochemistry, physiology, and structure of the organ are developmentally altered to influence appearance, texture, flavor, and aroma in ways designed to attract seed-dispersing organisms (Seymour et al., 1993). Although the specific biochemical programs resulting in ripening phenomena vary among species, changes typically include (1) modification of color through the alteration of chlorophyll, carotenoid, and/or flavonoid accumulation; (2) textural

modification via alteration of cell turgor and cell wall structure and/or metabolism; (3) modification of sugars, acids, and volatile profiles that affect nutritional quality, flavor, and aroma; and (4) generally enhanced susceptibility to opportunistic pathogens (likely associated with the loss of cell wall integrity). Although fruit species are classically defined physiologically on the basis of the presence (climacteric) or absence (nonclimacteric) of increased respiration and synthesis of the gaseous hormone ethylene at the onset of ripening (Lelievre et al., 1997), fruit displaying both ripening programs typically follow the general developmental changes described above. Examples of common climacteric fruits that require ethylene for ripening include tomato, apple, banana, and most stone fruits, whereas nonclimacteric fruits, including grape, citrus, and strawberry, are capable of ripening in the absence of increased ethylene synthesis. Interestingly, climacteric fruit span a wide range of angiosperm evolution, including both dicots (e.g., tomato) and monocots (e.g., banana). Nevertheless, members of the same (e.g., melon) or closely related (e.g., melon and watermelon) species are reported to include both climacteric and nonclimacteric varieties. The molecular distinctions underlying climacteric versus nonclimacteric ripening are poorly understood. Nevertheless, it seems likely that at least in instances of the same or closely related species with examples of both climacteric and nonclimacteric types, that nonclimacteric phenotypes may represent mutations in ethylene synthesis or signaling as opposed to more complex distinctions. Indeed, nonclimacteric melons are notoriously difficult to harvest compared with their climacteric counterparts because of reduced abscission, suggesting a defect in ethylene synthesis or response and a mature phenotype consistent with incomplete ripening (Perin et al., 2002). In this regard, it is especially important when selecting a system for the analysis of nonclimacteric ripening to be certain that the ripening physiology of the candidate species is well characterized and consistent with nonclimacteric ripening as opposed to inhibited ripening resulting from reduced ethylene synthesis or response. Although the specific role of climacteric respiration in fruit ripening remains unclear, the recruitment of ethylene as a coordinator of ripening in climacteric species likely serves to facilitate rapid and coordinated ripening. A great deal is known regarding specific downstream

ripening processes in a number of climacteric and nonclimacteric species, yet little is known about the regulation of ripening in nonclimacteric fruit or the upstream regulation of ethylene in their climacteric counterparts. Recent evidence of the MADS box regulation of ripening in both tomato and strawberry suggests common regulatory mechanisms operating early in both climacteric and nonclimacteric species (Vrebalov et al., 2002). The elucidation of the molecular basis of such early and common events represents an active frontier in fruit ripening research.

1.7.1 Tomato: primary model for climacteric fruit ripening

Tomato has emerged as the primary model for climacteric fruit ripening for a combination of scientific and agricultural reasons. The importance of tomato as an agricultural commodity has resulted in decades of public and private breeding efforts that have yielded numerous spontaneous and induced mutations, including many that affect fruit development and ripening (tomato germplasm can be viewed and ordered at the following World Wide Web sites: Tomato Genetic Resource Center [http://tgrc.ucdavis.edu/] and Hebrew University [http://zamir.sgn.cornell.edu/mutants/]). Simple diploid genetics, small genome size (0.9 pg per haploid genome [Arumuganathan and Earle, 1991]), short generation time, routine transformation technology, and availability of genetic and genomic resources, including mapping populations, mapped DNA markers (Tanksley et al., 1992), extensive EST collections (Van der Hoeven et al., 2002), publicly available microarrays, and a developing physical map, render tomato among the most effective model crop systems (http://www.sgn.cornell.edu). In addition, numerous single gene mutations that regulate fruit size, shape, development, and ripening combined with dramatic and readily quantifiable ripening phenotypes (ethylene, color index, carotenoids, softening) have enhanced the use of tomato as a model for climacteric ripening.

Differential screens, candidate gene analysis, gene expression profiling, and digital gene expression analysis have led to the identification of hundreds of genes whose expression profiles change during the course of fruit development and ripening (Alba et al., 2005; Fei et al., 2004; Picton et al., 1993a, b; Slater et al.,

1985; Zegzouti et al., 1999). Through a combination of approaches many of the downstream components that mediate the biochemical changes associated with ripening have been defined. For example, cell wall hydrolases, the enzymes involved in carotenoid synthesis and sugar metabolism, and some of the enzymes involved in the generation of flavor and aroma compounds have been characterized (Chen et al., 2004a, b; Fridman et al., 2004; Hirschberg 2001; Rose and Bennett 1999; Tieman et al., 2006). The pathways that determine the competency of a fruit to ripen or the signals that initiate the ripening program are less well defined, although the molecular identification of mutants that are impaired in fruit ripening are beginning to yield valuable insight into some of these genetic pathways, and multiple hormones, including jasmonates, auxin, and brassinosteroids, have all been implicated in the promotion of ripening in various species (Fan et al., 1998; Given et al., 1988; Manning et al., 2006; Vardhini and Rao 2002; Vrebalov et al., 2002). Signaling through the plant hormone ethylene, however, remains the most well-defined pathway that mediates the phenotypic changes that occur during ripening. Treatment of various fruits with inhibitors that block ethylene synthesis or action or the manipulation of these processes by transgenic or mutant approaches have revealed the essential role of this hormone in regulating fruit ripening (Hobson et al., 1984; Klee et al., 1991; Lanahan et al., 1994; Oeller et al., 1991; Picton et al., 1993a, b; Yang and Hoffman 1984).

Ripening-related cell wall metabolism and associated textural changes have been a major focus of ripening research since the isolation of the tomato fruit POLYGALACTURONASE (PG) gene. PG has been reported to represent ~1% of ripening fruit mRNA and results in substantial cell wall pectinase activity, in concert with the induction of ripening and softening (DellaPenna et al., 1989). PG expression is inhibited substantially by both the rin and nor mutations, with additional influence by ethylene (DellaPenna et al., 1989). Both antisense repression (Smith et al., 1988) and ectopic expression in unripe fruit (Giovannoni et al., 1989) indicated that PG alone is not sufficient for softening. Nevertheless, a reduction in ripe fruit susceptibility to postharvest pathogenesis in antisense PG fruit led to the commercialization of PG antisense tomatoes. The collapse of the hypothesis that PG represented the primary determinant of tomato fruit softening

caused attention to turn to the isolation and functional analysis of alternative cell wall–associated and/or metabolizing proteins (Brummell and Harpster, 2001; Orfila et al., 2001). Removal of pectin methylester groups from fruit cell walls before ripening by pectin methylesterase (PME) facilitates access of PG to its substrate. PME is expressed before ripening and is downregulated by ethylene as ripening begins. Although repression of tomato fruit PME via antisense resulted in increased juice viscosity attributable to the retention of preripening pectin chain length, softening was not altered measurably (Tieman et al., 1992). In addition to pectin-modifying enzymes, several hemicellulose-metabolizing enzymes have been characterized in ripening fruit. Repression of the ripening-related endo-ß-1,4-glucanases (also known as EGases or cellulases) CEL1 and CEL2 altered pedicel and fruit abscission, respectively, but did not influence fruit softening (Lashbrook et al., 1998; Brummell et al., 1999a). However, a ripening-related and ethylene-inducible tomato ß-galactosidase gene, TBG4, did have a modest impact on fruit softening when repressed via antisense (Smith et al., 2002), as did repression of the ripening expansin LeExp1 (Rose et al., 1997; Brummell et al., 1999b). The complexity of cell wall ultrastructure is matched by an equally complex repertoire of cell wall–metabolizing and structural activities, many of which are encoded by multigene families that likely contribute to the difficulty of determining the molecular basis of fruit cell wall metabolism. Although considerable progress has been made in determining the biochemical contribution of specific cell wall proteins during fruit ripening, the molecular basis of fruit softening is still poorly understood and remains an active area of investigation.

1.7.2 Strawberry: studied system for nonclimacteric ripening

Strawberry is the most widely studied system for nonclimacteric ripening, resulting in the identification and characterization of numerous ripening-related genes that affect cell wall metabolism, color, and aroma (Wilkinson et al., 1995b; Manning, 1998; Aharoni and O'Connell, 2002). The octaploid nature of cultivated strawberry has limited genetic analysis in this species, although strawberry is readily transformed (Woolley et al., 2001) and diploid varieties are available.

The biochemical events that occur during the ripening of strawberry result in important changes affecting fruit quality. These include the accumulation of red anthocyanin pigments, the loss of cell wall structure causing softening, an increase in the content of sucrose and hexoses, and the production of volatile flavour compounds. The biochemical characterization of these changes has been difficult because of the presence of high levels of phenolic compounds and viscous polysaccharides that interfere with enzyme isolation. To overcome these problems, molecular approaches have been used, firstly, to examine the extent of gene expression occurring during strawberry fruit development and, secondly, to identify the specific genes involved in ripening. Some of the qualitative changes in gene expression that occur in developing strawberry fruit and their hormonal control have been described in a preliminary study (Manning 1994).

Changes in the abundance of more than 50 mRNAs were observed between the immature and overripe stages, most of these occurring at or just before the appearance of anthocyanin pigmentation, used as a marker of ripening (Manning, 1998). As the fruit matured the expression of one group of genes increased, whereas another group showed a marked decrease before the onset of ripening. However, the expression of another groups of genes was prominent in immature green and ripe fruit but much reduced or undetectable just before the turning stage (Manning, 1998). Previous studies demonstrated that strawberry fruit ripening is independent of ethylene and therefore can be categorized as non-climacteric (Given et al. 1988). Auxin, produced by the achenes, is known to be essential for fruit growth but also acts as a repressor of ripening in this fruit. Evidence from in-vitro translation data indicates that expression of the ripening-enhanced genes in strawberry is co-ordinated by the hormone auxin (Manning 1994). The in-vitro translation data predict that in strawberry the highest number of genes related to ripening will be obtained by comparing fruit at the white and red stages. Wilkinson et al. (1995) used polymerase chain reaction (PCR) differential display to compare differences in gene expression between white and red strawberry fruit. Five mRNAs were identified as being ripening-enhanced, with three having homology to known proteins, including chalcone synthase. In another study, a cDNA subtractive library was used to compare genes expressed in red and green

fruit (Medina-Escobar et al.1997). During ripening, water solubility of pectins increases (Huber, 1984) but their depolymerization is limited (Nogata et al., 1996). This limited depolymerization correlates with the low PG activity detected in Toyonaka strawberries (Nogata et al., 1996). Moreover, a fruit specific PG gene was described (Redondo-Nevado et al., 2001), but the authors suggested that the predicted protein might be involved in the production of oligosaccharins rather than in pectin degradation. Based on these results, it has been suggested that the increase in pectin solubility could be due to the cleavage of pectin side chains (Nogata et al., 1996). Supporting this conclusion, a decrease of the content of galactose and arabinose, which are usually located in side chains, has been detected during strawberry ripening (Redgwell et al., 1997) and a β-galactosidase-like gene with enhanced expression in ripe strawberries has been reported (Trainotti et al., 2001). Metabolism of pectins could also be mediated by the action of pectate lyases (PL). Medina-Escobar et al. (1997) characterized a PL gene, whose expression was fruit specific and enhanced during ripening. Moreover, Jiménez-Bermúdez et al. (2002) reported a lower softening and pectin solubilization in strawberries with antisense expression of the mentioned gene.

Xyloglucan, the principal component of hemicelluloses in dicotyledons, is also considered to play an important role in cell wall structure, since it forms cross-linkages among the cellulose polymers. Endoglucanases, xyloglucan endotransglycosidases and expansins contribute to the depolymerization of xyloglucans during ripening (Brummel and Harpster, 2001). To account for this, an increased cellulase activity and endoβ-1,4-glucanases expression (Harpster et al., 1998; Llop-Tous et al., 1999) were detected during ripening. It was suggested that expansins debilitate interactions among cellulose and hemicelluloses, relaxing the network formed by these polymers (Brummel and Harpster, 2001). In strawberry, fruit specific expansins with enhanced expression during ripening have been described and characterized (Civello et al., 1999; Harrison et al., 2001). Besides, Salentijn et al. (2003) showed a relationship between different regulation of cynnamoil-CoA reductase (CCR) and cinnamyl alcohol dehydrogenase (CAD) genes and fruit firmness. Besides their role in lignin composition, the role of CCR and CAD reaction products on strength and/or disruption of cell wall polymers

should be taken into account. CCR and CAD enzyme activities and lignin deposition in strawberry fruits have been associated to vessels connecting achenes (Blanco-Portales et al. 2002).

Futhermore, during the ripening it have been observed a increase in the production of volatile flavour compounds. More than 300 compounds have been identified that can contribute to the complex process of aroma biosynthesis in strawberry (Maarse, 1991). The major components of strawberry flavor and aroma can be grouped into several chemical classes, including acids, aldehydes, ketones, alcohols, esters, and lactones. Other contributing groups are sulfur compounds, acetals, furans, phenols, epoxides, and hydrocarbons (Zabetakis and Holden, 1997). Esters are one of the most important classes of volatile compounds in fruit flavor; in strawberry alone, more than a hundred different esters have been detected (Honkanen and Hirvi, 1990). Esterification is the result of transacylation from acyl-CoA to an alcohol. The enzyme catalyzing the reaction is termed an alcohol acyltransferase (AAT), a key enzyme in aroma biochemistry. Aharoni et al. (2000) described the use of DNA microarrays and appropriate statistical analyses to dissect a complex developmental process. In doing so, they have identified a strawberry alcohol acyltransferase (SAAT) gene. The influence of esters (isoamyl and ethyl acetate) on beer flavor has made AAT one of the most important enzymes in the fermentation process performed by microorganisms. As such, it has been the subject of investigations with both yeast and fungi (Yamakawa et al., 1978; Yoshioka and Hashimoto, 1984; Yamauchi et al., 1989; Malcorps and Dufour, 1992; Fujii et al., 1994, 1996). In melon, banana, and strawberry, AAT proteins have been investigated in crude fruit extracts (Harada et al., 1985; Ueda et al., 1992; Perez et al., 1993, 1996; Olias et al., 1995). Ueda et al. (1992) concluded that the alcohol moieties of the esters produced by crude strawberry fruit extracts reflected the alcohols predominantly synthesized in the fruit and that the acid moieties reflected the acyl-CoA specificity of the AAT enzyme. Olias et al. (1995) compared strawberry and banana proteins possessing AAT activity and found clear differences between the alcohol and acyl-CoA specificity of the two enzymes. The strawberry AAT enzyme had high activity with hexanol and with acetyl- or butyl-CoAs. The banana enzyme, on the other

hand, had high activity with butanol and acetyl-CoA but showed less activity with butyl-CoA. A clear correlation could be observed between the substrate preference of the enzymes and the volatile esters present in both fruits. In this study, we report the cloning and characterization of a fruit gene encoding an AAT capable of catalyzing the formation of volatile esters in strawberry fruit (Beekwilder et al., 2004).

1.8 Pigments in fruit crops

Fruit attractiveness and nutritional value are important traits in nature and for humans, contributing to seed dispersal and thus increasing plant fitness. Polyphenols and carotenoids play a crucial role in this strategy, since they visually attract first flower pollinators, protect plant from biotic (pathogen attacks) and abiotic (UV radiations) stress, and provide nutritional benefits (sugars, nutraceuticals). They are major groups of phytochemicals that may contribute to the total antioxidant capacity (TAC) of plant foods with the traditional antioxidant vitamins such as vitamin C and vitamin E.

1.8.1 Tomato as important carotenoids source

In tomato fruit, the chloroplasts differentiate into carotenoid-containing chromoplasts, with lycopene being the principal carotenoid responsible for the red colour of ripe tomatoes (Harris and Spurr 1969).

Carotenoids are terpenoids synthesized in plastids as hydrocarbons (carotenes) and their oxygenated derivatives (xanthophylls) (Bramley, 1997), and serve essential roles in plants, as components of the photosynthetic apparatus and protectors against oxidation derived from excess light energy (Demmig-Adams and Adams, 1996). During plant development, carotenoids play role as dispensable colorants in flowers and fruits. They also provide the yellow, orange or red colouration characteristic of many flowers and fruits. Their importance is also recognized as nutritional components, vitamin A precursors, in the prevention of human diseases such as cancer, and from an industrial perspective (Bramley et al., 1993; Mayne, 1996; Olsen, 1989; Hirschberg, 1999; Sandmann, 2001).

The biochemistry of carotenoid biosynthesis has been well established. Genes and

cDNAs encoding some of the carotenogenic enzymes have been isolated and characterized in bacteria, algae, fungi and, more recently, in higher plants (Cunningham and Gantt, 1998; Hirschberg, 2001; Sandmann, 2001).

The first committed step in the carotenoid pathway is the synthesis of phytoene, catalysed by the enzyme phytoene synthase (PSY). Subsequently, the colourless phytoene undergoes four consecutive symmetrical desaturation steps. In plants and cyanobacteria these four desaturations are catalysed by two related enzymes, postulated to act coordinately (Cunningham and Gantt, 1998), phytoene desaturase (PDS) and ζ-carotene desaturase (ZDS), yielding the red carotene lycopene through the intermediate ζ-carotene (pale-yellow). These desaturase reactions require plastoquinone (Norris et al., 1995) and a plastid terminal oxidase as electron aceptors (Carol and Kuntz, 2001). In the next step of the pathway, cyclation of lycopene yields β-carotene and/or α-carotene, and subsequent substitutions by hydroxy, oxo, and/or epoxy groups produce xanthophylls with bright orange/yellow colours. Carotenoid biosynthesis in plants is connected with that of the plant growth regulator abscisic acid (ABA), which is produced through C15 intermediates after oxidative cleavage of specific xanthophylls (Marin et al., 1996; Schwartz et al., 1997; Milborrow, 2001). Indeed, many ABA deficient mutants identified are related to carotenoid synthesis (Taylor et al., 2000). Carotenoid complements of fruits and flowers vary considerably among species (Bramley, 1997), thus conferring colour singularities (fig. 3).

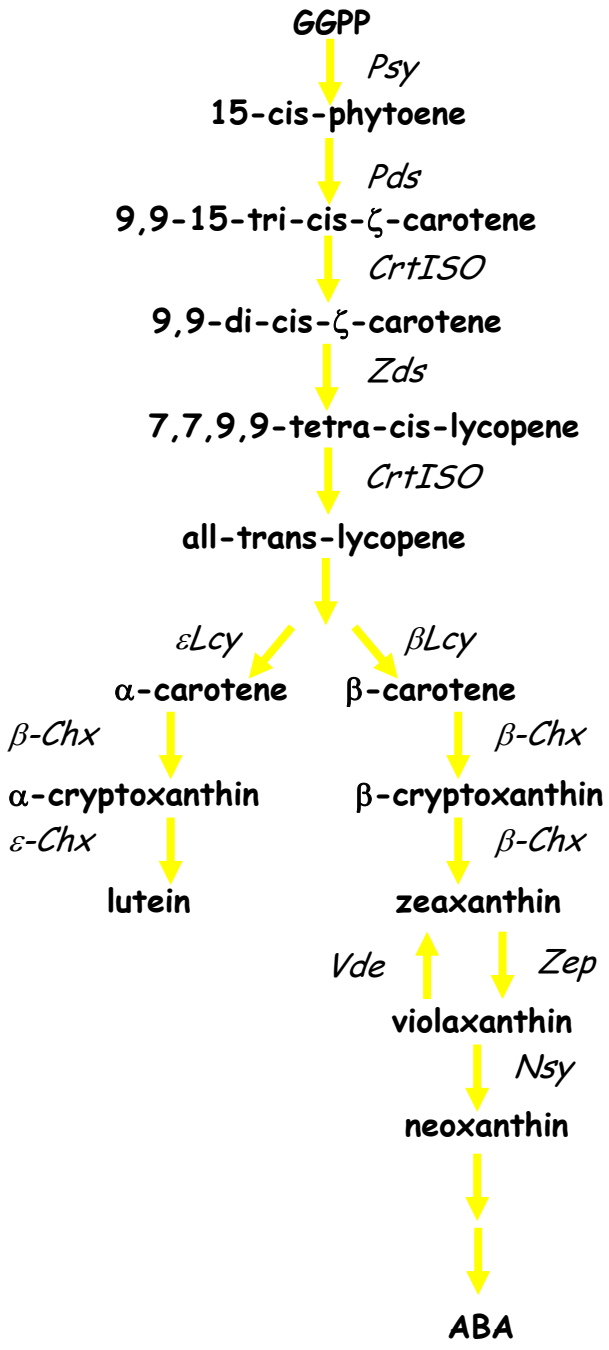

Figure 3: Carotenoid biosynthesis pathway in Tomato.

Genes encoding enzymes that catalyze carotenoid synthesis have been cloned from tomato and correspond to a number of previously defined pigmentation mutants (Bramley, 2002; Isaacson et al., 2002). Examples include the yellow-flesh (r) mutation, resulting in deletion of the ethylene-regulated phytoene synthase (PSY) gene (Fray and Grierson, 1993), loss of or reduced expression of the

carotenoid isomerase gene, resulting in the prolycopene-accumulating orange fruit of the tangerine mutants (Isaacson et al., 2002), and overexpression and knockout mutations of the lycopene-ß-cyclase gene, resulting in high-ß-carotene Beta (B) and deep-red crimson fruit, respectively (Ronen et al., 1999, 2000). It is known that PSY is strongly induced by ethylene during ripening, indicating a major control point for total fruit carotenoid accumulation (Lois et al., 2000). In addition, analysis of quantitative trait loci associated with tomato fruit carotenoid metabolism indicates that multiple loci, in addition to known structural components, contribute to carotenoid flux (Liu et al., 2003).

1.8.2 Flavonoids: the most important pigments in strawberry fruits

Flavonoids represent a large family of low molecular weight polyphenolic secondary metabolites that are widespread throughout the plant kingdom, ranging from mosses to angiosperms (Koes and Quattrocchio, 1994). In nature they are involved in a wide range of functions, for example (1) in providing pigmentation for flowers, fruits and seeds to attract pollinators and seed disperser, (2) in protection against ultraviolet light, (3) in plant defence against pathogenic micro organisms, (4) in plant fertility and germination of pollen, and (5) in acting as signal molecules in plant-microbe interactions (Koes and Quattrocchio, 1994; Dixon and Paiva, 1995; Dooner et., 1991). By definition, they all share the same basic skeleton, the flavan-nucleus, consisting of two aromatic rings with six carbon atoms (ring A and B) interconnected by a hetero cycle including three carbon atoms (ring C). According to the modifications of the central C-ring they can be divided in different structural classes like flavanones, isoflavones, flavones, flavonols, flavanols and anthocyanins. The huge diversity in flavonoid structures is due to modifications of the basic skeleton by enzymes such as glycosyl transferases, methyl transferases and acyl transferases. In a single plant species dozens of different flavonoids may be present and most of these are conjugated to various sugar moieties (Forkmann and Heller, 1999). Since flavonoids impart much of the colour and flavour of fruits, vegetables, nuts and seeds, they form an integral part of the human diet (Parr and Bowell, 2000). Rich dietary sources of flavonoids are for example soybean (isoflavones), citrus

(flavanones), tea, apple and cocoa (flavanols), celery (flavones), onions (flavonols) and berries (anthocyanins) (Rice-Evans et al., 1995; Ross and Kasum, 2002; Le Gall et al., 2003). Two classes of genes can be distinguished within the flavonoid pathway: (I) the structural genes encoding enzymes that directly participate in the formation of flavonoids, and (II) regulatory genes that control the expression of the structural genes. The precursors of the synthesis of most flavonoids are malonyl-CoA and p-coumaroyl-CoA, which are derived from carbohydrate metabolism and phenylpropanoid pathway, respectively (Forkmann and Heller, 1999). The biosynthesis of flavonoids is initiated by the enzymatic step catalysed by chalcone synthase (CHS), resulting in the yellow coloured chalcone. In the majority of plants chalcones are not the end-products, but the pathway proceeds with several enzymatic steps to other classes of flavonoids, such as flavanones, dihydroflavonols and finally to the anthocyanins, the major water-soluble pigments in flowers and fruits. Other flavonoid classes (i.e. isoflavones, aurones, flavones, pro-anthocyanidins (PA) and flavonols) represent side branches of the flavonoid pathway and are derived from intermediates in anthocyanin formation (Schijlen et al., 2004) (fig. 4).

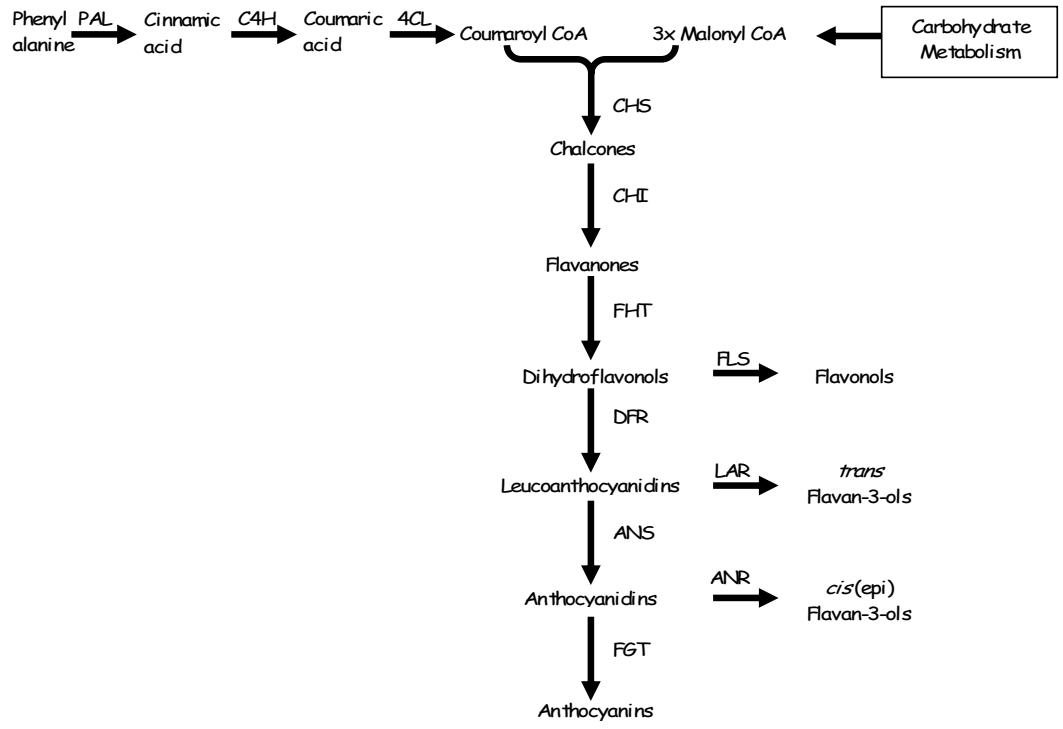

Figure 4: Flavonoid biosynthesis pathway in Strawberry.

Knowledge on genes involved in flavonoid biosynthesis is still scarce though as already mentioned, in the last few years the research effort on this subject increased a lot after it has begun clear that strawberry fruits have a high nutritional and antioxidant content. The L-Phe ammonia-lyase (pal), ubiquitous in higher plants, is the first enzyme of the phenylpropanoids pathway. It is upstream of several reactions which determine many fruit quality traits (antioxidants, colour, flavour, etc) (Hrazdina and Wagner, 1985). PAL gene has been characterized in strawberry by Given et al. (1988). In strawberry fruit the activity of pal enzyme shows two peaks, the first in the immature green stage and second a little before the full ripe stage, but it is not yet clear whether this can be the result of different gene expression of distinct PAL coding sequences. The first activity peak could, in principle, be connected to the biosynthesis of some flavonoids, like condensed tannins, and phenols which are abundant in the first stages of fruit development, while the second peak, near to the full ripe stage is certainly correlated to the anthocyanins accumulation (Cheng and Breen, 1985). Interestingly, the same pattern of pal activity has been reported for DFR and FGT genes at the RNA level (Perkin-Veazie, 1991; Moyano et al., 1998). Chs belongs to the polyketide synthase (pks) enzymes which are dimeric proteins that act directly on coenzyme A (CoA) thioesters of various carboxylic acids to extend the carbon backbone (Schröder, 1997). CHS gene was the first structural gene of the flavonoids biosynthesis pathway to be characterized. CHS has been an attractive target for genetic engineering and there are numerous examples of co-suppression or down regulation of this gene in order to modify flower colour towards pure white as a result of a complete absence of flavonoids. However, blocking the flavonoid pathway may also lead to pleiotropic effects such as male sterility (Napoli et al., 1999; Van der Meer et al., 1992; Ylstra et al., 1994; Jorgensen et al., 1996; Deroles et al., 1998).

From literature data emerge a great variability in the composition and concentration of flavonoids in strawberries. This is mainly the effect of different genetic backgrounds which determine the biosynthesis of specific enzymes and regulation factors. Besides, developmental stages and environmental factors may play a very important role for the differential accumulation of these metabolites.

The expression of genes involved in flavonoids biosynthesis is boosted a consequence to an increased exposition to light (Jaakola et al., 2004). Thus the establishing of these regulation mechanisms may be the result of the coordinated action of many regulation factors, mostly unknown, that finely modulate the abundance of specific metabolites on the basis of the plant physiological requirements. In strawberry has been cloned a gene (Fa-MYB1) probably involved in such modulation mechanisms. Fa-MYB1 codes for a 187 amino acids polypeptide belonging to the big family of myb transcription factors (Jin and Martin, 1999). These evidences suggest that Fa-myb1 in vivo may negatively influence the transcription of some genes involved in flavonoids biosynthesis in order to balance the pigment accumulation in late ripening stages and/or to modulate the accumulation of different flavonoid end-products (Aharoni et al., 2001).

1.9 Photoperception

Because photosynthetic organisms are dependent on photosynthetically active radiation as their source of energy, plant growth and development are intimately tied to changes in the light environment. Three classes of photoreceptors mediate light-induced development in response to light quantity, quality, directionality, and photoperiodicity: phytochromes, cryptochromes and phototropin (fig. 5).

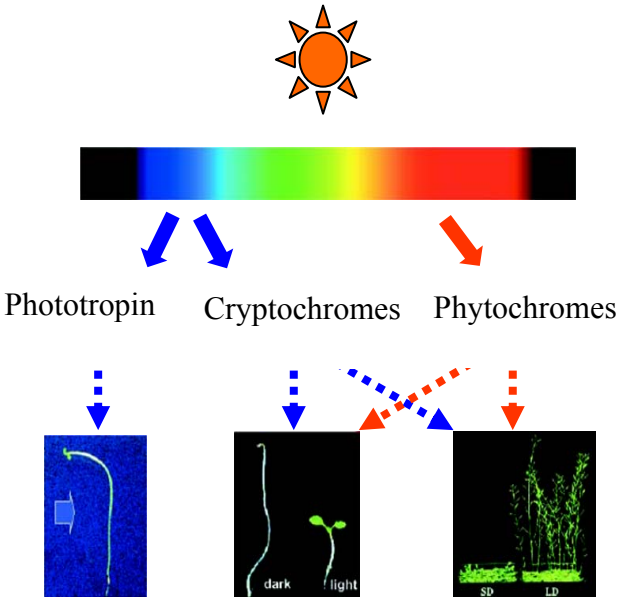

Figure 5: The plant photoreceptors.

Three classes of photoreceptors have been characterized from plants at the molecular level. (A) Phytochromes perceive red and far-red light of between 600 and 750 nm. (B) Cryptochromes perceive blue and UVA light (320-500 nm); (C) Phototropins also perceive blue and UVA light (320-500 nm).

Phytochromes (PHYA, PHYB, PHYC, PHYD and PHYE in *Arabidopsis*), the most thoroughly characterized class of plant photoreceptors, are chromoproteins that detect both red and far-red light. Individual plants contain several types of phytochromes, each of which is encoded by a distinct gene (Sharrock and Quail, 1989; Hauser et al., 1995). These red and far-red light receptors mediate numerous developmental processes throughout the plant's life cycle, including seed germination, de-etiolation, chloroplast development, stem elongation, flavonoid biosynthesis, and photoperiodic flowering (Kendrick and Kronenberg, 1994). In tomato five phytochrome genes have been discovered and analyzed so far: PHYA, PHYB1, PHYB2, PHYE and PHYF (Hauser et al., 1995).

Phylogenetic analyses showed ortology between PHYA, PHYE and PHYC/F gene pairs in *Arabidopsis* and tomato; tomato PHYB1 and PHYB2 were originated by an independent duplication (Pratt et al., 1995). Although attempts to define the role(s) of fruit-localized phytochrome in tomato ripening have been limited, existing evidence is consistent with the hypothesis that phytochromes play some regulatory role in this developmental process. An early study indicated that fruit-localized phytochromes regulate the accumulation of a "flavonoid-like" pigment in pericarp tissues (Piringer and Heinze, 1954). Subsequently it was reported that fruit-localized phytochromes mediate light-induced carotenoid biosynthesis in tomato (Khudairi and Arboleda, 1971; Thomas and Jen, 1975). A fourth investigation led to the conclusion that phytochrome-regulated carotenoid biosynthesis is correlated with red-light-induced ethylene production in tomato fruits, implying that fruit-localized phytochromes play a global regulatory role during the ripening of tomato fruit (Jen and Watada, 1977). Unfortunately, Jen and Watada (1977) used excessive irradiation treatments (14 h of high-fluence-rate red light) and neglected to address the far-red reversibility of red-light-induced ethylene production. Their conclusion that phytochromes regulate ethylene production in tomato fruits is thus only weakly supported at best. These studies, as well as others that indicate lycopene consumption decreases the incidence of prostate cancer in men (Giovannucci et al., 1995), raise a number of important questions about the exact role(s) of fruit-localized phytochrome in tomato ripening. Light has been shown to affect carotenoid accumulation in a number of species, including tomato. Alba et al. (2000) showed that phytochrome-mediated light signal transduction was required for normal ripe fruit pigmentation but did not affect other ripening attributes. Tomato high-pigment (hp1 and hp2) mutants, characterized by increased green fruit and leaf chlorophyll in addition to increased total ripe fruit carotenoids, have been shown to be hypersensitive to light (Peters et al., 1989). Ectopic expression of an oat phytochrome in tomato resulted in phenotypes similar to those exhibited by hp1 and hp2, further emphasizing the role of light in fruit carotenoid accumulation (Boylan and Quail, 1989). The hp2 locus has been cloned and shown to harbor the tomato homolog of the *Arabidopsis* DE-ETIOLATED1 (DET1) negative regulator of light signal

transduction, providing additional molecular evidence for the regulation of carotenoid synthesis via light signal transduction (Mustilli et al., 1999).

Cryptochromes (CRY1 and CRY2 in *Arabidopsis*) are flavoproteins that are found in various taxa and are thought to have evolved from photolyases. Unlike photolyases, however, CRY have no DNA-repair activity. The amino-terminal part of the CRY molecule binds two types of chromophore: pterin at one site and flavin adenine dinucleotide (FAD) at another. The carboxy-terminal parts of CRY1 and CRY2 contain a variable extension, which is not found in photolyases, and are essential for CRY function (Smith, 1982). The photochemical mechanism of signal capture and transfer by CRY is likely to involve a redox reaction. Most cryptochromes act as blue/UV-A light receptors. In *Arabidopsis*, cryptochromes mediate light control of stem elongation, leaf expansion, photoperiodic flowering, and the circadian clock. In tomato three cryptochrome genes have been discovered so far: two CRY1 (CRY1a and CRY1b) and one CRY2 gene (Perrotta et al., 2000; Perrotta et al., 2001). The role of one of the CRY1 genes, CRY1a, has been elucidated through the use of antisense (Ninu et al., 1999) and mutant (Weller et al., 2001) plants. CRY1a controls seedling photomorphogenesis, anthocyanin accumulation, and adult plant development. No effects of CRY1a on flowering time or fruit pigmentation have been observed. The overexpression of tomato CRY2 causes phenotypes similar to but distinct from their *Arabidopsis* counterparts (hypocotyls and internode shortening under both low and high fluence blue light), but also several novel ones, including a high-pigment phenotype, resulting in overproduction of anthocyanins and chlorophyll in leaves and of flavonoids and lycopene in fruits (Giliberto et al., 2005).

Phototropins (PHOT1 and PHOT2 in *Arabidopsis*) are also flavoproteins. They mediate photomovement rensponses including phototropism, chloroplast relocation, and stomal opening (Briggs and Christie, 2002; Lin, 2002). They carry two flavin mononucleotide (FMN) chromophores that are associated with the LOV (light, oxygen, voltage)/PAS (PER, ARNT, SIM) domain in the amino-terminal part of the molecule. PHOT1 and PHOT2 are blue-light-sensitive receptor kinases, whose carboxy-terminal parts contain a classical Ser/Thr kinase domain.

1.10 Rhythmic oscillations regulated by Circadian Clock

Plant have adapted their growth and development to use the diurnal cycling of light and dark. The day/night cycling of gene expression is called a diurnal rhythm and is achieved primarily by two mechanisms: first, by light, and second, by a free-running internal circadian clock. The circadian clock allows organisms to anticipate daily changes in the environment such as the onset of dawn and dusk, providing them with an adaptive advantage (Yan et al., 1998). Physiological processes regulated by the clock in higher plants include photoperiodic induction of flowering (Samach and Coupland, 2000) and rhythmic hypocotyls elongation, cotyledon movement, and stomatal opening (Kreps and Kay, 1997)

Our current understanding of the plant circadian clock derives mostly from genetic studies in *Arabidopsis* and rice (Hayama and Coupland, 2004). The circadian clock system is often divided into three general parts (Dunlap, 1999): an input pathway that entrains the clock, by transmitting light or temperature signals to the core oscillator; the central oscillator (the clock) that is the core of the system, responsible for driving 24-h rhythms; the output pathways that generates overt rhythms controlled by the core oscillator and represent a wide range of biochemical and developmental pathways. Therefore, the information flow should proceed along these three components in a unidirectional way: from the input systems the information arrives to the oscillator centre and then to the pathways which give rise to the physiological answers. This scheme is only a simplification of the extraordinary complexity of the relationships and regulations which happen in the various parts of the clock, as shown by recent studies (Valverde et al., 2004). Molecular analysis of the circadian-clock in animals and cyanobacteria reveal that the core oscillator is composed of an autoregulatory transcriptional and translational negative-feedback loop (Dunlap, 1999).

Genetic experiments with *Arabidopsis* mutants have established roles for PHYA, PHYB, PHYD, PHYE, CRY1 and CRY2 in the establishment of period length (Devlin and Kay, 2000; Millar et al., 1995; Somers et al., 1998). Many photoreceptor mutants are still able to be entrained to a light-dark cycle and retain rhythmicity, such as the cry1cry2 double mutant and the quadruple mutant

phyAphyBcry1cry2 (Devlin and Kay, 2000); making it clear that others photoreceptors (PHYC-PHYE, or others), can provide light input to the clock (Yanovsky et al., 2000). Indeed, a novel family of putative photoreceptors, ZEITLUPE (ZTL) and FLAVINBINDING KELCH REPEAT F-BOX (FKF) have recently been identified by a mutant phenotype of altered circadian rhythms (Jarillo et al., 2001; Nelson et al., 2000; Somers et al., 2000) and a third family member, LOV DOMAIN KELCH PROTEIN 2 (LKP2), has been recently identified, as well (Jarillo et al., 2001; Kiyosue and Wada, 2000). There is considerable interaction among photoreceptors. For instance, PHYA and CRY1 directly interact at the molecular level, with CRY1 serving as a phosphorylation substrate for PHYA in vitro (Ahmad et al., 1998). This suggests that CRY1 acts as a signal transduction component downstream from PHYA in the low intensity light input pathway to the clock (Devlin and Kay, 2001). Genetic studies have implicated two other genes, EARLY FLOWERING 3 (ELF3) and GIGANTEA (GI), in light signalling to the clock. elf3 loss of function alleles yield early flowering, hypocotyl elongation, and conditional arrhythmicity in continuous light (Covington et al., 2001; McWatters et al., 2000). ELF3 interacts with PHYB and seems to act as a negative modulator of PHYB signalling to the clock, as ELF3 overexpression both lengthens the circadian period and attenuates the resetting effects of red light pulses whereas loss of ELF3 function renders the plant hypersensitive to light signals (Covington et al., 2001; Liu et al., 2001; McWatters et al., 2000). In *Arabidopsis* GI positively regulates expression of the flowering time genes CONSTANS (CO) and FLOWERING LOCUS T (FT). GI encodes a nucleoplasmically localized protein that mediates a number of functions such as photoperiodic flowering, circadian rhythms and phytochrome/cryptochrome signaling (Martin-Tryon et al., 2007). The key roles played by GI are evident analyzing the effect of gi mutants over leaf movement and gene expression rhythms of multiple clock controlled and flowering genes, including GI itself (Fowler et al., 1999; Park et al., 1999).

The clock mechanism in the model plant, *Arabidopsis thaliana*, was first proposed to comprise a feedback loop in which two partially redundant genes, LATE ELONGATED HYPOCOTYL (LHY) and CIRCADIAN CLOCK ASSOCIATED

1 (CCA1), repress the expression of their activator, TIMING OF CAB EXPRESSION 1 (TOC1) (Alabadi et al, 2001). This circuit cannot fit all experimental data (Locke et al, 2005a), as a short-period rhythm persists for several cycles both in lhy;cca1 (Alabadi et al, 2002; Locke et al, 2005b) and in toc1 mutant plants (Mas et al, 2003). Previously a new circuit have been proposed comprising two interlocking feedback loops in order to explain the residual rhythm in the lhy;cca1 plant (Locke et al, 2005b)). This model predicted the existence and expression patterns of two hypothetical components X and Y. X is proposed to be activated by TOC1, and X protein then activates LHY transcription, as required by the expression profile of TOC1 protein (Mas et al, 2003). Y forms a second loop with TOC1, which is responsible for the short-period oscillation in the lhy;cca1 mutant. Based on the similarity of predicted and observed expression patterns, GI was identified as a candidate for Y (Locke et al, 2005b). Subsequently, this model have been extended to include the recently proposed feedback loop between PSEUDO-RESPONSE REGULATOR 7 (PRR7), PRR9 and LHY/CCA1 (Farre et al, 2005; Salome and McClung, 2005), resulting in a three-loop circuit. GI functions as a component of Y in a feedback loop with TOC1, and investigate the regulatory properties of the three-loop network (Locke et al., 2006).

Although there exists considerable knowledge about the core oscillator mechanisms, and some of the physiological and behavioral processes that are under circadian control, little is known about the connection between the oscillator and down-stream biological processes that are under clock control. Studies using DNA microarray technology have addressed these questions in a global fashion and identified rhythmically expressed in the higher plant *Arabidopsis* (Harmer et al., 2000; Shaffer et al., 2001). A large cluster of genes implicated in the light-harvesting reactions of photosynthesis were found to be under clock control. Light also regulates growth and development and resets the circadian clock. Genes encoding phytochrome B, cryptochrome 1, cryptochrome 2, and phototropin were clock-regulated (Harmer et al., 2000). The circadian clock may also orchestrate the production of photoprotective pigments early in the day.

Remarkably, phenylpropanoids biosynthesis genes peak before subjective dawn (Harmer et al., 2000).

A comparative analysis of the expression patterns utilizing the luciferase reporter system indicated that the promoter activities of all *Arabidopsis* photoreceptor genes followed a diurnal rhythm and exhibited maximum expression in the light phase (Tòth et al., 2001). Furthermore, these oscillations persisted under constant light or dark conditions with a period close to 24 h, proving that a circadian clock regulates the expression of these promoters. Measurements of mRNA transcribed from these genes in seedlings transferred to constant light indicated that the rhythmic expression was maintained at the level of mRNA accumulation. These findings were consistent with data on CRY1, CRY2, and PHYA, PHYB mRNA levels derived from microarray experiments (Harmer et al., 2000; Schaffer et al., 2001).

1.11 Aim of the PhD project

In order to investigate genes related to quality and quantity traits in crop plants, it is important to develop appropriate large scale molecular tools. In this context, we have investigated a number of developmental and physiological responses in strawberry (*Fragaria x ananassa*) and tomato (*Solanum lycopersicum*) species using extensive gene expression analyses by real time quantitative PCR (RT-qPCR) and microarray approaches.

These fruit crops provide a source of macronutrients and high levels of antioxidant which are finely regulated by biochemical processes that occur during ripening and which are related to genetic and environmental cues like temperature and light. The understanding of the molecular events related to plant metabolism could help to identify those genes that are associated to nutritional and qualitative characteristics and to the development of quality and quantity traits in plant.

Therefore the most important goal of this work was to gain information on the molecular mechanisms involved in fruit development in tomato and strawberry by the identification of a minimal set of fruit specific gene functions and by investigating the role of genes involved in light perception and responses. Moreover, studies were undertaken to elucidate gene/product relationships which influence key fruit quality traits in both species. Besides, here we report the characterization temporal transcripts oscillation of tomato genome, in order to identify genes involved in diurnal and circadian rhythms.

2. METHODS

Standard molecular biology protocols were followed as described in Sambrook et al., (Sambrook et al., 1989).

2.1 Plant material

For the comparative profiling of tomato fruits and leaves, tomato plants (*Solanum lycopersicum*, cv. Moneymaker) were grown under controlled greenhouse conditions with 16h photoperiod at 25 °C (day) and 20 °C (night). Green leaves (size approx 4 cm) and fruits at three different developmental stages (immature green, breaker and red ripe (ten days after breaker)) were collected between 4 and 6 hours after the onset of the light period. The locular tissue and seeds were discarded, and the pericarp was cut into small pieces.

To evaluating strawberry fruit quality traits and selecting improved genotypes by cDNA microarrays different strawberry genotypes (*Fragaria x ananassa*) were used: cultivar (cv.) Queen Elisa (QE) and its parentals, selection (sel.) USB35 (Lateglow x Seneca) and cv. Miss [(Comet x Honeoye) x Dana], cv. Maya (Design patent UE n° 7818) and cv. Onda [(78.65.1 x Honeoye) x Marmolada]. Strawberry red ripe fruits were harvested from field-grown plants at Institute for Fruit Breeding (ISF), Cesena, Italy.

For characterization of flavonoid biosynthesis pathway were used strawberry plants of cv. Queen Elisa (Miss × USB35) grown at Institute for Fruit Breeding experimental fields in Cesena, Italy. Fruit samples were collected at early green (G1, 7–10 days after anthesis, daa), intermediate green (G2, 12–14 daa), white (ca. 20 days after anthesis, daa), turning (ca. 25 daa) and ripe (ca. 30 daa) stages for RNA and metabolite extraction. Leaf, petal and root samples were also collected for RNA extraction.

To compare gene expression of strawberry genotypes with different phenolic compounds content and grown in different locations, first sampling of red ripe fruit of 34 different varieties of strawberry has been carried out. Of these, twenty genotypes were harvested from field-grown plants at Institute for Fruit Breeding (ISF), Cesena, Italy (Queen Elisa, Alba, Dora, Onda, Irma, Idea, 99.12.3,

99.159.8, 96.46.2, 97.306.9, 97.129.11, 98.86. 6, 99.194.13, 95.453.11, 96.57.1, 97.70.3, 97.167.9, 93.175.2, 92.340.3, 99.26.5), seven at Pantanello farm, Metaponto, Italy (96.j24.2 , TudlaNew, 99.163.19, 99.97.17, 99.121.9, Demeter, Rubea) and seven in both locations (99.163.14, Ventana, Candonga, 99.163.22, 99.20.1, Camarosa, 95.i59.2) . Then, were sampled fruits at five different ripening stages of genotypes with a high anthocyanin and flavan-3-ol content (cv. Camarosa and Candonga), with a high flavan-3-ol and proanthocyanidin content and medium anthocyanin content (sel. 99.163.14), and with a low anthocyanin and flavan-3-ol content (sel. 99.20.01 and cv. Onda).

Regarding transcriptional characterization of transgenic lines with high expression of CRY2 gene, plant material, as described in Giliberto et al. (2005), was provided by the laboratories of plant genomics of ENEA Casaccia research center (Giovanni Giuliano, phD).

For the analysis of temporal rhythmic oscillation of tomato mRNAs, *Solanum lycopersicum* (cv. Moneymaker) were grown in a growth chamber for 28 days in long day (LD) conditions (16 h light-25 °C/ 8 h dark-23 °C). Light intensity of about 100 μmol m^{-2} s^{-1} was provided by Osram (Munich) 11860 daylight lamps. For light continuous (LL) experiments, plants grown as described above for 28 days were shifted to continuous light at the dawn of 29^{th} day. The aerial parts of three plants were harvested at the times shown.

Plant sample of both strawberry and tomato crops were collected for RNA extraction and all sample were immediately frozen in liquid nitrogen and kept at -80 °C until use.

2.2 Total RNA isolation

Total cellular RNA was extracted from all tissues, according to the protocol described by R. Lopez-Gomez and MA Gomez-Lim (1992).

One gram of tissue, homogenized in liquid nitrogen, has been transfer in 1 ml of extraction buffer (Tris-borate 1M pH 7.5, EDTA 0.5 M, SDS 2%, water) containing 2β- mercaptoethanol 1% . The supernatant after addition of lithium chloride to a final concentration of 3M, was incubated at 4 °C for 3 hours. After centrifugation for 30' at 30000 xg and removal of supernatant, the pellet washed

in EtOH 80% was centrifuged for 10' at 15000 xg. RNA, suspended in H2O DEPC was centrifuged for 3' at 10000 xg. After spectrophotometric analysis 1 µg of RNA was loaded on the 2% agarose gel. After electrophoresis in TAE 0.5x, the gel was analyzed to UV rays.

2.3 DNA digestion

Total extracted RNA, split into aliquots of 40 µg, was digested with Deoxyribonuclease I (DNase I) (Bovine Pancreas) (GE Healthcare) to cleavage of DNA. For each reaction 40 µg RNA were digested with 2 µl of DNasi I (5000 U / ml), 3 µl buffer and DEPC water up to a final volume of 30 µl. After incubation for 20' at 37 °C, digestion products were purified with phenol-chloroform, and subjected to Electrophoresis on 2% agarose gels in presence of ethidium bromide (0.5 mg/ml).

2.4 Real Time RT-qPCR experiments

2.4.1 Reverse transcriptase (RT)

The 30 µl reaction volume have been used for 0.5–1 µg of total RNA. We have added the following components to a nuclease-free microcentrifuge tube: 0.2 µl of oligo$(dT)_{20}$ (100 µM), 0.5–1µg total RNA, DEPC water to 17 µl.

We have heated mixture to 80°C for 5 minutes and incubate on ice for at least 1 minute. We have collect the contents of the tube by brief centrifugation and we have added 6 µl 5X First-Strand Buffer, 3 µl 0.1 M DTT, 3 µl 2mM mM dNTP Mix (2 mM each dATP, dGTP, dCTP and dTTP at neutral pH), and 1 µl of SuperScript™ II or III RT (200 units/µl) (Invitrogen).

We have mixed by pipetting gently up and down and we have incubated at 42 °C for 60'. We have inactivate the reaction by heating at 80 °C for 10'.

Moreover, in order to remove RNA complementary to the cDNA we have incubated cDNA with 15 µl of NaOH 1M at 70 °C for 10'. We have added 15 µl of HCl 1M and we have purified the cDNA by Sepharose CL-6B (GE Healthcare) and using following procedures. We have added 500 µl of Sepharose CL-6B to columns and we have centrifuged for 3' at 3000xg. We have discarded the flow-through, we have added 300 µl of sterile water to columns and we have

centrifuged for 3' at 3000xg. We have discarded the flow-through, we have added the sample to columns and we have centrifuged for 3' at 3000xg. RT mix was quantified using a ND-1000 UV spectrophotometer (Nanodrop Technologies, Wilmington, USA).

2.4.2 Real time qPCR procedures

5-10 ng cDNA were used for real time RT-qPCR experiments, carried out with ABI 7700 and 7900 instruments, SybrGreen kit (AppliedBiosystems) and Platinum Sybr-Green kit (Invitrogen) according to manufacturers' instructions. Quantification was performed using standard dilution curves for each studied gene fragment. Relative gene expression data were obtained by normalizing the transcript level of each gene with that of the housekeeping elongation factor-1 alpha and/or actin for strawberry assays and of only actin for tomato assays.
The cycle PCR used was as follows:

Temperature	Time	
50 °C	2'	
95 °C	10'	
95 °C	15"	x45 cycles
58 °C	1'	
95 °C	5'	
60 °C	1'	
60→95 °C	30'	
95 °C	1'	

At the end of each analysis, software ABI Prism 7900 Sequence detection system has produced output where any amplified product has been linked to a specific value Ct. First, each studied gene fragment was amplified by using cDNA as template, therefore, the product has been estimated at spectrophotometer (Nanodrop ND1000) and was subsequently diluted six times (100 pg/µl, 10 pg/µl, 1 pg/µl, 100 fg/µl, 10 fg/µl, 1 fg/µl). The six dilutions of each fragment, repeated twice, were amplified by real time RT-qPCR; these obtained data allow to draw, for each of them, a correct calibration, putting axis in the logarithm of dilution factors and in order specific value of C_T.

$$Y = -mx + q$$

So, solving the equation for the unknown x is

$$X = Log_{10}[DNA] = (qy) / m$$

Where:

$$[DNA] = 10\,(qy) / m$$

The fragments were amplified with primers specific about 20 bp, designed by using McVector 1.5 software, in order to amplify sequences from selected portions approximately 100 bp long, at a annealing temperature of 58 °C.

Means from two independent experiments were subjected to calculation of standard deviation of repeats and/or to one-way ANOVA and Tukey's pairwise comparisons using PAST (http://folk.uio.no/ohammer/past/).

2.5 Microarray assays

2.5.1 Substrate microarray

2.5.1.1 TOM1 cDNA microarray

The array TOM1contains 12860 EST clones representing ~8,500 independent tomato loci onto glass slides coated with g-amino-propyl-silane (UltraGAPS; Corning Inc., NY) (http://bti.cornell.edu/CGEP/CGEP.html). These unigenes have been selected at random from a number different cDNA libraries made from a range of tissue including leaf, root, fruit, and flowers. As well as the random unigenes the arrays contain both positive and negative control spots.

cDNA was fixed to the slides by treatment with 300 mJoules (mJ) of UV irradiation followed by a two-hour incubation at 85 °C. Array fabrication was completed with a 2 minute wash in 0.2% SDS, three rinses in sterile water, and a final rinse in 90% EtOH. EtOH was removed immediately via centrifugation (2' at 500 rpm) and resulting microarrays were stored in a dust-free plexiglass chamber (~21°C, 0% Relative Humidity).

2.5.1.2 TOM2 oligonucleotide microarray

Oligoarrays (TOM2) contain ~12000 tomato oligonucleotides 70-mers longs (http://www.operon.com/arrays/oligosets_Tomato.php). The TOM2 microarrays

are printed on aminosilane-coated “Superamine” slides (Telechem) by University of Arizona.

Oligonucleotides were crosslinked to the slide surface by exposing the DNA-side of the microarray to UV irradiation at an energy level of 180 mJ.

Re-hydration and UV cross linking can be done well in advance before microarray hybridization, and the slides can be stored at room temperature for several months. Array fabrication was completed washing the slides in 1% SDS dissolved in sterile water for 5' at RT, rinsing the slides by plunging 10 times into sterile water, rinsing in 100% ETOH for 30" to 5', with gentle shaking, spinning dry the slides in a centrifuge at 1000 rpm for 2' and storing the slides in a light-proof box under cool dry conditions.

2.5.1.3 Strawberry cDNA microarray

For strawberry cDNA microarrays preparation, preparative PCR reactions (50 or 100 µl) were carried out using 1 µl of plasmid DNA extracted from representative EST strawberry clones. For PCR reactions we have used Taq DNA Polymerase (GE Healthcare).

For each clone PCR has been performed by following procedures:

Amount	Component
1 µl	Clone
10 µl	Buffer 10X
10 µl	dNTPs (2mM)
5 µl	T3 primer
5 µl	T7 primer
0.2 µl	Taq (1 unite)
68.8 µl	Water (sterile)

We have used GeneAmp PCR system 1700 instrument (Applied Biosystem) by following procedures:

Temperature	Time
94 °C	5'

94 °C	20"	
52 °C	20"	x35 cycles
72 °C	20"	
72 °C	5'	
15 °C	∞	

Products from duplicate 100 µl PCR reactions were combined and purified using Sepharose CL-6B (GE Healthcare) and 96-well filter plates (multiScreen MAHVN4510; Millipore Inc., MA) with following procedures:

We have added 300 µl of Sepharose CL-6B to filter plates and we have spun for 2' at 2000 xg. We have discarded the flow-through, we have added 200 µl of sterile water to filter plates and we have spun for 2' at 2000 xg. We have discarded the flow-through, we have added the sample to filter plates and we have spun for 4' at 2000 xg.

Purified products were dehydrated under vacuum, re-suspended in 3X SSC, and printed onto glass slides coated with g-amino-propyl-silane (UltraGAPS; Corning Inc., NY) using a SpotArray24 (Perkin Elmer). Temperature and humidity inside the arrayer were maintained at 45-55% relative humidity. cDNA was fixed to the slides by treatment with 300 mJ of UV irradiation. Array fabrication was completed with a 2' wash in 0.2% SDS, three rinses in sterile water, and a final rinse in 90% EtOH. EtOH was removed immediately via centrifugation (2' at 500 rpm) and resulting microarrays were stored in a dust-free plexiglass chamber (~21°C, 0% relative humidity).

The resulting microarrays have consisted of 5610 spots (1811 selected ESTs, 49 candidate genes, 10 controls, per three replicates).

2.5.2 Preparation of labeled target

We have used three different protocol for target labeling:

1. Direct-labeling by using SuperScript II reverse transcriptase (Invitrogen)
2. Indirect-labeling by using indirect cDNA labeling system (Invitrogen)
3. RNA amplification and indirect-labeling by using Aminoallyl Message Amp II kit (Ambion).

2.5.2.1 Direct-labeling

To anneal primers to total RNA, add the following labeling reaction components to a 1.5 ml amber microcentrifuge tube on ice:

Amount	Component
40 µg	Total RNA
1 µl	Anchored oligo-dT
Up to 11µl	Water (sterile)

Mix gently by pipetting up and down.

Incubate the reaction mixture at 70 °C for 5'.

Let the reaction mixture cool at room temperature for 10' to allow the primers to anneal with the total RNA template.

Spin down the reaction mixtures for 30" in a microcentrifuge to collect all reaction components at the bottom of the tube.

Place the annealed reaction mixture on ice and add the labeling components in the following order:

Amount	Component
4 µl	5x RT buffer
2 µl	0.1 M DTT
1 µl	d(AGC)TP nucleotide mix
1 µl	dUTP CyDye-labelled nucleotide
5 µl	SuperScript™ II RT (400 U/µl)

Incubate tube at 46°C for 2–3 hours

Degradation of RNA

Add 2 µl of 2.5 M NaOH into each microcentrifuge tube containing labelling reactions.

Mix the reaction mixtures by vortexing and spin them for 30" in a microcentrifuge.

Incubate the samples at 37 °C for 15'.

Add 2 µl of 2,5 M HCl to each reaction tube.

Purification of labelled cDNA with CyScribe GFX Purification kit

For every cDNA labelling reaction to be purified, place one GFX column into a clean collection tube. Add 500 µl of capture buffer to each column.

Transfer the unpurified labeled cDNA products into each GFX column

Centrifuge each column in a microcentrifuge at 13800 xg for 30"

Remove the GFX column and discard the liquid at the bottom of each collection tube. Return each GFX column into the used collection tube.

Add 600 µl of wash buffer to each column and centrifuge at 13800 xg for 30". Remove the GFX column and discard the collected liquid. Repeat wash step twice for a total of 3 washes. After the final wash, discard the liquid and place each column back in the used collection tube.

Centrifuge each column at 13800 xg for an additional 10" to remove all wash buffer in the tip of the column. Discard the collection tube.

Transfer each GFX column to a fresh 1.5 ml microcentrifuge tube and add 60 µl of elution buffer directly to the top of the glass fiber matrix in each GFX column.

Incubate the GFX column at room temperature for 1–5'.

Centrifuge at 13800 xg for 1' to collect the purified labeled cDNA.

2.5.2.2 Indirect-labeling

The following procedure is designed to convert 20 µg of total RNA into first-strand cDNA.

Amount	Component
20 µg	Total RNA
2 µl	Anchored Oligo(dT)$_{20}$ Primer (2.5 µg/µl)
Up to 18 µl	DEPC-treated water

Incubate tubes at 70 ºC for 5', and then place on ice for at least 1'.

Add the following to each tube on ice:

Amount	Component
6 µl	5X First-Strand buffer
1.5 µl	0.1 M DTT
1.5 µl	dNTP mix (including amino-modified nucleotides)
1 µl	RNaseOUT™ (40 U/µl)
2 µl	SuperScript™ III RT (400 U/µl)

Mix gently and collect the contents of each tube by brief centrifugation. Incubate tube at 46 °C for 2–3 hours.

After incubation, proceed directly to Alkaline Hydrolysis and Neutralization, below.

Hydrolysis and Neutralization

After cDNA synthesis, above, immediately perform the following hydrolysis reaction to degrade the original RNA:

Add 15 µl of 1 N NaOH to each reaction tube from. Mix thoroughly.

Incubate tube at 70º C for 10'.

Add 15 µl of 1 N HCl to neutralize the pH and mix gently.

Add 20 µl 3 M Sodium Acetate, pH 5.2, and mix gently.

Use the following procedure to purify the cDNA using the components of the Purification Module.

Add 500 µl of Loading Buffer to the neutralized cDNA

Place a S.N.A.P.™ Column on a collection tube and load your sample on the S.N.A.P.™ Column.

Centrifuge at 14000 xg at room temperature for 60". Remove the collection tube and discard the flow-through.

Place the S.N.A.P.™ Column onto the same collection tube and add 700 µl of Wash Buffer prepared

Centrifuge at 14000 xg at room temperature for 60". Remove the collection tube and discard the flow-through.

Repeat previous two steps.

Centrifuge one more time at 14000 xg at room temperature for 60". Remove the collection tube and discard the flow-through.

Place the S.N.A.P.™ Column onto a new 1.5-ml microcentrifuge tube.

Add 50 µl of DEPC-treated water to the S.N.A.P.™ Column and incubate at room temperature for 1 minute. Centrifuge at 14000 xg at room temperature for 1'.

Repeat previous step, using the same microcentrifuge tube.

In the second part of the purification procedure, perform an ethanol precipitation of the cDNA:

Add 10 µl of 3 M Sodium Acetate, pH 5.2

Add 2 µl of 20 mg/ml glycogen to the tube and mix.

Add 300 µl of ice-cold 100% ethanol, and incubate the tube at –20 ºC for at least 30'.

Spin the tube at 14000 xg at 4 ºC for 10–20'. Carefully remove and discard the supernatant.

Add 250 µl of ice-cold 75% ethanol and spin the tube at 14000 xg for 2'.

Carefully remove and discard the supernatant.

Air dry the sample for 10'.

Re-suspend the sample in 5 µl of 2X Coupling Buffer.

Follow the steps below to couple fluorescent dye to your amino-modified first-strand cDNA.

Cy3™ or Cy5™ dye vials (PA 23001, PA 25001; GE Healthcare): Add 45 µl DMSO directly to each dye vial.

Use 5 µl of this DMSO/dye solution in the next step.

Add the DMSO/dye solution to the tube from Ethanol Precipitation.

Mix well and incubate the tube at room temperature in the dark for 1 hour.

Use the following procedure to purify the cDNA:

Add 20 µl of 3 M Sodium Acetate, pH 5.2, to the dye-coupled cDNA solution

Add 500 µl of Loading Buffer plus isopropanol to the cDNA solution. Mix well by vortexing.

Place a S.N.A.P.™ Column onto a clear collection tube and load the cDNA/buffer solution onto the S.N.A.P.™ Column.

Centrifuge at 14000 xg at room temperature for 60". Remove the collection tube and discard the flow-through.

Place the S.N.A.P.™ Column on the same collection tube and add 700 µl of Wash Buffer plus ethanol to the column.

Centrifuge at 14000 xg at room temperature for 60". Remove the collection tube and discard the flow-through.

Repeat last two Steps above, using the same collection tube.

Centrifuge one more time at 14000 xg at room temperature for 60". Remove the collection tube and discard the flow-through.

Place the S.N.A.P.™ Column onto a new amber collection tube.
Add 50 µl of DEPC-treated water to the S.N.A.P.™ Column and incubate at room temperature for 1'.
Centrifuge at 14000 xg at room temperature for 1' and collect the flow-through.

2.5.2.3 RNA amplification and indirect-labeling

Before RNA amplification we are using Qiagen RNeasy MinElute Columns for RNA cleanup:
Adjust sample (20 µg total RNA) to a volume of 100 µl with RNAase-free water, add 350 µl RLT buffer (provided in the RNeasy kit), and mix thoroughly. At this point, the RNA samples are maintained at room temperature.
Add 250 µl of 100% ethanol to the diluted RNA, and mix thoroughly by pipetting. Do not centrifuge; continue immediately to the next step.
Add 700 µl of the sample to an RNeasy MinElute Spin Column in a 2 ml collection tube. Close the tube gently, and centrifuge for 15"at 8000 xg. Discard the flow-through.
Transfer the spin column into a new 2 ml collection tube. Pipet 500 µl RPE buffer (provided in the kit) onto the spin column. Close the tube gently, and centrifuge for 15" at 8000 xg to wash the column. Discard the flow-through.
Add 500 µl of 80% ethanol to the RNeasy MinElute Spin Column. Close the tube gently, and centrifuge for 2' at 8000 xg to dry the silica-gel membrane. Discard the flow-through.
Transfer the RNeasy MinElute Spin Column into a new microfuge collection tube. Open the cap of the spin column, and centrifuge in a microcentrifuge at full speed for 5'. Discard the flow-through and collection tube.
To elute, transfer the spin column to a new microfuge tube. Pipet 20 µl of DEPC water pre-heated to 55 °C directly onto the center of the silica-gel membrane. Close the tube gently, incubate at RT for 2', and centrifuge for 1' at maximum speed to elute. Repeat the elution one more time with additional 20 µl warm DEPC water (55 °C).
Measure the RNA concentration and proceed to the next step. Keep RNA solutions on ice after elution.

Measure the RNA amount using Nanodrop and use the Bioanalyzer to verify the quality of the total RNA.

RNA amplification and aRNA hybridization

Target Preparation I: Setting up the First Strand cDNA Synthesis

Place up to 1 µg of total RNA into a RNAase-free microfuge tube.

Add 1 µl of T7 Oligo(dT) Primer.

Add Nuclease-free Water to a final volume of 12 µl.

Incubate 5' at 70 °C in a thermocycler.

Remove the RNA samples from the 70 °C incubator and centrifuge briefly (~5 sec) to collect sample at bottom of tube and immediately transfer to ice.

Assemble the Reverse Transcription Master Mix at room temperature, then place on ice.

Amount	Component
2 µl	10X First Strand Buffer
1 µl	Ribonuclease Inhibitor
4 µl	dNTP Mix
1 µl	Reverse Transcriptase

Mix well by gently pipetting up and down or flicking the tube a few times. Centrifuge briefly (~5") to collect this master mix at the bottom of tube and place on ice.

Transfer 8 µl of Reverse Transcription Master Mix to each RNA sample, mix thoroughly by gently pipetting up and down or flicking the tube a few times, and place the tubes in a 42 °C incubator. We generally use a PCR machine with the lid temperature set at 48 °C.

After the 2 h incubation at 42 °C, centrifuge the tubes briefly (~5") to collect the reaction at the bottom of the tube. Place the tubes on ice, and proceed to Second Strand cDNA synthesis.

Target Preparation II. Second Strand cDNA Synthesis, and Setting Up for aRNA Synthesis

On ice, add the second strand cDNA synthesis reagents in the order listed to each sample.

Amount	Component
20 µl	cDNA sample
63 µl	Nuclease-free Water
10 µl	10X Second Strand Buffer
4 µl	dNTP Mix
2 µl	DNA Polymerase
1 µl	RNase H

Gently mix by pipetting up and down or by flicking the tube a few times, then centrifuge the tubes briefly (~5") to collect the reaction at the bottom of tube.
Incubate the tubes at 16 °C for 2 h
After the 2 h incubation at 16 °C, proceed to cDNA Purification (below), or immediately freeze reactions at –20 °C. Do not leave the reactions on ice for long periods of time.

Target Preparation V: cDNA Purification
Use the cDNA purification kit supplied with the messageamp-II kit or you can also use other PCR purification kits like Qiaquick.
Check that the cDNA filter cartridge is firmly seated in a 2 ml wash tube and pipet 50 µl cDNA binding buffer onto the filter in the cDNA filter cartridge.
Incubate at room temperature for 5'. Add 250 µl of cDNA binding buffer to each cDNA sample from the second strand cDNA synthesis and mix thoroughly by repeated pipetting.
Pipet the cDNA sample/cDNA Binding Buffer onto the center of an equilibrated cDNA Filter Cartridge.
Centrifuge for ~1' at 10000 xg, or until the mixture has passed through the filter.
Discard the flow-through and replace the cDNA filter cartridge in the 2 ml wash tube.
Apply 500 µl cDNA wash buffer to each cDNA filter cartridge. Centrifuge for ~1' at 10000 xg, or until all the cDNA wash buffer is through the filter.
Discard the flow-through and spin the cDNA filter cartridge for an additional minute to remove trace amounts of ethanol.

Transfer cDNA Filter Cartridge to a cDNA Elution Tube. To the center of the filter in the cDNA Filter Cartridge, apply 10 µl of nuclease free water that is preheated to 55 °C. Leave at room temperature for 2' and then centrifuge for ~1.5' at 10000 xg, or until all the nuclease-free water is through the filter.

Repeat the previous step with additional 10 µl of 55 °C pre-heated nuclease-free water. The double-stranded cDNA will now be in the eluate (~18 µl).

Discard the cDNA Filter Cartridge.

Target Preparation III: In Vitro Transcription for aRNA synthesis

Make the reaction mix by adding the reagents in the following order:

Amount	Component
16 µl	double-stranded cDNA
3 µl	aaUTP Solution (50 mM)
12 µl	ATP, CTP, GTP Mix (25 mM)
1 µl	UTP Solution (50 mM)
4 µl	T7 10X Reaction Buffer
4 µl	T7 Enzyme Mix

Mix well with pipette, centrifuge at 3000 xg for 30", then incubate over night the tube at 37 °C.

Stop the reaction by adding 60 µl nuclease-free water to each aRNA sample to bring the final volume to 100 µl. Mix thoroughly by gentle vortexing, and proceed to the aRNA purification step.

Target Preparation IV: aRNA Purification, Quantification, and Dye Coupling

Add 350 µl of aRNA binding buffer to each aRNA sample, then proceed to the next step immediately.

Add 250 µl of ACS grade 100% ethanol to each aRNA sample, and mix by pipetting the mixture up and down three times.

Proceed immediately to the next step as soon as you have mixed the ethanol into each sample. Any delay in proceeding could result in loss of aRNA because once the ethanol is added, the aRNA will be in a semi-precipitated state.

Pipet each sample mixture from step 2 onto the center of the filter in the aRNA filter cartridge, centrifuge for ~1' at 10000 xg, or continue until the mixture has passed through the filter.

Discard the flow-through, and replace the aRNA filter cartridge back into the aRNA collection tube.

Apply 650 µl wash buffer to each aRNA filter cartridge, centrifuge for ~1' at 10000 xg, or until all the wash buffer is through the filter.

Discard the flow-through, and spin the aRNA filter cartridge for an additional ~3' to remove trace amounts of wash buffer.

Transfer filter cartridge(s) to a fresh aRNA collection tube. To the center of the filter, add 100 µl nuclease-free water (pre-heated to 55 °C).

Leave at room temp for 2' and then centrifuge for ~1.5' at 10000 xg, or until the nuclease-free water is through the filter.

The aRNA will now be in the aRNA collection tube in ~100 µl of nuclease-free water.

Determine the concentration of RNA using either the Nanodrop or a conventional spectrophotometer.

Target Preparation V: Coupling AA-cRNA to the Cy Dye Ester

Preparation of Cy3 and Cy5 monoreactive dye. These dyes are supplied as five aliquots; the contents of each tube is sufficient for at least four labeling reactions. Dissolve the entire contents of a single tube in 22 µl DMSO by flicking the tube several times, and leaving at room temperature for at least 30' protected from light. Centrifuge at 1000 xg for 30" to collect the dye at the bottom of the tube. The dye is now ready for use, but can be stored at -20 °C for up to one month. Always protect the dye from light by wrapping with aluminum foil.

Dissolve the dried aRNA with 5 µl of coupling buffer by flicking the tube several times and leaving the tube at room temperature for at least 20'.

Add 5 µl of Cy3 or Cy5 (in DMSO) to each tube, and mix them thoroughly by flicking the tube several times.

Spin the tube at 1000 xg for 30".

Incubate the dye and aRNA mix in the tube at room temperature for 2 h while covered in aluminum foil.

Target Preparation VI: aRNA Purification (Post Dye-Coupling)

Quenching Reaction. This optional step involves quenching any unreacted Cy dye by adding an excess of primary amines.

Add 4.5 µl 4M hydroxylamine.

Incubate for 15' in the dark at RT.

Removal of Unincorporated Dye. The Qiagen RNeasy MinElute column is used for this purpose.

Adjust sample to a volume of 100 µl with RNAase-free water. Add 350 µl of RLT (kit) buffer, and mix thoroughly.

Add 250 µl of 96–100% ethanol to the diluted RNA, and mix thoroughly by pipetting.

Apply 700 µl of the sample to an RNeasy MinElute Spin Column in a 2 ml collection tube (supplied). Close the tube gently, centrifuge for 15" at 8000 xg, and discard the flow-through.

Transfer the spin column into a new 2 ml collection tube. Pipet 500 µl RPE buffer onto the spin column. Close the tube gently, and centrifuge for 15" at 8000 xg to wash the column. Discard the flow-through.

Add 500 µl of 80% ethanol to the RNeasy MinElute Spin Column. Close the tube gently, and centrifuge for 2' at 8000 xg to dry the silica-gel membrane. Discard the flow-through and collection tube.

Transfer the RNeasy MinElute Spin Column into a new 2 ml collection tube (supplied). Open the cap of the spin column, and centrifuge in a microcentrifuge at 12000 xg for 5'. Discard the flow-through and collection tube.

To elute, transfer the spin column to a new microfuge tube. Pipet 20 µl warm DEPC water (55 °C) and leave at RT for 2'. Close the tube gently, and centrifuge at 12000 xg for 1'.

Repeat previous step with an additional 20 µl of warm DEPC water (55 °C).

Measure the amount of dye incorporated into aRNA using a NanoDrop or conventional spectrophotometer.

2.5.3 Microarray hybridization

We have performed microarray hybridization by using three different protocols. Moreover following procedures concern manual approach but simultaneously we have also performed hybridization steps by using an automatic hybridization station (HybArray, Perckin-Elmer) following manufacturer's specifications.

2.5.3.1 TOM1 hybridization by using Amersham buffer

Purified Cy3- and Cy5-labelled cDNAs were dried in a speed-vac and resuspended in hybridization buffer (Amersham Bioscience) supplemented with 50% formamide, dispensed over the glass slide and incubated at 42 °C overnight in corning chambers with agitation in a water bath. Slides were washed in decreasing SSC concentrations (2X - 0.1X) and 0.1% SDS at 42 °C and room temperature, respectively. The last wash was carried out in 0.1X SSC at room temperature.

2.5.3.2 TOM1 and strawberry hybridization by using Corning buffer

Prehybridization

This step has the purpose of blocking the unused surface of the slide and removing loosely bound probe DNA. It is recommended that all target cDNAs be characterized prior to the start of prehybridization.

The preparation of the hybridization solutions can be completed during the time arrays are being prehybridized.

Prepare prehybridization solution consisting of 50% formamide, 5X SSC, 0.1% SDS, and 0.1 mg/mL BSA. The volumes required to process a given number of arrays depends on type of glassware available. Use Coplin jars to simultaneously process up to 5 arrays using only 50 ml of solution per step.

Warm prehybridization solution to 42 ºC.

Immerse arrays in prehybridization solution and incubate at 42 ºC for 45 to 60'.

Transfer prehybridized arrays to 0.1X SSC and incubate at ambient temperature (22 to 25 ºC) for 5'.

Repeat previous step.

Transfer arrays to purified water and incubate at ambient temperature for 30".

Dry arrays by blowing high-purity nitrogen over the array or by centrifugation at 1600 rpm, for 2'. Keep arrays in a dust-free environment while completing the preparation of the hybridization solution.

Hybridization

Carefully pipette the target cDNA onto the arrayed surface.

Avoid touching the array with the pipette tip and creating air bubbles.

When using cover glass, apply the target cDNA in small volumes along the middle of the array.

Transfer array/cover glass assembly to Corning Hybridization Chamber. Submerge chamber-array assembly in a water bath or place in a hybridization oven kept at 42 °C. Hybridize arrays at 42 °C for 12 to 16 h.

Post-Hybridization Washes

Immerse arrays in 2X SSC, 0.1% SDS at 42 °C until the coverslip moves freely away from the slide.

Transfer arrays to 2X SSC, 0.1% SDS at 42 °C for 5'.

Transfer arrays to 0.1X SSC, 0.1% SDS at room temperature for 5'.

Repeat previous step.

Transfer arrays to 0.1X SSC at room temperature for 1'.

Repeat previous Step four times.

Rinse arrays in 0.01X SSC for 10".

Dry arrays by centrifugation at 1600 xg for 2'.

2.5.3.3 TOM2 hybridization

Mix the following in a microfuge tube:

Amount	Component
6 µl	20X SSC
3.6 µl	Liquid Block (GE Healthcare)
2.4 µl	2% SDS
200-300 pmols	Both Labeled Targets
Up to 60 µl	Sterile water

Denature labeled target by incubating tube at 65 °C for 5'.

Transfer tube to ice immediately or apply on to the slides directly.

Rinse Hybridization Cassette with distilled water and dry thoroughly.
Make sure flexible rubber gasket is seated evenly in gasket channel.
Add 15 µl water to the lower groove inside the cassette chamber.
Insert the microarray into cassette chamber, DNA side up.
Place the lifter slip over the microarray slide
Apply the PRE-HEATED sample slowly to the one end of the lifterslip and let it disperse.
Quickly place the clear plastic cassette lid on top of the cassette chamber.
Place the cassette into a hybridization oven set at 55 °C.
Allow the hybridization reaction to proceed for 8-12 h.

Microarray Washing
Wash slide in the following solutions for 5' each:
2X SSC, 0.5% SDS at 55 °C
0.5X SSC at room temperature
0.05X SSC at room temperature

Washing is done by immersing the slides in a glass slide-staining jar containing the appropriate volume of wash buffer, followed by placing it on a belly shaker at 60 rpm. Pre-heat the first wash solution, and make sure the slides are completely immersed in wash buffer.
After completion of the washes, spin dry the slide in centrifuge at no more than 1000 rpm for 2-4'.

2.5.4 Image detection

Immediate scanning is recommended. We have performed image detection by using ScanArray Lite (PerkinElmer).
Examine the scanned images immediately to determine the number of elements that are near zero or are saturated (for a 16-bit scanner, that represents a value of 65400). The proportion of these elements should be acceptably low, since information is lost in either case.

It is much more preferable to rescan with altered gain settings on the scanner than to proceed with analysis of images containing large proportions of zero or saturated elements. We have found that, even though the absolute value of the spots may be reduced by scanning a second or third time, the relative fluorescence distribution is preserved, so the information is not lost.

Scanning a second time at higher PMT/laser values can also be done to move low intensity elements higher within the dynamic range. The two intensity distributions (at low and high PMT/laser values) can then be merged to provide an increased combined dynamic range. Save the image as a .TIFF file.

Feature extraction is a critical step which must be done carefully and thoughtfully, as it greatly influences the outcome of your microarray experiment! Feature extraction is carried out by spot-finding programs, which convert the digital scanned images to numerical values representing the signal intensities of each spot.

Raw hybridization signals were filtered by imposing a minimal signal/noise ratio of 2.0 or 3.0 and flagging the non-passed spots. Raw values were then normalized with the locally weighted linear regression (LOWESS) method using the 20% of data for smoothing (Cleveland and Devlin, 1998) and gene expression analysis of the array data were performed using GeneSpring version 7.3 (Silicon Genetics, http://www.chem.agilent.com/). Cluster Analyses analyses were performed using Cluster and Treeview algorythms (Eisen et al., 1998).

3. RESULTS

3.1 Comparative profiling of tomato fruits and leaves evidences a complex modulation of global transcript profiles

To get further insight into the molecular mechanisms involved in fruit ripening in tomato and identify new genes and functions possibly involved in light perception and responses, we have investigated the gene transcription changes during fruit ripening in the cultivar Moneymaker (*Solanum lycopersicum*). The monitoring of the gene expression has been carried out using comparative transcription profiling using both cDNA microarray and quantitative Real Time reverse transcription-polymerase chain reaction (RT-PCR) approaches.

The results are shown in the following attached paper (Carbone et al., 2005).

Available online at www.sciencedirect.com
SCIENCE DIRECT®
Plant Science 169 (2005) 165–175
PLANT SCIENCE
www.elsevier.com/locate/plantsci

Comparative profiling of tomato fruits and leaves evidences a complex modulation of global transcript profiles

Fabrizio Carbone [a], Daniele Pizzichini [b], Giovanni Giuliano [b], Carlo Rosati [a], Gaetano Perrotta [a,*]

[a] *ENEA, Trisaia Research Center, 75026 Rotondella (MT), Italy*
[b] *ENEA, Casaccia Research Center, S.S. 106 Jonica – Km 419,500 P.O. Box 2400, Rome 00100, Italy*

Received 7 October 2004; received in revised form 14 March 2005; accepted 14 March 2005
Available online 1 April 2005

Abstract

Recently, transcription profiling of ripening tomatoes has provided some information about genes involved in fruit maturation and ripening. Nevertheless, many fundamental molecular mechanisms need to be better investigated. Besides, despite their deep impact on fruit development, very little is known about the regulation of photosensory and light signalling genes during fruit ripening.

Using the Tom1 microarray, we have compared the extent of transcriptional changes in three different stages of fruit development (immature green, breaker, and fully ripe) versus leaf in the *cultivar* Money Maker.

The extent of transcriptional modulation was confirmed through quantitative real time RT-PCR on selected genes, showing significant levels of regulation during fruit development.

Furthermore, real-time RT-PCR was used to study the regulation of transcripts encoding photosensory receptors, light signalling proteins, and carotenoid biosynthesis genes. Some of these transcripts are highly regulated during tomato fruit development, suggesting that light responsiveness of carotenoid biosynthesis tomato fruits could be at least partially regulated at the transcriptional level.

Keywords: Tomato fruit ripening; Microarray; Light signalling genes; Carotenoid biosynthesis

1. Introduction

In their constant effort to obtain competitive and vital progenies plants have developed, during evolution, numerous mechanisms for the dispersion of seeds. The fruits are an integral part of this strategy. During ripening, fleshy fruits become attractive with bright colours and flavours in order to attract a variety of organisms that will act as vehicle of seed propagation.

The ripening process represents a unique event in the development of seed plants, still more important for its implications in the human diet. Tomato fruit ripening is the result of a series of biochemical and physiological changes aimed at render the fruit particularly attractive to animals and humans. Generally such changes, though variable through different plant species, involve modifications in the ultra-structure and texture of the cell wall, the conversion of the starch in sugar, the onset of pigment biosynthesis pathways and the increment of aroma and flavour [1,2].

Fruits can be classified into climacteric and not climacteric ones according to the rate of ethylene biosynthesis and the respiratory burst [3,4]. In contrast to non-climacteric ones, climacteric fruits like tomato synthesize high levels of ethylene in order to coordinate and complete the ripening process, as shown from the analysis of tomato plants treated with inhibitors of the biosynthesis and perception of ethylene [5].

Although a large amount of information is currently available about the molecular aspects of ripening in tomato, it is still largely unknown how metabolic pathways, apparently not correlated to each other, act in a synchronized

* Corresponding author. Tel.: +39 0835974746; fax: +39 0835974749.
E-mail address: gaetano.perrotta@trisaia.enea.it (G. Perrotta).

0168-9452/$ – see front matter
doi:10.1016/j.plantsci.2005.03.011

way during the several steps of fruit development. Understanding these phenomena is important not only to increase our knowledge of an important aspect of plant biology, but also for the remarkable impact it can have in agricultural practice. Tomato is a major food commodity especially in the Mediterranean countries. It represents a source of fibres, carbohydrates, proteins, lipids, minerals as well as of several vitamins and anti-oxidants, namely lycopene, that plays an important role in the prevention of some diseases like prostate cancer [6].

The relative concentration of all these substances in fruit tissues is finely regulated by biochemical processes that occur during ripening and which are related to genetic and environmental cues. Therefore, the understanding of the molecular events related to fruit metabolism will help to identify those genes that are associated to nutritional and qualitative characteristics and to the development of desirable traits in fruits.

The expansion of high-throughput automated DNA sequencing and gene cloning strategies have accelerated the exploitation of molecular data obtained from genomes. Until a few years ago, sequence information on important key genes as well as significant functional data over any biological system were virtually non existent or, if available, represented the result of researches conducted for many years using classic approaches. Nowadays, the ''omics'' sciences have paved the way to the study of structural and functional aspects of genes on a global scale [7].

Tomato, a model Solanaceaous plant, is the focus of several research projects aimed at elucidating the informational content of its genome as well as gene structure/function relations. For this purpose, a database containing more than 160,000 expressed sequences tags (ESTs) representing over 30,000 unigenes is currently available (http://www.tigr.org; http://sgn.cornell.edu) [8]. At the Cornell University genomic information has been exploited to produce a cDNA microarray (TOM1) containing about 12,000 tomato ESTs (http://bti.cornell.edu/CGEP/CGEP.html).

DNA microarray technology offers many advantages for the investigation of gene function. The most important one is the ability of monitoring the gene expression of virtually every single gene of a genome in a single experiment. Moreover, the use of solid substrates as chemically modified glass, the robotics precision and the optimization of the fluorescence detection methods are able to give results in relatively short time and with greater accuracy compared with methods based on filters and radioactive detection [9].

Recently, transcription profiling of ripening tomatoes has provided some information about genes involved in fruit maturation and ripening (http://ted.bti.cornell.edu) [10,11]. Nevertheless, many fundamental molecular mechanisms need to be better investigated. Indeed, despite their deep impact on fruit development, very little is known about the regulation of photosensory and light signalling-related genes.

Higher plants are able to monitor the environmental light conditions by using multiple wavelength-specific photoreceptors including red/far-red absorbing phytochromes [12] and blue/UVA absorbing cryptochromes and phototropins [13,14]. Some evidences hint that distinct light signalling pathways initiated by multiple photoreceptors trigger the activation of a bZIP transcription factor (Hy5) whose protein stability is finely regulated by the constitutive photomorphogenic repressor Cop1 [15].

Light-mediated responses promote de-etiolation through the inhibition of hypocotyl elongation, cotyledon expansion, chloroplast development, stomatal opening and pigment biosynthesis. Moreover, many studies have demonstrated that alteration of light perception deeply affects the plant adult phenotype. Notably, tomato *hp* mutants, characterized by exaggerated photoresponsiveness, and transgenic tomato with increased expression of cryptochromes bear fruits with more intense pigmentation than those of wild type plants [16,17].

We have monitored the fruit versus leaf gene expression profiling in tomato using both cDNA microarray and quantitative real time reverse transcription polymerase chain reaction (QRT-PCR) approaches. The aim of this work was to gain information on the molecular mechanisms involved in fruit development in tomato by the identification of a minimal set of fruit specific gene functions and by investigating the possible role of genes involved in light perception and responses.

2. Methods

2.1. Plant material

Tomato plants (cv Money Maker) were grown under controlled greenhouse conditions with 16h photoperiod at 25 °C (day) and 20 °C (night). Green leaves (size approx 4 cm) and fruits at three different developmental stages – immature green (I), breaker (B) and mature red (M, ten days after breaker) – were collected between 4 and 6 h after the onset of the light period. The locular tissue and seeds were discarded, and the pericarp was cut into small pieces, quick-frozen in liquid nitrogen and stored at −80 °C until RNA extraction.

2.2. Nucleic acid manipulations

Standard molecular biology protocols were followed as described by Sambrook et al. [18].

Total RNA was isolated from pools of tomato leaf and fruit tissues, representing at least six different leaves or fruits from two different plants following the procedure described by Lopez-Gomez and Gomez-Lim [19], with minor modifications.

2.3. Preparation of labelled probes and hybridisation

Tomato TOM1 microarrays were purchased from the Center for Gene Expression Profiling (CGEP) at Cornell University (http://bti.cornell.edu/CGEP/CGEP.html).

Microarrays were pre-hybridized in 50% formamide buffer at 42 °C for 1 h and rinsed briefly in sterile water. RNA labelling was achieved using two different protocols using direct-labelling and indirect-labelling methods. For each direct-labelling reaction, 40 μg of DNA-free total RNA were reverse transcribed using SuperScript II reverse transcriptase (Invitrogen) and oligo-dT primer in the presence of Cy3- or Cy5-labelled dUTP using the SuperScript II reverse transcriptase (Invitrogen). Unincorporated nucleotides were eliminated using GFX-PCR columns (Amersham Biosciences) following manufacturer's specifications. The indirect-labelling reactions were carried out with 20 μg of DNA-free total RNA using indirect cDNA labelling system (Invitrogen) following the manufacturer specifications. Purified Cy3- and Cy5-labelled cDNAs were dried in a speed-vac and resuspended in hybridization buffer (Amersham Bioscience) supplemented with 50% formamide, dispensed over the glass slide and incubated at 42 °C overnight with agitation in a water bath. Slides were washed in decreasing SSC concentrations ($2x - 0.1x$) and 0.1% SDS at 42 °C and room temperature, respectively. The last wash was carried out in $0.1x$ SSC at room temperature. Hybridized microarrays were then scanned using the ScanArray Lite (Perkin–Elmer) and the resulting Cy3 and Cy5 images were analyzed with the software ScanArray Express (Perkin–Elmer) in order to measure the Cy3/Cy5 spot intensities.

2.4. Microarray data analysis

Raw hybridization signals were filtered by imposing a minimal signal/noise ratio of 3.0. Non-passed spots were flagged and not further considered.

Raw values were then normalized with the locally weighted linear regression (LOWESS) method using the 20% of data for smoothing [20].

2.5. Real time RT-PCR

For experiments, first strand cDNA was synthesized from 1 μg total RNA in 30 μl with oligo-dT and Superscript II (Invitrogen), according to manufacturer's instructions. The RT mix was diluted to 1:3 and 2-μl aliquots were used for quantitative QRT-PCR experiments, carried out with gene-specific primers, using ABI 7700 instrument and SyBr-Green kit (cat. 4309155; Applera) according to manufacturer's instructions. PCR conditions were: 5′ at 95 °C followed by 45 cycles of incubations at 95 °C × 15″ and at 58 °C × 60″. Quantification was performed using standard dilution curves for each studied gene fragment and the data were normalized for the quantity of actin transcript.

The primer sequences are:

Phototropin1 (SGN-U216278)
CTAGTTGCACTCCGATGAAGTACTG; CTAAGACTGG CAAAAAGTTCTGGAA
Cop1 (AF029984)
CAACAGACAGTACTCTACG; GATGTCCTTCAGCACA ATG
Hy5 (SGN-U221674)
CATCATGAACTCAAAGAAGGTATGGA; ACCGGCGG CCGATACT
Cryptochrome1A (AF130424)
TCCTTGCTAACTTTTTGTTAGTATCTGTG; TACGATC TTTTGTTAGCCTGCCT
Cryptochrome1B (AF348462)
ATATCGATGTAATGCAAGAACTATGGA; TCTGGTAC AGAGAAGTAGAGGCATCA
Cryptochrome 2 (AF130426)
CAAAGGGTGCCATCAATGC; GCTTGTTATCATTGAG CTTCTTTGTT
Phytochrome A (AJ001914)
GAATCGAAGGTGACTATAGAGCGATT; GAACACCAG CCAAATTGATCAG
Phytochrome B1 (AJ002281)
GGGCTTCCTCCTGAATTGG; GCTCAGTCCTAGGCCT TCCTG
Phytochrome B2 (AF122901)
TGATTTCTTACAGATTATGGC AAGCT; TTGGTCGAA-GATGGACTTCTACC
Phytochrome E (AF178571)
TTGCTTAGTGTAGTGCA CCATGC; GTTTCAAA CCAGGTAACACCTTGA
Phytochrome F (U32444)
TTGAGCAAGGATCAAAGGCA; GTGTCGTCAATGAT CTTGGCTAGT
Phytoene synthase 1 (X60441)
GGGCGGCCATTTGACAT; AATGGCTGAATATCAAC TGGAAAGT
Phytoene synthase 2 (L23424)
CGGTTGATATTCAGCCATTCAG; GCGACATAGTAAC AATAGAGATATAGCTCAT
Phytoene desaturase (M88683)
CCGGTGACTACACGAAACAGAA; AAGTAACTCATA ATCCTGTACAATAGCTTGA
Zeta-carotene desaturase (AF195507)
TTGGAGCGTTCGAGGCAAT; AGAAATCTGCATCTG GCGATAGA
Carotene isomerase (AF416727)
TACTTTATAGGGCAAATGTTACAAGTATCAT; ATCTG GTAGCATTCGATACTATGGTTT
Lycopene beta cyclase (X86452)
TCGTTGGAATCGGTGGTACAG; AGCTAGTGTCCTT GCCACCATATAA
Lycopene epsilon cyclase (Y14387)
AGTTGAGGTTGATAACAACAATCCATTTG; AGATTG AGCGTCGTGTCTGAGA
Carotene hydroxylase 1 (Y14809)
CGAACTTTTTATTTCCGTCATTCA; TTCTTCTAGACC TCAAAATTGGGC
Carotene hydroxylase 2 (Y14810)
CGTTTCTCAGTCCAAAATCCG; CAGCACAAAACAA ACCGCC

Zeaxanthin epoxidase (Z83835)
ATGATAGACCGCCAACCTTTAGTT; CCATGCATCCC CCTTGAC
Violaxanthin de-epoxidase (AF385366)
GCGCTTGCCCCTCATTC; TCGGAAGCCTTGATCCAA CTTG
Lycopene cyclase B (Y18297)
TGTTATTGAGGAAGAGAAATGTGTGAT; TCCCACCA ATAGCCATAACATTTT
Actin (SGN-U213638)
AGGTATTGTGTTGGACTCTGGTGAT; ACGGAGAATG GCATGTGGAA
Ubiquitin (SGN-U143513)
GCGATTGTACTCCCTTTTATTCTC; TGCGGCAATACT TACATCCA
Pectinesterase 1 (SGN-U143700)
ATGCTTGCGTCTTTGACAACT; GAACTCACCCAAGA TGGCATT
Alcohol Dehydrogenase 2 (SGN-U143271)
AAGTGTGGCTATATTTGGACTAGGA; TCGAGGCACC AGCAATTCT
Glutamine Synthetase (SGN-U146805)
ACATCAGCGGGATCAATGGT; ATGCCAACAGAAGG TCCAACTT
2-oxoglutarate-dependent dioxygenase (SGN-U155526)
GATGAAAATAATAAAGCTGCTGGAT; CCATTAACTT GATTTTGCGATATAAA
Fructose-bisphosphate aldolase (SGN-U143932)
GCCCGAGATCCTTGTCGAT; CAAGAACGCGCTCGG TAAC
Late embryogenesis (LEA) (SGN-U143432)
TTCTCAGCAGGCGTGGAT; CCTTTTGCTACACCGGA AAC

3. Results and discussion

3.1. Microarray expression profiling

The development of tomato fruit is the result of several physiological changes controlled by hormonal and environmental signals. At the genetic level, metabolic changes during ripening are assumed to be due to variations in the gene expression patterns that lead to the constitution of the ripe phenotype.

Taking the green leaf tissue (L) as reference, we have monitored the gene expression at the immature green (I), breaker (B) and mature (M) stages.

Each expression profiling analysis was carried out using different replications. One (‘‘dye swap’’) consisted in swapping the Cy3 and Cy5 dyes between reference (L) and test (I, B and M) RNAs, in order to minimize artefacts due to different efficiencies in dye incorporation or detection. The other replications (‘‘biological replicas’’) used RNA samples extracted from different tomato plants and a different labelling protocol, as described in Section 2. A total of six replicate hybridizations (three biological replicas, each with two dye swaps) have been run and analyzed for each of the comparisons (I/L, B/L, M/L, respectively), resulting in 18 hybridized slides. Following the scanning, intensity dependent normalizations (LOWESS) have been applied to raw data (see Section 2).

We have selected good quality spots imposing a minimal signal/noise ratio of 3.0. Only selected spots present in at least three out of the six hybridized slides of a single experiment (I/L, B/L and M/L) were considered for further analysis.

In order to identify transcripts that were differentially regulated in all fruit stages versus leaf, spots showing up- or downregulation of at least two-fold between test and reference were considered significant only when the corresponding CV among replicate slides was <50% (Fig. 1, Table 1).

The terms up- and downregulation will be used hereinafter to designate significant transcript accumulation disparity between test and reference samples though we are aware that given the developmental divergence between fruit and leaf tissues, variation in gene expression pattern are not in obvious correlation.

Stage-specific comparisons allow to draw a general picture of the metabolic pathways more affected during ripening as shown in Fig. 2.

Most of the genes involved in photosynthetic metabolism appear to be downregulated in fruits (I/F 18%, B/F 14%, M/F 18% of all the downregulated genes), while genes involved in energy pathways, hormone responses and protein biosynthesis/degradation are mostly upregulated. The increased expression of the latter set of genes is probably correlated to a considerable increase of protein synthesis or turnover during fruit development and, consequently, with a greater need for molecular chaperones, required for the correct folding of native proteins (Fig. 2).

The majority of transcripts encoding putative light regulated genes involved in photosynthetic machinery are down-regulated in fruits (Fig. 2), as expected. When considering genes involved in perception and transduction pathways of light signals, we observe that many of the corresponding spots over the TOM 1 microarray did not pass the quality control settings, mainly because the spot intensities were not sufficiently high (data not shown). However, passed spots did not show appreciable gene expression differences between test and reference samples (Supplementary data).

Nevertheless, the functional role of a great number of up- and downregulated sequences with unassigned identity remains to be investigated. Since no significant blast hits were obtained for these EST sequences, it is plausible that some of this genes encode tomato-specific proteins with particular roles in fruit development (Fig. 2).

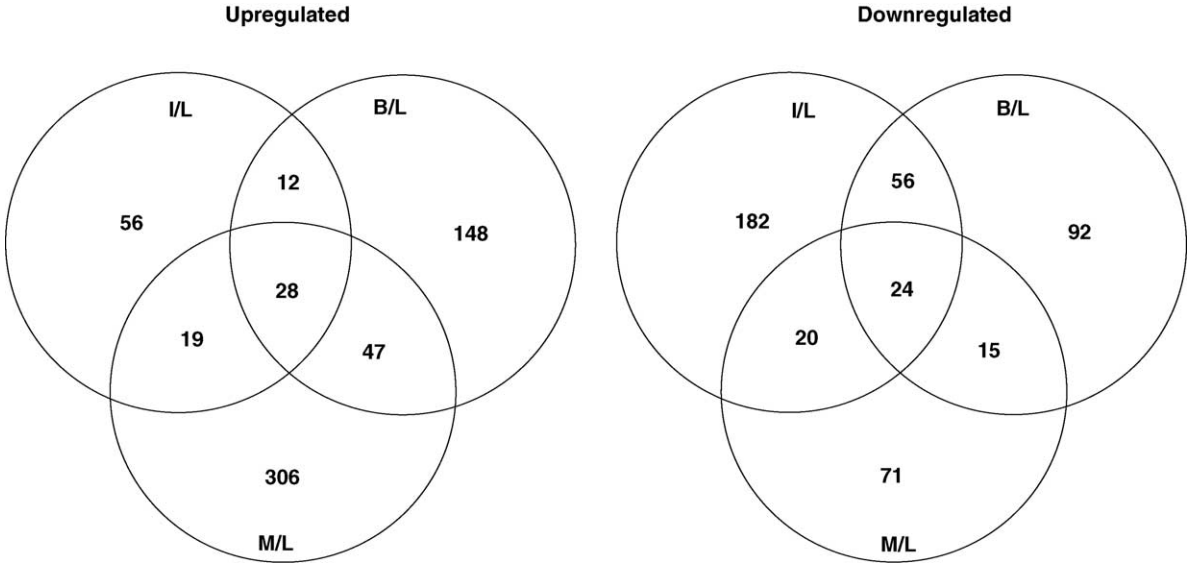

Fig. 1. Venn diagram of upregulated and downregulated transcripts in immature (I), breaker (B) and mature red (M) tomato fruit compared to leaf (L).

Table 1
Putative genes upregulated simultaneously in I, B and M fruit stages in comparison to leaf tissues

Array id	Immature			Breaker			Mature			Annotation	QRT-PCR
	Mean ratio	S.D.	CV	Mean ratio	S.D.	CV	Mean ratio	S.D.	CV		
1-1-5.2.2.2	9.53	3.34	35.01	2.27	1.03	45.45	2.07	0.97	47.01	Acyl-CoA-binding protein (ACBP)	
1-1-5.4.15.16	2.59	1.13	43.67	3.97	0.05	23.03	4.32	1.85	42.71	ADP-ribosylation factor	
1-1-2.3.4.17	2.22	0.95	42.52	2.01	0.73	36.50	2.03	0.62	30.61	Calmodulin PCM2/PCM4/PCM5/PCM6/PCM7/PCM8-potato	
1-1-7.3.9.5	2.84	1.09	38.29	2.40	0.62	25.76	3.44	1.21	35.33	Disease resistance protein kinase (EC 2.7.1.) Pto - tomato	
1-1-5.2.1.10	2.06	0.40	19.16	4.22	2.10	49.72	3.01	0.97	32.21	Expressed protein [*Arabidopsis thaliana*]	
1-1-3.1.13.3	2.67	1.14	42.71	3.29	1.40	42.64	4.02	1.53	38.07	Expressed protein [*Arabidopsis thaliana*]	
1-1-4.1.16.7	2.98	1.10	36.95	5.57	2.08	37.25	13.20	4.39	33.27	Fructose-bisphosphate aldolase [*Persea americana*]	Yes
1-1-4.2.17.1	3.98	1.44	36.12	3.34	0.66	19.00	2.07	0.62	29.81	Glycosyltransfeerase family 8 [*Arabidopsis thaliana*]	
1-1-1.3.2.10	12.28	3.63	29.59	25.45	12.65	49.71	18.80	7.15	38.00	Induced stolen tip protein tubs	
1-1-5.4.6.8	13.62	6.17	45.35	18.92	8.89	47.01	9.38	4.64	49.46	Induced stolen tip protein tubs	
1-1-8.1.20.21	5.75	2.36	40.97	2.15	0.99	46.08	2.06	0.60	28.95	Late-embryogenesis protein homolog - tomato	Yes
1-1-4.1.9.3	2.04	0.82	40.12	2.17	0.90	41.46	2.86	1.03	35.92	No sequence	
1-1-5.1.10.19	2.42	0.84	34.85	2.08	0.60	28.67	2.90	0.91	31.57	No sequence	
1-1-1.3.9.14	2.87	1.18	41.29	3.03	1.16	38.41	2.30	1.06	45.97	No sequence	
1-1-8.2.6.20	3.40	1.42	41.77	2.18	0.69	31.74	4.71	2.00	42.30	No sequence	
1-1-2.1.17.4	3.62	1.46	40.21	2.45	0.88	36.03	2.85	1.29	45.28	No sequence	
1-1-2.4.9.5	4.19	2.03	48.48	2.55	0.51	19.81	3.90	1.74	44.63	No sequence	
1-1-2.1.10.21	5.29	0.80	15.05	6.72	2.44	36.29	4.92	1.75	35.52	No sequence	
1-1-7.3.9.4	2.58	1.06	41.19	2.98	1.45	48.50	5.87	2.25	38.27	Outer membrane lipo protein - like [*Arabidopsis thaliana*]	
1-1-3.1.12.11	2.21	1.02	46.27	2.07	0.91	44.04	3.16	1.52	48.05	Phosphoglycerate kinase; cytosolic	
1-1-1.4.9.15	2.04	0.61	30.11	18.80	8.53	45.38	6.90	3.24	46.92	Phytoene synthase 1; chloroplast precursor (fruit ripening specific protein p TOM5)	
1-1-7.2.8.7	5.65	2.68	47.56	6.86	2.92	42.48	4.97	2.06	41.49	Phytoene synthase 1; chloroplast precursor (fruit ripening specific protein pTOM5)	Yes
1-1-6.2.14.11	2.25	1.11	49.19	2.07	0.47	22.60	3.36	1.41	41.91	Ribosomal Pr 117 [*Triticum aestivum*]	
1-1-6.1.2.14	2.80	1.31	46.84	2.97	1.44	48.61	5.43	2.41	44.35	Ribosomal protein L 11-like [*Nicotiana tabacum*]	
1-1-6.2.9.7	4.93	1.70	34.58	2.25	0.37	16.36	2.87	1.35	47.23	Ribosomal protein L27a [*Petunia × hybrida*]	
1-1-3.1.9.8	2.19	0.76	34.73	2.55	0.68	26.46	4.58	1.83	39.96	Ribosomal protein L33 [*Castiinea sativa*]	
1 1-3.4.2.13	3.03	1.25	41.25	3.56	1.55	43.65	2.05	0.83	40.43	Ribosomal protein S26; cytosolic [imported] – garden pea	
1-1-2.3.10.19	3.02	1.12	37.03	3.93	1.77	45.12	2.38	0.92	38.7l	Ubiguitin conjugating protein [*Avicennia marinal*]	

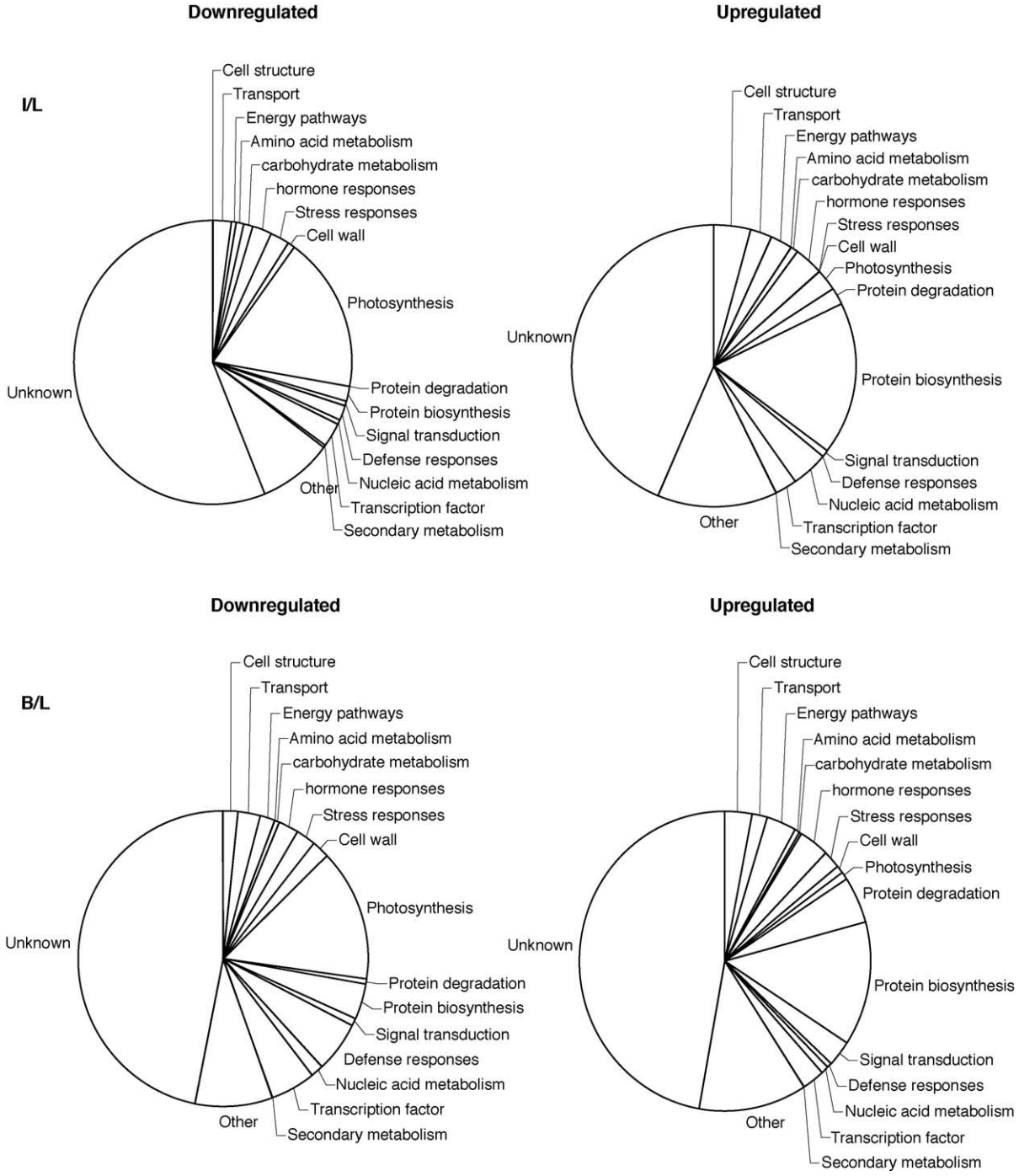

Fig. 2. Graphical representation of upregulated and downregulated genes, grouped by putative functional categories. I/L = immature vs. leaf; B/L = breaker vs. leaf; M/L = mature vs. leaf.

3.2. Fruit-induced genes

We have selected 28 fruit upregulated spots (Fig. 1) that correspond to 26 putative genes, since two spots are constituted by redundant genetic information (Table 1).

Notably, transcripts which share significant homology with the gene encoding fructose-bisphosphate aldolase (array id: 1-1-4.1.16.7) are upregulated. The above-mentioned enzyme is known to play a major role in the biosynthesis of volatile compounds [21]. Therefore, the higher transcript levels in the ripening fruits could eventually lead to the synthesis of aroma- and flavour-related compounds in red ripe tomato (Table 1).

The largest group of fruit upregulated genes is constituted by putative ribosomal protein encoding genes. We have found five different ribosomal protein genes, corresponding to 18% of all the upregulated genes (array id: 1-1-6.2.9.7, 1-1-6.2.14.11, 1-1-6.1.2.14, 1-1-3.1.9.8, 1-1-3.4.2.13). These

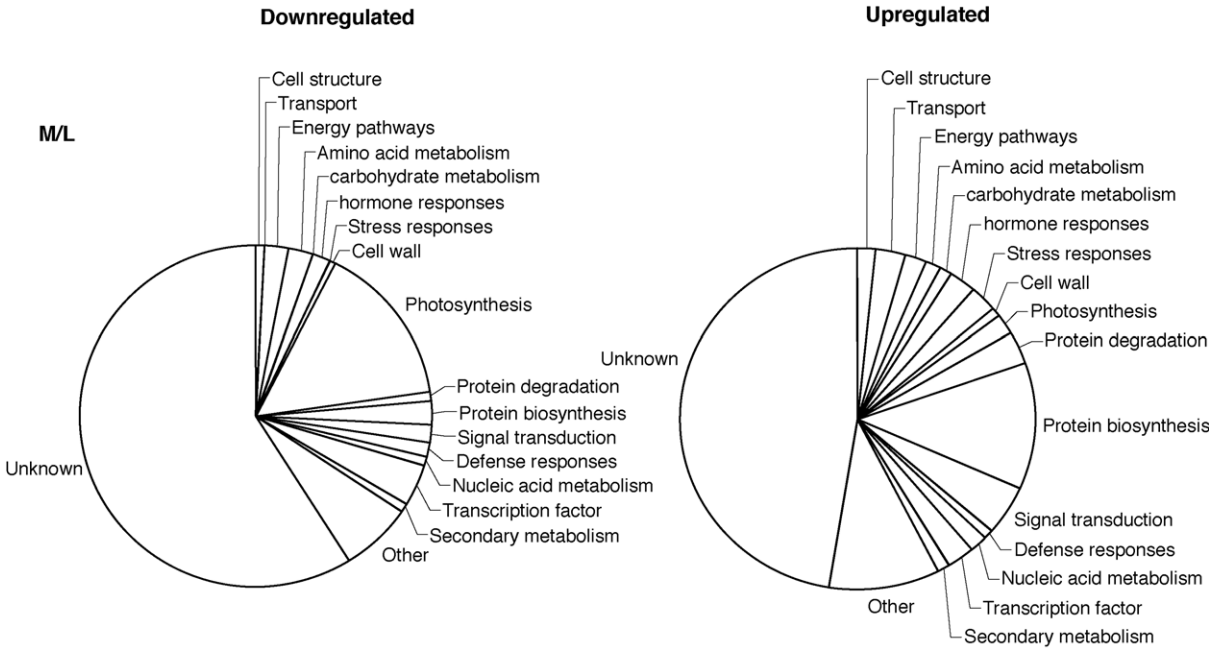

Fig. 2. (*Continued*).

results, together with the upregulation of ubiquitin-conjugating enzyme transcripts (array id: 1-1-2.3.10.19) suggests that these proteins are probably required for the high protein turnover existing in the ripening fruit, partly due to the activation of ubiquitin-dependent proteolytic systems [22]. The incremented metabolic activity in the ripening fruit could also account for the upregulation of transcripts related to cytoskeleton (array id: 1-1-1.3.2.10, 1-1-5.4.6.8) and energy production/carbohydrate-lipid metabolism (array id: 1-1-4.1.16.7, 1-1-3.1.12.11, 1-1-5.2.2.2).

We have also detected the upregulation of phytoene synthase 1 (*Psy1*) putative gene (array id: 1-1-7.2.8.7, 1-1-4.9.15) (Table 1) which is involved in carotenoid and ABA biosynthesis [23,24].

In the relevant section we will discuss in further detail the expression pattern of *Psy1* and other genes involved in carotenoid biosynthesis pathway.

The upregulation of some transcripts is not easily explainable, such as that of genes encoding a late embryogenesis protein homolog (LEA, array id: 1-1-8.1.20.21) (Table 1). Moreover, remains to be further investigated the functional role of as many as nine transcripts, about one third of the total upregulated ones, which do not share significant similarity with any known gene (array id: 1-1-5.2.1.10, 1-1-3.1.13.3, 1-1-4.1.9.3, 1-1-5.1.10.19, 1-1-1.3.9.14, 1-1-8.2.6.20, 1-1-2.1.17.4, 1-1-2.4.9.5, 1-1-2.1.10.21) (Table 1).

To confirm the microarray expression data, we performed (QRT-PCR) experiments on 4 transcripts, of the 28 transcripts found to be upregulated in all fruit stages (Table 1). Such analyses confirmed the upregulation of fructose-bisphosphate aldolase, ubiquitin-conjugating enzyme and Late embryogenesis and LEA transcripts at all fruit stages, while Phytoene synthase 1 transcripts, in contrast to microarray data, did not show any upregulation in the immature green stage (Table 2A).

QRT-PCR has also been used to verify fruit versus leaf expression of four additional transcripts that, though

Table 2
QRT-PCR quantification of expression of genes upregulated in microarray experiments. A, B: see text for details

	Gene	Relative expression level		
		Immature vs. leaf	Breaker vs. leaf	Mature vs. leaf
A	Ubiquitin-conjugating protein (SGN-U143513)	159.81 ± 27.95	191.28 ± 10.56	41.22 ± 29.15
	Fructose-bisphosphate aldolase (SGN-U143932)	13.14 ± 0.75	25.94 ± 4.06	63.54 ± 17.88
	Late embryogenesis (LEA) (SGN-U143432)	63.46 ± 15.72	5.11 ± 2.61	1.80 ± 0.88
	Phytoene synthase 1 (X60441)	0.75 ± 0.02	117.84 ± 3.25	203.81 ± 12.48
B	Pectinesterase 1 (SGN-U143700)	5685.54 ± 1213.75	8190.69 ± 1948.69	3772.21 ± 1133.71
	Alcohol dehydrogenase 2 (SGN-U143271)	88.68 ± 5.21	296.90 ± 55.29	697.58 ± 34.39
	2-oxoglutarate-dependent dioxygenase (SGN-U155526)	13.73 ± 2.39	49.32 ± 2.28	53.86 ± 2.84
	Glutarnine synthetase (SGN-U146805)	4.97 ± 0.97	9.60 ± 2.98	5.76 ± 1.38

Data are normalized for the actin transcript.

represented by mostly upregulated spots over the TOM 1 microarray were not considered since CV value among replicate experiments was grater than 50% (Supplementary data and Table 2B). Indeed, putative pectinesterase 1 (array id: 1-1-3.3.17.12, 1-1-7.1.3.6, 1-1-8.2.8.14), alcohol dehydrogenase 2 (array id: 1-1-4.3.1.2, 1-1-5.1.4.2, 1-1-5.3.3.12, 1-1-7.3.20.8, 1-1-8.2.16.17), 2-oxoglutarate-dependent dioxygenase (array id: 1-1-2.3.13.14, 1-1-3.4.15.7, 1-1-4.4.9.19) and glutamine synthetase (array id: 1-1-2.2.14.12) transcript upregulation has been confirmed by QRT-PCR essays (Supplementary data and Table 2B).

In conclusion, the QRT-PCR analysis has widely confirmed the upregulations found in microarray experiments, suggesting that genes actually upregulated in all fruit stages versus leaf could be more than those selected by our criteria. The stringency of microarray analysis criteria could partially explain the fact that fruit upregulated genes listed in Table 1 are represented by one or a few array IDs, though some of them are actually present in more microarray positions as different EST clones of a same contig assembly (http://sgn.cornell.edu). Whatever the case, the upregulation of the genes listed in Tables 1 and 2 is confirmed by QRT-PCR analysis in the vast majority of the cases tested. Previous reports also confirm that some of the listed genes are highly expressed in fruits [4,21,23,25,26].

We note that, in contrast to our RNA expression data (Table 2B), glutamine synthetase enzyme activity has been shown to decrease at both B and M stages [27]. This apparent contrast between mRNA levels and enzymatic activity would imply that the latter could be regulated by a post-transcriptional mechanism.

In conclusion, to better understand the molecular and regulatory mechanisms that are established since the early stages of the fruit biogenesis and that are still active in the red ripe tomato, many of the genes listed in Table 1 deserve a deeper functional characterization. In this regard it is fundamental to investigate the open reading frames of unknown function (Table 1).

3.3. Quantitative real time RT-PCR of genes involved in light perception and related responses during fruit ripening

Despite the over 12,000 EST sequences present in the TOM1 microarray that in principle allow sub-genomic scale transcriptome monitoring, microarray data analysis was not able to resolve with sufficient accuracy the transcription profile of more than 50% of the spotted genes. Many genes involved in signal perception/transduction have mRNA levels that are at the limit of microarray detection, or are absent from the TOM1 microarray.

Former studies have confirmed that light quantity and quality is very important for the induction of fruit pigment synthesis in tomato. In particular, lycopene accumulation is stimulated by both phytochrome and cryptochrome action [17,28]. Therefore, in order to better investigate effect of light in tomato fruit development and ripening, comparative profiling QRT-PCR experiments were carried out to measure the transcript level changes of structural genes of the carotenoid biosynthesis pathway and of genes involved in light signal transduction at different fruit stages (Tables 3 and 4).

3.4. Carotenoids

We have designed primers (see Section 2) to analyze the expression of twelve structural genes of the carotenoid pathway by QRT-PCR (Table 3). Carotenoid synthesis starts with the formation of phytoene from condensation of two molecules of geranylgeranyl pyrophosphate by PSY and proceeds with subsequent desaturation and isomerization steps to yield all-*trans* lycopene. Lycopene is then converted into either ε/ε+β-ring carotenes or β-β-ring xanthophylls.

Fruits of tomato accumulate lycopene as the major carotenoid pigment, beta-carotene to a lesser extent, and traces of xanthophylls. Fruit ripening is the result of dramatic changes from the I stage, with photosynthetically active chloroplasts, to the M stage, characterized by the

Table 3
QRT-PCR quantification of expression of genes encoding enzymes of the carotenoid biosynthesis pathway

	Relative expression level		
Gene	Immature vs. leaf	Breaker vs. leaf	Mature vs. leaf
Phytoene synthase 1 (X60441)	0.75 ± 0.02	117.84 ± 3.25	203.81 ± 12.48
Phytoene synthase 2 (L23424)	0.26 ± 0.00	0.16 ± 0.01	0.25 ± 0.00
Phytoene desaturase (M88683)	0.36 ± 0.01	1.13 ± 0.18	1.68 ± 0.15
Zeta-carotene desaturase (AF195507)	0.07 ± 0.02	0.41 ± 0.08	0.88 ± 0.24
Carotene isomerase (AF416727)	0.17 ± 0.05	2.38 ± 0.12	11.43 ± 0.07
Lycopene beta cyclase (X86452)	0.21 ± 0.03	0.16 ± 0.01	0.13 ± 0.02
Lycopene epsilon cyclase (Y14387)	0.05 ± 0.01	0.01 ± 0.00	0.00 ± 0.00
Lycopene cyclase B (Y18297)	2.48 ± 0.70	2.26 ± 0.12	2.87 ± 0.61
Carotene hydroxylase 1 (Y14809)	1.09 ± 0.16	1.28 ± 0.16	1.90 ± 0.38
Carotene hydroxylase 2 (Y14810)	0.53 ± 0.05	0.57 ± 0.06	0.59 ± 0.05
Zeaxanthin epoxidase (Z83835)	0.03 ± 0.01	0.03 ± 0.02	0.10 ± 0.04
Violaxanthin de-epoxidase (AF385366)	0.21 ± 0.01	0.40 ± 0.04	0.15 ± 0.05

Data are normalized for the actin transcript.

Table 4
QRT-PCR quantification of expression of genes encoding blue/red/far-red light photo receptors and regulators of light signalling in plants

Gene	Relative expression level		
	Immature vs. leaf	Breaker vs. leaf	Mature vs. leaf
Cop1 (AF029994)	0.22 ± 0.00	0.27 ± 0.00	0.08 ± 0.00
Hy5 (SGN-U221674)	10.09 ± 3.59	62.02 ± 19.95	22.90 ± 9.48
Phototropin1 (SGN-U216278)	0.40 ± 0.10	0.26 ± 0.01	1.17 ± 0.20
Cryptochrome1A (AF130424)	0.99 ± 0.01	1.61 ± 0.43	2.81 ± 0.50
Cryptochromel B (AF348462)	1.13 ± 0.06	0.19 ± 0.06	0.04 ± 0.00
Cryptochrome 2 (AF130426)	0.67 ± 0.15	0.34 ± 0.28	2.56 ± 0.53
Phytochrome A (AJ001914)	0.57 ± 0.12	1.53 ± 0.19	18.18 ± 0.00
Phytochrome B1 (AJ002281)	0.59 ± 0.01	0.27 ± 0.04	0.81 ± 0.09
Phytochrome B2 (AF122901)	1.59 ± 0.29	1.72 ± 0.54	2.55 ± 0.74
Phytochrome E (AF178571)	0.20 ± 0.6	0.02 ± 0.00	0.01 ± 0.00
Phytochrome F (U32444)	8.81 ± 0.88	10.72 ± 4.23	36.50 ± 11.52

Data are normalized for the actin transcript.

complete development of chromoplasts. The transition from chloroplasts to chromoplasts in fruits visually determines the B stage, marked by the transcriptional activation of carotenoid genes leading to lycopene biosynthesis [23,24].

Psy1 and phytoene desaturase (*Pds*) - two early genes involved in lycopene formation – are clearly upregulated at the B and M stages, in agreement with previous reports [23]. In contrast, the second phytoene synthase (*Psy2*) transcript is downregulated at all fruit developmental stages, confirming its secondary role in fruit carotenogenesis [29,30]. We also found a previously undescribed relative increase of zeta-carotene desaturase (*Zds*) gene expression during ripening, though fruit transcript levels remain below leaf ones. The carotene isomerase (*CrtISO*) gene, controlling the isomerization of zeta-carotene and lycopene from the *cis* to the *trans* form [24], showed a progressive increase at the B and M stages, in agreement with Isaacson et al. [24] (Table 3). The three lycopene cyclase genes, controlling the formation of cyclic carotenoids from lycopene, show different expression profiles: *ε-Lcy* is downregulated, consistent with the trace amounts of the β-ε xanthophyll lutein present in tomato fruit. As for genes involved in β-carotene synthesis, *β-Lcy* is downregulated and *B* is upregulated at all ripening stages with respect to leaf. This contrasts with the hypothesized role of B as a neoxanthin synthase [31] since neoxanthin is a leaf-specific carotenoid. In general, experiment data on lycopene cyclase genes are in agreement with previous findings [32,33,34] demonstrating the complex regulation of carotenoid pathway at lycopene/carotene stage.

The transcription profile for the two carotene hydroxylase (*Chy*) genes indicates that a strict distinction between leaf- and fruit-specific genes cannot be made. Transcript levels of the zeaxanthin epoxidase (*Zep*) and violaxanthin de-epoxidase (*Vde*) genes were found to be constantly lower than those found in leaf (Table 3).

Overall, our investigations on the expression of carotenoid biosynthetic genes indicate an upregulation of the early part of the pathway, leading to the synthesis of the major fruit carotenoid, lycopene, and a downregulation of the later part of the pathway, with the exception of *B*, whose upregulation is probably responsible for the amounts of beta-carotene (5–10% of total carotenoids) found in ripe fruits. These observations are in agreement with tomato fruit ripening physiology.

3.5. Genes involved in light perception and signal transduction

QRT-PCR was also used to measure the transcript levels in fruits and leaves of four genes encoding blue light photoreceptors: phototropin 1 (*Phot1*), cryptochrome 1a (*Cry1A*), cryptochrome 1b (*Cry1B*), and cryptochrome 2 (*Cry2*) [13,14], and five genes coding for red/far-red photoreceptors: phytochrome A (*PhyA*), phytochrome B1 (*PhyB1*), phytochrome B2 (*PhyB2*), phytochrome E (*PhyE*) and phytochrome F (*PhyF*) [14]. In addition, we have analyzed the fruit/leaf relative mRNA abundance of *Cop1* and *Hy5* genes encoding a repressor of the photomorphogenesis and a bZIP transcription factor, respectively. Both genes play key roles as regulators of light signalling in *Arabidopsis* [15] and tomato [35].

Photoreceptor genes were downregulated at the I stage, with the exception of *Cry1A, Cry1B, PhyB2* and *PhyF* (Table 4). Conversely, at the M stage we observed the upregulation of some photoreceptor genes, with the exception of *Cry1B*/*PhyE* (downregulated), and *PhyB1*/*Phot1* (not significantly affected) (Table 4).

Cry1B and *PhyE* genes were found to be strongly downregulated at B and M stages, suggesting that their protein products play a marginal role in fruit ripening. On the other hand, the fact that *PhyB2* and *PhyF* transcripts are preferentially expressed (especially *PhyF*) in ripening fruits, in accord with a previous report [36], may hint a fruit-specific action of these phytochromes (Table 4). These data are in agreement with the decrease in fruit pigmentation observed when the phyB2 mutation is added in a phyA-phyB1 background [37].

Cop1 shows a strong downregulation, while *Hy5* shows a considerable induction at all stages (Table 4). This opposite

trend in transcriptional regulation corresponds to the roles the corresponding gene products play in *Arabidopsis*: many light signalling pathways involve the activation of light-responsive genes via the Hy5 transcription factor. In the dark, the negative regulator of photomorphogenesis Cop1 is able to target Hy5 for degradation, while in the presence of light Cop1 interacts with other proteins, such as Cry photoreceptors (and maybe others), and inhibits this process allowing Hy5 to accumulate and promote photomorphogenic responses [15]. Recently has been shown that Cop1 is also able to repress photoperception signals by targeting the Hfr1 transcription factor for degradation, in dark [38].

This model suggests that the degree of light responsiveness is at least partially dependent on the cellular balance of cryptochrome photoreceptors and Hy5 on one side, and Cop1 on the other. The tomato proteins, LeCry2, LeHy5 and LeCop1LIKE (a Cop1 paralog) have been shown to act as inducers (Cry2 and LeHy5) and repressors (LeCop1LIKE), respectively, of fruit pigmentation [17,35]. Thus, the modulation of transcript abundance we observe, if reflected at the protein level, could play a major role in the modulation of fruit pigmentation, and perhaps of other fruit developmental processes. Whether this fluctuation of transcript abundance reflects actual variations at the protein level, remains to be shown.

On the other hand, the strong induction of PhyA/F-type phytochromes late in fruit development suggests that they may play a role at these stages where the biosynthesis of pigments – especially lycopene – is boosted. The cryptochrome 1 paralog *Cry1B* shows a quite different transcription pattern compared to *Cry1A*. It is downregulated and therefore, presumably does not play a major role in late fruit development. The function of this cryptochrome, which is derived from a recent duplication of *Cry1*, that occurred in tomato, but not in *Arabidopsis* [39] is currently under investigation.

Microarray expression data of putative *Hy5, Phot1* and *Cry1B* spots, when available, did not show significant expression differences in fruit versus leaf experiments (Supplementary data). One possible explanation is that, in the case of *Phot1* and *Cry1B*, specific QRT-PCR oligos were designed using coding sequences (see Section 2) that do not overlap neither with the EST sequences spotted on the array nor with the correspondent unigene assembly. Besides it should be considered that QRT-PCR essays are much more selective compared to cDNA microarrays and are able to detect transcripts from a single element of similar coding sequences.

In conclusion, our results suggest that during tomato fruit development and ripening the transcripts coding for photosensory receptors and light signalling proteins are highly regulated, and that tomato light responsiveness during fruit development may be modulated by these wide fluctuations in transcript abundance.

Acknowledgements

This work was financed by the Italian Ministry of Research (GENEFUN and FIRB projects). We thank F. Giorno for the assistance in the early phase of this work, JJ Giovannoni and Rob Alba for critical reading of the manuscript.

Appendix A. Supplementary data

Supplementary data associated with this article can be found, in the online version, at doi:10.1016/j.plantsci.2005.03.011.

References

[1] M.J.C. Rhodes, The maturation and ripening of fruits, in: K.V. Thimann, F.L. Boca Raton (Eds.), Senescence in Plants, CRC Press, 1980, pp. 157–205.
[2] G.B. Seymour, J.E. Taylor, G.A. Tucker, Biochemistry of Fruit Ripening, Chapman and Hall, London, New York, 1993.
[3] J.M. Lelievre, A. Latche, B. Jones, M. Bouzayen, J.C. Pech, Ethylene and fruit ripening, Physiol. Plant 101 (1997) 727–739.
[4] J. Giovannoni, Molecular biology of fruit maturation and ripening, Annu. Rev. Plant Physiol. Plant. Mol. Biol. 52 (2001) 725–749.
[5] L. Alexander, D. Grierson, Ethylene biosynthesis and action in tomato: a model for climacteric fruit ripening, J. Exp. Bot. 53 (2002) 2039–2055.
[6] P.H. Gann, F. Khachik, Tomatoes or Lycopene versus prostate cancer: is evolution anti-reductionist? J. Nat. Cancer Inst. 95 (2003) 1563–1565.
[7] C. Somerville, S. Somerville, Plant functional genomics, Science 285 (1999) 380–383.
[8] G.E. Bartley, B.K. Ishida, Digital fruit ripening: data mining in the tigr tomato gene index, Plant Mol. Biol. Rep. 20 (2002) 115–130.
[9] M. Schena, D. Shalon, R.W. Davis, P.O. Brown, Quantitative monitoring of gene expression patterns with a complimentary DNA microarray, Science 270 (1995) 467–470.
[10] S. Moore, J. Vrebalov, P. Payton, J. Giovannoni, Use of genomics tools to isolate key ripening genes and analyse fruit maturation in tomato, J. Exp. Bot. 53 (2002) 2023–2030.
[11] Z. Fei, X. Tang, R.M. Alba, J.A. White, C.M. Ronning, G.B. Martin, S.D. Tanksley, J.J. Giovannoni, Comprehensive EST analysis of tomato and comparative genomics of fruit ripening, Plant J. 40 (2004) 47–59.
[12] H. Smith, Phytochromes and light signal perception by plants—an emerging synthesis, Nature 407 (2000) 585–591.
[13] C. Lin, D. Shalitin, Cryptochrome structure and signal transduction, Ann. Rev. Plant Biol. 54 (2003) 469–496.
[14] E. Liscum, D.W. Hodgson, T.J. Campbell, Blue light signalling through the cryptochromes and phototropins. so that's what the blues is all about, Plant Physiol. 133 (2003) 1429–1436.
[15] P. Gyula, E. Schafer, F. Nagy, Light perception and signalling in higher plants, Curr. Opin. Plant Biol. 6 (2003) 446–452.
[16] E.V. Wann, E.L. Jourdain, R. Pressey, B.G. Lyon, Effect of mutant genotypes hp ogc and dg ogc on tomato fruit quality, J. Am. Soc. Hortic. Sci. 110 (1985) 212–215.
[17] L. Giliberto, G. Perrotta, P. Pallara, J.L. Weller, P.D. Fraser, P.M. Bramley, A. Fiore, M. Tavazza, G. Giuliano, Manipulation of the blue light photoreceptor Cryptochrome 2 in tomato affects vegetative

development, flowering time, and fruit antioxidant content, Plant Physiol. 137 (2005) 199–208.
[18] J. Sambrook, E.F. Fitsch, T. Maniatis, Molecular Cloning: A Laboratory Manual, Cold Spring Harbor Press, Cold Spring Harbor, 1989.
[19] R. Lopez-Gomez, M.A. Gomez-Lim, A method for extracting intact RNA from fruits rich in polysaccharides using ripe mango mesocarp, Hort. Sci. 27 (1992) 440–442.
[20] W. Cleveland, S. Devlin, Locally weighted linear regression: an approach to regression analysis by local fitting, J. Am. Stat. Assoc. 83 (1988) 596–609.
[21] W. Schwab, A. Aharoni, T. Raab, A. Garcia Perez, C. Sanz, Citosolic aldolase is a ripening related enzyme in strawberry fruits (Fragaria × ananassa), Phytochem 56 (2001) 407–415.
[22] C. Ingvardsen, B. Veierskov, Ubiquitin- and proteasome-dependent proteolysis in plants, Physiol. Plant 112 (2001) 451–459.
[23] G. Giuliano, G.E. Bartley, P.A. Scolnik, Regulation of carotenoid biosynthesis during tomato development, Plant Cell 5 (1993) 379–387.
[24] T. Isaacson, G. Ronen, D. Zamir, J. Hirschberg, Cloning of tangerine from tomato reveals a carotenoid isomerase essential for the production of beta-carotene and xanthophylls in plants, Plant Cell 14 (2002) 333–342.
[25] J. Speirs, E. Lee, K. Holt, K. Yong-Duk, N.S. Scott, B. Loveys, W. Schuch, Genetic manipulation of alcohol dehydrogenase levels in ripening tomato fruit affects the balance of some flavor aldehydes and alcohols, Plant Physiol. 117 (1998) 1047–1058.
[26] J. Gray, S. Picton, J. Shabbeer, W. Schuch, D. Grierson, Molecular biology of fruit ripening and its manipulation with antisense genes, Plant Mol. Biol. 19 (1992) 69–87.
[27] S.B. Boggio, J.F. Palatnik, H.W. Heldt, E.M. Valle, Changes in amino acid composition and nitrogen metabolizing enzymes in ripening fruits of Lycopersicon esculentum Mill, Plant Sci. 159 (2000) 125–133.
[28] R. Alba, L.M.M. Cordonnier-Pratt, L.H. Pratt, Fruit-localized phytochromes regulate lycopene accumulation independently of ethylene production in tomato, Plant Physiol. 123 (2000) 363–370.
[29] G.E. Bartley, P.A. Scolnik, cDNA cloning, expression during development, and genome mapping of PSY2, a second tomato gene encoding phytoene synthase, J. Biol. Chem. 268 (1993) 25718–25721.
[30] P.D. Fraser, J.W. Kiano, M.R. Truesdale, W. Schuch, P.M. Bramley, Phytoene synthase-2 enzyme activity in tomato does not contribute to carotenoid synthesis in ripening fruit, Plant Mol. Biol. 40 (1999) 687–698.
[31] F. Bouvier, A. D'Harlingue, R. Backhous, M.H. Kumagai, B. Camara, Identification of neoxanthin synthase as a carotenoid cyclase paralog, Eur. J. Biochem. 267 (2000) 6346–6352.
[32] G. Ronen, M. Cohen, D. Zamir, J. Hirschberg, Regulation of carotenoid biosynthesis during tomato fruit development: expression of the gene for lycopene epsilon-cyclase is down-regulated during ripening and is elevated in the mutant Delta, Plant J. 17 (1999) 341–351.
[33] G. Ronen, L. Carmel-Goren, D. Zamir, J. Hirschberg, An alternative pathway to beta-carotene formation in plant chromoplasts discovered by map-based cloning of beta and old-gold color mutations in tomato, Proc. Natl. Acad. Sci. 97 (2000) 11102–11107.
[34] I. Pecker, R. Gabbay, F.X. Cunningham, J. Hirschberg, Cloning and characterization of the cDNA for lycopene beta-cyclase from tomato reveals decrease in its expression during fruit ripening, Plant Mol. Biol. 30 (1996) 807–819.
[35] Y. Liu, S. Roof, Z. Ye, C. Barry, A. van Tuinen, J. Vrebalov, C. Bowler, J. Giovannoni, Manipulation of light signal transduction as a means of modifying fruit nutritional quality in tomato, Proc. Natl. Acad. Sci. USA 101 (2004) 9897–9902.
[36] B.A. Hauser, L.H. Pratt, M.M. Cordonnier-Pratt, Absolute quantification of five phytochrome transcripts in seedlings and mature plants of tomato (Solanum lycopersicum L.), Planta 201 (1997) 379–387.
[37] J.L. Weller, M.E. Schreuder, H. Smith, M. Koornneef, R.E. Kendrick, Physiological interactions of phytochromes A, B1 and B2 in the control of development in tomato, Plant J. 24 (2000) 345–356.
[38] J. Yang, R. Lin, J. Sullivan, U. Hoecker, B. Liu, L. Xu, X.W. Deng, H. Wang, Light regulates COP1-mediated degradation of HFR1, a transcription factor essential for light signaling in arabidopsis, Plant Cell 17 (2005) 804–821.
[39] G. Perrotta, G. Yahoubyan, E. Nebuloso, L. Renzi, G. Giuliano, Tomato and barley contain duplicated copies of cryptochrome 1, Plant Cell Environ. 24 (2001) 991–997.

3.2 Development of molecular and biochemical tools to investigate fruit quality traits in strawberry elite genotypes

We have analyzed gene expression alterations in red ripe fruits in five cultivated strawberry genotypes (*Fragaria x ananassa* Duch.) which show striking differences for several fruit quality traits.

A strawberry cDNA microarray was constructed with 3573 expressed sequence tags (ESTs) selected from a fruit EST collection previously made in our lab. cDNA microarray comparative profiling experiments were carried out using cultivar (cv) Queen Elisa, which show outstanding fruit quality and yield capacity, as our reference genotype. Thus total RNA extracted from Queen Elisa red fruits has been compared to RNA extracted from its parental genotypes (Miss and USB35) as well as to the RNA extracted from red fruits of cv Maya and Onda, respectively. Data selected from microarray experiments were further validated by Real-Time reverse transcription PCR analyses.

The results are shown in the following attached paper (Carbone et al., 2006).

Mol Breeding (2006) 18:127–142
DOI 10.1007/s11032-006-9017-2

Development of molecular and biochemical tools to investigate fruit quality traits in strawberry elite genotypes

Fabrizio Carbone · Fabienne Mourgues · Franco Biasioli · Flavia Gasperi · Tilmann D. Märk · Carlo Rosati · Gaetano Perrotta

Received: 21 September 2005 / Accepted: 22 April 2006 / Published online: 17 August 2006

Abstract Molecular and biochemical studies were undertaken to elucidate gene/product relationships which influence key fruit quality traits in cultivated strawberry (*Fragaria* × *ananassa* Duch.). Comparative transcription profiling experiments in selected genotypes pointed out a number of differentially-expressed genes, possibly related to important fruit quality traits as aroma and fruit firmness. Some of the altered cDNAs encode putative cinnamyl alcohol dehydrogenase, cinnamoyl CoA reductase, cellulase and expansin genes, involved in the early steps of lignin biosynthesis and in cell wall structure, respectively. Parallel biochemical analyses studied the spectra of volatile compounds by Proton Transfer Reaction-Mass Spectrometry (PTR-MS) and alcohol acyl transferase (AAT) specific activity in red fruits. A correlation between the expression of an *aat* gene, total AAT activity and the presence of related esters in fruit headspace was found.

Keywords Comparative gene expression profiling · Enzyme assays · Fruit quality · Functional Genomics · Proton Transfer Reaction-Mass Spectrometry

F. Carbone · F. Mourgues · C. Rosati · G. Perrotta (✉)
ENEA, Trisaia Research Center, S.S. 106, km 419+500, 75026 Rotondella, MT, Italy
e-mail: gaetano.perrotta@trisaia.enea.it

F. Biasioli · F. Gasperi
Istituto Agrario di S. Michele all'Adige, Via E. Mach, 2, 38010 S. Michele, TN, Italy

T. D. Märk
Institut für Ionenphysik, Universität Innsbruck, Technikerstr. 25, A-6020 Innsbruck, Austria

Introduction

Cultivated strawberry (*Fragaria* × *ananassa* Duch.) is a popular fruit crop, which provides a source of macronutrients and high levels of antioxidants. Though strawberry varieties typically show limited geographical adaptation capacity, this crop is grown over a wide range of latitudes and environments, which influence important traits as yield and fruit quality. The octoploid background and outbreeding of cultivated strawberry has long discouraged genetic studies. However, genetic maps have been developed for diploid and octoploid *Fragaria* species, using a variety of molecular and morphological markers (Davis and Yu 1997; Lerceteau-Köhler et al. 2003; Sargent et al. 2004). Moreover, strawberry has recently been studied as model non-climateric fruit, especially for genes and processes related to ripening (Aharoni et al. 2000, Aharoni et a1. 2002; Aharoni and O'Connell 2002).

Strawberry fruit ripening produces dramatic changes in fruit firmness, color, taste and aroma, involving the coordinated expression of hundreds of genes. In particular, the full red stage is the most important for both taste and aroma, since it corresponds to the maximum emission of volatile compounds (Ménager et al. 2004) and accumulation of sugars. Firmness and aroma are among the main quality parameters for fruits, the latter being of outmost commercial and industrial relevance for strawberry (Azodanlou et al. 2003). Esters, among the most important constituents of strawberry aroma (Pérez et al. 2002; Azodanlou et al. 2003), are produced via esterification of alcohols in the presence of acyl-CoA by the enzyme alcohol acyl transferase (AAT). Strawberry AAT has been characterized from the biochemical and molecular point of view, and substrate specificity of AAT extracted from different genotypes has been demonstrated (Pérez et al. 1996; Aharoni et al. 2000; Olías et al. 2002).

Early molecular reports on strawberry ripening studied limited sets of genes (e.g., Manning 1998; Nam et al. 1999; Marty et al. 2000). Progress in knowledge and dramatic advances in technology have provided the researchers with tools to evaluate the expression of genome-wide sets of genes (Schadt et al. 2003; Yamada et al. 2003). Despite the still limited knowledge of *Fragaria* genome, also for strawberry the characterization of gene expression has taken advantage of microarray technology (Aharoni et al. 2000; Aharoni et al. 2002; Salentijn et al. 2003). However, multidisciplinary molecular and biochemical research is mandatory to understand the regulatory mechanisms underlying fresh product quality (Fiehn 2002).

In the marketing chain of fresh and processed foods, non-destructive real-time methods have been implemented to monitor quality traits online (e.g., Dorfner et al. 2004; Tsuchikawa and Hamada 2004). Among analytical approaches, Proton Transfer Reaction-Mass Spectrometry (PTR-MS) is a relatively new but established technique where the issue is the fast and sensitive detection of volatile compounds (Lindinger et al. 1998). It is based on a particular implementation of chemical ionization that allows a direct injection of the volatile mixture in the ionization chamber (drift tube) without any pretreatment. Common air constituents are not detected, thus air can be used as carrier gas. The detection of compounds present in amounts as low as few parts per trillion has been reported (Hansel et al. 1999). In food science and technology, PTR-MS combines some of the advantages of time-consuming gas chromatography techniques and other more immediate approaches but either not enough sensitive (e.g., electronic noses) or unsuitable for measuring complex mixtures (e.g., spectroscopic methods). Correlation of PTR-MS data with other analytical techniques (Boscaini et al. 2003) and with sensory data (Gasperi et al. 2001; Biasioli et al. 2006) has been investigated as well as the application to shelf life study of berry fruits (Boschetti et al. 1999). Coupling of PTR-MS anonymous fingerprinting with class modeling and linear discriminant analysis (Biasioli et al. 2003) or artificial neural networks (Mott et al. 2004) provided a tool for the discrimination of strawberry genotypes based on non-destructive analyses of single fruits. Recently, the correlation of PTR-MS spectra with molecular markers has been proposed to find Quantitative Trait Loci (QTLs) related to volatile organic compounds (Zini et al. 2005).

Microarray profiling experiments were carried out to detect differentially-expressed genes in red fruits of five strawberry genotypes. Results of comparative gene expression profiling were consistent with phenotypic differences in fruit firmness, AAT activity and PTR-MS volatile compound spectra, showing the feasibility to study some complex polygenic traits with combined molecular and biochemical approaches.

Materials and methods

Plant material and sampling

Strawberry genotypes used in this study were cultivar (cv) Queen Elisa (QE) and its parentals, selection USB35 (Lateglow × Seneca) and cv Miss [(Comet × Honeoye) × Dana], cv Maya (Design patent UE no 7818) and cv Onda [(78.65.1 × Honeoye) × Marmolada]. Red ripe fruits were harvested from field-grown plants at

Institute for Fruit Breeding (ISF), Cesena, Italy. For molecular analyses, fruits were cut into quarters and immediately frozen at –80°C.

PTR-MS data presented in this work are a subset of the data collected over 2 years (2002–2004) to characterize the fruit quality of strawberry genotypes in northern Italy. Red fruits were harvested and brought the same day to the Istituto Agrario di S. Michele all'Adige laboratories for PTR-MS analyses. Data set A: fruits were collected at ISF collection between May 19th and May 25th. For QE, Miss, and USB35, 10 fruits were analyzed the day after the harvest and after 4 days of storage at 4°C. Data set B: analyses were carried out on fruits of QE and Miss harvested in two locations (Cesena and Verona). Samples were collected on April 29th (Verona, plastic tunnel, 38 fruits), May 9th (Cesena, plastic tunnel, 17 fruits) and May 17th (Cesena, open field, 10 fruits). Data set C: for all genotypes were collected 15 fruits between in May 22nd and May 24th (ISF, open field). Samples were partly stored at room temperature and partly at 4°C. Measurements were carried out 1 day after harvest and after 4 days of storage at room temperature or 4°C. In this study, the evolution of fruit volatile compounds during shelf life was disregarded. Instead, different fruit samples should account for the variability that can be expected for each genotype due to different locations, harvest times, cultivation methods, shelf life and storage conditions.

Nucleic acid manipulations

When not specified, experiments were carried out according to standard procedures (Sambrook et al. 1989). RNA was extracted from fruits according to Lopez-Gomez and Gomez-Lim (1992) with minor modifications.

Construction of a strawberry cDNA microarray

For preparation of DNA microarrays, preparative PCR reactions (50 or 100 µl) were carried out using plasmid DNA extracted from representative EST clones. Purified PCR products were resuspended in 3× SSC at a DNA concentration of 100 ng/µl and printed, in triplicate, using a SpotArray24 (Perkin–Elmer) on GapsII slides (Corning). The resulting microarrays consisted of 5,610 spots, with an inter-spot distance of 300 µm, in 32 sub-arrays. Slide post-processing was carried out by hydration of the spots in a humid chamber followed by UV cross-linking.

Preparation of labeled probes and microarray hybridization

Microarrays were pre-hybridized in 50% formamide buffer at 42°C for 1 h and rinsed briefly in sterile water. RNA labeling was achieved using two different protocols using direct labeling and indirect labeling methods. For each direct labeling reaction, 40 µg of DNA-free total RNA were reverse transcribed using and oligo-dT primer in the presence of Cy3- or Cy5-labelled dUTP using the SuperScript II reverse transcriptase (Invitrogen). Unincorporated nucleotides were eliminated using GFX-PCR columns (Amersham Biosciences) following manufacturer's specifications. The indirect labeling reactions were carried out with 20 µg DNA-free total RNA using Indirect cDNA Labeling System (Invitrogen) following the manufacturer's specifications. Purified Cy3- and Cy5-labelled cDNAs were dried in a speed-vac and resuspended in hybridization buffer (Amersham Bioscience) supplemented with 50% formamide, dispensed over the glass slide and incubated at 42°C overnight with agitation in a water bath. Slides were washed in decreasing SSC concentrations (2×–0.1×) and 0.1% SDS at 42°C and room temperature, respectively. The last wash was carried out in 0.1× SSC at room temperature. Hybridized microarrays were then scanned using the ScanArray Lite (Perkin–Elmer) and the resulting Cy3 and Cy5 images were analyzed with the ScanArray Express (Perkin–Elmer) software in order to measure the Cy3/Cy5 spot intensities.

Microarray data analysis

Raw hybridization signals were filtered by imposing a minimal signal/noise ratio of 3.0 and flagging the non-passed spots. We filtered microarray data imposing good quality spots to be

present in at least three out of four hybridized slides. For Maya/QE and Onda/QE only spots present in both replicate experiments were considered for further analyses. Raw values were then normalized with the locally weighted linear regression (LOWESS) method using 20% of data for smoothing (Cleveland and Devlin 1998).

Quantitative real-time RT-PCR

For quantitative real-time reverse transcription PCR (qRT-PCR) experiments, first strand cDNA was synthesized from 1 μg total RNA in 30 μl with oligo-d$(T)_{17}$ and Superscript II (Invitrogen) according to manufacturer's instructions. The RT mix was diluted to 1:3 and 2-μl aliquots were used for qRT-PCR experiments, carried out with an ABI 7700 instrument, SybrGreen kit (Applied Biosystems cat. 4309155) and Platinum Sybr-Green kit (Invitrogen cat. 11733–046) according to manufacturers' instructions. Quantification was performed using standard dilution curves for each studied gene fragment. Relative gene expression data were obtained by normalizing the transcript level of each gene with that of the housekeeping elongation factor-1 alpha. Comparable data were obtained using another highly expressed EST clone, a type 2 MT-like gene (data not shown).

Gene-specific oligonucleotide primers used in qRT-PCR:

Beta xylosidase 1 (*xyl1*) (AY486104)
GGAGCTAGGGATGGAACTCACA,
TGTTTGCGGCCCATTTTC;
Beta-galactosidase 1 (*beta-gal1*) (AJ278703)
CCATGTCCAAATGTCATGAAGA,
TTCGTGTACTTGAGACTCAGAATCA;
Pectate liase (*pl*) (U63550)
TGATCACAACTCGCTCTCGAA,
GGCAGTAGAACCCATGATAGCA;
Cinnamyl alcohol dehydrogenase (*cad*) (U63534)
GCGTTTAGTCAAAGCAGATGTCA,
GCAGAATTTAAGTGCTAGCCTTCA;
Auxin-regulated (*aux-reg*) (AF041393)
TTGCTAGAAGTGGAGCTTGGTG,
CACAGAGAACCAGGAATAGAAAGGA;
Cinnamoyl CoA reductase (*ccr*) (AY285922)
CAAACCCAAGTCTTGTAGCTTCTG,
CCCACCAAGTTGAAAGATGAT;
Cellulase 1 (*cel1*) (AF051346)
GACAACGTGAAGTTCGGGTTT,
CATGACCCTCCCGAAGTCTATAA;
O-methyltransferase (*omt*) (CO381730)
CAGCCAACTTTCATCGATATCCT,
CATCCACATGGCAGCCAAACT;
Cystein protease (*cysp*) (CO380301)
CTGTTCTTGCTGTTGGGTATGG,
CCAGCTTTGTCCCCAAGAGTT;
Alcohol acyl transferase (*aat*) (AF193789)
GAATCTGCAAGTTGCAAGTTCATAA,
TCTTCTTCTAGATTCACCCACGC;
Expansin 4 (*exp4*) (AF226701)
GAGCAATGTGCTGGAATACA,
CCCTAACAATGCTGGGGGA;
Expansin 1 (*exp1*) (AF163812)
CGCTTGCTTCGAGATCAAG,
ATGGAGGGCTTTCCGGCA;
Expansin 2 (*exp2*) (AF159563)
CAGCACTTCGATTTGGCCG,
ACACAAGCAACTCTTCTGAAT.

PTR-MS analyses

For this study, two commercial PTR-MS instruments (Ionicon Analytik, Innsbruck) were used: a high-sensitivity version with an additional pumping stage to increase sensitivity and reduce background for data set A and C; a standard setup for set B. Fruit measurements were performed as described by Biasioli et al. (2003). Briefly, single whole fruits were placed in a glass vessel (400 ml) at room temperature for 1 h, to allow the saturation of the vessel with emitted volatiles. Then, the headspace mixture was directly injected for 4 min at 9.3 cm^3/min at atmospheric pressure. This corresponds to five complete spectra from mass/charge ratio (m/z) = 20 to m/z = 240. Spectral intensities in counts per seconds (cps) were converted into concentration (ppm or ppb) using the relation reported by Lindinger et al. (1998) with a reaction constant $k = 2 \times 10^{-9}$ cm^3/s. Absolute comparison with data published elsewhere must take into account the actual value of k for each compound (Lindinger et al. 1998). To avoid spurious effects, a dummy sample was measured at the beginning of each measuring session and measurement order was randomized.

Preliminary measurements and data published by Buhr et al. (2002) on the fragmentation of alcohols, aldehydes, ketones and esters indicate that the m/z ratio corresponding to the molecular ions of esters (75, 89, 103, 117, 131, 145,159, 173, ... = 75 + 14n) are not present in the fragmentation of the other considered classes. Moreover, among esters, only acetates produce a significant fragment at m/z = 61. Therefore, the signal at m/z = 75 + 14n was considered as a measure of the concentration of esters in the headspace of the strawberry samples and m/z = 61 as an indication of the presence of acetate esters.

AAT enzyme assays

All reagents were purchased from Sigma or Fluka. Frozen red fruits were ground to a fine powder in liquid nitrogen and dispersed (1:2 w/v) in extraction buffer (0.5 M Tris–HCl pH 8.0, 0.2% Triton X-100, 10% glycerol). Crude enzyme extracts were obtained by filtration and centrifugation (15,000 *g*, 20 min) and either used directly or flash-frozen in liquid nitrogen for subsequent tests. Proteins were quantified using the Bradford reagent (Bradford 1976) using BSA as standard.

Standard assay mixtures (285 µl) contained 0.5 M Tris–HCl (pH 8.0), 4.5 mM $MgCl_2$, 130 µM Acetyl CoA, 3.5 mM alcohol substrate (1-butanol, 1-octanol or 1-decanol) and crude enzyme extract (5 µg total proteins). The mixture was incubated at 35°C for 30 min, then 10 µl of 10 mM 5,5-dithiobis(nitrobenzoic acid) (DTNB) were added. The kinetics of increased absorbance at 412 nm, due to the formation of yellow thiophenol by the reaction of DTNB with the free HS-CoA, was recorded over 20 min using a spectrophotometer (Beckman Coulter DU-70). AAT specific activity was calculated according to Li et al. (2006) and AAT relative activity was determined taking USB35 values obtained in octanol assays = 100%.

Results

QE was chosen as reference variety in gene expression experiments for its outstanding characteristics. Main fruit quality and plant yield data characterizing the studied genotypes are resumed in Table 1 (W. Faedi et al., personal communication).

Microarray expression profiling

A cDNA microarray of more than 5,600 spots was produced by selecting fruit EST sequences from an annotated database available at http://fragariaest.trisaia.enea.it/. Two representative EST clones for each contig (to give an intra-array replicate) and the unique clone for singletons were tentatively processed. Successful preparative amplifications were obtained from 1,811 clones of which 1,193 from singleton clones. The final microarray layout contained 5,610 spots representing 1,811 EST clones, 49 ripening-related genes already available in public databases (GCxx clone codes) and 10 genes used as negative controls (spot report alien cDNA kit, Stratagene), all spotted in triplicate.

Taking QE as reference, we have monitored the gene expression of its parentals USB35 and Miss. Each expression profiling analysis was carried out using different replicates. One (''dye swap'') consisted in swapping the Cy3 and Cy5 dyes between reference and test RNAs. A second replicate experiment was performed using different RNA samples.

In order to gather more information on distinctive gene expression of QE, a second single set of microarray experiments, with one ''dye swap'' replicas, were performed using the unrelated genotypes Maya and Onda (Maya/QE, Onda/QE).

Table 1 Major fruit quality and yield traits of genotypes studied in this work (average 3-year data ± SD)

Genotype	Firmnes[a]	SSC[b]	TA[c]	Yield[d]
Queen	571 ± 15	7.3 ± 0.5	9.9 ± 0.6	910 ± 45
Miss	334 ± 24	6.1 ± 0.3	7.9 ± 0.4	696 ± 20
USB	434 ± 13	7.8 ± 0.4	12.5 ± 0.5	530 ± 16
Maya	345 ± 22	6.6 ± 0.4	10.3 ± 0.7	826 ± 24
Onda	340 ± 9	6.1 ± 0.6	7.9 ± 0.4	615 ± 20

[a]6-mm diameter penetrometer test (g)

[b]Soluble solid content (°Brix)

[c]Titratable acidity (meq/100 g fw)

[d]Total yield (g/plant)

Good quality (GQ) spots were selected imposing a minimal signal/noise ratio of 3.0. In order to identify transcripts that were differentially regulated, GC spots showing a mean expression change of at least 2-fold between test and reference sample were considered up- or down-regulated.

In Miss versus QE experiments, only 14 transcripts showed a significant up-regulation, while 7 transcripts were found to be down-regulated (Table 2). USB35 versus QE experiments revealed a slightly higher number of differentially expressed sequences, with 16 up- and 26 down-regulated clones (Table 3). Common up-regulated transcripts in both parental lines were related to genes coding for alcohol acyl transferase (*aat*; FRA0488 and GC10), cinnamoyl CoA reductase (*ccr*; FRA0423) and small nuclear RNA (*psu2*; FRA1794).

On the other hand, transcripts related to cinnamyl alcohol dehydrogenase (*cad*; FRA1563) and an unknown putative protein (FRA1655) were down-regulated in both parental lines (Tables 2, 3). Notably, *aat* and *psu2* transcripts seem to be generally down-regulated in QE fruits since they are accordingly also altered in Maya-Onda versus QE experiments. Moreover, the *ccr* and *cad* transcript regulations observed in Miss versus QE and USB35 versus QE experiments are confirmed in Maya versus QE, but not in Onda versus QE ones (Tables 2, 3).

Above-mentioned genes are known to play a key role in metabolic pathways controlling major

Table 2 Up- and down-regulated putative genes in Miss versus QE microarray experiments

Miss versus QE						
Lab code	Putative ID (blastx)	Maya versus QE	Onda versus QE	Mean	SD	CV
Down-regulated						
FRA 1098	Putative casein kinase (AAM51279)			0.26	0.06	22.48
FRA 1563	Cinnamyl alcohol dehydrogenase (AAD10327)	*		0.35	0.08	23.31
FRA 1491	Unknown			0.41	0.05	11.96
FRA 1655	Unknown putative protein (CAB80819)			0.45	0.20	43.13
FRA 1004	Unknown			0.47	0.13	26.80
FRA 1374	Unknown			0.49	0.22	45.36
FRA 0623	Peptidylprolyl isomerase (XP483423)			0.49	0.22	45.03
Up-regulated						
FRA 0423	Cinnamoyl-CoA reductase (AAP46143)	*		18.09	4.65	25.68
FRA 0488	Alcohol acyltransferase (AAG13130)	*		12.43	5.86	47.12
FRA 1794	PSU2 for U2 snRNA (X15936)	*	*	4.52	1.72	38.07
GC10	Alcohol acyltransferase (AF193789)	*	*	4.24	1.6	37.67
FRA 0195	Unknown			3.39	1.31	38.71
FRA 1796	Unknown			2.71	0.72	26.47
FRA 0925	Unknown protein (AAM51341)			2.44	1.02	41.89
FRA 0816	Unknown protein (BAD37732)			2.37	1.01	42.55
FRA 0497	Unknown			2.31	0.59	25.80
FRA 0512	Unknown hypothetical protein (CAE73868)			2.26	1.13	49.95
FRA 0950	Unknown			2.21	1.10	49.73
FRA 1015	FSGTP1 (CAA67153)			2.19	0.94	42.68
FRA 0792	Endo-β-1,4-glucanase (AJ414709)			2.09	0.93	44.52
FRA 0028	Polygalacturonase (AAP37458)			2.01	0.65	32.50

Regulated transcripts consistently altered in Maya versus QE and Onda versus QE experiments are marked with an asterisk

Table 3 Up- and down-regulated putative genes in USB35 versus QE microarray experiments

Lab code	Putative ID (blastx)	Maya versus QE	Onda versus QE	Mean	SD	CV
Down-regulated						
FRA 1563	Cinnamyl alcohol dehydrogenase (AAD10327)	*		0.22	0.04	19.59
FRA 1672	Unknown			0.22	0.03	14.14
FRA 0102	Metallothionein-like protein (AAD31477)			0.26	0.11	44.34
FRA 0093	Putative auxin-induced protein (NP917700)			0.35	0.15	44.10
FRA 1655	Putative protein (CAB80819)			0.36	0.03	8.32
FRA 0291	Glutathione disulfide reducuctase (T09151)			0.36	0.15	42.33
FRA 0466	Salicylic acid glucosyltransferase (BAD34360)			0.37	0.09	23.87
FRA 0524	S-adenosylmethionine decarboxylase (BAC55114)			0.37	0.12	32.42
FRA 0179	Elongation factor 2 (AB026185)			0.39	0.16	42.34
FRA 0627	b-Tubulin (AAQ92664)			0.39	0.14	35.47
FRA 0784	Putative pollen thioesterase (AAS90598)			0.41	0.09	22.05
FRA 0431	Cytochrome b (CAD90557)			0.41	0.07	17.78
FRA 0716	Unknown			0.42	0.16	38.23
FRA 0042	Unknown			0.44	0.13	28.67
FRA 1248	Glycine max mRNA for ribosomal protein L2(GMA404848)			0.44	0.18	40.88
FRA 1065	Unknown			0.44	0.19	42.74
FRA 1714	Unknown			0.45	0.12	26.58
FRA 0280	Unknown			0.45	0.11	25.37
FRA 0734	Unknown			0.45	0.15	33.81
FRA 0551	Nucleic acid binding protein-like (AAM64729)			0.45	0.22	49.68
FRA 0284	Quinone reductase (AAN41337)			0.45	0.15	34.28
FRA 0230	NADH dehydrogenase 1-like(1211235CV)			0.45	0.18	39.41
FRA 0553	Glutaredoxin(AAL04507)			0.47	0.07	15.85
FRA 0965	Flavonol synthase (BAD34463)			0.47	0.16	33.15
FRA 0133	Unknown			0.49	0.18	37.43
FRA 1071	Unknown			0.49	0.08	16.32
Up-regulated						
FRA 0423	Cinnamoyl-CoA reductase (AAP46143)	*		25.71	16.5	64.2
GC10	Alcohol acyltransferase (AF193789)	*	*	24.34	9.58	39.34
FRA 1794	PSU2 gene for snRNA (X15936)	*	*	18.76	6.80	36.25
FRA 0488	Alcohol acyltransferase (AAG13130)	*		7.55	6.28	83.15
GC15	Cellulase (Cel1; AF051346)			5.16	1.46	28.21
FRA 0951	Chitinase-like protein (AAQ56598)			3.22	0.97	30.19
FRA 0849	Heat shock protein (CAA67867)			2.93	1.18	40.16
GC30	Pectate lyase (U63550)			2.82	1.25	44.39
FRA 0937	Unknown protein (BAC42796)			2.80	0.42	14.84
FRA 1471	HyPRP mRNA (AF026382)			2.56	0.98	38.33
GC08	Auxin-repressed mRNA (X52429)			2.53	0.51	20.00
FRA 0887	O-methyltransferase (AF220491)			2.50	0.94	37.45
FRA 0964	Unknown			2.21	0.51	23.35
FRA 0694	40S ribosomal protein S17 (XP_468565)			2.16	0.97	44.95
FRA 1510	Pyruvate decarboxylase (AAG13131)			2.04	0.87	42.88
FRA 1317	Unknown (AAM65231)			2.02	0.87	42.94

Regulated transcripts consistently altered in Maya versus QE and Onda versus QE experiments are marked with an asterisk

fruit quality traits as aroma and firmness. Indeed, AAT is involved in fruit flavor biosynthesis (Pérez et al. 1993, 1996) and is induced during ripening (Aharoni et al. 2000) to produce esters peaking their concentration at full red stage (Ménager et al. 2004); on the other hand *ccr* and *cad* genes are mostly expressed in the vascular tissue of strawberry fruit and achenes (e.g., Blanco-Portales et al. 2002) and are involved in the biosynthesis of phenylpropanoid compounds

and lignin precursors (Anterola and Lewis 2002). Concurrent up-regulation of *ccr* and down-regulation of *cad* genes, together with up-regulation of cell wall-related genes, were consistent with the lower firmness of Miss, USB35 and Maya fruits (Table 1).

Quantitative real time RT-PCR

qRT-PCR experiments were carried out to validate microarray data on selected genes such as the up-regulated *aat*, and the abundantly expressed O-methyltransferase (*omt*), cystein protease (*cysp*) and auxin-regulated (*aux-reg*) genes (Fig. 1a).

In ripe fruits, further qRT-PCR analyses were carried out to confirm or complete expression data of genes putatively involved in firmness and cell wall metabolism (Fig. 1b). The expression of three members of the strawberry expansin multigene family (*exp1*, *exp2* and *exp4*), beta-galactosidase 1 (*beta-gal1*), cellulase 1 (*cel1*), beta-xylosidase 1 (*xyl1*), and pectate lyase (*pl*) genes, not sufficiently resolved by microarray experiments, were further studied by designing specific primers based on information from sequence databases.

Although relative gene expression values were generally increased, qRT-PCR analyses produced results mostly in agreement with those of microarray experiments. Up-regulation of *aat*, *ccr* and down-regulation of *cad* transcripts were confirmed (Fig. 1a, b). As for the expansin family, qRT-PCR data showed an overall up-regulation of the 3 expansin (*exp*) genes in Miss, USB35, Maya and Onda. A stronger up-regulation of *exp4*

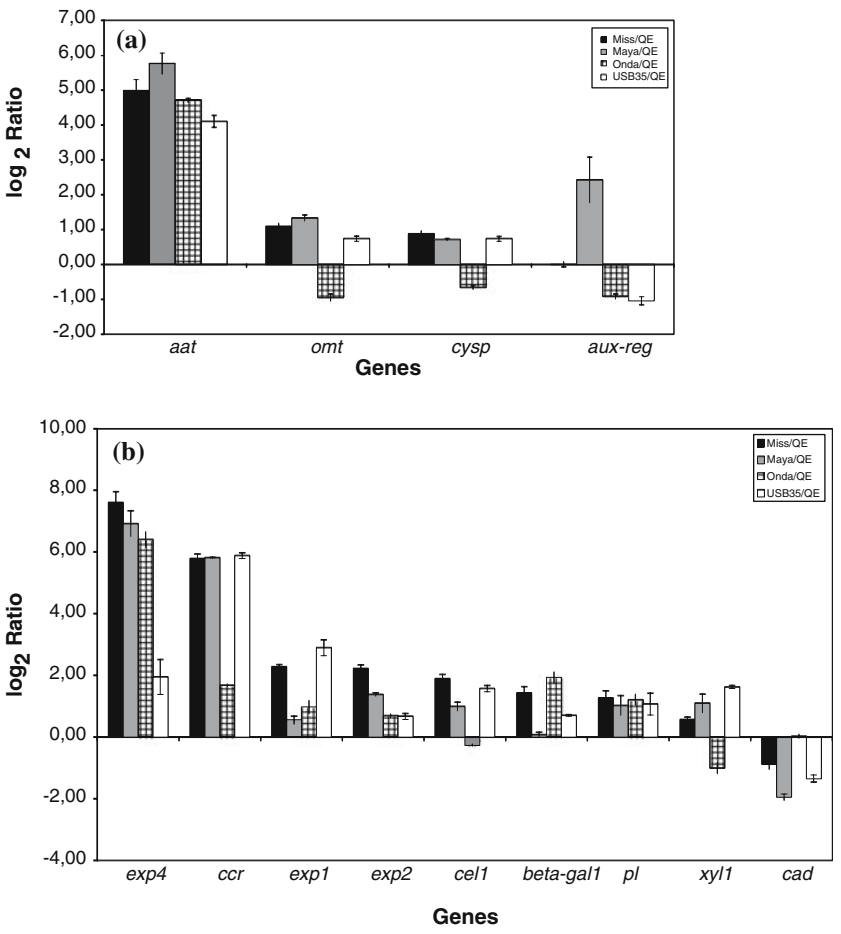

Fig. 1 Analysis of gene expression by quantitative Real-Time RT-PCR. The relative expression (log 2 ratio) of selected genes Black bars: Miss/QE. Grey bars: Maya/QE. Cross-hatched bars: Onda/QE. White bars: USB35/QE. See text for gene acronyms. Normalizing. Data were normalized for elongation factor-1 alpha transcript

was found in Miss, Maya and Onda, while relative differences in transcript levels of *exp1*, *exp2* and *pl* were less evident. Finally, *cel1* and *xyl1* transcripts were up-regulated in all genotypes but Onda with respect to QE; while *beta-gal1* transcripts are unchanged in Maya versus QE experiment (Fig. 1b).

PTR-MS analyses and AAT enzyme assays

The average PTR-MS spectra of QE, Miss, USB35, Maya and Onda, referring to measurements on sample set C, are shown in Fig. 2. Non parametric analysis of variance (Kruscal–Wallis test) indicated that many peaks significantly distinguish the five genotypes. In particular, the series of peaks at $m/z = 75 + 14n$, corresponding to esters, is the dominant feature of the high m/z region of USB35, Miss, Onda and Maya spectra. Such peaks are dramatically less intense in the case of QE. Peaks corresponding to esters with spectrum odd m/z values of carbon atoms are typically higher, the peak at $m/z = 103$ being the most intense. Comparison with volatile compound databases (Boelens 1996) and with known fragmentation patterns (Buhr et al. 2002) suggests that $m/z = 103$ peak should be tentatively attributed to methylbutanoate (>80%) and ethylpropanoate. On the other hand, few peaks have comparable intensities for all varieties, e.g. $m/z = 33$ (methanol), $m/z = 59$ (acetone and propanale) and $m/z = 37$ (protonated water dimer). These peaks are markers of catabolic processes (e.g. $m/z = 33$, Boschetti et al. 1999)

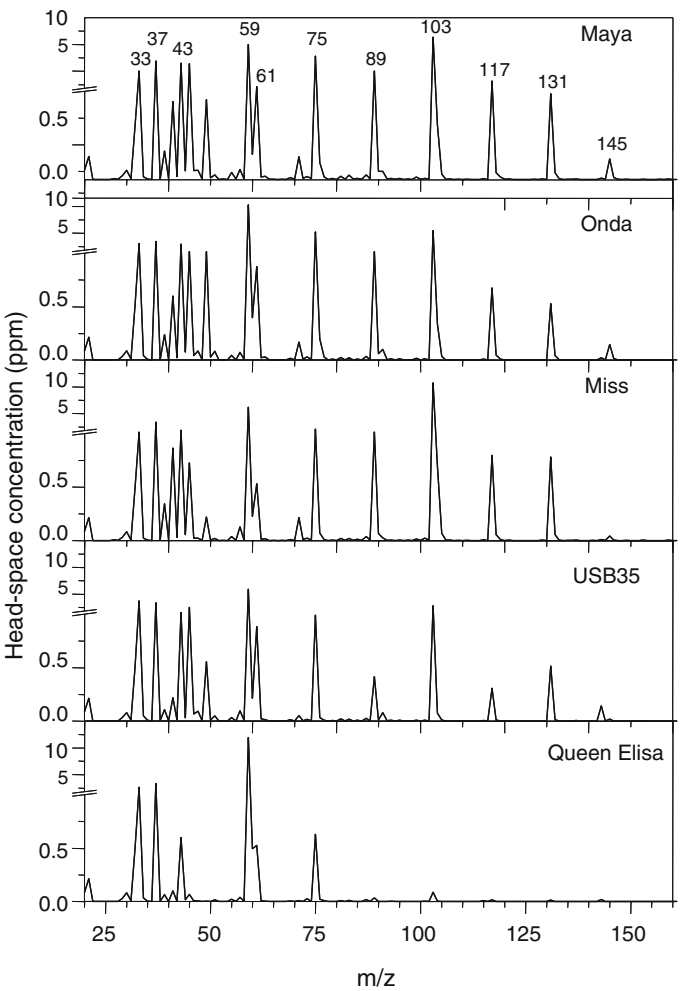

Fig. 2 Average spectra of the genotypes studied in this work (data set C). m/z value of the most relevant peaks (see Results) are indicated in the case of Maya

or water content of the gaseous mixture (m/z = 37, Lindinger et al. 1998), and confirm the stability of the measuring procedure and homogeneity of fruit samples. Similar results were obtained from fruits of data set A concerning QE, Miss and USB35 genotypes (data not shown).

Data set B contains more data (65 for each genotype), recorded from different storage conditions and growing locations (see Materials and methods). Miss and USB35 gave similar patterns (data not shown), therefore only data from Miss and QE are reported. Figure 3 shows the whisker-box plot of m/z values related to esters of sample set B. The pattern easily discriminates Miss and QE fruits, confirming the possibility presented by Biasioli et al. (2003) to unambiguously identify genotypes by rapid and non-destructive PTR-MS measurements of single fruits. Miss fruits had a significantly higher emission than those of QE for all masses except m/z = 61 and m/z = 75. Data of Fig. 3 are in good agreement with those of Fig. 2: the emission values at $m/z = 75 + 14n$ are always higher for Miss (1 or 2 orders of magnitude in average). A different situation is represented by m/z = 61 (fragment of acetate esters), that showed no significant difference between Miss and QE. This is likely to indicate that acetates are not responsible of the observed differences in volatile emission. Again, the separation of QE from its parent Miss is evident: distributions are clearly separated for most masses (note the logarithmic scale) and, based on this trait, only few fruit samples could not be unambiguously assigned to the right clone. This is quite a remarkable result, since these data refer to many samples collected in three locations at three harvest times, with different storage conditions and duration.

The total headspace concentration of esters, calculated by summing the intensity of all related peaks, is reported in Fig. 4 for all genotypes (data set C). Ester levels of QE are always lower, more than one order of magnitude in average, than those of the other genotypes. Miss, Maya and Onda are not statistically different among each other and have higher ester concentrations than USB35.

Finally, normalization of spectra on total intensity, carried out in order to compensate the possible effects related to fruit size, or

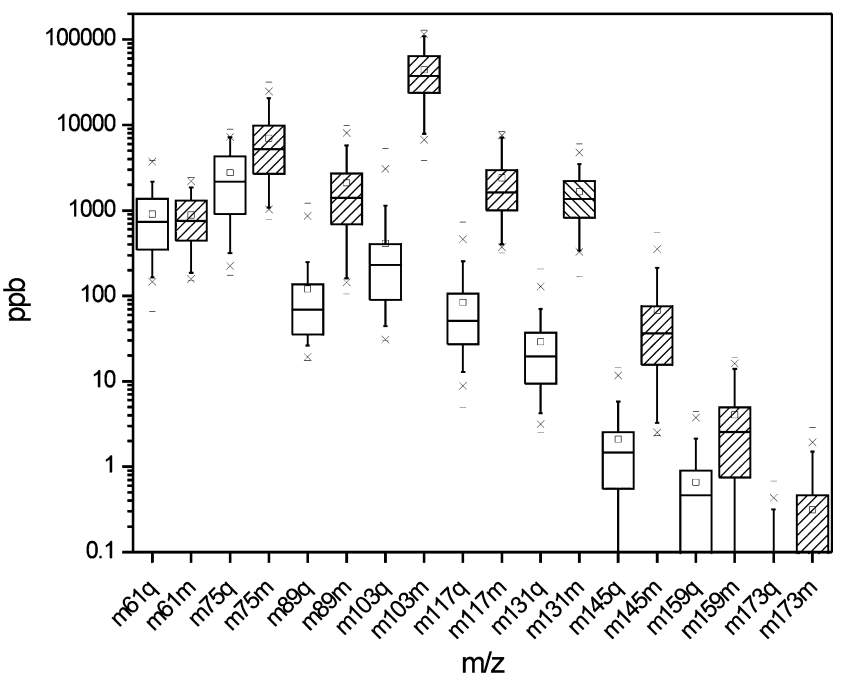

Fig. 3 Volatile compound emission intensity for Miss (pattern) and QE (open box) obtained from data set B. Boxes indicate 25%, 50% and 75% percentiles. Mean value (), maximum value (—), 1% and 99% (x) percentiles are also indicated

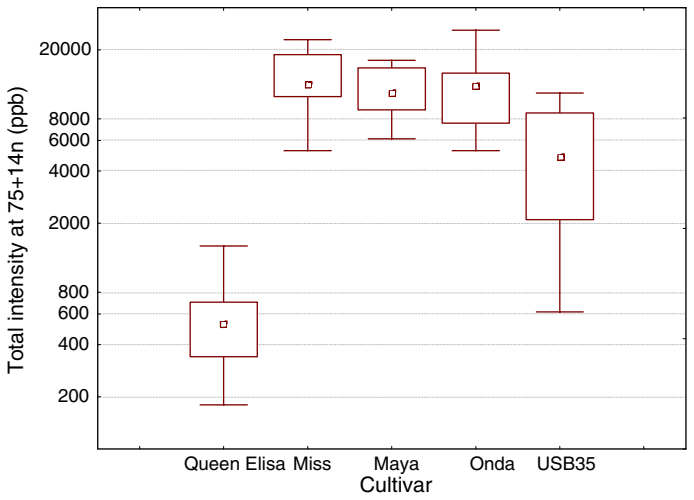

Fig. 4 Box and whisker plots for ester concentration in fruits headspace of all genotypes (Data set C), see text). Total emission at *m*/*z* 75, 89, 103, 117, 131, 145 is reported. Points indicate medians, boxes 25% and 75% percentiles and whiskers max and min values

measurements on cut fruits further confirmed the results (data not shown).

In order to compare ester biosynthesis and the relative enzymatic activities in strawberry fruits, AAT enzyme activity was measured using crude extracts of red fruits in all five genotypes (Fig. 5). Alcohols with variable chain length (butanol, octanol and decanol) and acetyl-CoA were used as alcohol and acyl group donor substrates, respectively. In general, octanol was the preferred alcohol substrate in AAT assays. QE showed the lowest relative AAT activity levels irrespective of the alcohol substrate used in tests, in agreement with results of gene expression and PTR-MS analyses. The other genotypes had variable patterns of AAT activity depending on alcohol chain length.

Discussion

Identification of key genes involved in the control of polygenic traits is a challenging task. However, the parallel implementation of high throughput genomics and biochemical approaches look promising especially in species with complex genetic organization.

In this work, gene transcript levels, enzyme activity and emission of volatile compounds were investigated in genotype-to-genotype comparisons at red stage, when changes in transcript levels and/or metabolite concentration should account for differences in the expression of major quality traits as aroma and firmness. Our main results point out a set of cell wall-related genes and *aat* gene and enzyme(s) whose

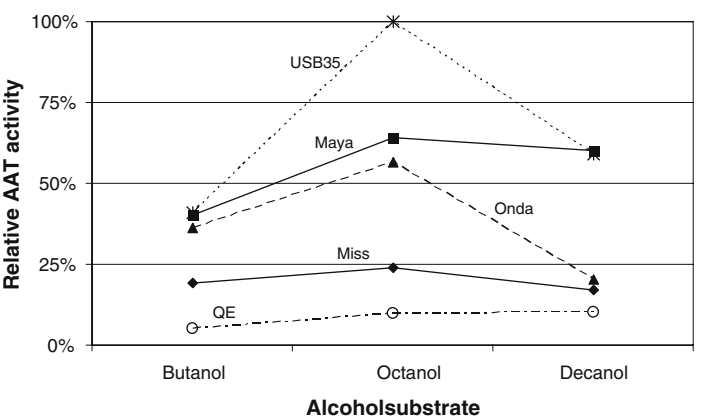

Fig. 5 Relative AAT activity of crude enzyme extracts from red fruits of strawberry genotypes. Alcohol substrates incubated were used for all genotypes. Two independent experiments were carried out using each alcohol substrate ($N = 6$)

differential expression is most likely to be related to changes in fruit firmness and headspace ester emission.

cDNA microarrays and Real-Time RT-PCR monitor ripening-related genes and are able to detect differentially expressed genes associated with differences in fruit quality traits among genotypes

As high-throughput tools become more and more affordable, the complexity of fruit ripening physiology is being studied with functional genomics approaches in a number of economically important species as grape, peach, pear, strawberry and tomato (Aharoni et al. 2000; Carbone et al. 2005; Fei et al. 2004; Fonseca et al. 2004; Trainotti et al. 2006; Waters et al. 2005). Comparative analysis of EST collections and microarray expression experiments on further species will allow to gain general and species-specific insight of fruit ripening.

Gene expression analyses evidenced altered genes related to changes in aroma profile and fruit firmness among the élite genotype QE and its parents Miss and USB35. A second set of microarray experiments was also carried out using two additional genotypes, Maya and Onda, unrelated to QE and with fruit firmness similar to that of Miss and USB35 (Table 1).

Microarray data were generally validated by qRT-PCR experiments, although the latter method of analysis often magnified differences in gene expression. Multiple factors could account for this: spot saturation with labeled probe RNAs in microarray experiments, higher sensitivity of qRT-PCR technology or possible cross-hybridizations of homolog transcripts, which alter microarray gene expression ratios.

The key role of *aat* in ester production was shown when comparing genotypes with different levels of volatile compound emission. Expression of *aat* increases during fruit ripening, peaking at full red stage with high levels of transcript (Aharoni et al. 2000). *aat* was strongly up-regulated in QE parental, Maya and Onda genotypes, and differences in transcript levels were confirmed by qRT-PCR experiments. Biosynthesis of volatile compounds in fruits is a very complex phenomenon and, in strawberry and also due to its broad substrate specificity (Pérez et al. 1993; Li et al. 2006; El-Sharkawy et al. 2005), *aat* is the major gene controlling differences in ester levels in strawberry fruits (Aharoni et al. 2000).

Cell wall metabolism has great influence on fruit firmness. The molecular basis of cell wall degradation during strawberry ripening are still unclear. Recent evidences show that fruit softening is mostly the result of pectin degradation and the degree of pectin depolymerization rather than the effect of cellulose and hemicellulose hydrolysis (Rosli et al. 2004). However, the degree of firmness is probably the effect of the coordinated action of many different enzymatic activities related to cell wall metabolism and finely modulated at the genetic level. We, indeed, show that there is a coordinated expression of a number genes involved in cell wall metabolism among different genotypes with contrasting fruit firmess. qRT-PCR analyses showed an activation of expansin, *cel1*, *pl*, *beta-gal1* and *xyl1* genes in all tested genotypes with respect to the firmest genotype QE (Table 1; Fig. 1b), with the exception of *cel1* and *xyl1* transcripts in Onda versus QE experiment and of *beta-gal1* transcripts in Maya versus QE experiment (Fig. 1b). All cited genes and related enzymes are expressed either sequentially or simultaneously during fruit ripening, and play a role in the softening process of different fruits (Benitez-Burraco et al. 2003; Fonseca et al. 2004; Lloup-Tous et al. 1999; Martinez et al. 2004; Trainotti et al. 2001; Trainotti et al. 2003). In non-climateric fruits as strawberry, activation of above-mentioned genes coding cell wall degrading is not catalyzed by ethylene but rather by hormones, developmental and environmental cues, and shows the maximum expression at final ripening stages (Medina-Escobar et al. 1997; Civello et al. 1999; Lloup-Tous et al. 1999). Moreover, these enzymes are encoded by multigene families, with differences in spatial and temporal expression patterns. In the case of endo-β-1,4-glucanase genes, Lloup-Tous et al. (1999) showed that accumulation of *cel1* transcripts starts at late stages of ripening and strongly peaks at red stage. Therefore, higher expression of *cel1* at red stage might determine major differences in fruit firmness. On the other hand, *cel2* mRNA is

steadily accumulated from early onset of turning stage and its level remains constantly elevated, though lower than that of *cel1* peak at red stage. These aspects are of paramount importance when analyzing gene expression data, since expression levels of specific members are probably underestimated by cross-hybridization in microarray experiments. With the exception of Onda, up-regulation of *ccr* and down-regulation of *cad* genes were correlated with lower firmness of USB35, Miss Maya and Onda fruits with respect to QE. These results on *ccr* and *cad*, apparently unrelated to fruit firmness, agree with those from Salentijn et al. (2003) and point out further genes controlling this polygenic trait. Confirmation of microarray analyses by different research groups, furthermore validated by Northern blot or qRT-PCR experiments, adds robustness to expression data themselves. Besides their role in lignin composition, the role of CCR and CAD reaction products on strength and/or disruption of cell wall polymers should be taken into account. CCR and CAD enzyme activities and lignin deposition in strawberry fruits have been associated to vessels connecting achenes (Blanco-Portales et al. 2002).

All together, our results point out a wide set of candidate genes (*cad*, *ccr*, *cel1*, *pl*, *beta-gal1*, *xyl1* and *exp* family) whose coordinated and differential expression could be related with the variation of fruit firmness, a major quantitative breeding trait. Remarkably, *exp4* transcripts seem to be positively correlated to relative fruit firmness: in the firmest genotype QE, *exp4* transcripts are less abundant, while they peak in the softest genotypes Maya, Miss and Onda. On the other hand, differences in the transcript levels of *ccr*, *cel1*, *pl*, *beta-gal1* and *xyl1* genes were less dramatic, and were sometimes contrasting mostly in Onda (Table 1; Fig. 1b), suggesting that the actual complexity of the genetic control of fruit firmness in strawberry deserves further investigations.

PTR-MS analyses of headspace volatiles correlate with expression of genes and enzymes involved in ester aroma biosynthesis

While many applications of PTR-MS have been proposed and tested in food science and technology, in this work we combined PTR-MS with molecular approaches to study volatile emission. The direct correlation between *aat* gene expression, enzyme activity and volatile ester emission was very encouraging, and opens the way to broader studies where PTR-MS can provide a link between gene expression and sensory data (Gasperi et al. 2001, Biasioli et al. 2006).

AAT assays provided information on both enzyme activity and substrate specificity of studied genotypes. Every genotype showed a distinct AAT activity pattern. Besides the lowest AAT activity of QE, strictly correlated with gene expression and ester emission levels (Figs. 1b, 3), our analyses confirmed octanol as the preferred straight-chain alcohol substrate for AAT (Fig. 5), in agreement with previous findings (Aharoni et al. 2000). The broad array of alcohols and acyl group donors concurring to ester formation (Aharoni et al. 2000; Olias et al. 2002; Perez et al. 1996) make impossible to strictly correlate headspace ester composition and AAT activity. Nevertheless, the AAT assay data shown in our work are consistent with the ester emission pattern of the five genotypes.

The PTR-MS proved to be a powerful approach to discriminate varieties based on volatile compound emission, and has important features such as sensitivity (single-fruit measurements), absence of sample treatment (whole fruits, possibility to measure the same fruits with different techniques) and quickness (statistics on many fruits and dynamic measurements). PTR-MS classification of fruits showed to be robust with respect to year-to-year variation and culture technique, since data sets A, B and C were recorded in different years, and, for data set B, samples of each genotype were collected from open field- and plastic tunnel-grown plants from two locations. This confirms the consistent classification of cultivars over several seasons by monitoring aroma profile on single fruits (Biasioli et al. 2003). The absence of separation is the main drawback of PTR-MS analysis because it does not allow unambiguous identification of compounds. Even if not mandatory in the context of the present work, however, improved PTR-MS experimental procedures are being developed to distinguish the contribution of each class of esters in headspace mixture.

The observed differences among genotypes for *aat* transcript levels corresponded to differences in AAT activity and were magnified (10- to 100-fold) for ester emission in the fruit headspace. Indeed, analysis of literature and volatile compounds databases (Boelens 1996–1999) indicate that also acids can contribute to the signal at $m/z = 75 + 14n$. The contribution of acids to the fruit headspace, estimated by following the decay of the PTR-MS signal after the removal of the samples—fast for esters, much slower for the less volatile acids—was found to be less than 5% and thus ignored. Another aspect to be considered is that fragmentation decreases with increasing molecular weight or chain length, and ramified ester and unsaturated esters exhibit lesser fragmentation (Buhr et al. 2002).

In this study we focused on esters, since they represent the major compound of the PTR-MS spectra of the studied genotypes. However, it is worth mentioning that other m/z peaks can fingerprint cultivars as well as fruit shelf life and post-harvest physiology. This was not relevant for the preliminary investigations of this work but will be developed in the future.

In conclusion, we used a multidisciplinary approach to characterize fruit quality traits of several strawberry genotypes and reveal differences among genotypes at ripening and post-harvest stages. Differential expression of a limited number of genes involved in major fruit quality traits as firmness and aroma biogenesis was shown and validated by qRT-PCR analyses. PTR-MS analyses provided tools for distinguishing varieties based on their volatile compound spectra at full ripening and during post-harvest, and showed a direct correlation between ester spectra pattern and the expression of *aat* gene and enzyme involved in the biosynthesis of such aroma compounds.

Acknowledgements Work supported by the Italian MIUR QualiFraPe project, the Austrian FWF of Vienna, and the European ComMission, We thank ISF staff for data on quality traits, F. Giorno for her assistance.

References

Aharoni A, O'Connell AP (2002) Gene expression analysis of strawberry achene and receptacle maturation using DNA microarrays. J Exp Bot 53:2073–2087

Aharoni A, Keizer LCP, Bouwmeester HJ, Sun Z, Alvarez-Huerta M, Verhoeven HA, Blaas J, van Houwelingen AMML, De Vos RCH, van der Voet H, Jansen RC, Guis M, Mol J, Davis RW, Schena M, van Tunen AJ, O'Connell AP (2000) Identification of the SAAT gene involved in strawberry flavor biogenesis by use of DNA microarrays. Plant Cell 12:647–661

Aharoni A, Keizer LCP, Van Den Broeck HC, Blanco-Portales R, Munoz-Blanco J, Bois G, Smit P, De Vos RCH, O'Connell AP (2002) Novel insights into vascular, stress, and auxin-dependent and -independent gene expression programs in strawberry, a non-climateric fruit. Plant Physiol 129:1019–1031

Anterola AM, Lewis NG (2002) Trends in lignin modification: a comprehensive analysis of the effects of genetic manipulations/mutations on lignification and vascular integrity. Phytochemistry 61:221–294

Azodanlou R, Darbellay C, Luisier JL, Villettaz JC, Amadò R (2003) Quality assessment of strawberries (*Fragaria* species). J Agric Food Chem 51:715–721

Benítez-Burraco A, Blanco-Portales R, Redondo-Nevado J, Bellido ML, Moyano E, Caballero J-L, Mun~oz-Blanco J (2003) Cloning and characterization of two ripening-related strawberry (Fragaria × ananassa cv. Chandler) pectate lyase genes. J Exp Bot 54:633–645

Biasioli F, Gasperi F, Aprea E, Mott D, Boscaini E, Mayr D, Märk TD (2003) Coupling proton transfer reaction-mass spectrometry with linear discriminant analysis: a case study. J Agric Food Chem 51:7227–7233

Biasioli F, Gasperi F, Aprea E, Endrizzi I, Framondino V, Marini F Mott D, Märk TD (2006) Correlation of PTR-MS spectral fingerprints with sensory characterisation of flavour and odour profile of ''Trentingrana'' cheese. Food Qual Prefer 17:63–75

Blanco-Portales R, Medina-Escobar N, Lopez-Raez JA, Gonzalez-Reyes JA, Villalba JM, Moyano E, Caballero JL, Munoz-Blanco J (2002) Cloning, expression and immunolocalization pattern of a cinnamyl alcohol dehydrogenase gene from strawberry (Fragaria × ananassa cv. Chandler). J Exp Bot 53:1723–1734

Boelens MH (1996–1999) VCF (2000) Volatile compounds in food, qualitative and quantitative data, 7th edn. (1996), Suppl 1 (1997), Suppl 2 (1999), Huizen, BACIS

Boscaini E, Van Ruth S, Biasioli F, Gasperi F, Märk TD (2003) Gas chromatography-olfactometry (GC-O) and proton transfer reaction-mass spectrometry (PTR-MS) analysis of the flavor profile of Grana Padano, Parmigiano Reggiano, and Grana Trentino cheeses. J Agric Food Chem 51:1782–1790

Boschetti A, Biasioli F, van Opbergen M, Warneke C, Jordan A, Holzinger R, Prazeller P, Karl T, Hansel A, Lindinger W, Iannotta S (1999) PTR-MS real time monitoring of the emission of volatile organic compounds during postharvest aging of berryfruit. Postharvest Biol Technol 17:143–151

Bradford MM (1976) A rapid and sensitive method for the quantitation of microgram quantities of protein utilizing the principle of protein dye binding. Anal Biochem 72:248–254

Buhr K, van Ruth S, Delahunty C (2002) Analysis of volatile flavour compounds by Proton-Transfer Reaction-Mass Spectrometry: fragmentation patterns and discrimination between isobaric and isomeric compounds. Int J Mass Spectrom 221:1–7

Carbone F, Pizzichini D, Giuliano G, Rosati C, Perrotta G (2005) Comparative profiling of tomato fruits and leaves evidences a complex modulation of global transcript profiles. Plant Sci 169:165–175

Civello PM, Powell ALT, Sabehat A, Bennett AB (1999) An expansin gene expressed in ripening strawberry fruit. Plant Physiol 121:1273–1279

Cleveland W, Devlin S (1998) Locally weighted linear regression: an approach to regression analysis by local fitting. J Am Stat Assoc 83:596–609

Davis TM, Yu H (1997) A linkage map of the diploid strawberry, *Fragaria vesca*. J Hered 88:215–221

Dorfner R, Ferge T, Yeretzian C, Kettrup A, Zimmermann R (2004) Laser mass spectrometry as on-line sensor for industrial process analysis: process control of coffee roasting. Anal Chem 76:1386–1402

El-Sharkawy I, Manríquez D, Flores FB, Regad F, Bouzayen M, Latché A, Pech J-C (2005) Functional characterization of a melon alcohol acyl-transferase gene family involved in the biosynthesis of ester volatiles. Identification of the crucial role of a threonine residue for enzyme activity. Plant Mol Biol 59:345–362

Fei Z, Tang X, Alba RM, White JA, Ronning CM, Martin GB, Tanksley SD, Giovannoni JJ (2004) Comprehensive EST analysis of tomato and comparative genomics of fruit ripening. Plant J 40:47–59

Fiehn O (2002) Metabolomics – the link between genotypes and phenotypes. Plant Mol Biol 48:155–171

Fonseca S, Hackler L Jr, Zvara A, Ferreira S, Baldé A, Dudits D, Pais MS, Puskás LG (2004) Monitoring gene expression along pear fruit development, ripening and senescence using cDNA microarrays. Plant Sci 167:457–469

Gasperi F, Gallerani G, Boschetti A, Biasioli F, Monetti A, Boscaini E, Jordan A, Lindinger W, Iannotta S (2001) The mozzarella cheese flavour profile: a comparison between judge panel analysis and proton transfer reaction mass spectrometry. J Sci Food Agric 81:357–363

Hansel A, Jordan A, Warneke C, Holzinger R, Wisthaler A, Lindinger W (1999) Proton-transfer-reaction mass spectrometry (PTR-MS): on-line monitoring of volatile organic compounds at volume mixing ratios of a few pptv. Plasma Sources Sci Technol 8:332–336

Lerceteau-Köhler E, Guerin G, Laigret F, Denoyes-Rothan B (2003) Characterization of mixed disomic and polysomic inheritance in the octoploid strawberry (*Fragaria* × *ananassa*) using AFLP mapping. Theor Appl Genet 107:619–628

Li D, Xu Y, Xu G, Gu L, Li D, Shu H (2006) Molecular cloning and expression of a gene encoding alcohol acyltransferase (MdAAT2) from apple (cv. Golden Delicious). Phytochemistry 67:658–667

Lindinger W, Hansel A, Jordan A (1998) On-line monitoring of volatile organic compounds at pptv level by means of Proton-Transfer-Reaction Mass Spectrometry (PTR-MS). Medical application, food control and environmental research. International Int J Mass Spectrom Ion Process 173:191–241

Lloup-Tous I, Domínguez-Puigjaner E, Palomer X, Vendrell M (1999) Characterization of two divergent endo-β-1,4-glucanase cDNA clones highly expressed in the nonclimacteric strawberry fruit. Plant Physiol 119:1415–1421

Lopez-Gomez R, Gomez-Lim MA (1992) A method for extracting intact RNA from fruit rich in polysaccharides using ripe mango mesocarp. HortScience 27:440–442

Manning K (1998) Isolation of a set of ripening-related genes from strawberry: their identification and possible relationship to fruit quality traits. Planta 205:622–631

Martínez GA, Chaves AR, Civello PM (2004) β-xylosidase activity and expression of a β-xylosidase gene during strawberry fruit ripening. Plant Physiol Biochem 42:89–96

Marty I, Douat C, Tichit L, Jungsup K, Leustek T, Albagnac G (2000) The cystathionine-β-synthase gene involved in methionine biosynthesis is highly expressed and auxin-repressed during wild strawberry (*Fragaria vesca* L.) fruit ripening. Theor Appl Genet 100:1129–1136

Medina-Escobar N, Cárdenas J, Moyano E, Caballero JL, Muñoz-Blanco J (1997) Cloning, molecular characterization and expression pattern of a strawberry ripening-specific cDNA with sequence homology to pectate lyase from higher plants. Plant Mol Biol 34:867–877

Ménager I, Jost M, Aubert C (2004) Changes in physicochemical characteristics and volatile constituents of strawberry (cv. Cigaline) during maturation. J Agric Food Chem 52:1248–1254

Mott D, Biasioli F, Gasperi F, Aprea E, Marini F, Märk TD (2004) Characterisation of strawberry genotypes by PTRMS spectral fingerprinting. Acta Horticult 649:65–68

Nam YW, Tichit L, Leperlier M, Cuerq B, Marty I, Lelièvre JM (1999) Isolation and characterization of mRNAs differentially expressed during ripening of wild strawberry (*Fragaria vesca* L.) fruits. Plant Mol Biol 39:629–636

Olías R, Perez AG, Sanz C (2002) Catalytic properties of alcohol acyltransferase in different strawberry species and cultivars. J Agricult Food Chem 50:4031–4036

Pérez AG, Sanz C, Olías JM (1993) Partial purification and some properties of alcohol acyltransferase from strawberry fruits. J Agric Food Chem 41:1462–1466

Pérez AG, Sanz C, Olías R, Ríos JJ, Olías JM (1996) Evolution of strawberry alcohol acyltransferase activity during fruit development and storage. J Agric Food Chem 44:3286–3290

Pérez AG, Olías R, Luaces P, Sanz C (2002) Biosynthesis of strawberry aroma compounds through amino acid metabolism. J Agric Food Chem 50:4037–4042

Rosli HG, Civello PM, Marti'nez GA (2004)Changes in cell wall composition of three *Fragaria* × *ananassa* cultivars with different softening rate during ripening. Plant Physiol Biochem 42:823–831

Salentijn EMJ, Aharoni A, Schaart JG, Boone MJ, Krens FA (2003) Differential gene expression analysis of strawberry cultivars that differ in fruit-firmness. Physiol Plant 118:571–578

Sambrook J, Fritsch EF, Maniatis T (1989) Molecular cloning: a laboratory manual, 2nd edn. Cold Spring Harbor, New York

Sargent DJ, Davis TM, Tobutt KR, Wilkinson MJ, Battey NH, Simpson DW (2004) A genetic linkage map of microsatellite, gene-specific and morphological markers in diploid Fragaria. Theor Appl Genet 109(7):1385–1391

Schadt EE, Monks SA, Drake TA, Lusisk AJ, Chek N, Colinayok V, Ruff TG, Milligan SB, Lamb JR, Cavet G, Linsley PS, Mao M, Stoughton RB, Friend SH (2003) Genetics of gene expression surveyed in maize, mouse and man. Nature 422:297–302

Trainotti L, Spinello R, Piovan A, Spolaore S, Casadoro G (2001) β-Galactosidases with a lectin-like domain are expressed in strawberry. J Exp Bot 52:1635–1645

Trainotti L, Zanin D, Casadoro G (2003) A cell wall-oriented genomic approach reveals a new and unexpected complexity of the softening in peaches. J Exp Bot 54:1821–1832

Trainotti L, Bonghi C, Ziliotto F, Zanin D, Rasori A, Casadoro G, Ramina A, Tonutti P (2006) The use of microarray to investigate transcriptome changes during transition from pre-climacteric to climacteric phase in peach fruit. Plant Sci 170:606–613

Tsuchikawa S, Hamada T (2004) Application of time-of-flight near infrared spectroscopy for detecting sugar and acid contents in apples. J Agric Food Chem 52:2434–2439

Waters DLE, Holton TA, Ablett EM, Lee LS, Henry RJ (2005) cDNA microarray analysis of developing grape (Vitis vinifera cv. Shiraz) berry skin. Funct Integr Genomics 5(1):40–58

Yamada K, Lim J, Dale JM, Chen H, Shinn P, Palm CJ, Southwick AM, Wu HC, Kim C, Nguyen M, Pham P, Cheuk R, Karlin-Newmann G, Liu SX, Lam B, Sakano H, Wu T, Yu G, Miranda M, Quach HL, Tripp M, Chang CH, Lee JM, Toriumi M, Chan MMH, Tang CC, Onodera CS, Deng JM, Akiyama K, Ansari Y, Arakawa T, Banh J, Banno F, Bowser L, Brooks S, Carninci P, Chao Q, Choy N, Enju A, Goldsmith AD, Gurjal M, Hansen NF, Hayashizaki Y, Johnson-Hopson C, Hsuan VW, Iida K, Karnes M, Khan S, Koesema E, Ishida J, Jiang PX, Jones T, Kawai J, Kamiya A, Meyers C, Nakajima M, Narusaka M, Seki M, Sakurai T, Satou M, Tamse R, Vaysberg M, Wallender EK, Wong C, Yamamura Y, Yuan S, Shinozaki K, Davis RW, Theologis A, Ecker JR (2003) Empirical analysis of transcriptional activity in the Arabidopsis genome. Science 302:842–846

Zini E, Biasioli F, Gasperi F, Mott D, Aprea E, Märk TD, Patocchi A, Gessler C, Komjanc M (2005) QTL mapping of volatile compounds in ripe apples detected by Proton Transfer Reaction-Mass Spectrometry. Euphytica 145:269–279

3.3 Characterization of major enzymes and genes involved in flavonoid and proanthocyanidin biosynthesis during fruit development in strawberry (*Fragaria x ananassa*).

Biochemical and molecular analyses were carried out to characterize the flavonoid pathway in strawberry (*Fragaria x ananassa* Duch.). Real-Time RT-qPCR experiments were carried out to determine the expression pattern of strawberry flavonoid genes in a reference strawberry genotype (cv Queen Elisa). The results show fine modulations of the transcript abundance of genes involved in flavonoid biosynthesis and of a number of other coding sequences related to fruit quality.

The results are shown in the following attached paper (Almeida et al., 2007).

Available online at www.sciencedirect.com
ScienceDirect
Archives of Biochemistry and Biophysics 465 (2007) 61–71
ABB
www.elsevier.com/locate/yabbi

Characterization of major enzymes and genes involved in flavonoid and proanthocyanidin biosynthesis during fruit development in strawberry (*Fragaria* × *ananassa*) ☆

João R.M. Almeida [a,1], Eleonora D'Amico [a], Anja Preuss [b], Fabrizio Carbone [a], C.H. Ric de Vos [c], Bettina Deiml [d], Fabienne Mourgues [a], Gaetano Perrotta [a], Thilo C. Fischer [d], Arnaud G. Bovy [c], Stefan Martens [b], Carlo Rosati [a,*]

[a] *ENEA, Trisaia Research Center, Department of Genetics and Genomics, S.S.106, km 419+500, 75026 Rotondella, MT, Italy*
[b] *Philipps Universität Marburg, Institut für Pharmazeutische Biologie, Deutschhausstrasse 17A, 35037 Marburg, Germany*
[c] *Plant Research International, 6700 AA Wageningen, The Netherlands*
[d] *Technical University Munich, Department of Plant Sciences, Ornamental Plants and Horticultural Plant Breeding, Am Hochanger 4, 85350 Freising, Germany*

Received 19 March 2007, and in revised form 23 April 2007
Available online 21 May 2007

Abstract

The biosynthesis of flavonoids and proanthocyanidins was studied in cultivated strawberry (*Fragaria* × *ananassa*) by combining biochemical and molecular approaches. Chemical analyses showed that ripe strawberries accumulate high amounts of pelargonidin-derived anthocyanins, and a larger pool of 3′,4′-hydroxylated proanthocyanidins. Activities and properties of major recombinant enzymes were demonstrated by means of *in vitro* assays, with special emphasis on specificity for the biologically relevant 4′- and 3′,4′-hydroxylated compounds. Only leucoanthocyanidin reductase showed a strict specificity for the 3′,4′-hydroxylated leucocyanidin, while other enzymes accepted either hydroxylated substrate with different relative activity rates. The structure of late flavonoid pathway genes, leading to the synthesis of major compounds in ripe fruits, was elucidated. Complex developmental and spatial expression patterns were shown for phenylpropanoid and flavonoid genes in fruits throughout ripening as well as in leaves, petals and roots. Presented results elucidate key steps in the biosynthesis of strawberry flavonoid end products.

Keywords: Flavonoids; Fruit ripening; Developmental gene expression; Proanthocyanidins; Recombinant enzyme activity; Strawberry; Substrate preference

Fruit attractiveness and nutritional value are important traits for humans and in nature, where they contribute to plant seed dispersal, thus increasing plant fitness. Polyphenols play a crucial role in this strategy, since they first visually attract flower pollinators and then animals feeding on fruits. Moreover, they protect plants from biotic and abiotic stresses, and provide nutritional benefits [1–3].

The phenylpropanoid and flavonoid pathways (Fig. 1) have been thoroughly investigated by genetic, biochemical and molecular studies e.g. [4 and references therein]. The pathways are modulated by developmental and environmental cues through structural genes and transcription

☆ Sequence data from this work are in the Genbank database under the following accession numbers. cv 'Queen Elisa': *FaANR*, DQ664192 and DQ664193; *FaANS*, AY695817 and AY695818; *FaDFR*, AY695812 and AY695813; *FaFGT*, AY695815 and AY695816; *FaFHT*, AY691918 and AY691919 (cDNA and gDNA, respectively). cv 'Queen Elisa' gDNAs: *FaFLS* DQ834905; *FaLAR* DQ834906. cv 'Korona' cDNAs: *FaFLS* DQ087252; *FaLAR* DQ087253.

* Corresponding author. Fax +39 0835974749.
E-mail address: carlo.rosati@trisaia.enea.it (C. Rosati).
[1] Present address: Department of Applied Microbiology, Lund University, P.O. Box 124, S-221 00 Lund, Sweden.

0003-9861/$ - see front matter © 2007 Elsevier Inc. All rights reserved.
doi:10.1016/j.abb.2007.04.040

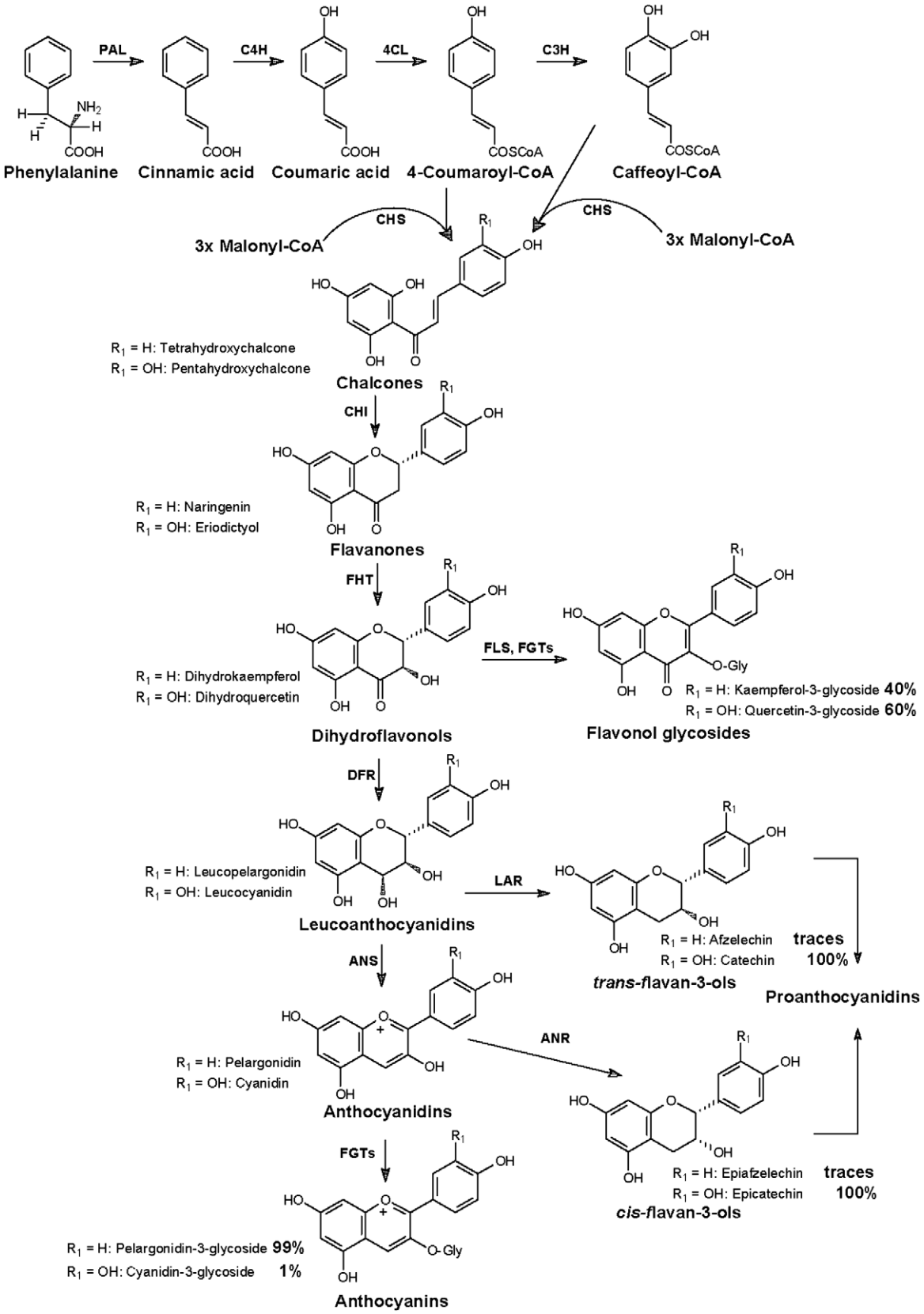

Fig. 1. Schematic representation of the phenylpropanoid and flavonoid pathways. Structures of metabolites which are most relevant for this work, and relative percentage levels within each class of end-products present in ripe fruits of cv. Queen Elisa (cf. Table 1), are shown. Enzyme abbreviations: 4CL, *p*-coumarate:CoA ligase; ANR, anthocyanidin reductase; ANS, anthocyanidin synthase; C3H, *p*-coumaroyl-CoA 3-hydroxylase; C4H, cinnamic acid 4-hydroxylase; CHI, chalcone isomerase; CHS, chalcone synthase; DFR, dihydroflavonol 4-reductase; FGTs, flavonoid glycosyltransferases; FHT, flavanone 3β-hydroxylase; FLS, flavonol synthase; LAR, leucoanthocyanidin reductase; PAL, phenylalanine ammonia-lyase.

factors (TFs)[2], which result in a complex regulation [5 and references therein]. Recent works addressed the synthesis [6,7] and the oxidative polymerization [8] of flavan-3-ols, which serve for proanthocyanidin (PA) biosynthesis (Fig. 1). Many flavonoid pathway enzymes leading to major aglycones belong to the reductase or 2-oxoglutarate-/Fe^{2+}-dependent dioxygenase superfamilies. Furthermore, some cytochrome P450 enzymes perform hydroxylation reactions at 3′ or at 3′,5′ position of the B-ring, which are critical for flavonoid patterns [2].

The Rosaceae family includes many economically important fruit crops, among which the most prominent "berry" species belong to the genera *Fragaria* and *Rubus*. Despite their octoploid level, *F.* × *ananassa* [9–12] and its wild progenitors *F. chiloensis* and *F. virginiana* [13,14] have been the object of molecular studies. In ripe strawberry fruits (hereafter, strawberry receptacle will be referred to as fruit), anthocyanins are the major flavonoid compounds compared to flavonols, flavan-3-ols and simple phenols. Information on levels and qualitative composition of flavan-3-ol polymers PAs in strawberry is scarce and does not precisely describe PA levels and qualitative composition [e.g. 15]. Levels of phenolic compounds have been reported to vary as a function of genetic, environmental and post-harvest factors [16–20]. Some strawberry flavonoid genes and enzymes have been shown to follow a two-phase expression pattern during fruit development [21,22] i.e., early after anthesis and in the final ripening phase. During strawberry ripening, up-regulation of chalcone synthase (*FaCHS*), flavanone 3β-hydroxylase (*FaFHT*), dihydroflavonol 4-reductase (*FaDFR*) and flavonoid glycosyltransferase (*FaFGT*) genes [21,23] corresponds to an increase in enzyme activity in fruit extracts [22], which result in anthocyanin accumulation at ripe red stage. In contrast to model species, comprehensive parallel characterization of structural genes and major enzymes controlling the formation of flavonoid end products in strawberry fruits is still lacking.

In this work, biochemical and molecular analyses were combined to advance in the knowledge of the strawberry flavonoid and PA metabolism. The composition of phenolic compounds in ripe fruits and the spatial and developmental accumulation of major flavonoids in strawberry fruits were analyzed. The activities and substrate specificities of prominent recombinant enzymes involved in flavonoid biosynthesis were studied, and the organization of corresponding genes was elucidated. Expression patterns of main structural genes of phenylpropanoid and flavonoid pathways were analyzed in different organs and during fruit ripening.

Materials and methods

Growing and sampling of strawberry plant material

Strawberry plants of cv 'Queen Elisa' were grown at Institute for Fruit Breeding experimental fields in Cesena, Italy. Potted strawberry plants of cv 'Korona' were field-grown at Department of Plant Science, Freising, Germany. Fruit samples were collected at early green (G1, 7–10 days after anthesis, daa), intermediate green (G2, 12–14 daa), white (W, ca. 20 daa), turning (T, ca. 25 daa) and ripe red (R, ca. 30 daa) stages for RNA and metabolite extraction. Developed leaf, petal and root samples were collected for DNA and RNA extraction. All samples were immediately frozen in liquid nitrogen and kept at −80 °C until use.

Cloning of flavonoid genes

Fruit cDNA sequences of flavonoid genes were obtained by RT-PCR approaches using gene-specific primers (GSPs, listed in Suppl. Table 1S). Red fruit cDNA was used as template for all genes except leucoanthocyanidin reductase (*FaLAR*) (G2 fruit cDNA). For anthocyanidin reductase (*FaANR*), degenerate primers designed from ANR protein alignment (Suppl. Fig. 1S) allowed the amplification of a 686-bp fragment with 91% amino acid homology to *Malus ANR* (AAZ12184). Then, *FaANR* GSPs were designed for 3′ and 5′ rapid amplification of cDNA ends (RACE). Anthocyanidin synthase (*FaANS*) and *FaFHT* full sequences were cloned by 3′ and 5′RACE with GSPs designed from published ESTs (*ANS*: AF041396; *FHT*: AF041385). For cloning of *FaDFR* and *FaFGT* full length coding sequences, GSPs were designed based on available sequence information (*DFR*: AF029685; *FGT*: AY575056). Flavonol synthase (*FaFLS*) was cloned first by designing RoFLSfor and RoFLSrev primers based on a *FLS* sequence from *Rosa* (AB038247), which led to the amplification of a partial 1050-bp fragment, followed by 5′RACE with GSPs. *FaLAR* was cloned by 3′RACE with GSPs designed from LAR protein alignment (Suppl. Fig. 2S). The resulting 839-bp fragment contained an ORF of 588 nucleotides with 87% amino acid homology to *Malus LAR1* (AY830131). *FaLAR* GSPs were successively designed for 5′RACE. Corresponding genomic sequences were obtained using genomic DNA (gDNA) as template in PCR reactions with appropriate primers, or by using a PCR-based walking strategy adapted from [24]. Full cDNA sequences were cloned and sequence-verified in pET15b or pYES2 expression vectors using suitable primers (Suppl. Table 1S) and *Pfu* DNA polymerase.

Molecular procedures

If not otherwise stated, standard molecular procedures were adopted [25]. gDNA was extracted from young leaves following a CTAB method [26]. Total RNA was extracted from fruits, leaves, petals and roots [27]. For quantitative Real Time reverse transcription PCR (qRT-PCR) experiments, first strand cDNA was synthesized from 1 μg total RNA in 30 μl with oligo-d$(T)_{17}$ and Superscript III (Invitrogen, Milan, Italy), according to manufacturer's instructions. cDNA concentration in the RT mix was quantified using a ND-1000 UV spectrophotometer (Nanodrop Technologies, Wilmington, USA), and 5 ng cDNA were used for qRT-PCR experiments, carried out with GSPs (Suppl. Table 2S) designed with Primer Express (Applied Biosystems, Monza, Italy), using an ABI 7900 thermocycler (Applied Biosystems, Monza, Italy) and Platinum Sybr-Green kit (Invitrogen, Milan, Italy) according to manufacturer's instructions. An actin gene, having constant expression levels (data not shown), was used to normalize raw data and calculate relative transcript levels. Means from independent experiments were subjected to one-way ANOVA

[2] *Abbreviations used*: 4CL, *p*-coumarate:CoA ligase; ANR, anthocyanidin reductase; ANS, anthocyanidin synthase; C4H, cinnamic acid 4-hydroxylase; CHI, chalcone isomerase; CHS, chalcone synthase; DFR, dihydroflavonol 4-reductase; DMACA, *p*-methylaminocinnamaldehyde; F3′H, flavonoid 3′-hydroxylase; Fa, *Fragaria* × *ananassa*; FGT, flavonoid glycosyltransferase; FHT, flavanone 3β-hydroxylase; FLS, flavonol synthase; FW, fresh weight; GSP, gene-specific primer; LAR, leucoanthocyanidin reductase; LC, liquid chromatography; MS, mass spectrometry; PA, proanthocyanidin; PAL, phenylalanine ammonia-lyase; PDA, photodiode array; PTFE, polytetrafluoroethylene; qRT-PCR, quantitative Real Time reverse transcription PCR; QTOF, quadrupole time of flight; TF, transcription factor.

and Tukey's pairwise comparisons using PAST (http://folk.uio.no/ohammer/past/). Automated sequencing was carried out with ABI 3700 or ABI 3730*xl* (Applied Biosystems, Monza, Italy) DNA sequencers.

Substrate specificity assays with recombinant enzymes

Flavonoid standards and other chemicals were from TransMIT Flavonoidforschung (Giessen, Germany), Phytolab (Vestenbergsgreuth, Germany), Roth (Karlsruhe, Germany), Sigma (Deisenhofen, Germany) and MBI Fermentas (St. Leon-Roth, Germany). [2-^{14}C]-malonyl-CoA and UDP-[U-^{14}C]-glucose were from Hartmann Analytik (Braunschweig, Germany) and Amersham Biosciences (Freiburg, Germany), respectively. Synthesis of labeled substrates is described by [28,29].

Yeast heterologous expression experiments were carried out as described [28]. Construction of bacterial expression vector pET15b-FaFGT, transformation of *Escherichia coli* strain BL21, growth, induction and protein isolation was done according to manufacturer's description (Invitrogen).

Reaction mixtures (0.5 ml) contained 250–500 μg total protein. Bacterial and yeast cultures with empty pET15b or pYES2, and boiled protein extracts, were used as controls. Assay conditions of each test are summarized in Suppl. Table 3S. Reaction products were extracted twice with 200 μl EtOAc. EtOAc extracts were applied to cellulose TLC plates for separation. LAR and ANR assay extracts were quantified by HPLC-DAD (Merck-Hitachi, Darmstadt, Germany) as described in Refs. [6] and [7], respectively.

Chemical analyses of fruit polyphenols

Flavonoids and other phenolics were extracted and analyzed essentially as described in [30], with some modifications. Briefly, 0.5 g of frozen strawberry powder was extracted with 1.5 ml cold methanol containing 0.1% formic acid, followed by 15 min sonication. Samples were then centrifuged at 2500 rpm for 10 min and the supernatants were filtered over 0.2 μm PTFE. Analysis was carried out using a Waters W600 system and a Luna C18 column (150 × 4.6 mm, 3μ; Phenomenex, Torrance, CA, USA) heated to 40 °C. A 5–35% acetonitrile gradient in 0.1% trifluoroacetic acid (1 ml min^{-1} flow rate) was used for separation. Samples were monitored continuously from 210 to 600 nm by a Waters 996 PDA detector. Data were analyzed using Waters Empower software. Absorbance spectra and retention times of eluting peaks were compared with those of commercial standards (Sigma, Zwijndrecht, The Netherlands; Extrasynthèse, Genay, France; Apin Chemicals, Abingdon, UK). Dose–response curves of standards (0–50 μg ml^{-1}) were determined and used to quantify these compounds and derivatives thereof showing similar absorbance characteristics in the extracts. Identity of compounds was confirmed by LC-PDA-QTOF MS and MS/MS [31]. Analysis of PA composition was carried out by treating samples with phloroglucinol as reported [32].

Results

Assessment and localization of anthocyanin and flavan-3-ol major flavonoid compounds in developing strawberry fruits

The spatial and developmental accumulation of flavan-3-ols was studied in cvs 'Queen Elisa' and 'Korona' by treating fruit sections with *p*-dimethylaminocinnamaldehyde (DMACA; Fig. 2). DMACA specifically reacts with flavan-3-ol-containing compounds to give a blue coloration

Fig. 2. DMACA staining of longitudinal and transversal sections of strawberry fruits at G1 (top left), G2 (top right), white (middle left), turning (middle right) and red (bottom) stages of cv 'Korona'. Blue coloration indicates the presence of flavan-3-ols and their derivatives in tissues. DMACA treatment of 'Queen Elisa' fruits produced comparable staining results (data not shown).

[33]. Fruits of both 'Queen Elisa' and 'Korona' varieties gave a similar pattern: from W to R stage, red-orange anthocyanin levels increased, while flavan-3-ol-associated DMACA staining generally decreased. Interestingly, DMACA staining was spatially associated with vascular, epidermis and core fruit tissues at W stage, and mostly restricted to vascular tissues at T and R stages.

Chemical analyses of polyphenol composition in fruits

Targeted analyses of fruit methanol extracts detected four major classes of phenolic compounds (Table 1). Anthocyanins were the most abundant monomer compounds, with a total concentration of more than 180 mg kg^{-1} berry fresh weight (FW). Pelargonidin derivatives were by far the major anthocyanins, among which pelargonidin-3-glucoside and pelargonidin-3-*O*-malonyl glucoside accounted for 80% and 14% of total anthocyanins, respectively. Total flavonol and monomer flavan-3-ol concentration was 23 and 36 mg kg^{-1} FW, respectively. Quercetin and kaempferol derivatives had a balanced 3:2 ratio. As to flavan-3-ols, catechin was virtually the only aglycone present: epicatechin was detected only in trace amounts, as well as 4′-hydroxylated afzelechin, whose mass spectrometry signal was about 25-fold lower than that of catechin in 'Queen Elisa' (data not shown). Phloroglucinol treatment [32] revealed an unprecedented large flavan-3-ol pool in the form of oligomeric and polymeric PAs. PA terminal units predominantly consisted of catechin units (10-fold more than epicatechin). In contrast, epicatechin level as extension unit was 4-fold that of catechin (Table 1). Sugar or acyl substitutions were all at the 3 position of identified flavonoids. Flavonols were present as either glucosides or glucuronides, while a more complex pattern was observed for anthocyanins, with mono- (glucose, arabinose) or disaccharide (rutinose) and acylated (malonylated) substitutions of pelargonidin and only small amounts of cyanidin glucosides, in addition to three unidentified pelargonidin derivatives (Table 1). Finally, *p*-coumaric and ellagic acid derivatives were present in relatively high amounts in red fruits, while levels of chlorogenic acid derivatives were below 1 mg kg^{-1} (data not shown).

Recombinant enzyme assays

Full coding sequences of *FaANR*, *FaANS*, *FaDFR*, *FaFGT*, *FaFHT*, *FaFLS* and *FaLAR* were expressed in *E. coli* or *Saccharomyces cerevisiae*, respectively using pET15b (FaFGT) or pYES2 (other enzymes) vectors (see Methods). Cell extract preparations were obtained from transformed bacterial or yeast cultures after induction of protein expression, and standard assays for each enzyme were developed (Suppl. Table 3S). A number of physiologically relevant substrates according to the analytical data (Table 1 and Suppl. Table 3S) were assayed for each enzyme. All expressed flavonoid genes produced functional enzymes with the assigned activity (Table 2). In particular, 4′-hydroxylated flavonoids were the preferred substrates of FaANS, FaDFR, FaFHT and FaFLS, whereas FaLAR and FaANR showed a higher activity on 3′,4′-hydroxylated compounds. A strict substrate specificity was found only for FaLAR, which used only leucocyanidin as substrate. Combined FaDFR + FaANS enzyme assays using dihydrokaempferol as substrate yielded both pelargonidin and kaempferol (Fig. 3): this demonstrated not only the postulated activity of both enzymes (conversion of dihydrokaempferol into pelargonidin *via* the leucopelargonidin intermediate), but also FaANS side reactions [34]. Other qualitative assays on unnatural substrates showed minor flavanone reductase activity of FaDFR, and FaLAR activity on 3-deoxyleucoanthocyanidins (data not shown). Concerning glycosylation of flavonoid end products, FaFGT displayed a strong 3-*O*-glucosyltransferase activity on both tested anthocyanidins, while flavonols seem to be only a minor substrate (Table 2). Competition experiments providing various substrates gave similar ratios of product formation as those obtained from standard assays (data not shown).

Molecular characterization of flavonoid structural genes

Genomic sequences were obtained by PCR with GSPs using gDNA of 'Queen Elisa' as template (see Materials and methods). Comparison between cDNA and gDNA sequences revealed the presence of introns in all genes (Suppl. Fig. 3S): one in *FaANS* and *FaFGT*; two in *FaFHT* and *FaFLS*; four in *FaLAR* and *FaANR*; and five in *FaDFR*. The number and position of gene introns were generally conserved when compared with those of other species. Intron length varied between 94 bp (intron I of *FaDFR*) and 1383 bp (intron I of *FaFLS*). Length polymorphisms were found between introns of *FaANS*, *FaDFR* and *FaFHT* genes and the corresponding introns of gene homologs in *F. vesca* [35]. Amino acid sequence analysis revealed several catalytic domains for all enzymes (Suppl. Fig. 3S). For instance, FaFGT contains the PSPG box, critical for substrate binding [36]. FaLAR has the RFLP, ICCN and THD motifs (named after the codes of "signature" amino acids) specific of LAR proteins [37], as well as a Gly-rich NAD(P)H-binding site [38] starting at G20.

Southern analyses (data not shown) detected a variable number of bands for each above-studied gene in 'Queen Elisa': one for *FaFGT*; up to two for *FaANR*; up to 4–5 for *FaANS*, *FaDFR*, *FaFHT* and *FaLAR*; and as many as eight for *FaFLS*.

Gene expression analyses

qRT-PCR experiments were carried out to determine gene transcript levels in various organs and developing fruits. In order to perform a more complete analysis, phenylalanine ammonia-lyase (*FaPAL*), cinnamic acid 4-hydroxylase (*FaC4H*), *p*-coumarate:CoA ligase (*Fa4CL*), four *CHS* (*FaCHS1*, *FaCHS2*, *FaCHS3*, and *FaCHS5*),

Table 1
Levels of phenolic compounds in red fruits of cv 'Queen Elisa'

Compound class	Metabolite	Level (mg kg^{-1} fresh weight)
Anthocyanins	Pelargonidin-3-*O*-glucoside	145.7
	Pelargonidin-3-*O*-rutinoside	4.9
	Pelargonidin-3-*O*-arabinoside	0.4
	Pelargonidin-3-*O*-malonyl glucoside	25.4
	Pelargonidin derivative (28.7)	1.4
	Pelargonidin derivative (34.5)	2.2
	Pelargonidin derivative (41.6)	0.2
	Cyanidin-3-*O*-glucoside	2.4
Flavonols	Quercetin-3-*O*-glucoside	2.5
	Quercetin-3-*O*-glucuronide	11.1
	Kaempferol-3-*O*-glucoside	2.1
	Kaempferol-3-*O*-glucuronide	3.4
	Kaempferol-3-*O*-glucoside derivative (31.1)	3.7
Flavan-3-ols	Catechin monomer	35.8
	Epicatechin monomer	<0.2
	Catechin (as PA extension unit)	104.3
	Epicatechin (as PA extension unit)	436.4
	Catechin (as PA terminal unit)	108.8
	Epicatechin (as PA terminal unit)	10.1
Other phenolics	*p*-Coumaroyl glucoside	55.9
	p-Coumaric acid derivative (14.7)	12.9
	Ellagic acid derivative (23.2)	3.3
	Ellagic acid derivative (23.5)	13.8
	Ellagic acid derivative (24.4)	12.5

Figures within parentheses following unidentified derivative compounds indicate their retention time (in min).

FaCHI and the TF *FaMYB1* [39] genes were also assayed in qRT-PCR experiments, by designing suitable GSPs from available sequences of either closely-related Rosaceae species (only for *PAL*, *C4H* and *4CL*) or strawberry (Suppl. Table 2S). Primers were designed in conserved regions of genes, to allow the detection of multiple gene copy/allele transcripts and thus broad-spectrum transcript analysis of each gene.

Comparative expression analyses in leaves, petals, roots, and R fruits showed that flavonoid pathway genes leading to anthocyanin formation were generally most strongly expressed in fruits (Fig. 4). On the other hand, relative expression levels of all genes were consistently low in leaves, while petals and roots showed distinct expression patterns when compared to each other and to red fruits. Phenylpropanoid pathway genes *FaPAL*, *FaC4H* and *Fa4CL* were strongly expressed in petals, while only *Fa4CL* was up-regulated in roots. Concerning *FaCHS* genes, petals showed the highest levels of expression of all four members with respect to roots and leaves, *FaCHS2* and *FaCHS5* being the most strongly expressed. The expression pattern of flavonoid pathway genes in petals seems to support the synthesis of flavonol derivatives: *FaCHI*, *FaFHT* and *FaFLS* were up-regulated, while *FaDFR* and *FaANS* were repressed. Roots exhibited a quite different pattern: only *FaLAR* and *FaANR* genes were clearly up-regulated, with *FaLAR* more expressed than *FaANR*.

In fruits, developmental expression analysis showed a transcript peak at T stage for all studied genes (Fig. 5). In order to highlight common regulatory mechanisms, genes were grouped according to their expression patterns. Phenylpropanoid genes *FaPAL*, *FaC4H* and *Fa4CL* had a similar two-phase expression pattern with a decrease of transcript levels at W stage, although statistically significant differences were found only for *Fa4CL* gene (Fig. 5A). *FaCHS* transcripts also showed a two-phase expression pattern, and the highest relative expression

Table 2
Activity and substrate specificity of flavonoid recombinant enzymes expressed in bacterial (FaFGT) and yeast (other enzymes) systems

Enzyme	Substrate	Relative activity (%)	Reaction products
FaFHT	Naringenin	100	Dihydrokaempferol
	Eriodictyol	67	Dihydroquercetin
FaFLS	Dihydrokaempferol	100	Kaempferol
	Dihydroquercetin	2.5	Quercetin
FaDFR	Dihydrokaempferol	100	Leucopelargonidin
	Dihydroquercetin	43	Leucocyanidin
FaANS	Leucopelargonidin	100	Pelargonidin
	Leucocyanidin	37	Cyanidin
FaLAR	Leucopelargonidin	0	Afzelechin
	Leucocyanidin	100	Catechin
FaANR	Pelargonidin	24	Epiafzelechin
	Cyanidin	100	Epicatechin
FaFGT	Pelargonidin	100	Pelargonidin-3-*O*-glucoside
	Cyanidin	87	Cyanidin-3-*O*-glucoside
	Kaempferol	3	Kaempferol-3-*O*-glucoside
	Quercetin	8	Quercetin-3-*O*-glucoside

For each enzyme, relative activity on physiologically relevant substrates was measured (conversion rate of the main substrate = 100%).

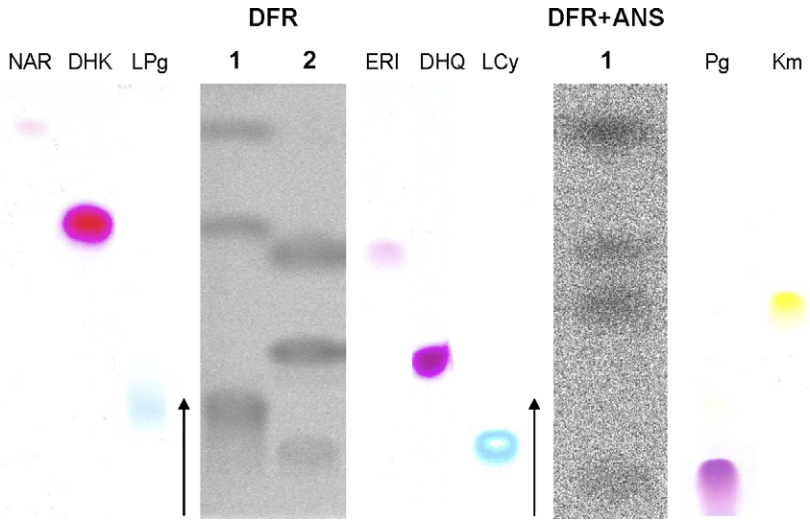

Fig. 3. Thin layer chromatography of reaction products from FaDFR alone (left) and coupled FaDFR + FaANS (right) enzyme assays, using ^{14}C-dihydrokaempferol (1) or ^{14}C-dihydroquercetin (2) as substrates. Unlabeled standards were run along with labeled reaction products as references. Plates were run in CAW (chloroform:acetic acid:water; 50:45:5). Arrows indicate the direction of solvent run. Staining of standards was performed by spraying with 0.1% DMACA in 6N HCl:EtOH 1:1 (v/v) [33] or with zinc–HCl [52]. Traces of ^{14}C-NAR and ^{14}C-ERI are due to incomplete synthesis of the respective dihydroflavonols. DHK, dihydrokaempferol; DHQ, dihydroquercetin; ERI, eriodictyol; Km, kaempferol; LCy, leucocyanidin; LPg, leucopelargonidin; NAR, naringenin; Pg, pelargonidin.

values at T stage among all studied genes; strong differences between expression levels at T stage from independent experiments prevented statistical significance of mean values (Fig. 5B). Flavonoid pathway genes could be clearly classified in two groups according to their expression pattern: *FaANR*, *FaANS*, *FaCHI*, *FaFHT* and *FaLAR* had two transcription peaks at early and late stages (Fig. 5C), while *FaDFR*, *FaFGT*, *FaFLS* and *FaMYB* showed an up-regulation trend with a single peak at T and/or R stage (Fig. 5D). Only *FaFLS* and *FaLAR* showed a significant down-regulation at R stage with respect to T stage (Fig. 5C–D).

Discussion

The increasing interest in new sciences such as food nutrigenomics requires interdisciplinary knowledge of main plant natural product pathways [40]. Flavonoids and PAs are important food secondary metabolites, with a strong impact on visual aspect, sensorial attributes and health benefits of fresh and processed fruit products. The knowledge gap on strawberry PAs prompted parallel biochemical and molecular investigations, allowing a deep insight of strawberry flavonoid metabolism.

Developmental regulation of flavonoid biosynthesis in strawberry fruits

Overall results of expression analyses evidenced a coordinated control of transcription of all studied genes in fruits. Careful design of qRT-PCR primers in conserved protein domains enabled a theoretical maximum coverage of expressed alleles/copies for each gene, in order to obtain comprehensive information on gene expression, especially in fruits. The only exception was *FaCHS* gene family, for which four sequences were already present in public databases, whose analysis revealed marked differences in spatial rather than developmental patterns. A general up-regulation of all genes occurred at T stage (Fig. 5), which is related to relevant enzyme activity and formation of flavonoid end-products in ripe fruits. However, non negligible amounts of phenylpropanoid metabolites are also directed towards the synthesis of simple phenolics, assisted by the up-regulation of *FaPAL*, *FaC4H* and *Fa4CL* transcripts (Fig. 5A), showing that metabolite synthesis is not completely directed into flavonoid formation despite the strong up-regulation of *FaCHS* genes.

Similarly to *Fa4CL*, the strong up-regulation of all *FaCHS* members in fruits highlights the central role of CHS in flavonoid biosynthesis. While all *FaCHS* genes had a similar developmental expression pattern in fruits, a significant spatial regulation of the *FaCHS* family was found: *FaCHS2* and *FaCHS5* were more expressed in petals, while *FaCHS1* and *FaCHS3* transcripts were more abundant in red fruits (Fig. 5). Expression of multiple polyketide synthase genes is organ-specific and developmentally regulated also in *Petunia*, *Rubus* and *Vitis* [41–43]. In our experiments, the very high transcript levels of *FaCHS* gene(s) at T/R stages are somewhat in contrast with the low CHS activity found by [22] at late ripening stages, and might indicate genotype-related differences and/or post-transcriptional control of the expression of *FaCHS* genes.

Striking differences were found in the expression of genes involved in anthocyanin *vs* flavonol/flavan-3-ol biosynthesis. The critical stage was R, at which the steady up-regulation of anthocyanin genes, and down-regulation of *FaFLS*, *FaLAR* (and, to a lesser extent, *FaANR*),

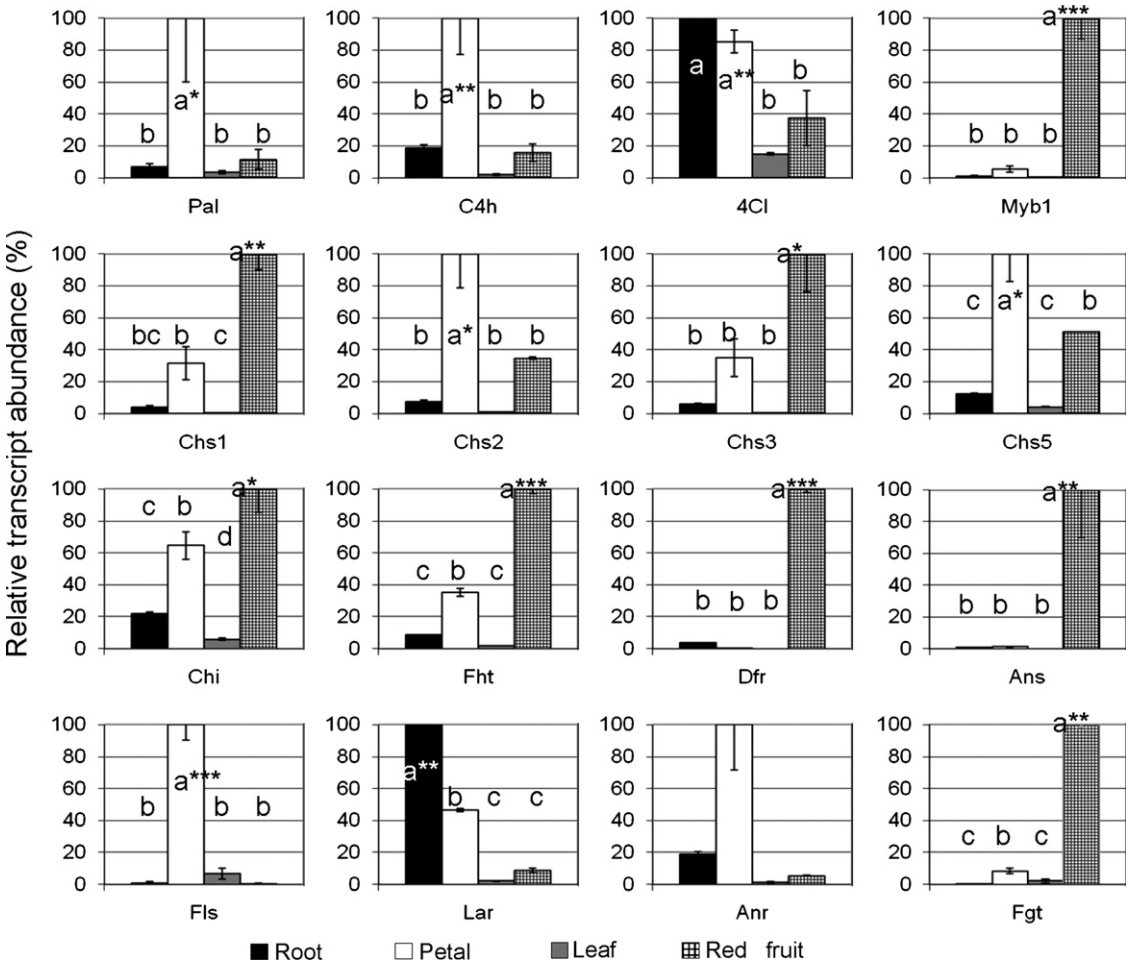

Fig. 4. Spatial qRT-PCR analysis of gene expression in leaves, petals, roots and red fruits of cv 'Queen Elisa'. Relative gene expression levels are shown, following normalization with actin transcript values, and compared with those of fruits (highest value = 100%). For gene acronyms, see text. Values and error bars represent the average and standard deviation from two independent experiments, respectively. For each gene, different letters indicate significant differences among mean values ($^{*}p \leqslant 0.05$; $^{**}p \leqslant 0.01$; $^{***}p \leqslant 0.001$).

determine the massive synthesis of pelargonidin derivatives against flavonols and flavan-3-ols. Among ripening-induced genes, the strong up-regulation of *FaFGT* throughout fruit ripening stages agrees with previous reports [21] and is related to the final glycosylation step of flavonoid end-products. The expression pattern of *FaDFR* is noteworthy, since it is different from the two-phase pattern reported in Ref. [23], and common to most other flavonoid genes (Fig. 5). Since Southern analyses showed that FaDFR is encoded by a small multigene family in strawberry ([23], this work), it is possible that our *FaDFR*, cloned from late ripening fruit cDNA, is associated to anthocyanin biosynthesis, and that other sequence-divergent, developmentally-regulated *FaDFR*s might be expressed at earlier stages. As to PA biosynthesis, because catechin is predominantly used as terminal unit and epicatechin as extension unit, it can be inferred that (1) FaLAR is the key enzyme for the initiation of PA molecules, while FaANR is likely to provide the substrates for the synthesis of PA oligo- and polymers and (2) a substrate specificity of polymerizing enzyme(s) based on *cis*/*trans* isomerism of flavan-3-ols should be considered. The specific localization of flavan-3-ols/PAs in fruit vascular bundles has analogies with the expression pattern of cinnamyl alcohol dehydrogenase and cinnamoyl CoA reductase enzymes, respectively associated with lignified fruit and xylem vascular tissues [44,45], and that of a HyPRP protein considered to possess a polyphenol anchoring function [46]. Thus, the interplay between polyphenol-containing polymers (PAs, lignin) and associated proteins in vascular tissues should be further addressed. Concerning the levels of flavan-3-ol and PA compounds, one should take into account not only the action of biosynthetic enzymes—LAR, ANR for flavan-3-ols, and flavan-3-ol polymerizing proteins for PAs—but also the possible role of still uncharacterized depolymerizing and/or degrading enzymes throughout fruit ripening. Polyphenol oxidase and peroxidase enzymes have been shown to degrade flavonoids in non-cell systems (processed food) as well as *in vivo* [47 and references therein]. Active degradation of anthocyanins *in planta* has been recently proposed in *Brunfelsia* as a senescence-independent mechanism not associated with browning, likely

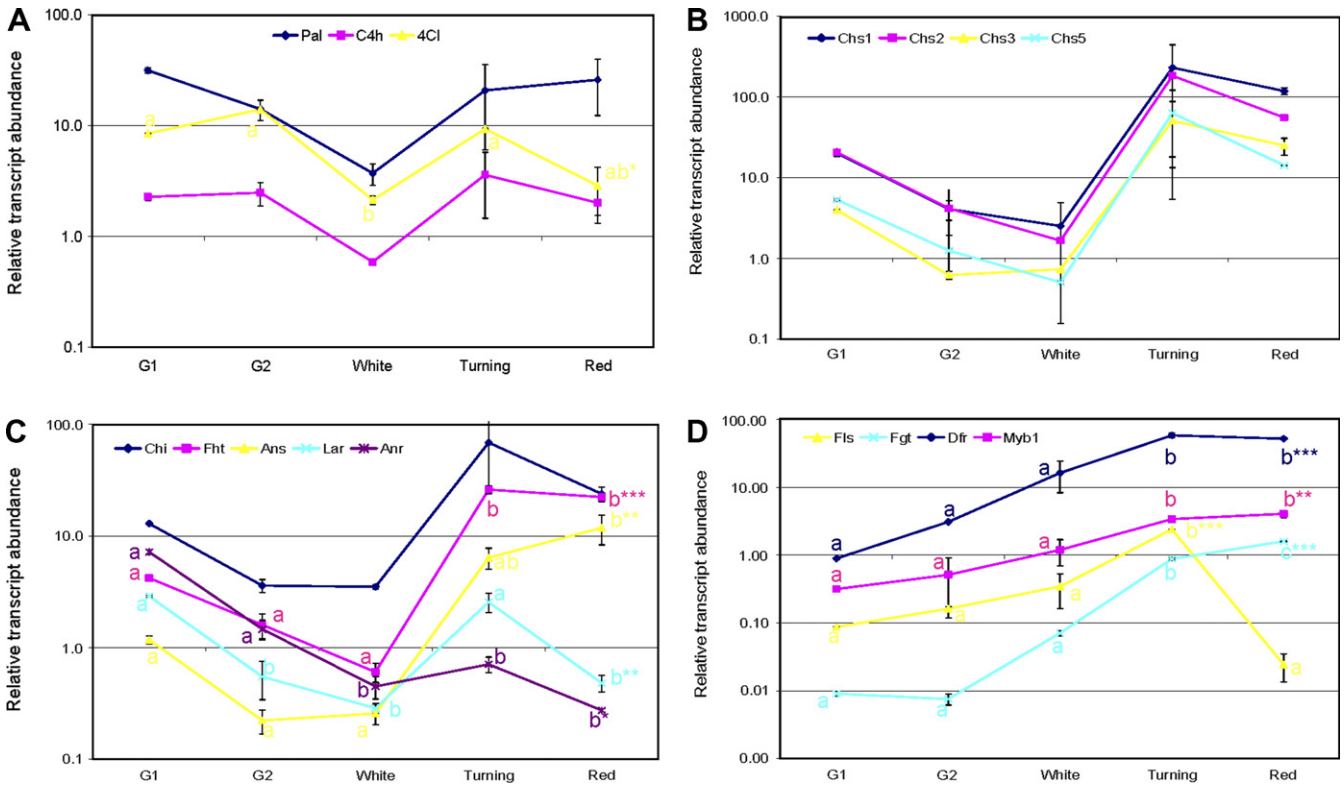

Fig. 5. Developmental qRT-PCR analysis of gene expression in fruits of cv 'Queen Elisa' at different stages (G1, G2, W, T and R). Relative gene expression levels are shown (*Y* axis in Log scale), following normalization with actin transcript values. (A) Phenylpropanoid pathway genes. (B) *FaCHS* gene family. (C) Flavonoid pathway genes showing a two-phase expression pattern. (D) Flavonoid pathway genes and *FaMYB1* TF showing a one-phase expression pattern. For gene acronyms, see text. Values and error bars represent the average and standard deviation from two independent experiments, respectively. For each gene, different letters indicate significant differences among mean values ($^{*}p \leqslant 0.05$; $^{**}p \leqslant 0.01$; $^{***}p \leqslant 0.001$).

driven by the action of peroxidases postulated to act in the vacuoles, the subcellular compartment where flavonoids accumulate [48].

The transcription patterns of structural genes suggest the action of distinct sets of TFs, regulating e.g. flavan-3-ol/PA biosynthesis at early developmental stage(s), flavonols at R stage and anthocyanin synthesis at T/R stages. This is similar to Arabidopsis, maize and petunia, where MYB-, MYC- and WDR-types of TFs form complexes regulating these three branches of the flavonoid pathway [5 and references therein]. The low but steadily increasing expression of *FaMYB1* throughout ripening in cv 'Queen Elisa' is consistent with its role as TF and with the pattern of cv 'Elsanta' [39]. Specific interactions among a broader number of TFs need to be thoroughly studied to determine regulation networks in strawberry fruits.

Flavonoid biosynthesis is spatially regulated in strawberry organs

The observed spatial regulation of flavonoid gene expression has multiple biological meanings. In fruits, accumulation of red-orange anthocyanins at final ripening stage imparts a visual cue to animals and humans for fruit consumption. On the other hand, the progressive reduction of flavan-3-ol and PA levels from whole fruits to vascular tissues during fruit development indicates different (1) regulation and/or transport mechanisms controlling their spatial and developmental accumulation and (2) biological action of these compounds.

In flowers, the transcriptional block of *FaDFR* and *FaANS* and the high transcript levels of upstream genes are likely to promote the biosynthesis of flavonols for pollinator attraction [1,49]. In leaves, flavonoids are mostly accumulated in the epidermal layers to serve as UV light-protectants: the observed low expression probably reflects a homeostasis situation, where low levels of transcripts are sufficient to maintain the levels of flavonoid compounds. Up-regulation of *Fa4CL* most likely indicates the central role of coumaroyl-CoA in the synthesis of lignin precursors in roots.

Hydroxylation state of flavonoid pools and substrate specificity of recombinant enzymes

Several factors can concur, simultaneously or separately, to determine the hydroxylation pattern of flavonoid end products: (1) enzyme substrate specificity; (2) flavonoid 3′-hydroxylase (F3′H) activity, generally acting on substrates upstream of DFR; and (3) the presence of multiple (iso)enzymes with different catalytical properties. Chemical analyses were in agreement with the preference

of anthocyanidin-related enzymes (FaFHT, FaDFR and FaANS) for 4′-hydroxylated flavonoids and, more markedly, of flavan-3-ol-related enzymes (FaLAR and FaANR) for 3′,4′-hydroxylated flavonoids. Considering FaFHT preference for naringenin with respect to eriodictyol, F3′H activity on flavanones and/or dihydroflavonols is a common scenario for the simultaneous presence of kaempferol and quercetin flavonols. The preference of FaDFR for dihydrokaempferol is an important feature for the synthesis of pelargonidin-derived anthocyanins. On the other hand, the conversion of dihydroquercetin into leucocyanidin by FaDFR is a prerequisite for the formation of 3′,4′-hydroxylated flavan-3-ols. In this respect, the exclusive accumulation of 3′,4′-hydroxylated flavan-3-ols (Table 1) suggests a spatial or temporal regulation of F3′H gene expression and/or enzyme activity. The last point is theoretically compatible with the results of Southern analyses for most genes except *FaFGT*, which show the presence of small to large gene families. This is a common situation for flavonoid genes, possibly further enhanced by the polyploidy of cultivated strawberry. Nevertheless, sequencing work evidenced only one cDNA member and Southern analyses the presence of large gene families only for *FaFLS* (data not shown). These results are likely to indicate the dominance of one transcript for each analyzed gene and/or low polymorphism of flavonoid genes in the octoploid background of *F.* × *ananassa*. Finally, flavanone 4-reductase activity of FaDFR and 3-deoxyflavanol reductase activity of FaLAR, found also in other fruit species, and multifunctionality of FaANS, are indicative of enzyme evolution and the possible presence of alternative pathways [34,50,51].

In conclusion, the presented biochemical and molecular studies give a comprehensive insight of flavonoid metabolism in strawberry. This work provides the basis for comparative analyses of strawberry genotypes with different flavonoid accumulation in fruits and functional characterization of alleles within each gene family. New knowledge will also allow to tailor genetic engineering approaches to improve the nutritional value of strawberry.

Acknowledgments

Funding by EU Project FLAVO (FOOD CT-2004-513960) and Bayerisches Staatsministerium für Landesentwicklung und Umweltfragen is acknowledged. Authors thank ENEA Casaccia Genelab for generous support in gene sequencing, Dr. Salvatore Arpaia for helpful advice in statistical analyses, and Prof. Gert Forkmann for critical reading of the manuscript.

Appendix A. Supplementary data

Supplementary data associated with this article can be found, in the online version, at doi:10.1016/j.abb.2007.04.040.

References

[1] R.A. Dixon, C.L. Steele, Trends Plant Sci. 4 (1999) 394–400.
[2] G. Forkmann, W. Heller, U. Sankawa (Eds.), Comprehensive natural products chemistry, Polyketides and other secondary metabolites including fatty acids and their derivatives, vol. 1, Elsevier, Oxford, 1999, pp. 713–748.
[3] S.M. Hannum, Crit. Rev. Food Sci. Nutr. 44 (2004) 1–17.
[4] K.M. Davies, K.E. Schwinn, in: O.M. Andersen, K.R. Markham (Eds.), Flavonoids—Chemistry, Biochemistry and Applications, CRC Taylor & Francis, Boca Raton, 2006, pp. 143–218.
[5] L. Lepiniec, I. Debeaujon, J.M. Routaboul, A. Baudry, L. Pourcel, N. Nesi, M. Caboche, Annu. Rev. Plant Biol. 57 (2006) 405–430.
[6] G.J. Tanner, K.T. Francki, S. Abrahams, J.M. Watson, P.J. Larkin, A.R. Ashton, J. Biol. Chem. 278 (2003) 31647–31656.
[7] D.Y. Xie, S.B. Sharma, N.L. Paiva, D. Ferreira, R.A. Dixon, Science 299 (2003) 396–399.
[8] L. Pourcel, J.M. Routaboul, L. Kerhoas, M. Caboche, L. Lepiniec, I. Debeaujon, Plant Cell 17 (2005) 2966–2980.
[9] A. Aharoni, L.C.P. Keizer, H.J. Bouwmeester, Z. Sun, M. Alvarez Huerta, H.A. Verhoeven, J. Blaas, A.V. Houwelingen, R.C.H. De Vos, H. Voet, R.C. vd Jansen, M. Guis, J. Mol, R.W. Davis, M. Schena, A.J.V. Tunen, A.P. O'Connell, Plant Cell 12 (2000) 647–661.
[10] E. Lerceteau-Köhler, G. Guérin, F. Laigret, B. Dénoyès-Rothan, Theor. Appl. Genet. 107 (2003) 619–628.
[11] F. Carbone, F. Mourgues, F. Biasioli, F. Gasperi, T.D. Märk, C. Rosati, G. Perrotta, Mol. Breed. 18 (2006) 127–142.
[12] S. Lunkenbein, M. Bellido, A. Aharoni, E.M.J. Salentijn, R. Kaldenhoff, H.A. Coiner, J. Muñoz-Blanco, W. Schwab, Plant Physiol. 140 (2006) 1047–1058.
[13] M.V. Ashley, J.A. Wilk, S.M.N. Styan, K.J. Craft, K.L. Jones, K.A. Feldheim, K.S. Lewers, T.L. Ashman, Theor. Appl. Genet. 107 (2003) 1201–1207.
[14] M.G. Martinez Zamora, A.P. Castagnaro, J.C. Diaz Ricci, Mol. Genet. Genom. 272 (2004) 480–487.
[15] L. Gu, M.A. Kelm, J.F. Hammerstone, G. Beecher, J. Holden, D. Haytowitz, R.L. Prior, J. Agric. Food Chem. 51 (2003) 7513–7521.
[16] W. Kalt, C.F. Forney, A. Martin, R.L. Prior, J. Agric. Food Chem. 47 (1999) 4638–4644.
[17] S.H. Häkkinen, A.R. Törrönen, Food Res. Int. 33 (2000) 517–524.
[18] S.H. Häkkinen, S.O. Kärenlampi, H.M. Mikkänen, I.M. Heinonen, A.R. Törrönen, Eur. Food Res. Technol. 212 (2000) 75–80.
[19] M.P. Kähkönen, A.I. Hopia, M. Heinonen, J. Agric. Food Chem. 49 (2001) 4076–4082.
[20] S.Y. Wang, H.S. Lin, J. Agric. Food Chem. 48 (2000) 140–146.
[21] K. Manning, Planta 205 (1998) 622–631.
[22] H. Halbwirth, I. Puhl, U. Haas, K. Jesik, D. Treutter, K. Stich, J. Agric. Food Chem. 54 (2006) 1479–1485.
[23] E. Moyano, I. Portero-Robles, N. Medina-Escobar, V. Valpuesta, J. Muñoz-Blanco, J.L. Caballero, Plant Physiol. 117 (1998) 711–716.
[24] P.D. Siebert, A. Chenchik, D.E. Kellogg, K.A. Lukyanov, S.A. Lukyanov, Nucleic Acids Res. 23 (1995) 1087–1088.
[25] J. Sambrook, E.F. Fritsch, T. Maniatis, Molecular Cloning: A Laboratory Manual, second ed., Cold Spring Harbor, New York, 1989.
[26] S.M. Aljanabi, L. Forget, A. Dookun, Plant Mol. Biol. Rep. 17 (1999) 1–8.
[27] R. Lopez-Gomez, M.A. Gomez-Lim, Hortscience 27 (1992) 440–442.
[28] S. Martens, T. Teeri, G. Forkmann, FEBS Lett. 531 (2002) 453–458.
[29] S. Martens, G. Forkmann, L. Britsch, F. Wellmann, U. Matern, R. Lukačin, FEBS Lett. 544 (2003) 93–98.
[30] A.G. Bovy, C.H.R. De Vos, M. Kemper, M. Almenar Pertejo, S. Muir, G. Collins, S. Robinson, M. Verhoeyen, S. Hughes, A.J. van Tunen, Plant Cell 14 (2002) 2509–2526.
[31] S. Moco, R.J. Bino, O. Vorst, H.A. Verhoeven, J. De Groot, J.A. Van Beek, J. Vervoort, C.H.R. De Vos, Plant Physiol. 141 (2006) 1205–1218.

[32] J.A. Kennedy, G.P. Jones, J. Agric. Food Chem. 49 (2001) 1740–1746.
[33] W. Feucht, D. Treutter, E. Christ, Tree Physiol. 10 (1992) 169–177.
[34] R. Lukačin, F. Wellmann, L. Britsch, S. Martens, U. Matern, Phytochemistry 62 (2003) 287–292.
[35] C. Deng, T.M. Davis, Theor. Appl. Genet. 103 (2001) 316–322.
[36] T. Vogt, P. Jones, Trends Plant Sci. 5 (2000) 380–386.
[37] J. Bogs, M.O. Downey, J.S. Harvey, A.R. Ashton, G.J. Tanner, S.P. Robinson, Plant Physiol. 139 (2005) 652–663.
[38] D.Y. Xie, S.B. Sharma, N.L. Paiva, R.A. Dixon, Arch. Biochem. Biophys. 422 (2004) 91–102.
[39] A. Aharoni, C.H.R. De Vos, M. Wein, Z. Sun, R. Greco, A. Kroon, J.N.M. Mol, A.P. O'Connell, Plant J. 28 (2001) 319–332.
[40] M.J. Rist, U. Wenzel, H. Daniel, Trends Biotechnol. 24 (2006) 172–178.
[41] R.E. Koes, R. van Blokland, F. Quattrocchio, A.J. van Tunen, J.N.M. Mol, Plant Cell 2 (1990) 379–392.
[42] W. Wiese, B. Vornam, E. Krause, H. Kindl, Plant Mol. Biol. 26 (1994) 667–677.
[43] A. Kumar, B.E. Ellis, Phytochemistry 62 (2003) 513–526.
[44] E. Lacombe, S. Hawkins, J. Van Doorsselaere, J. Piquemal, D. Goffner, O. Poeydomenge, A.M. Boudet, J. Grima-Pettenati, Plant J. 11 (1997) 429–441.
[45] R. Blanco-Portales, N. Medina-Escobar, J.A. López-Ráez, J.A. González-Reyes, J.M. Villalba, E. Moyano, J.L. Caballero, J. Muñoz-Blanco, J. Exp. Bot. 53 (2002) 1723–1734.
[46] R. Blanco-Portales, J.A. López-Ráez, M.L. Bellido, E. Moyano, G. Dorado, J.A. González-Reyes, J.L. Caballero, J. Muñoz-Blanco, Plant Mol. Biol. 55 (2004) 763–780.
[47] L. Pourcel, J.M. Routaboul, V. Cheynier, L. Lepiniec, I. Debeaujon, Trends Plant Sci. 12 (2006) 29–36.
[48] H. Vaksin, A. Bar-Akiva, R. Ovadia, A. Nissim-Levi, I. Forer, D. Weiss, M. Oren-Shamir, Planta 222 (2005) 19–26.
[49] P. Kevan, M. Giurfa, L. Chittka, Trends Plant Sci. 1 (1996) 280–284.
[50] T.C. Fischer, H. Halbwirth, B. Meisel, K. Stich, G. Forkmann, Arch. Biochem. Biophys. 412 (2003) 223–230.
[51] J. Pfeiffer, C. Kühnel, J. Brandt, D. Duy, P.A.N. Punyasiri, G. Forkmann, T.C. Fischer, Plant Physiol. Biochem. 44 (2006) 323–334.
[52] G.M. Barton, J. Chromatogr. 34 (1968) 562.

3.4 Comparative profiling of strawberry genotypes with different flavonoid content

Strawberries are one of the best natural sources of antioxidants, natural compounds that are very effective against free radicals damaging. Among these, phenolic compounds in strawberries have been increasingly found to have even stronger antioxidant capacity comparable to that of vitamin C and E. Phenolic acids and flavonoids (such as anthocyanins and proanthocyanidins (PAs)) are among the most important (poly)phenol compounds (Schijlen et al, 2004). A vast amount of knowledge on flavonoids has accumulated (Forkmann and Martens, 2001). Among flavonoids, PAs, or condensed tannins, represent a class of big branched molecules derived from the polymerization of catechins (flavan-3-ols). Catechins are lateral intermediates of the main flavonoids pathway resulted by reduction of anthocyanidins and leucoanthocyanidins by the action of anthocyanidin reductase (anr) and leucoanthocyanidin reductase (lar) (Tanner et al., 2003). The branch of the pathway leading to PAs biosynthesis is less known and awaits further investigations.

An integrated approach has been used to correlate flavonoid accumulation pattern and gene expression differences in fruits of cultivated strawberry genotypes (*Fragaria x ananassa* Duch.).

First of all, red ripe fruits of different strawberries varieties and lines were collected. The plant material includes 27 different genotypes grown in North of Italy (Cesena) (99.163.14, Ventana, Candonga, 99.163.22, 99.20.1, Camarosa, 95.i59.2, QueenElisa, Alba, Dora, Onda, Irma, Idea, 99.12.3, 99.159.8, 96.46.2, 97.306.9, 97.129.11, 98.86.6, 99.194.13, 95.453.11,96.57.1, 97.70.3, 97.167.9, 93.175.2, 92.340.3, 99.26.5) and 14 genotypes grown in South of Italy (Metaponto (MT))(99.163.14, Ventana, Candonga, 99.163.22, 99.20.1, Camarosa, 95.i59.2, 96.j24.2, TudlaNew, 99.163.19, 99.97.17, 99.121.9, Demetra, Rubea). Seven genotypes of them were grown in both northern and southern Italian areas to study environment influence on flavonoid accumulation (99.163.14, Ventana, Candonga, 99.163.22, 99.20.1, Camarosa, 95.i59.2).

In order to select among the strawberry genotypes those containing extreme amount of particular classes of flavonoids, have been performed

spectrophotometric analysis of juice. Polyphenols were extracted according to Heinonen et al. (1998). Anthocyanins were quantified by measuring the absorbance at 510 nm. While total flavan-3-ols and PAs content was measured at 640 nm using p-dimethylaminocinnamaldehyde (DMACA) (Treutter, 1989). The analyses have showed considerable differences in the accumulation pattern of either anthocyanins and flavan-3-ols/PAs not only among different genotypes but also within the same genotypes grown in different geographical areas (fig. 6) .

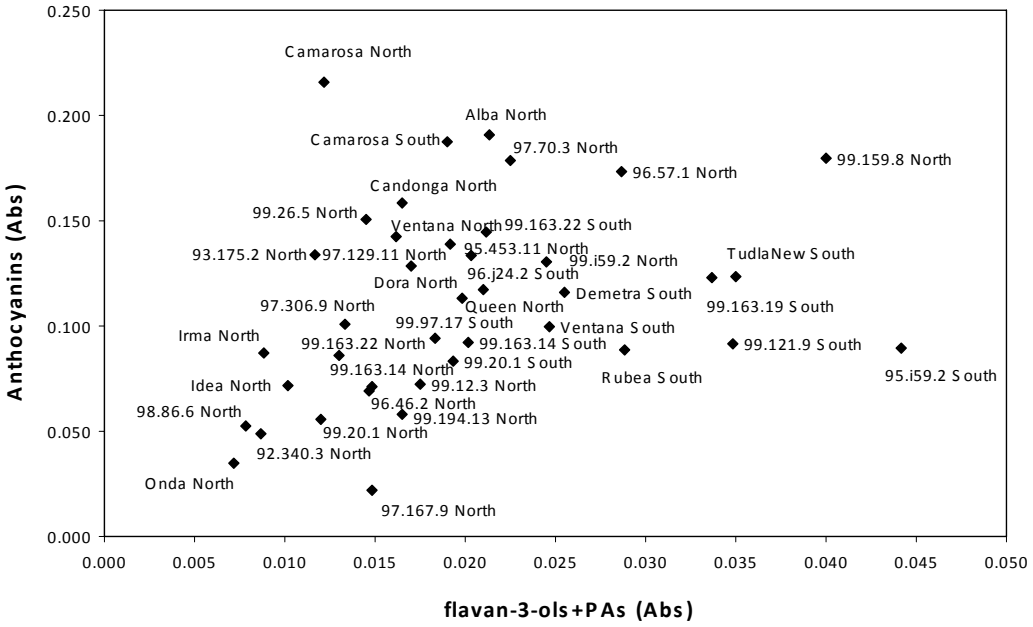

Figure 6: Analysis of the total content of anthocyanins and flavan-3-ols by spectrophotometric analyses of juices and coloring DMACA (see text for details). Abs: Absorbance.

Moreover a part of each samples have been sent to “Plant Research International” for flavonoid content analysis by liquid chromatography - quadrupole time of fligh – mass spettrometry (LC-QTOF-MS). By these data, the production of different classes of flavonoids has been shown clearly dependent by genetic factors (fig. 7).

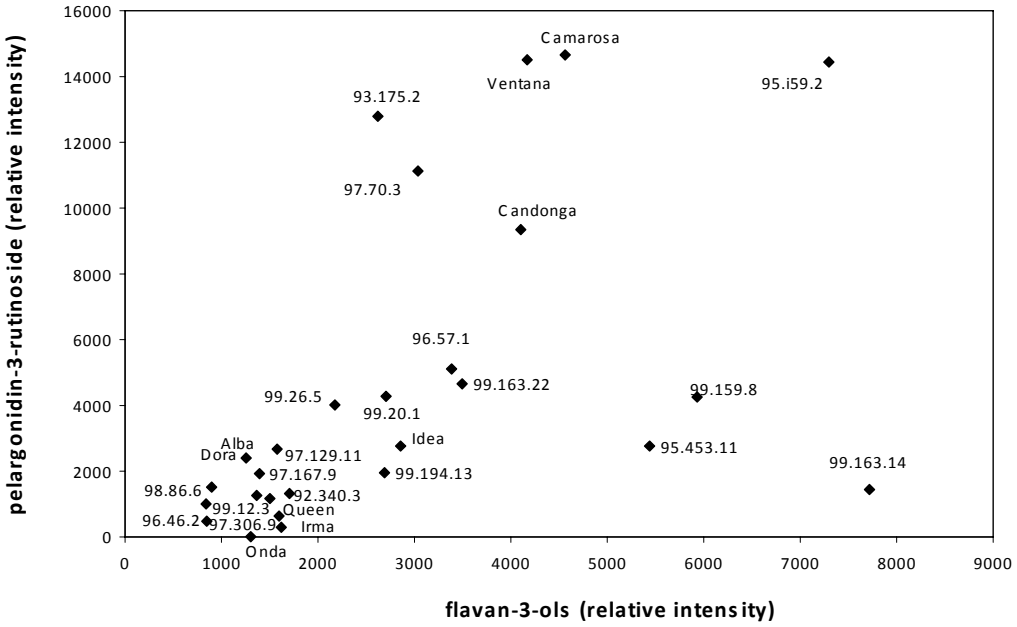

Figure 7: Pelargonidin-3-rutinoside and flavan-3-ols relative content of red fruits of genotypes harvested in northern location by LC-QTOF-MS analysis (PRI, Wageningen).

For this reason, three genotypes have been selected for different flavonoid accumulation pattern and harvested in the north of Italy: 99.163.14 with high content of PAs and flavan-3-ols, Onda with low levels of anthocyanins and Pas and Camarosa with high anthocyanin content. Moreover, in order to observe environmental biases, Camarosa and 99.163.14 have been sampled also in a different area (South of Italy). Besides other two genotypes, 99.20.1 and Candonga with low flavonoid and high anthocyanin content respectively, have been selected in both southern and northern areas. Finally, Queen Elisa have been used as reference genotype. cv. Onda, like as cv. Queen Elisa, were sampled in only northern location because it is impossible to grown these genotypes to inferior latitude. Fruit samples of different strawberries varieties and lines were collected at early green (G1, 7–10 days after anthesis, daa), intermediate green (G2, 12–14 daa), white (W, ca. 20 daa), turning (T, ca. 25 daa) and ripe red (R, ca. 30 daa) stages (fig. 8). A part of each samples has been sent to "Plant Research International" for flavonoid content analysis.

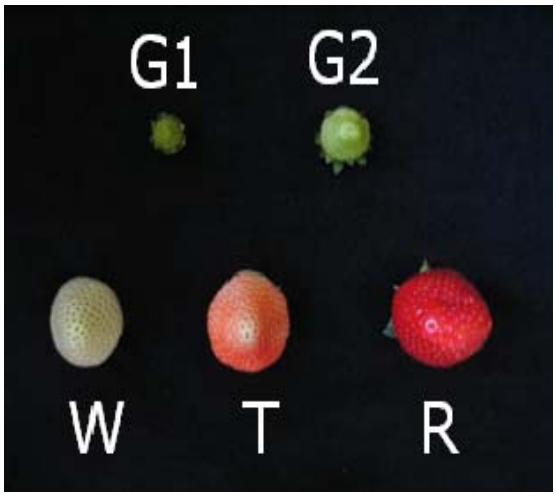

Figure 8: Fruit harvested at five different development stages: early green (G1, 7–10 days after anthesis, daa), intermediate green (G2, 12–14 daa), white (W, ca. 20 daa), turning (T, ca. 25 daa) and ripe red (R, ca. 30 daa).

To better understand the molecular and regulatory mechanisms that control these differences, we have carried out real time RT-qPCR experiments to analyze the transcripts levels of the genes involved in the flavonoid pathways in fruits of strawberry genotypes selected for their different flavonoid content.

We have designed specific primers to analyze the expression of nine structural genes of the flavonoid pathway: chalcone synthase (CHS), flavanone 3β-hydroxylase (FHT), flavonoid 3'-hydroxylase (F3'H), dihydroflavonol 4-reductase (DFR), anthocyanidin synthase (ANS), flavonoid glycosyltransferase (FGT), flavonol synthase (FLS), leucoanthocyanidin reductase (LAR), and anthocyanidin reductase (ANR) genes.

Gene expression patterns of CHS, CHI, FHT, DFR genes observed in cv Queen Elisa (please see attached paper: Almeida et al., 2007) have been confirmed and constant among genotypes and aerials. In fact CHS, CHI, and FHT had two transcription peaks at early and late stages showing a expression increment at T and R stages, while DFR have showed an up-regulation trend with a single peak at R stage (fig. 9). The same regulation of these genes among the different strawberry genotypes it is probably necessary to ensure proper channeling of precursors. The only exception is represented by FHT gene which have showed higher transcript levels in the southern genotypes at G1 and G2 stages and by

DFR gene which have showed higher transcript levels in the southern genotypes at G1 stage.

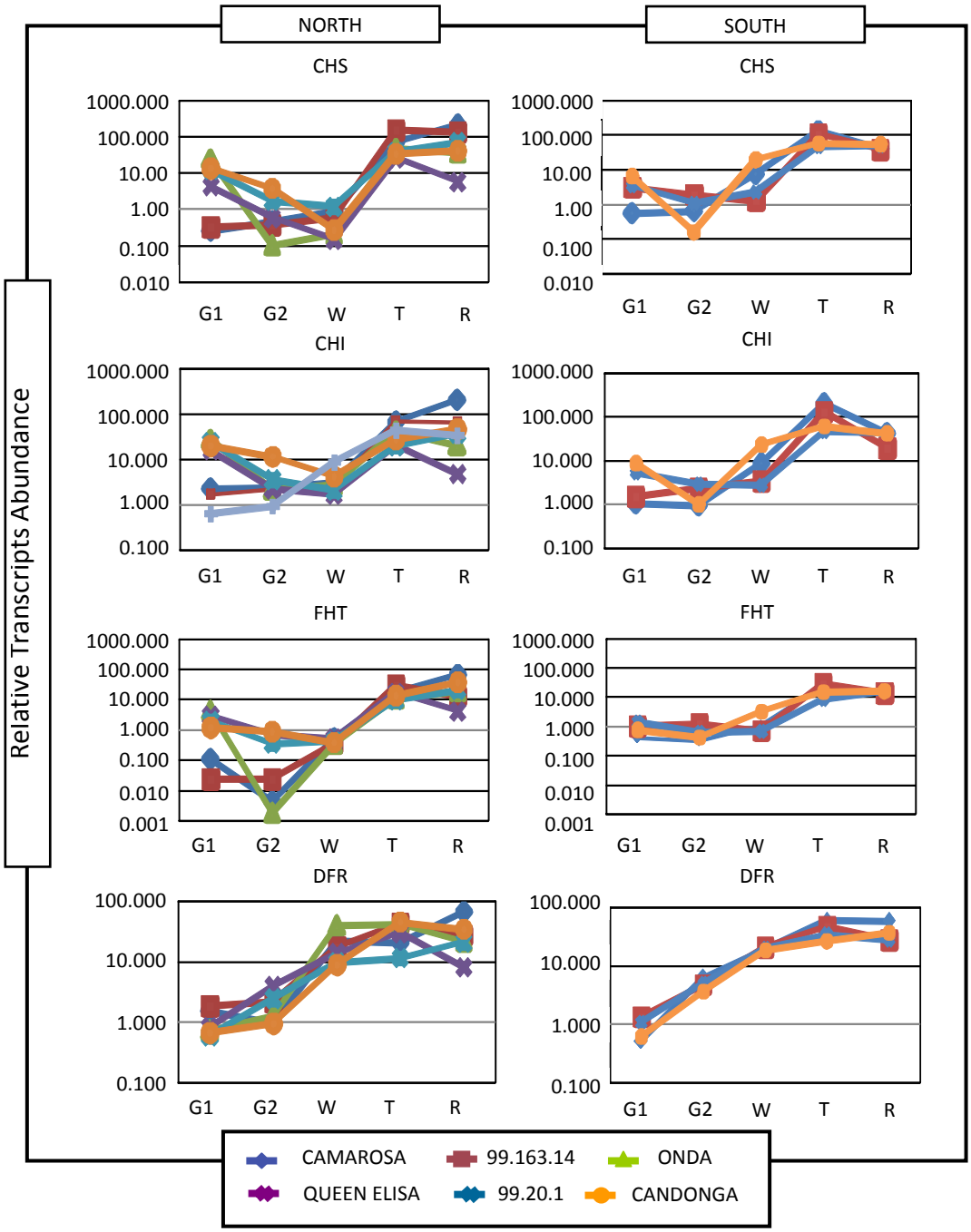

Figure 9: Developmental qRT-PCR analysis of gene expression in fruits of extreme genotypes grown in two different locations (North and South of Italy) at different stages (G1, G2, W, T and R). Relative gene expression levels are shown (Y axis in Log scale), following normalization with actin transcript values. For gene acronyms, see text.

Moreover, FLS and F3'H showed a constant decrement during the ripening in agreement with a decrease of flavonols and Pas along fruit development (Jaakola

et al., 2002), and we haven't observed appraisable differences among different genotypes (fig. 10).

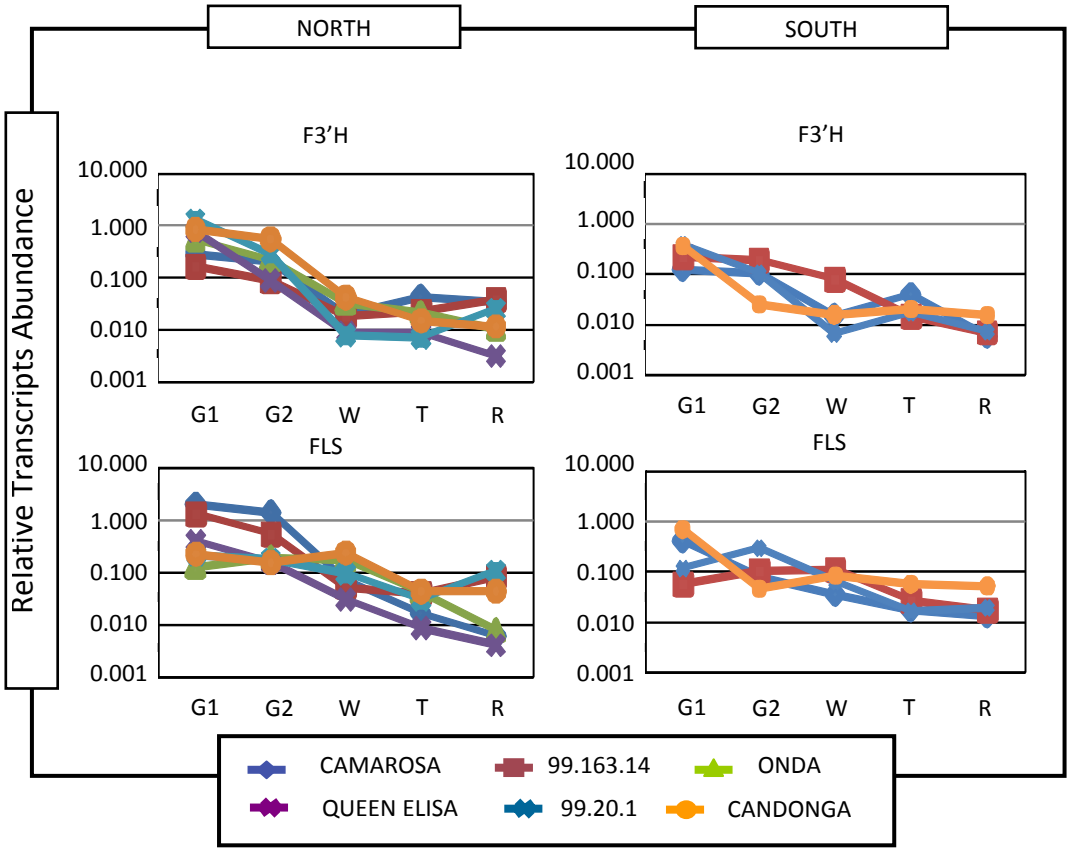

Figure 10: Developmental qRT-PCR analysis of gene expression in fruits of extreme genotypes grown in two different locations (North and South of Italy) at different stages (G1, G2, W, T and R). Relative gene expression levels are shown (Y axis in Log scale), following normalization with actin transcript values. For gene acronyms, see text.

The genes involved in lateral branches like as, ANR and LAR, and in the last step like as ANS and FGT of the principal flavonoids pathway have showed differences among genotypes and aerials in gene expression patterns. In particular, the genotype with highest PAs and Flavan-3-ols content (99,163,14) have showed higher levels of LAR transcripts in the final ripening stages in both southern and northern varieties (fig. 11).

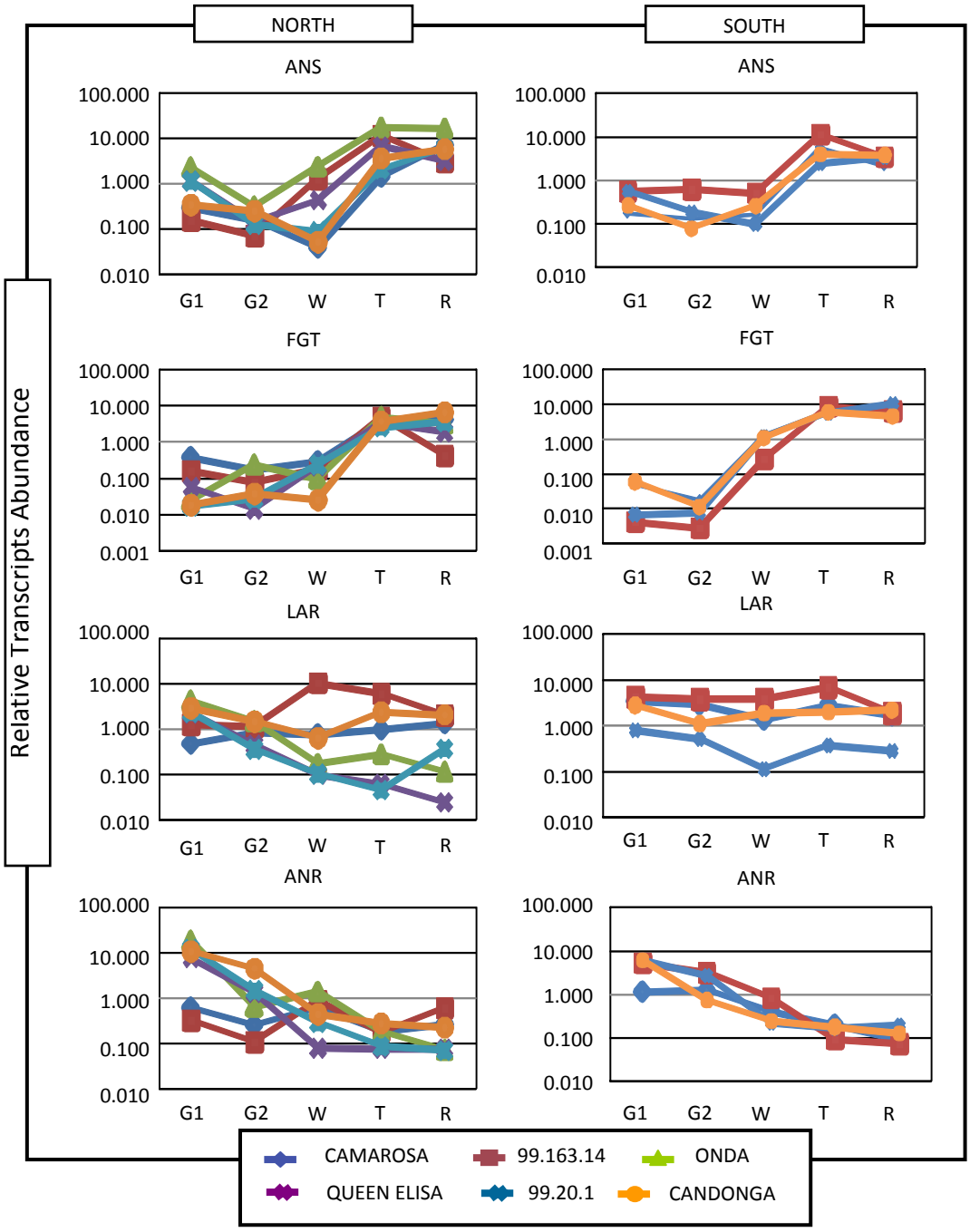

Figure 11: Developmental qRT-PCR analysis of gene expression in fruits of extreme genotypes grown in two different locations (North and South of Italy) at different stages (G1, G2, W, T and R). Relative gene expression levels are shown (Y axis in Log scale), following normalization with actin transcript values. For gene acronyms, see text.

Finally, to better understand eventually difference flavonoids gene regulation pattern among genotypes grown in the different locations, we have arranged real time RT-qPCR data by cluster analysis according to similarity of gene expression (Eisen et al., 1998). These analysis have shown very low influences of

environment on flavonoid transcript regulation. It is evident a stronger genetic influence: Candonga, 99.163.14, and 99.20.1 show expression pattern very similar in both southern and northern locations. The only exception is observed in Camarosa that considering all flavonoid gene expression pattern present a more environment influence. On the other hand, cluster analysis confirms correlation among genotypes with high flavonoid content and high flavonoid gene expression (fig. 12).

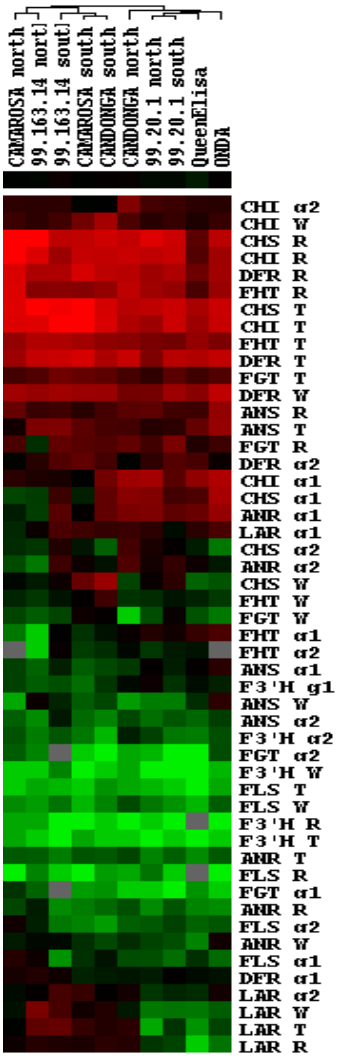

Figure 12: The real time RT-qPCR expression data were clustered. 13 representative patterns, each with an idealized graph representing patterns of expression, are shown. For the clusters, black represents normalized values of expression similar to 1, green < 1 and red > 1. See text for details.

3.5 Transcriptional characterization of CRY2-overexpressing tomato plants by microarrays

Transgenic cryptochrome 2 overexpressed (CRY2OX) plants from two individual lines were selected for further characterization by microarray experiments.

Cryptochromes are blue light photoreceptors found in plants, bacteria, and animals. In *Arabidopsis*, CRY2 is involved primarily in the control of flowering time and in photomorphogenesis under low-fluence light. In tomato (*Solanum lycopersicum*) the expression of CRY2 gene was altered through a combination of transgenic overexpression and virus-induced gene silencing (Giliberto et al., 2005). Tomato CRY2 overexpressors show phenotypes similar to but distinct from their *Arabidopsis* counterparts (hypocotyl and internode shortening under both low- and high-fluence blue light), but also several novel ones, including a high-pigment phenotype, resulting in overproduction of anthocyanins and chlorophyll in leaves and of flavonoids and lycopene in fruits (fig. 13). CRY2 overexpression causes an unexpected delay in flowering, observed under both short- and long-day conditions, and an increased outgrowth of axillary branches. Virus-induced gene silencing of CRY2 results in a reversion of leaf anthocyanin accumulation, of internode shortening, and of late flowering in CRY2OX plants, whereas in wild-type plants it causes a minor internode elongation (Giliberto et al., 2005).

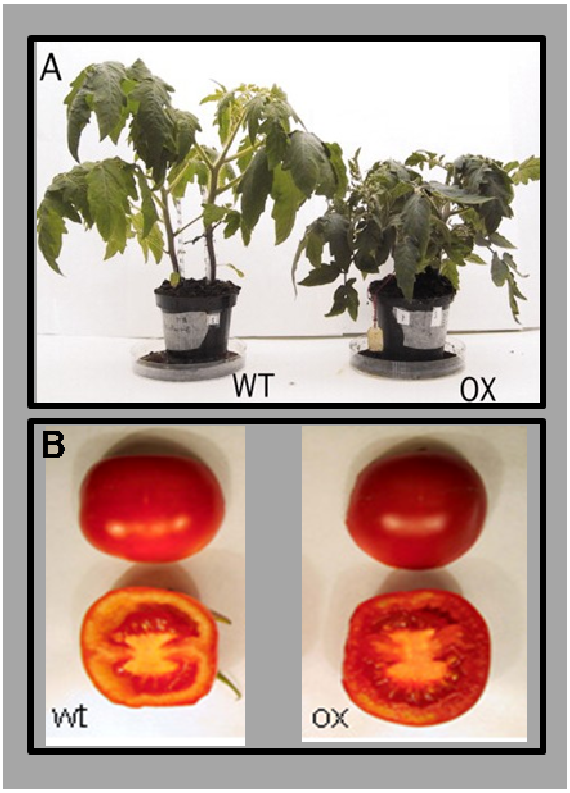

Figure 13: Transgenic cryptochrome 2 overexpressed (CRY2OX) plants show phenotypes with a hypocotyl and internode shortening under both low- and high-fluence blue light anthocyanins and higher chlorophyll in leaves and of flavonoids and lycopene contents in fruits (Giliberto et al., 2005)

We have designed an experimental setup that was balanced with respect to the use of Cyanine3 (Cy3) or Cyanine5 (Cy5) in the labeling reactions and which took into account the limitations in number of slides available. The strategy was to analyze differential gene expression between the two lines CRY2OX-3C and CRY2OX-8D, and wild type (Wt) line in tomato fruits to monitor the genome response to the over-expression of CRY2 (fig. 14).

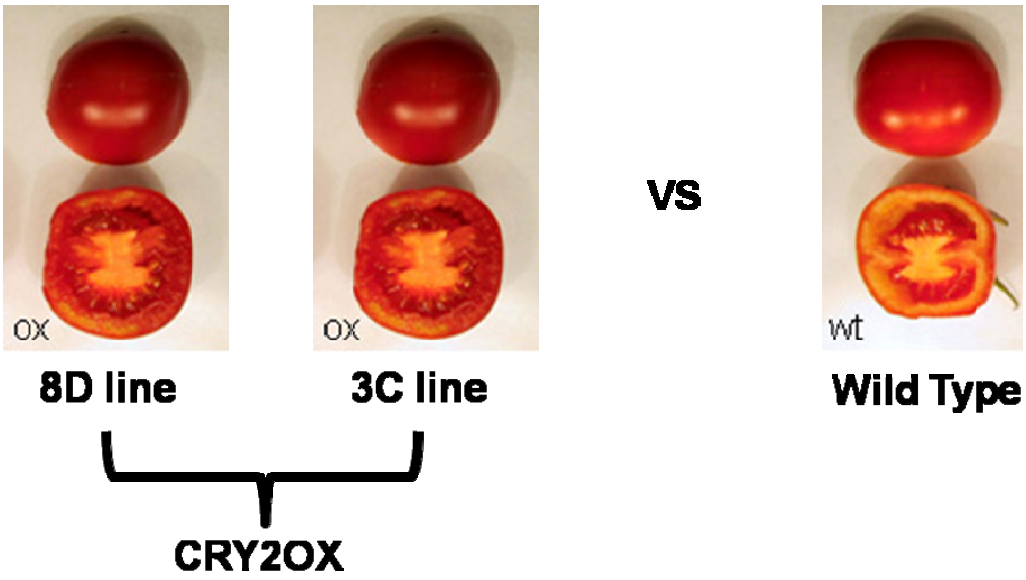

Figure 14: Comparating profiling by oligoarray. The fruits at red ripe stage of two transgenic lines CRY2OX-3C and CRY2OX-8D were compared to fruits of wild type (Wt) harvested at the same ripening stage.

Two experiments comparing tomato fruit of CRY2OX-3C line with Wt, and CRY2OX-8D line with Wt were performed. In each experiment, one mRNA population (target) was labeled with Cy3 and the other with Cy5. The labeled targets were then mixed and hybridized simultaneously to a microarray. To exclude artifacts, we have performed two independent biological replicates each with a reciprocal labeling experiment with each pair of targets, using the same techniques of the first experiment except that the labels were exchanged. A total of 8 hybridizations were assayed (4 CRY2OX-3C vs. Wt, and 4 CRY2OX-8D vs. Wt). After hybridization, the fluorescence pattern of each microarray was recorded. Raw hybridization signals were filtered by imposing a minimal signal/noise ratio of 2.0 and flagging the non-passed spots. In order to obtain a homogeneous dataset for all hybridized slides we have filtered microarray data imposing good quality spots to be present in at least three out of four hybridized slides (two dye-swap and two biological replicas, respectively) for each experimental point. Raw values were then normalized with the locally weighted linear regression (LOWESS) method using the 20% of data for smoothing (Cleveland and Devlin, 1998). Transcripts showing an expression difference

greater than three-fold between two CRY2OX lines and Wt and with a p-value among repeats <0.05 were classified as differentially regulated.

According to this criterion, were identified 741 uni-genes (sgn-) up-regulated and 712 down-regulated in CRY2OX-8D vs. Wt and 303 genes up-regulated and 103 down-regulated in CRY2OX-3C vs. Wt. Among the up-regulated genes, 225 are common in both CRY2-OX lines, 85 have been identified only in CRY2OX-3C line and 522 in CRY2OX-8D line. Among the down-regulated genes, 74 are common in both CRY2-OX lines, 29 have been identified only in line CRY2OX-3C and 640 in CRY2OX-8D line (fig. 15).

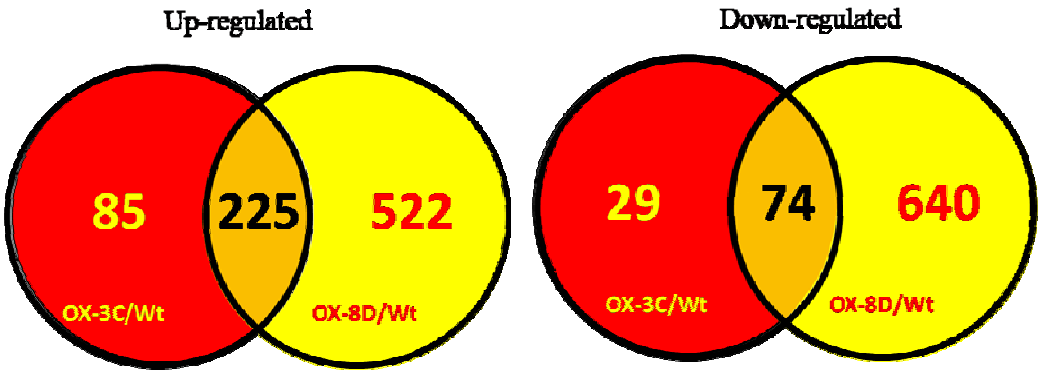

Figure 15: Venn diagram of upregulated and downregulated transcripts in red ripe fruits of two different tomato CRY2OX lines (OX-3C, and OX-8D) compared to Wild type (Wt).

The CRY2OX-8D line show a stronger up-regulation of cryptochrome 2 transcripts (CRY2, AF130425) with respect to the CRY2OX-3C line probably related to more regulated genes in CRY2OX-8D with respect to Wt (fig. 16).

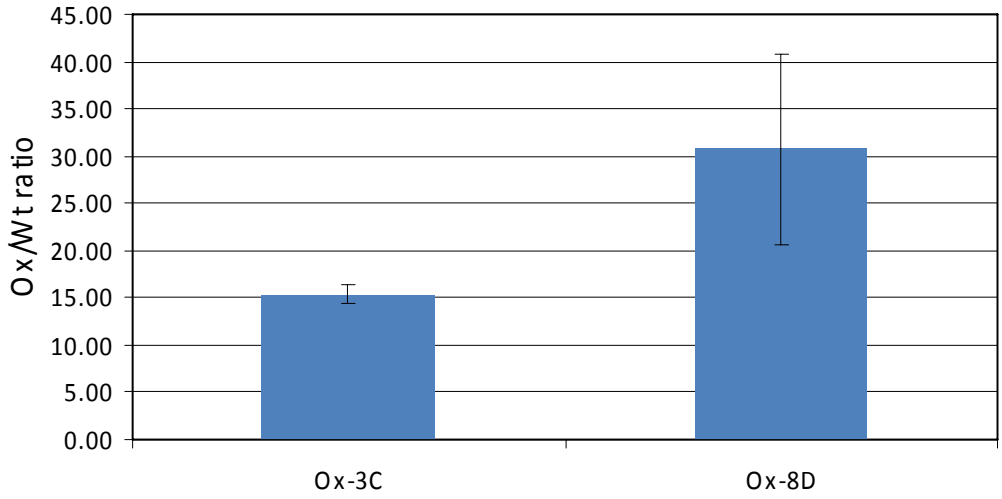

Genotype	Gene_ID	Annotation	Ox_a	Ox_b	Ox_c	Ox_d	Mean	SD	CV	p-Value
Ox-3C	AF130425	Cryptochrome 2 [Lycopersicon esculentum]	15.59	13.99	15.69	16.19	15.36	0.95	6%	1.52E-08
Ox-8D	AF130425	Cryptochrome 2 [Lycopersicon esculentum]	45.44	24.59	23.71	29.33	30.77	10.09	33%	1.62E-04

Figure 16: Comparating profiling by oligoarray. For each comparing Cry2OX_3C vs. Wt e Cry2OX_8D vs. Wt have been represented relative expression (OX vs WT ratio) of CRY2 gene following normalization with the locally weighted linear regression (LOWESS) method using the 20% of data for smoothing. Values and error bars represent the mean and standard deviation (SD) from four independent experiments, respectively. CV = variation coefficient (SD/Mean).

Combining the results from all two experiments, after correction for redundancy, a total of 1575 unique genes differentially expressed at least once were identified (832 and 743 up- and down-regulated with respect to Wt, respectively). Each gene was assigned to one of 18 categories (including unknown and other genes) on the basis of its BLAST search output (fig. 17).

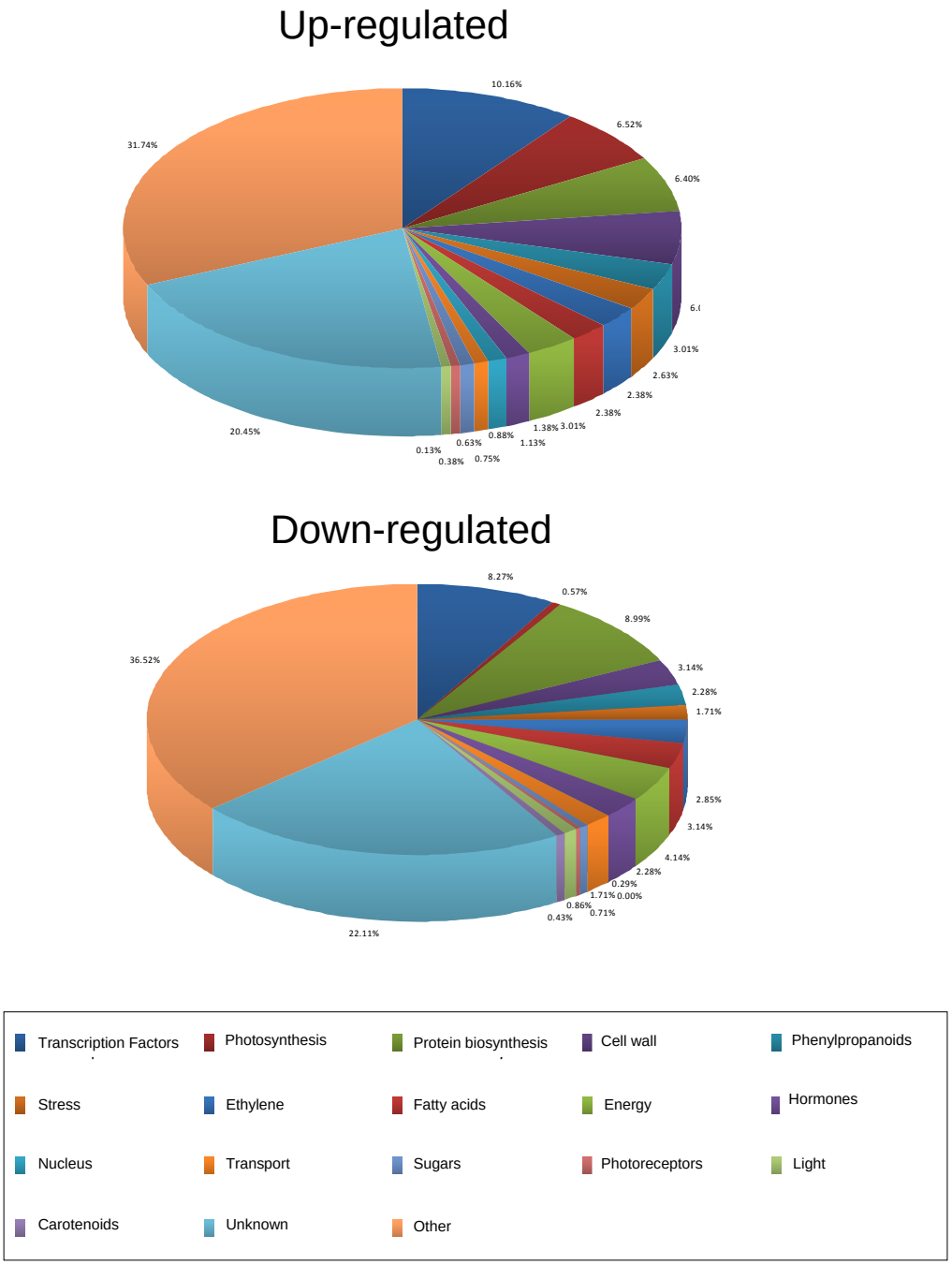

Figure 17.: Graphical representation of up-regulated and down-regulated genes, grouped by putative functional categories.

We have observed that the majority of up-regulated genes encode proteins involved in the photosynthetic processes (52 transcripts). Moreover, 24 genes, coding enzymes involved in the phenylpropanoids and flavonoids pathways, show higher transcript levels in transgenic lines compared to Wt. These results are in accordance with the highest chlorophyll and water-soluble antioxidants contents

measured in tomato fruits CRY2 overexpressors (Giliberto et al., 2005). Of the up-regulated genes involved in photosynthesis, we have found genes conding chlorophyll a/b-binding protein (CAB), Photosystem I and II subunit precursor, Photosystem I and II oxygen-evolving system, Photosystem I and II stability/assembly factors, chloroplast precursors, and ribulose bisphosphate carboxylase (RuBisCO). Many flavonoid genes were more expressed in CRY2OX lines coding a Leucoanthocyanidin dioxygenase (ANS), Dihydroflavonol reductase (DFR), Flavonol synthase 1 (FLS1), two different flavanone 3-hydroxylase (F3H), Flavonol 3-O-glucosyltransferase (F3GT), Isoflavone reductase (IFR) and flavonoid 3'-hydroxylase (F3'H) (F3'5'H) while among phenylpropanoids we have found altered transcripts of GCN5-related N-acetyltransferase (GNAT), Cinnamyl-alcohol dehydrogenase (CAD), two different 4-coumarate:CoA (4CL), Caffeic acid O-methyltransferase (COMT) and 4-coumarate:CoA ligase 2 (4CL2) genes.

Besides the observed increase of DNA replication and transcription were associated with an increased expression of transcriptional factors and structural nucleosome proteins. Of the up-regulated genes, we have found 81 genes coding TFs and 9 nuclear proteins. Of the 9 nuclear protein identified, 6 code histones or hystone related.

3.6 Analysis of temporal rhythmic oscillation of tomato mRNAs: cryptochromes can alterate transcription fluctuations of photoreceptor and circadian regulated genes

In order to identify genes involved diurnal rhythms in tomato, we have performed a large scale comparative analysis over TOM2 microarray.

Wild type (Wt) tomato plants were grown under a daily light cycle of 16h light/8h darkness(LD) and sampled every 8h for 24 hours.

This approach allowed us to examine the daily expression pattern of ~7000 transcripts (U-sgn). Our results showed that one-fifth of the transcripts/genes examined showed significant light-regulated expression pattern, with an expression difference greater than three-fold in at least one time point analyzed.

The results of this study are shown in the following attached paper actually in preparation.

Paper in preparation

Analysis of temporal rhythmic oscillation of tomato mRNAs: cryptochromes can alterate transcription fluctuations of photoreceptor and circadian regulated genes

Authors (presently strictly alphabetic order)

Carbone F., Facella P., Giuliano G., Lopez L., Perrotta G.

Introduction

Plants have adapted their growth and development to make use of the diurnal light/dark cycle. This is manifested at both the physiological level, with leaf movement, growth modulation, stomatal opening, and photoperiodic flowering, and at the molecular level, with expression of some genes at definite times of the day. The day/night cycling of gene expression is accomplished, primarily, by light and, secondly, by a free-running internal molecular timekeeper called circadian clock. The intimate connection between light signalling pathways and the circadian oscillator allows the anticipation of the environmental transitions and the measurement of day-length as an indicator of changing seasons.

Our current understanding of plant circadian clock derives mostly from genetic studies in *Arabidopsis* and rice (Hayama and Coupland, 2004). Commonly, the circadian clock system is divided into three general parts (Dunlap, 1999): an input pathway that entrains the clock, by transmitting light or temperature signals to the core oscillator; the central oscillator (the clock) that is the core of the system, responsible for driving 24-h rhythms; the output signals that generates the fluctuation of a wide range of biochemical and developmental pathways.

Plants have evolved several classes of photoreceptors to monitor their environmental light signals. The photoreceptors include red and far-red-light–absorbing phytochromes (PHYs) and UV-A/blue light–absorbing cryptochromes (CRYs) and phototropins (Deng and Quail, 1999; Neff *et al.,* 2000). Recent evidence shows that green light also has discrete effects on plant biology, and the mechanisms that sense this light quality are now being elucidated. Green light has been shown to affect plant processes via cryptochrome-dependent and cryptochrome-independent means (Folta and Maruhnich, 2007).

Among the photoreceptors, phytochromes and cryptochromes mediate several responses such as seedling de-etiolation, photoperiodic flowering, and circadian rhythm (Guo *et al.,* 1998; Mas *et al.,* 2000).

In *Arabidopsis*, the phytochrome gene family has five members, *PHYA* through *PHYE* (Clack *et al.,* 1994). Genetic experiments with *Arabidopsis* mutants have established roles for PHYA, PHYB, PHYD, PHYE, CRY1 and CRY2 in the establishment of period length (Devlin and Kay, 2000; Millar *et al.,* 1995; Somers *et al.,* 1998). Light-labile PHYA is the predominant photoreceptor for the clock at low intensity of red or blue

light, whereas PHYB and CRY1 dominate at high intensities of red and blue light, respectively (Somers *et al.,* 1998). Double mutant studies demonstrated a role for CRY2 at intermediate intensities of blue light, although that role is redundantly specified by CRY1 (Devlin and Kay, 2000). Many photoreceptor mutants are still able to be entrained to a light-dark cycle and retain rhythmicity, such as the *cry1cry2* double mutant and the quadruple mutant *phyAphyBcry1cry2* (Devlin and Kay, 2000); making it clear that others photoreceptors (PHYC-PHYE, or others), can provide light input to the clock (Yanovsky *et al.,* 2000). Indeed, a novel family of putative photoreceptors, ZEITLUPE (ZTL) and FLAVINBINDING KELCH REPEAT F-BOX (FKF) have recently been identified by a mutant phenotype of altered circadian rhythms (Jarillo *et al.,* 2001; Nelson *et al.,* 2000; Somers *et al.,* 2000) and a third family member, LOV DOMAIN KELCH PROTEIN 2 (LKP2), has been recently identified, as well (Jarillo *et al.,* 2001; Kiyosue and Wada, 2000).

There is considerable interaction among photoreceptors. For instance, PHYA and CRY1 directly interact at the molecular level, with CRY1 serving as a phosphorylation substrate for PHYA *in vitro* (Ahmad *et al.,* 1998). *In vivo*, CRY1 is phosphorylated in response to red light in a far-red reversible manner (Ahmad *et al.,* 1998). A *cry1* null mutant shows lengthened period in low intensity red or white light and there is no additivity seen in the double *phyAcry1* mutant (Devlin and Kay, 2000). This suggests that CRY1 acts as a signal transduction component downstream from PHYA in the low intensity light input pathway to the clock (Devlin and Kay, 2001).

Genetic studies have implicated two other genes, *EARLY FLOWERING 3* (*ELF3*) and *GIGANTEA* (*GI*), in light signalling to the clock. *elf3* loss of function alleles yield early flowering, hypocotyl elongation, and conditional arrhythmicity in continuous light (Covington *et al.,* 2001; McWatters *et al.,* 2000). Genetic experiments suggest substantial redundancy in ELF3 and PHYB function (Reed *et al.,* 2000). ELF3 interacts with PHYB and seems to act as a negative modulator of PHYB signalling to the clock, as *ELF3* overexpression both lengthens the circadian period and attenuates the resetting effects of red light pulses whereas loss of ELF3 function renders the plant hypersensitive to light signals (Covington *et al.,* 2001; Liu *et al.,* 2001; McWatters *et al.,* 2000).

In *Arabidopsis* GI positively regulates expression of the flowering time genes *CONSTANS (CO)* and *FLOWERING LOCUS T* (*FT*). *GI* encodes a nucleoplasmically localized protein that mediates a number of functions such as photoperiodic flowering, circadian rhythms and phytochrome/cryptochrome signaling (Martin-Tryon *et al.,* 2007). The key roles played by GI are evident analyzing the effect of *gi* mutants over leaf movement and gene expression rhythms of multiple clock controlled and flowering genes, including *GI* itself (Fowler *et al.,* 1999; Park *et al.,* 1999).

Latest intensive studies on the model higher plant *Arabidopsis thaliana* have begun to shed light on the molecular mechanisms underlying the functions of the central clock. The current best candidates for *Arabidopsis* clock components are CIRCADIAN CLOCK ASSOCIATED 1 (CCA1) and its redundant homolog LATE ELONGATED HYPCOTYL (LHY), which are transcription factors (TF) containing a single MYB domain (Schaffer *et al.,* 1998, Wang and Tobin 1998, Mizoguchi *et al.,* 2002). Furthermore, five *PRR*

genes that belong to a small family of *PSEUDO-RESPONSE REGULATORS* including *TIMING OF CAB EXPRESSION* (*TOC1*), *GIGANTEA* (*GI*), *ZEITLUPE/ADAGIO* (*1ZTL/ADO1*), *LOV KELCH PROTEIN* (*2LKP2*), *EARLY FLOWERING 3* and *4* (*ELF3* and *ELF4*), *LUX ARRHYTHMO/PHYTOCLOCK* (*1LUX/PCL1*), *TIME FOR COFFEE* (*TIC*), *SENSITIVITY TO RED LIGHT REDUCED* (*1SRR1*) and *TEJ* (Gardner *et al.,* 2006, McClung, 2006) have also been involved in the circadian machinery.

The clock mechanism in *Arabidopsis* was first proposed to comprise a feedback loop in which two partially redundant genes, *LHY* and *CCA1*, repress the expression of their activator, *TOC1* (Alabadi *et al.,* 2001). This circuit cannot fit all experimental data (Locke *et al.,* 2005a) as a short-period rhythm persists for several cycles both in *lhy;cca1* (Alabadi *et al.,* 2002; Locke *et al.,* 2005b) and in *toc1* mutant plants (Mas *et al.,* 2003). Subsequently, many other clock-associated genes were identified and incorporated into the simple model, resulting in a somewhat complicated interlocking multiloop model comprising the feedback loop between LHY, CCA1 and TOC1, and a predicted, interlocking feedback loop involving TOC1 and a hypothetical component Y (Locke *et al.,* 2005b). Experiments based on model predictions suggested GI as a candidate for Y. Analysis of the three-loop network suggests that the plant clock consists of morning and evening oscillators, coupled intracellularly, which may be analogous to coupled, morning and evening clock cells in *Drosophila* and the mouse (Locke *et al.,* 2006).

In recent years the list of plant genes reported to be controlled by light has grown from a few dozen to thousands thanks to microarray experiments. The functional significance of a large proportion of these genes is still unknown. Light signals typically trigger rapid changes in the mRNA levels of TFs, but the position that they occupy in a putative transcriptional cascade and the steps interposed between the photoreceptors and the first raw of TFs have not been fully established (Casal and Yanovsky, 2005). Recent work using an expressed sequence tag (EST)-based DNA microarray has suggested that nearly one-third of the genome is regulated in white light. In addition, the genome expression patterns largely overlap in 6-days-old seedlings grown under white, far-red, red, and blue light. More than 26 cellular pathways, ranging from DNA replication to transcription, metabolism, protein degradation, plant defense, and developmental regulation, have been found to be commonly regulated by all light signals (Ma et al., 2001). However, the expression of many early-responsive genes to light signals during the dramatic and rapid transitions of seedling development are likely to be missed by examining the effect of light after only 24-h or 6-days irradiation. In an independent microarray study, approximately 10% of about 8000 genes examined were found to be regulated by PHYA in far-red light. From a detailed kinetic study, it was evident that a large portion of the genes, which respond to light signals within 1 h, encodes multiple classes of transcription factors (Tepperman et al., 2001). Thus it was concluded that transcriptional cascades are likely to be involved in far-red-light regulation of gene expression.

Schaffer and collaborators (Schaffer *et al.,* 2001) by analysis of gene expression using *Arabidopsis* cDNA array which represents approximately 7800 unique genes, observed that 11% of genes showed differential expression at one or more of the phases tested during the light/dark cycle (Schaffer *et al.,* 2001).

Besides, a large fraction of genes that showed diurnal regulation was also circadian-regulated, as revealed by differential transcript abundance under light constant conditions (Harmer *et al.,* 2000; Schaffer *et al.,* 2001).
The cataloging of plant clock-controlled genes began with Kloppstech's (Kloppstech, 1985) observation of a circadian oscillation in mRNA abundance of a chlorophyll a/b binding protein gene (LHCB or CAB). Oligo-based microarrays experiments, performed by Harmer *et al.,* (Harmer *et al.,* 2000), allowed the detection of circadian oscillations in mRNA abundance of 5-6% of the 8200 genes examined.
A comparative analysis of the expression patterns utilizing the luciferase reporter system indicated that the promoter activities of all *Arabidopsis* photoreceptor genes followed a diurnal rhythm and exhibited maximum expression in the light phase (Tòth *et al.,* 2001). Furthermore, these oscillations persisted under constant light or dark conditions with a period close to 24 h, proving that a circadian clock regulates the expression of these promoters. Measurements of mRNA transcribed from these genes in seedlings transferred to constant light indicated that the rhythmic expression was maintained at the level of mRNA accumulation. These findings were consistent with data on *CRY1*, *CRY2*, and *PHYA*, *PHYB* mRNA levels derived from microarray experiments (Harmer et al., 2000; Schaffer et al., 2001).
Here we report the characterization temporal transcripts oscillation of tomato genome. Focused analyses over photoreceptor gene transcripts in both wild type tomato and genotypes with alternated cryptochromes, provided useful information about possible functional interactions between cryptochromes and the circadian clock machinery, and on intra-photoreceptor regulations, as well.

Results

In order to identify genes involved in diurnal and circadian rhythms and to establish possible functional relations between photoreceptors and circadian clock machinery in tomato, we performed extensive transcription analyses either using TOM2 microarray and a by QRT-PCR of *PHYA*, *PHYB1, PHYB2, PHYE, PHYF* (Hauser *et al.,* 1995) and *CRY1a, CRY1b, CRY2* genes (Perrotta *et al.,* 2000; Perrotta *et al.,* 2001).
Wild-type (wt) tomato plants were grown under a daily light cycle of 16h light/8h darkness (LD), as described in experimental procedures, and sampled every 4h for 24 hours. Because diurnal changes of gene expression frequently reflect an underlying circadian rhythm, tomato plants entrained in LD, were transferred to light constant conditions (LL), and then genes expression was monitored for additional 40 h at 4h intervals.
Transcription analyses were also performed on the two genotypes with altered cryptochromes, *cry1a*- and *CRY2-OX* (Weller *et al.,* 2001; Giliberto *et al.,* 2005), grown and sampled as the wt plants.
Additional genes already known to be regulated by circadian clock in other plant species were also investigated by QRT-PCR, including *GI* and *CAB* in both LD and LL conditions (Fowler *et al.,* 1999; Giuliano *et al.,* 1988).
To classify time points in which the sampling was carried out we used Zeitgeber time (ZT) that is the time in hours from the start of a normal 16 h light–8 h dark cycle (Zerr *et al.,* 1990).

Transcription profiling using TOM2 microarray

In order to draw an extensive picture of genes potentially involved in diurnal transcription cycles in tomato we assayed TOM2 microarray with target RNAs extracted from ZT0 (presumptive dawn), ZT8 (eight hours after dawn), ZT16 (presumptive dusk) and ZT20 (four hours after dusk), in LD conditions (see Experimental procedures). These comparisons comprehended three experimental points taking ZT0 as a common reference: ZT8 *vs*. ZT0, ZT16 *vs*. ZT0 and ZT20 *vs*. ZT0.

Transcripts showing an expression difference greater than three-fold in at least one of the time points were classified as light-regulated. According to this criterion, 1372 transcripts (U-sgn) showed a light-regulated expression pattern, corresponding to 20% of all genes (6953) which passed quality controls (as described in Experimental procedures) at the corresponding microarray spots. When we placed light-regulated genes into phase clusters of peak expression time, we observed a major concentration of genes in the middle of the light phase (ZT8) (39,7%), whereas comparatively fewer genes peaked near dusk (ZT16) (14,7%) (Figure 1).

The structural genes of the nucleus and the cell wall appeared to be consistently more expressed at dawn (ZT0), with respect to the other time points, while the majority of the genes coding for mitochondrial and cytosolic proteins peaked in the mid of the light phase (ZT8) together with genes coding for plastidial proteins, involved in photosynthetic reaction (Figure 2A). Genes coding for ribosomal, plastidial and tylacoidal proteins were preferentially expressed at dusk (ZT16). Notably, many genes coding for cytoplasmatic membrane proteins showed a maximum of expression in the dark phase (ZT20) (Figure 2A). Finally, it is remarkable that several genes coding for proteins involved in "transporter and transferase activity" showed a peak of expression around dusk (ZT16), while many genes peaking at ZT20 (about 33% of all ZT20 peaking genes) resulted to be involved in the transcription control machinery ("transcription factor activity, nucleic acid binding and DNA or RNA binding" categories) (Figure 2B).

In order to identify representative expression patterns of photoregulated genes we have carried out cluster analysis according to similarity of gene expression (Eisen et al., 1998).

A single cluster representing genes with an expression peak at ZT0 contained 27 transcripts, mostly involved in light signaling and flowering (Cluster 1 Figure 3) as the putative myb-related transcription factor *Late Elongated Hypocotyl* (*LHY*), one member of YABBY family (*Abnormal Floral Organs Protein* (*AFO*)), *Constans Like 1* (*COL1*), the *Suppressor of Phytochrome A* (*SPA1*) and the *Early Light Inducible* (*ELIP*) genes (Ledger *et al.,* 2001; Ishikawa *et al.,* 2006; Laubinger *et al.,* 2006, Bruno and Wetzel, 2004).

The converse cluster that represents transcripts peaking from ZT8 to ZT20 and with comparatively low expression at dawn (ZT0) is the largest one and includes 94 mRNAs (Cluster 2 Figure 3). Here we found some transcripts involved circadian rhythm, light transduction and flowering - *Pseudo-Response Regulator 7* (*PRR7*), *Flavin-Binding*, *Kelch Repeat*, *F-Box 1* (*FKF1*) and the flowering time gene *GI* (Kaczorowski KA and Quail PH, 2003; Nelson *et al.,* 2000; Fowler *et al.,* 1999) as well as a number of other potential

transcriptional regulators, two zinc finger protein, one tdr4 transcription factor and three members of WRKY family (Eulgem *et al.,* 2000).

A cluster with transcripts down-regulated at ZT8 included 41 transcripts (Cluster 5 Figure 3) mostly involved in cellular communication and signal transduction as *calcium binding protein*, *Calmodulin-Related Protein 3 Touch-Induced* (*TCH3*) and a *Leucine-Rich Repeat Trans-Membrane Protein Kinase*.

We have found only three transcripts coding for Glutamate Synthase and a Phosphoenolpyruvate Carboxylase 1-Related Protein, up-regulated at dusk (ZT16) (Cluster 7 Figure 3). While, a little more transcripts (10) are represented in the mirror cluster of spots repressed at dusk (Cluster 6 Figure 3). Furthermore, 10 transcripts in cluster 9 (Figure 3), which include coding elements for ATPase Subunit 1, an enzyme involved in the phenylpropanoid biosynthetic pathway (Glutathione-Transferase) and an ABA-Responsive Protein, are induced in darkness (ZT20) and repressed by light. As expected, seven of the 17 genes repressed in darkness (ZT20) in its mirror cluster (Cluster 8 Figure 3) are putatively implicated in the light-harvesting reactions of photosynthesis.

Finally, a number of spots showed several other patterns such as transcripts peaking at ZT8 and ZT20 (Cluster 3 Figure 3), peaking at ZT8 (Cluster 4 Figure 3), peaking at ZT8 and ZT16 (Cluster 10 Figure 3) or at ZT0 and ZT20 (Cluster 11 Figure 3), up-regulated/down-regulated at ZT0/ZT20 (Cluster 12 Figure 3) and its reciprocal (Cluster 13 Figure 3).

Remarkably, no single group was detected with high expression in both dawn (ZT0) and dusk (ZT20).

Among light regulated genes we find regulatory structural coding sequences such as TF, genes implicated in the biosynthesis of metabolites involved in photo-protection, like carotenoids and flavonoids, as well as genes involved in important developmental and processes such as flowering and photo-sensory pathways.

Our results showed that 141 putative TF transcripts of several families were regulated by light (Table 1). In particular, members from all main TF families known in *Arabidopsis*, Zinc Finger, WRKY, bHLH, bZIP, MYB, HD, AP2, GRAS, MADS Box, ERF/DBRE (Jiao *et al.,* 2003), were found to be altered by light in tomato, with either induction or repression. A large portion of TFs exhibited striking co-regulation, with most peaking both at ZT8 and in the dark at ZT20 (Table 1).

Among light regulated TF genes, it is noteworthy that transcripts encoding the well known HY5, able to recognize G-box DNA-binding sites in target gene promoters regulating photo-sensory responses (Ang *et al.,* 1998; Holm *et al.,* 2002), was up-regulated at ZT0 and ZT16 (Table 2). At the same way, *COL1*, member of the light input for circadian regulation and photoperiodic control of flowering-associated CO-like zinc-finger factor subfamily of the C2C2 family (Ledger *et al.,* 2001), showed early response to light and its transcripts peaked at ZT0 as well (Table 2). Moreover, the MYB super-family with many members involved in light signal transduction (Riechmann, 2002), has the biggest number of TF genes showing an early response at dawn (ZT0) (Table 1).

The majority of carotenoid related genes, represented over TOM2 microarray, showed up-regulation at dawn followed by a decrement of transcripts during the day (Table 2). Indeed, *Phytoene Synthases*, *PSY1-PSY2* (sgn-U212842, sgn-U212843, sgn-U212844, 20B19M84744 and 25N10L23424), *Lycopene β-Cyclase* (sgn-

U234580) and *β-Carotene Hydroxylase 1* (sgn-U215829, sgn-U233360 and 9K08Y14809), show the expression peak at dawn (or 4 hours before dawn: sgn-U212842) (Table 2). Conversely, transcripts encoding the downstream enzymes involved xanthophyll cycle: Zeahanthin Epoxidase (ZEP) (24M18Z83835 and sgn-U221254) and Violaxanthin Depoxidase (VDE) (4G14AF385366 and sgn-U222306) have a different pattern, the first being up-regulated during the light phase with an expression peak at ZT8, the latter showing a slight decrement during the first part of the day and a peak at ZT16, though with a reduced amplitude (Table 2).

A number of sequences corresponding to genes involved in the flavonoid biosynthesis show a clearly light-regulated transcription pattern. Two out of five sequences putatively corresponding to *Flavonoid Glucosyltransferase* (*FGT*) gene family (sgn-U217139 and sgn-U242106) have a transcription peak at dawn (ZT0) and a decrease during light hours. While the other three putative *FGT* (sgn-U217841, sgn-U215136 and sgn-U215140) show an opposite transcription pattern with peak levels during presumptive day (ZT8-ZT16) (Table 2). Moreover, all but one sequences putatively coding for flavonoid dioxygenases (*Flavonol Synthase-Fls*, *Anthocyanidin Synthase-Ans* and *Flavonone Hydroxylase-Fht*) show a very high transcription peak during the light phase (sgn-U213371, sgn-U213372 and sgn-U215281) (Table 2).

A number of flowering-time and photosensory-related genes have been previously reported to show an expression pattern strictly light-regulated in a circadian way (Hayama and Coupland, 2004). Seven putative flowering-time genes of tomato (*LHY*, *ELF4*, *COL1*, *GI*, *SPA1*, *PRR7* and *FKF1*) have a light-regulated transcription pattern (Table 2). Besides, two sequences encoding GI, well known to be involved in flowering in *Arabidopsis* (Araki and Komeda, 1993) (sgn-U214381 and sgn-U218528) showed a maximum of expression at dusk (ZT6) (Table 2). Also the so called "evening genes" *ELF4* (sgn-U226837) and *FKF1* (sgn-U223492) exhibited an expression peak at dusk, like their *Arabidopsis* counterparts (Table 2) (Doyle *et al.,* 2002; Nelson *et al.,* 2000). Finally, two putative homolog of *Arabidopsis Consitutively Photomorphpgenic 1* (*COP1*) gene (sgn-U216241) (Ledger *et al.,* 2001), either exhibit an expression pattern overlapped to that of *SPA1* (maximum of expression at ZT0) or in the morning (ZT8) (sgn-U237464) (Table 2).

We also tested the transcription pattern of cryptochrome and phytochrome genes, however these genes were also essayed more in deep by QRT-PCR with similar results (Figure 4). Given the higher resolution of the latter test, we report the QRT-PCR data below.

Day/night mRNA oscillations of tomato photoreceptor genes

We analyzed the temporal transcription pattern of tomato phytochrome (*PHYA*, *PHYB1*, *PHYB2*, *PHYE*, *PHYF*) and cryptochrome (*CRY1a*, *CRY1b*, *CRY2*) genes and measured changes of mRNA accumulation under LD at intervals of 4 h for 24 h by QRT-PCR. Although with differences in amplitude, all tomato photoreceptor transcripts but *CRY1b* (Figure 5), exhibited maximum transcription peak in the presumptive afternoon (ZT 12), and decline dramatically in darkness (Figure 5).

The majority of the tested photoreceptor genes (*CRY1a*, *CRY2*, *PHYA*, *PHYB2* and *PHYE*) were expressed throughout a day with fluctuations that suggest diurnal rhythms and show transcription peaks in the light phase from ZT8 to ZT12 (Figure 5B-C). In darkness, transcripts of these genes declined (from ZT16 to ZT20) and then generally started to increase before the onset of light (from ZT20 to ZT24) (Figure 5B-C). This pre-dawn "anticipatory" rise of expression, may suggest that these genes are under the control of an endogenous circadian clock.

PHYF is expressed with amplitude and fluctuations significantly reduced relative to that observed in other tomato photoreceptors (Figure 5D), with an expression peak at ZT12. A similar pattern, though with a greater oscillation is also detected for *PHYB1* (Figure 5A).

The expression pattern of *CRY1b* photoreceptor is quite divergent from the other tomato photoreceptors (Figure 5A). It doesn't show any significant fluctuation in light/dark cycles, and the abundance of the *CRY1b* mRNAs is uniformly high throughout the 24 h period. Only at early-morning (ZT4), *CRY1b* transcripts abruptly decrease (Figure 5A). These evidences suggest that *CRY1b* expression is not strongly regulated by light, and it is quite constitutively expressed in tomato plant entrained in LD conditions.

In general, comparative analyses of the diurnal expression patterns of phytochrome and cryptochrome genes show qualitatively comparable oscillation phases though significant changes in mRNA abundance were detected throughout the complete 24 h monitoring period (Figure 5A-D).

CRY1b was the most abundant tomato photoreceptor gene with its transcripts uniformly high throughout the 24 h period. *CRY1b* transcripts are about 3-fold higher compared to *PHYB1*, 6-fold higher compared to *CRY2*, 10 to 12-fold higher compared to *CRY1a*, *PHYA*, *PHYB2* and *PHYE*, and more than 30-fold higher compared to *PHYF* (Figure 5A-D).

Concerning the amplitude of oscillations, photoreceptor transcripts show modest fold changes compared to other light-regulated and circadian genes like *CAB4* and *GI* (see below), spanning from 2 (*PHYF*) to 9 (*PHYB2*) fold (Figure 5). At dawn (ZT0) and in darkness the quantity of all transcripts ere comparatively low, but a detectable transcription activity is still maintained (Figure 5A-D).

Changes in mRNA accumulation of tomato photoreceptor genes in LL conditions

One of the most reliable diagnostic feature of circadian rhythms is that they persist under light constant conditions. Therefore, to determine whether the rhythmic fluctuation of the tomato photoreceptors observed in LD are maintained in LL conditions, we measured their transcription in plants transferred in LL, after entraining the clock in LD. Samples were harvested at 4h intervals during a period of 40 h.

In LL transcript levels cryptochromes and phytochromes continue to cycle indicating that circadian clock controls the expression of these genes (Figure 6A-D). Conversely, *PHYB1* and *PHYE* transcripts lose any detectable oscillation under LL (Figure 6A-C). However, as compared to LD conditions (Figure 5A-D), we observe both similarities and differences in the phase and amplitude of the transcription peaks. The majority of circadian photoreceptor transcripts maintain an exact 24h periodicity thus they show an expression peak at

ZT36 (*CRY1b*, *CRY2*, *PHYB2* and *PHYF*) (Figure 6A-D); while *CRY1a* and *PHYA* genes anticipate the transcription peak at ZT32 (Figure 6B), suggesting that light may have a partial resetting effect on their transcription rhythm. However the circadian oscillation when not supported by normal light/dark cycles, results in weaker transcription alterations and sometimes in slight differences in the oscillation phase.
Although *CRY1b* and, especially, *PHYF* transcripts didn't show dramatic perturbations in LD, once under constant light conditions their transcript levels increase up to ZT36 (Figure 6A-D).

Effects of cryptochromes on light-induced expression of tomato photoreceptor genes in day/night cycles

To study the effect of the light signal via cryptochrome (*CRY1a* and *CRY2*) genes on the expression profiles of tomato photoreceptor genes, we compared the mRNA levels changes in LD, among wt, CYRY1 deficient mutant (*cry1a*-) and *CRY2* over-expressing transgenic (*CRY2-OX*) (Weller *et al.,* 2001; Giliberto *et al.,* 2005) tomatoes. The results indicated that loss of CRY1a as well as the over-expression of CRY2 influences the daily transcription profiles of several tested tomato genes (Figure 7 and Figure 8). In both *cry1a*- and *CRY2-OX* plants, most tomato photoreceptor transcripts continued to cycle in LD conditions, in the same phase as in wt, although with reduced or increased amplitude.
Major alterations involve *CRY1a*, *CRY2*, *PHYA*, *PHYB2* and *PHYF* transcripts. Most notably, in the *cry1a*- background the transcription *CRY1a* gene (non functional) is increased. The increase is about 2-fold from ZT4 to ZT20 with the highest levels 4h before (ZT8), with respect to wt (Figure 7). In *CRY2-OX* plants, as expected for the presence of the transgene, *CRY2* mRNAs is about 10-15 fold more abundant relative to that observed in wt (Figure 7). Remarkably, over-expression of *CRY2* didn't depress the normal cycling of *CRY2* transcript (Figure 7). These data could establish both transcript and protein as components of a positive feedback circuit capable of generating a stable oscillation. Besides, *PHYA* transcripts are altered in a similar manner in both *cry1a*- and *CRY2-OX* background, consisting in a decrease of mRNA abundance especially at ZT12 (Figure 8). Conversely, the effect of tomato genotype is opposite for *PHYB2,* indeed, *cry1a*- increases while *CRY2-OX* reduces the oscillation amplitude at most the time points analyzed (Figure 8). Finally, *PHYF* mRNAs are more abundant in *cry1a*- while the effect is minor in *CRY2-OX* genotype (Figure 8).

Effects of cryptochromes on light-induced expression of tomato photoreceptor genes under LL

In order to determine possible effects of the light signal via cryptochromes on the circadian expression profiles, we compared the changes in the mRNA abundance of photoreceptor genes, among wt, *cry1a*- and *CRY2-OX* plants grown under LL. Our results underlined that loss of CRY1a as well as the over-expression of the CRY2 influenced the transcription profiles and the circadian regulation of a number of genes, including *CRY1a*, *CRY2*, *PHYA*, *PHYB2* and *PHYF* transcripts (Figure 9 and Figure10).
Under LL, the effect of the *cry1a*- and *CRY2-OX* genetic backgrounds on *CRY1a* transcription result in a slight delay of the expression peak from ZT32 to ZT36 (Figure 9).

As already observed in LD, the cyclical pattern of *CRY2* expression is not affected by *CRY2* over-expression, although the transcript levels are 10-15 fold more abundant relative to that observed in wt (Figure 9). Circadian oscillations of *PHYA,* that cycled in wt plants, are repressed following the transfer of mutant and transgenic plants to LL conditions (Figure 10). However, in the mutant the presence of low-amplitude oscillation (ZT36) can not be excluded (Figure 10). *CRY2* over-expression also changed *PHYB2* transcription pattern reducing the oscillation amplitude at all the time points analyzed (Figure 10). Circadian oscillations of *PHYB2* that cycled in the wt plants are also fully suppressed in the transgenic plants but not in *cry1a-* (Figure 10). Finally, as already observed for LD experiments, *PHYF* transcript oscillation pattern remain unclear also under LL; however in *cry1a-* background its *PHYF* transcripts were more abundant and oscillated with robust amplitudes (Figure 10).

Diurnal oscillation of tomato GI and CAB4 mRNA in day/night cycles

Our results confirmed that *GI* and *CAB4* mRNAs fluctuate within a cycle, showing a direct light regulation. On the whole, *GI* transcripts cycle, with the highest amount at 12h after the onset of light (ZT12) and the lowest level at presumptive dawn (ZT0) with amplitude of more than 700-fold (Figure 11). Peak levels of *CAB4* transcription occurred 4 h earlier (ZT8) (Figure 11) and reached trough levels 12 h later (ZT20) as *GI*, after transition to darkness (Figure 11). Also, the amplitude of *CAB4* transcript oscillations was wide, 120-fold at ZT8 over ZT20 (Figure 11). Interestingly, *CAB4* transcripts increased slightly in darkness from ZT20 to ZT24, showing, here again, the anticipation of "light-on" that is typical of circadian-regulated genes (Figure 11) (Tòth *et al.,* 2001).
Under LL *GI* mRNA levels continue to cycle with an exactly 24h periodicity (ZT36) (Figure 12), showing that the transcription of this gene is controlled by the endogenous circadian clock. However, peak level at ZT36 decreased, while trough levels increased compared with LD (Figure 11 and Figure 12). In addition, at subjective dark, increases of the GI transcripts were observed from ZT16 to ZT20 (Figure 12). As expected, also *CAB4* transcript levels were controlled by the circadian clock. *CAB4* mRNAs peaked during the light constant condition as observed under LD (Figure 12). LL conditions affected both the amplitude/phase of the transcripts oscillations as well as the mRNAs abundance (Figure 12).

Effects of cryptochromes on light-induced expression of tomato GI and CAB4 genes in day/night cycles

In *cry1a-* background, *GI* transcripts cycled as they did in wt (Figure 11). However, loss of CRY1a caused a 2 fold reduction peak of *GI* transcript levels at ZT12 and ZT16 (Figure 11). A similar effect was also observed for *CAB4* where the loss of CRY1a determined reduced amplitude of the transcriptional oscillations when lights were on. In addition was evident a slight phase shift which anticipated the transcription peak at ZT4 (Figure 11). Conversely, *CRY2-OX* background did not affect significantly *GI* as well as *CAB4* transcription pattern (Figure 11).

The effect of CRY1a loss and *CRY2* over-expression on the expression of tomato *GI* and *CAB4* genes were considered also under LL. In *cry1a-* plants, *GI* transcripts continued to cycle as observed in wt (Figure 12), while in *CRY2-OX* circadian expression of *GI* is disrupted (Figure 12). Loss of CRY1a produced a negative regulation of *CAB4* gene expression in LL and a very weak alteration of rhythmicity, if any, from ZT24 to ZT40 (Figure 12); while in transgenic tomato, *CAB4* transcription changes were less evident (Figure 12).

Discussion

Diurnal expression of tomato genome

Using TOM2 microarray containing 12160 oligonucleotides, we identified 1372 genes that were regulated in a diurnal pattern corresponding to 20% of the genes that passed quality controls. Though by using artificial cutoff values we might exclude a certain number of gene transcripts cycling with lower amplitude, it is still evident that in tomato, as it occurs in *Arabidopsis* (Nozue and Maloof 2006), light has a huge impact on growth and development. The majority of light regulated genes reached their max transcript levels at midday (ZT8), otherwise the other transcription peaks appeared quite evenly distributed during a 24h period (Figure 1) supporting the occurrence of highly coordinated and alternated metabolic processes.

As expected, the majority of genes involved in cell wall biosynthesis, mitochondrial, cytosolic and plastidial proteins involved in photosynthesis were up-regulated by light (Figure 2A). This could indeed account for the biosynthetic processes correlated to photosynthesis and energy metabolism that are usually driven by light. Whereas the fact that several genes coding for proteins involved in transporter and transferase activity showed a peak of expression around dusk (ZT16), and those involved in the transcription control machinery peak mainly at dark (ZT20) (Figure 2B) indicate that tomato cells retain number of biochemical activity correlated with developmental pathways, lipid oxidation and others.

Reduction of data complexity by clustering light regulated genes with similar transcription trend was very useful to get a quick picture over the coordinated genomic activity. For example, the several genes more expressed during daylight, grouped in the clusters 1, 4, 8, 10 and 12 (Figure 3) encode for protein elements involved in photosynthesis, fatty acid biosynthesis, secondary metabolites with photo-protective properties, light signaling and flowering; while most of the genes repressed during daylight, included in the clusters 2, 5, 9, 11 and 13 (Figure 3), serve to prepare the plant organism to the biochemical processes to be accomplished during dark hours. Among the latter genes we found elements involved in degradation of cell wall and oxidation of fatty acids. Moreover, genes involved in nitrogen and sulfur assimilation were down-regulated

by light as well as key enzymes involved in ethylene biosynthesis and cell wall loosening as xyloglucan endotransglycosylase and expansin. Most of these genes are already known to be down-regulated by light in *Arabidopsis* (Ma *et al.,* 2001). Thus, it is conceivable that light temporal regulated genes influence the same diurnal based biochemical processes in *Arabidopsis* and tomato.

As expected, many genes involved in metabolites with antioxidant properties, such as carotenoids and flavonoids, were more expressed during light hours in order to protect cells and tissues from the damaging effects of free radicals and singlet oxygen generated by the excess of light. In green tissues, carotenoids prevent the chlorophyll-photosensitized formation of highly destructive singlet oxygen by intercepting the chlorophyll triplet states and may also scavenge additional singlet oxygen present. Furthermore, they perform an antenna function by transferring the energy of absorbed light at the singlet excited state level to the chlorophyll system for the execution of photosynthesis. Thus the up-regulation of most of the carotenoids related genes over TOM2 microarray in correspondence of the presumptive dawn is perfectly accountable with the predicted function of carotenoids in tomato green tissues (Table 2). Coincidently, most of the genes involved in flavonoids that in green tissues also provide protection against light induced oxidation states, albeit they do not take direct part in photosynthesis, were up-regulated at early hours (ZT0-ZT8) (Table 2).

Temporal modulations of cryptochromes and phytochromes gene expression

Previous experiments in *Arabidopsis* have established a fundamental role of phytochromes and cryptochromes in providing light input to the plant circadian clock (Devlin and Kay, 2001; Tòth *et al.,* 2001). In tomato, like *Arabidopsis*, we observed a sort of regulatory bi-directional crosstalk between the clock machinery and photoreceptors which allowed the latter to determine significant changes on the temporal transcription pattern of genes under the control of the first.

As it occurs in *Arabidopsis* (Toth *et al.*, 2001), tomato *PHY* and *CRY* genes follow a diurnal rhythm and exhibited maximum expression in the light phase (Figure 5A-D). Tomato, photoreceptor transcripts, except *CRY1b,* appeared to be quite synchronized and peaked at presumptive afternoon (ZT 12), (Figure 5A-D). While, in *Arabidopsis* the photoreceptor genes coding for light-stable proteins are intensively transcribed at the beginning (PHYC, PHYD, and PHYE) or in the first half (PHYB and CRY1) of the light phase, the photo-labile PHYA and CRY2 reached their maximum transcript abundance close to the end of the light interval. Unfortunately, data on the photo-stability of tomato photoreceptors are not yet available; by the way, the massive synthesis of most of the tomato photoreceptor transcripts, including *CRY-DASH* (Facella *et al.,* 2006), in late afternoon could be interpreted as a physiological adaptation which prepares tomato plants to the following day light stimuli.

It is very interesting to note that, in LD all cryptochromes and PHYA presented a minimum level of transcript quantity 4h after the presumptive dawn (ZT4) (Figure 5A-B) (Facella *et al.,* 2006). It is possible that this expression trough represents a “light-on” signal that may potentially result in clock resetting.

The temporal regulation of *CRY1b* expression, whose mRNAs were the most abundant among the analysed photoreceptors, didn't show remarkable fluctuation during the day and was quite different from that of the other *CRY* genes (Figure 5A). Despite its high sequence similarity with *CRY1a,* this gene is not yet functionally characterized so we cannot rule out a specific and different role of *CRY1b* in light perception process of tomato plants. The close similarities of the expression pattern of *PHYA*, *CRY1a* and *CRY2* genes in both LD an LL (Figure 5B and Figure 6B): they presented high levels of expression in the second part of the day (ZT8-16) and very low transcript abundance during the night, could be potentially related to overlapping functions and cooperation in their physiological roles.

PHYB1 transcript levels were definitely the most abundant among phytochromes followed by *PHYB2*, *PHYE* and *PHYA* which showed a decrease of about 4-5 fold of their transcripts; while *PHYF* remain by far the less expressed phytochrome in tomato green tissues (Figure 5). In LD the expression peak of phytochrome genes was overlapped at ZT12 with no major phase differences. Also the amplitude of the oscillation was quite modest with the sole exception of *PHYB2* that showed a 9-fold difference between through and peak transcript levels (Figure 5). These data contrast with a previous report (Hauser *et al.,* 1998) which show a clear difference in diurnal rhythms of expression of *PHYB1* and *PHYB2*, which are out of phase by approximately 10 hours. However, it must be taken in account that the authors used a quite different experimental set up with tomato plants grown in greenhouse and without supplemental illumination. Besides, the quite constant relative phases of peak expression that we observe around ZT12, diverges from data published by Hauser et al. 1998; also in *Arabidopsis PHY* and *CRY* genes show expression peaks at four different times along the light phase (Tòth *et al.,* 2001). The specific timing of the photoreceptor transcripts accumulation could suggest that the photoreceptor mediated input signalling to the clock machinery must be particularly synchronized in tomato. However it should be considered that in our experiments tomato plants were grown in growth chamber under artificial light of constant intensity and spectrum composition (see Experimental procedures), this artificial environment could potentially affect to some extension the diurnal gene expression.

The fact that, under LL all tomato cryptochromes plus *PHYA*, *PHYB2* and *PHYF* kept the oscillations following a period close to 24 hours, though with minor changes in the phase of the peaks (*CRY1a* and *PHYA* transcripts reached their maximum 4 hours earlier) (Figure 6A-D), hints that a circadian clock regulates the expression of these photoreceptors, as in *Arabidopsis* (Harmer *et al.,* 2000). Notably, the transcription of *PHYB1* and *PHYE* lost their rhythmicity in LL, hence they seem to escape the influence of the circadian machinery, in tomato (Figure 6A-C).

In LL, at the beginning of presumptive night (ZT20), it is generally evident a certain increment of the transcripts with respect to the correspondent LD point (Figure 6). This difference may be explained postulating a direct activation driven by light. The actual transcript levels appear to be then partially restored to the "normal" light/dark oscillation; this is possibly caused by some feedback action mediated by the clock machinery. This hypothetic feedback action is totally consistent with the model proposed by Tòth *et al.,* in (Toth *et al.*, 2001) by which the photoreceptors send the "light-on" signal to the clock core and the core

regulates their expression, forming a regulatory loop. This regulatory loop could serve to increase the perception of resetting light signals at the right times and to neutralize signals from non-predictable environmental cues, which could cause an incorrect resetting of the circadian clock.

Photoreceptors genes expression in plants with altered cryptochrome under LD and LL

Alterations in cryptochrome accumulation caused minor effects on the LD transcription of the cryptochrome genes except some increment in mRNA abundance. Interestingly, the expression of *CRY1a* gene was up-regulated in *cry1a-* plants (Figure 7); we infer that this could be the effect of some auto-regulatory feedback mechanism caused by the absence of a CRY1a functional protein. Following this hypothesis, in normal conditions, accumulation of CRY1 protein would repress the transcription of its own gene.

The increment of *CRY2* transcripts in transgenic tomato over-expressing cryptochrome 2 is fully expected by the effect of the transgene, what is more difficult to interpret is the still marked temporal fluctuation *CRY2* transcripts with the same cyclic trend of wt plants (Figure 7 and Figure 9). However a similar situation is, for example evident in a transgenic line over-expressing *GI* (Mizoguchi *et al.,* 2005). In principle, the transgene mRNAs, under the control of the 35S promoter, should not undergo diurnal and circadian rhythms; however we must consider that in *CRY2OX* genotype the population of *CRY2* mRNAs are a mixture of endogenous and transgenic ones. It is possible that the additional *CRY2* stimulate to some extend the expression of the endogenous gene. So we cannot rule out that the persisting cycling phase of *CRY2* mRNAs in the transgenic line is the result of an enhanced activity of the endogenous CRY2 promoter.

We demonstrated that cryptochromes act as important transcriptional regulators of phytochromes. Indeed, genotypes with altered cryptochromes showed profound effects on the transcription of the phytochrome genes which involve both transcript abundances, phase changes and reduced/increased cycling amplitude.

The fact that in LD the mRNA levels of *PHYA* and *PHYB2* were strongly reduced in *cry1a-*, while they are reduced and increased, respectively in *CRY2-OX* genotypes with respect to wt plants (Figure 8), is probably the result of a direct control on these two genes by cryptochrome 1 and 2 which act cooperatively repressing the transcription of *PHYB2* and antagonistically over the transcription of *PHYA*, promoted by *CRY1a* and repressed by *CRY2* (Figure 8 and Figure 13). In *Arabidopsis* there is evidence for a direct interaction between PHYA and CRY1, with PHYA mediating a light-dependent phosphorylation of CRY1 (Ahmad *et al.,* 1998), and between PHYB and CRY2, with the cryptochrome 2 probably suppressing *PHYB* signalling (Mas *et al.,* 2000). Furthermore, in *Arabidopsis* CRY1 operates as a signal transduction component downstream of PHYA in light input to the clock (Devlin and Kay, 2000). Assuming that also in tomato *PHYA* light signalling to the clock is mediated by CRY1a, our results show that, under high fluence white light, CRY1a has an epistatic effect on *PHYA* expression. Also, in tomato the suppression of the PHYB type signalling could take place by the coordinated repressive action of both CRY1a and CRY2 over *PHYB2*, but not *PHYB1*, transcripts (Figure 8 and Figure 13). To further prove of the complexity of the interactions

between phytochromes and cryptochromes, there was the about 2-fold increase of *PHYF* transcripts at all time points as a result of the lack of a functional *CRY1a*.

Under LL conditions the transcription pattern often become more perturbed and sometimes of difficult interpretation. However, cryptochromes showed no significant effects on the transcription of cryptochrome genes, except the changes in mRNA abundance already described in LD (Figure 7 and Figure 9). In general, the lack of CRY1a has little or no effect also over the LL transcription of phytochromes, while the evident arhythmicity of *PHYA, PHYB2* and *PHYF* genes caused by the over-expression of CRY2 (Figure 10) is quite intriguing. Excess of CRY2, indeed, can influence the transcription of phytochromes, either directly altering their transcripts abundance in diurnal cycles, either via the circadian machinery removing the clock feedback control over all the *PHY* genes that continue to oscillate in LL (Figure 10 and Figure 13). We can hypothesize that the presence of constitutive protein CRY2 disrupts the specific pace-maker mechanism of the core that normally causes the oscillations of these two phytochromes in wt plants.

Expression CAB4 and GI expression are altered by cryptochromes

In tomato wt plants, *GI* and *CAB4* transcript levels cycled similarly to their putative counterparts in *Arabidopsis* (Fowler *et al.,* 1999; Millar, 1999) and their strong diurnal oscillations (about 700- 100-fold, respectively) suggests that also in tomato they are deeply controlled by a time keeping machinery. Although the lower amplitude of oscillations in LL, hints that the mRNA quantity of both tomato *CAB4* and *GI* is more affected by a continuous high fluence light treatment than in *Arabidopsis* (Fowler *et al.,* 1999; Millar, 1999) (Figure 11 and Figure 12). Interestingly, lack of *CRY1a*, but not over-expression of *CRY2*, triggered the decrease of the diurnal expression of both *GI* and *CAB4*, which means that both genes, directly or indirectly, were activated by CRY1a. A recent report showed that *Arabidopsis* mutant *cry1-cry2* plants displayed a severely reduced *GI* response to blue light, while CRY2 had no affect on the daily transcription of *GI* (Paltiel *et al.,* 2006). According to these features, our results demonstrated that CRY1a plays a main role in the activation of tomato *GI,* under high fluence white light. Besides, following the hypothesis of GI as the "factor Y" in an interlocked feedback loop through light affecting TOC1 expression (Locke *et al.*, 2005) we may then assume that CRY1a must have a direct influence on the tomato circadian core system. Despite the fact that Patiel and colleagues (Paltiel *et al.,* 2006) did not report any connection between the cryptochrome 2 and *GI* transcription, when we consider the tomato genotype over-expressing CRY2, we observe the loss of circadian oscillations of *GI*. However, we must point out that the transcription pattern of *GI* and, especially, *CAB4* genes in LL become quite perturbed (Figure 12). If this effect is real, it could be either due by a direct repression of *GI* transcription driven by the excess of CRY2 in absence of dark-light input, either mediated by PHYB2, as a consequence for the reduction of its mRNAs and for the loss of their circadian rhythm in *CRY2-OX* plants under LL (Figure 10). It is, indeed, reasonable to hypothesize that CRY2 controls the transcription pattern of *PHYB2* that, at its turn, regulates the expression of *GI*. This model is consistent with

some experimental evidences in *Arabidopsis* in which GI acts as a positive mediator of PHYB signalling to the clock (Huq *et al.,* 2000; Mizoguchi *et al.,* 2005). Whatever the case and given the delicate role of GI in determining the flowering time (Imaizumi and Kay, 2006), the late flowering phenotype of tomato *CRY2OX* genotype in short and long day conditions, as well (Giliberto *et al.*, 2005), could be the effect of CRY2 on the input elements (phytochromes and cryptochromes) of the circadian system that regulate tomato flowering time.

Experimental procedures

Standard molecular biology protocols were followed as described in Sambrook *et al.,* (Sambrook *et al.,* 1989).

Solanum lycopersicum (cv *Moneymaker*), *cry1a-* and transgenic *CRY2-OX* (Weller *et al.,* 2001; Giliberto *et al.,* 2005) were grown in a growth chamber for 28 days in LD conditions (16 h light-25°C/8 h dark-23°C). Light intensity of about 100 µmol m^{-2} s^{-1} was provided by Osram (Munich) 11–860 daylight lamps. For LL experiments, plants grown as described above for 28 days were shifted to continuous light at the dawn of 29th day. The aerial parts of three plants for each genotype (wt, *cry1a-* and *CRY2-OX*) were harvested at the times shown.

Microarray analyses

Samples were assayed on the Tomato TOM2 oligo-arrays printed by University of Arizona contain 12160 oligonucleotides (**http://www.operon.com/arrays/oligosets_Tomato.php**).

For each experiment, 2 ug of DNA-free total RNA were retro-transcribed and amplified using the Aminoallyl Message Amp II kit (AMBION http://www.ambion.com/) following manufacturer's instructions. 2ug of amplified aminoallyl-modified RNA were labeled in the presence of Cy3 and Cy5 for 2 hours at room temperature. Unincorporated dyes were eliminated using RNeasy MinElute column (Qiagen Inc.; http:// www.qiagen.com/) according to the manufacturer's specifications.

200 pmoles of purified Cy3- and Cy5-labelled aRNAs were added in a buffer containing 2x SSC, 0.08% SDS and Liquid Blocking Reagent (Amersham Biosciences; http://www5.amershambiosciences.com/) dispensed over the glass slide and incubated at 55°C overnight with agitation. Slides were washed in decreasing SSC concentrations (2x _ 0.1x) and 0.1% SDS at 55 °C and room temperature, respectively. The last wash was carried out in 0.1x SSC at room temperature. The both hybridization and post-hybridization washes were performed on a automatic hybridization station (HybArray 12, Perkin-Elmer http://www.perkinelmer.com/). Hybridized microarrays were then scanned using the ScanArray Lite (Perkin–Elmer http://www.perkinelmer.com/) and the resulting Cy3 and Cy5 images were analyzed with the

software ScanArray Express (Perkin–Elmer http://www.perkinelmer.com/) in order to measure the Cy3/Cy5 spot intensities.

Raw hybridization signals were filtered by imposing a minimal signal/noise ratio of 2.0 and flagging the non-passed spots. In order to obtain a homogeneous dataset for all hybridized slides we have filtered microarray data imposing good quality spots to be present in at least three out of four hybridized slides (two dye-swap and two biological replicas, respectively) for each experimental point. Raw values were then normalized with the locally weighted linear regression (LOWESS) method using the 20% of data for smoothing (Cleveland and Devlin, 1998) and gene expression analysis of the array data were performed using GeneSpring version 7.3 (Silicon Genetics, http://www.chem.agilent.com/). Data generated from 4 replicates (2 independent biological replicates and 2 dye-swap experiments) were averaged and standard deviations were calculated. Genes that met at least one of the following two conditions in at least two time points were considered light-regulated: 1) genes showing equal to or more than 3-fold change in all repeats; 2) genes showing the mean value from all repeats at least 3-fold changed and the standard deviation was less than 50% of the mean. Cluster analyses were performed using Cluster and Treeview algorythms (Eisen *et al.,* 1998).

Quantitative RT-PCR

Total RNA (1 μg) was retro-transcribed with oligo-dT and Superscript III (Invitrogen, http://www.invitrogen.com/), according to the manufacturer's instructions. First strand cDNA (5 ng) was used as template for quantitative real time RT-PCR (QRT-PCR). QRT-PCR assays were carried out with gene-specific primers, using an ABI PRISM 7900HT (Applied Biosystems, http://www.appliedbiosystems.com/) and the Platinum SYBR Green master mix (Invitrogen, http://www.invitrogen.com/), according to manufacturer's instructions. PCR conditions were: 50 at 95°C followed by 45 cycles at 95°C X 15'' and at 58°C X 60''. Quantification was performed using standard dilution curves for each studied gene fragment and the data were normalized for the quantity of the β-actin transcript.

Acknowledgements

References

1 **Ahmad. M., Jarillo J.A., Smirnova O. and Cashmore, A.R.** (1998) The CRY1 blue light photoreceptor of Arabidopsis interacts with phytochrome A in vitro. *Mol. Cell*, **1**, 939-48.

2 **Alabadi, D., Oyama, T., Yanovsky, M.J., Harmon, F.G., Mas, P. and Kay, S.A.** (2001) Reciprocal regulation between TOC1 and LHY/CCA1 within the Arabidopsis circadian clock. *Science,* **293**, 880–883.

3 **Alabadi, D., Yanovsky, M.J., Mas, P., Harmer, S.L. and Kay S.A.** (2002) Critical role for CCA1 and LHY in maintaining circadian rhythmicity in arabidopsis. *Curr. Biol,* **12,** 757–761.

4 **Ang, L.H., Chattopadhyay, S., Wei, N., Oyama, T., Okada, K., Batschauer, A. and Deng, X.W.** (1998) Molecular interaction between COP1 and HY5 defines a regulatory switch for light control of Arabidopsis development. *Mol. Cell,* **1,** 213-222.

5 **Araki, T. and Komeda, Y.** (1993) Analysis of the role of the late-flowering locus, GI, in the flowering of *Arabidopsis thaliana*. *Plant J*, **3**, 231-39.

6 **Bruno, A.K. and Wetzel, C.M.** (2004) The early light-inducible protein (ELIP) gene is expressed during the chloroplast-to-chromoplast transition in ripening tomato fruit. *J. Exp. Bot,* **55**, 2541-2548.

7 **Casal, J.J. and Yanovsky, M.J.** (2005) Regulation of gene expression by light. *Int. J. Dev. Biol,* **49**, 501-511.

8 **Clack, T., Mathews, S. and Sharrock, R.A.** (1994) The phytochrome apoprotein family in Arabidopsis is encoded by five genes: the sequences and expression of PHYD and PHYE. *Plant Mol. Biol*, **25**, 413-427.

9 **Cleveland, W.S. and Devlin, S.J.** (1998) Locally weighted regression: an approach to regression analysis by local fitting. J. of Am. Stat. Assoc, **83,** 596-610.

10 **Covington, M.F., Panda, S., Liu, X.L., Strayer, C.A., Wagner, D.R. and Kay, S.A.** (2001) ELF3 Modulates Resetting of the Circadian Clock in Arabidopsis. *Plant Cell,* **13**, 1305–1316.

11 **Deng, X.W. and Quail, P.H.** (1999) Signalling in light-controlled development. *Semin Cell Dev. Biol,* **10**, 117-119.

12 **Devlin, P.F. and Kay, S.A.** (2000) Cryptochromes are required for phytochrome signaling to the circadian clock but not for rhythmicity. *Plant Cell*, **12**, 2499-2510.

13 **Devlin, P.F. and Kay, S.A.** (2001) Circadian photoreception. *Annu. Rev. Physiol*, **63**, 677-694.

14 **Doyle, M.R., Davis, S.J., Bastow, R.M., McWatters, H.G., Kozma-Bognar, L., Nagy, F., Millar, A.J. and Amasino, R.M.** (2002) The ELF4 gene controls circadian rhythms and flowering time in *Arabidopsis thaliana*. *Nature,* **419**, 74-77.

15 **Dunlap, J.C.** (1999) Molecular bases for circadian clocks. *Cell,* **96,** 271-290.

16 **Eisen, M.B., Spellman, P.T., Brown, P.O. and Botstein, D.** (1998) Cluster analysis and display of genome-wide expression patterns. *Proc. Natl. Acad. Sci. USA,* **95**, 14863-14868.

17 **Eulgem, T., Rushton, P.J., Robatzek, S. and Somssich, I.E.** (2000) The WRKY superfamily of plant transcription factors. *Trends Plant Sci,* **5**, 199-206.

18 **Facella, P., Lopez, L., Chiappetta, A., Bitonti, M.B., Giuliano, G. and Perrotta G.** (2006) CRY-DASH gene expression is under the control of the circadian clock machinery in tomato. *FEBS Lett*, **580**, 4618-4624.

19 **Folta, K.M. and Maruhnich, S.A.** (2007) Green light: a signal to slow down or stop. *J. Exp. Bot*, **146**, 227-228.

20 **Fowler, S., Lee, K., Onouchi, H., Samach, A., Richardson, K., Morris, B., Coupland, G. and Putteril, J.** (1999) GIGANTEA: a circadian clock-controlled gene that regulates photoperiodic flowering in *Arabidopsis* and encodes a protein with several membrane-spanning domains. *EMBO J*, **18,** 4679-4688.

21 **Gardner, M.J., Hubbard, K.E., Hotta, C.T., Dodd, A.N. and Webb, A.A.** (2006) How plants tell the time. *Biochem. J*, **397**, 15–24.

22 **Giliberto, L., Perrotta, G., Pallara, P., Weller, J.L., Fraser, P.D., Bramley, P.M., Fiore, A., Tavazza, M. and Giuliano, G.** (2005) Manipulation of the blue light photoreceptor cryptochrome 2 in tomato affects vegetative development, flowering time, and fruit antioxidant content. *Plant Physiol*, **137**, 199-208.

23 **Giuliano, G., Hoffman, N.E., Ko, K., Scolnik, P.A. and Cashmore, A.R.** (1988) A light-entrained circadian clock controls transcription of several plant genes. *EMBO J*, **7,** 3635-3642.

24 **Guo, H., Yang, H., Mockler, T.C. and Lin, C.** (1998) Regulation of flowering time by Arabidopsis photoreceptors. *Science,* **279**, 1360-1363.

25 **Harmer, S.L., Hogenesch, J.B., Straume, M., Chang, H.S., Han, B., Zhu, T., Wang, X., Kreps, J.A. and Kay, S.A.** (2000) Orchestrated transcription of key pathways in *Arabidopsis* by the circadian clock. *Science* **290**, 2110-2113.

26 **Hauser, B.A., Cordonnier-Pratt, M.M. and Pratt, L.H.** (1998) Temporal and photoregulated expression of five tomato phytochrome genes. *Plant J*, **14**, 431-439.

27 **Hauser, B.A., Cordonnier-Pratt, M.M., Daniel-Vedele, F. and Pratt, L.H.** (1995) The phytochrome gene family in tomato contains a novel subfamily. *Plant Mol. Biol*, **29**, 1143-1155.

28 **Hayama, R. and Coupland, G.** (2004) The molecular basis of diversity in the photoperiodic flowering responses of *Arabidopsis* and Rice. *Plant Physiol*, **135**, 677-684.

29 **Holm, M., Ma, L.G., Qu, L.J. and Deng, X.W.** (2002) Two interacting bZIP proteins are direct targets of COP1-mediated control of light-dependent gene expression in *Arabidopsis*. *Genes Dev*, **16**, 1247-1259.

30 **Huq, E., Tepperman, J.M. and Quail, P.H.** (2000) GIGANTEA is a nuclear protein involved in phytochrome signalling in *Arabidopsis*. *Proc. Natl. Acad. Sci. USA*, **97**, 9654-58.

31 **Imaizumi, T. and Kay, S.A.** (2006) Photoperiodic control of flowering: not only by coincidence. *Trends Plant Sci,* **11**, 550-558.

32 **Ishikawa, M., Kiba, T. and Chua, N.H.** (2006) The *Arabidopsis* SPA1 gene is required for circadian clock function and photoperiodic flowering. *Plant J*, **46**, 736–746.

33 **Jarrillo, J.A., Capel, J., Tang, R.H., Yang, H.Q., Alonso, J.M., Ecker, J.R. and Cashmore, A.R.** (2001) An *Arabidopsis* circadian clock component interacts with both CRY1 and phyB. *Nature*, **410**, 487-490.

34 **Jiao, Y., Yang, H., Ma, L., Sun, N., Yu, H., Liu, T., Gao, Y., Gu, H., Chen, Z., Wada, M., Gerstein, M., Zhao, H., Qu, L.J. and Deng, X.W.** (2003) A genome-wide analysis of blue-light regulation of *Arabidopsis* transcription factor gene expression during seedling development. *Plant Physiol*, **133**, 1480-1493.

35 **Kaczorowski, K.A. and Quail, P.H.** (2003) *Arabidopsis* PSEUDO-RESPONSE REGULATOR7 is a signaling intermediate in phytochrome-regulated seedling deetiolation and phasing of the circadian clock. *Plant Cell*, **15**, 2654-2665.

36 **Kiyosue, T. and Wada, M.** (2000) LKP1 (LOV kelch protein 1): a factor involved in the regulation of flowering time in *Arabidopsis*. *Plant J*, **23**, 807-15.

37 **Kloppstech, K.** (1985) Diurnal and circadian rhytmicity in the expression of light-induced nuclear messenger RNAs. **Planta**, **165**, 502-506.

38 **Laubinger, S., Marchal, V., Le Gourrierec, J., Wenkel, S., Adrian, J., Jang, S., Kulajta, C., Braun, H., Coupland, G. and Hoecker, U.** (2006) *Arabidopsis* SPA proteins regulate photoperiodic flowering and interact with the floral inducer CONSTANS to regulate its stability. *Development*, **133**, 3213-3222

39 **Ledger, S., Strayer, C., Ashton, F., Kay, S.A. and Putterill, J.** (2001) Analysis of the function of two circadian-regulated CONSTANS-LIKE genes. *Plant J*, **26**, 15-22.

40 **Liu, X.L., Covington, M.F., Fankhauser, C., Chory, J. and Wagner, D.R.** (2001) ELF3 encodes a circadian clock-regulated nuclear protein that functions in an *Arabidopsis* PHYB signal transduction pathway. *Plant Cell,* **13**, 1293-1304.

41 **Locke, J.C., Kozma-Bognar, L., Gould, P.D., Feher, B., Kevei, E., Nagy, F., Turner, M.S., Hall, A. and Millar, A.J.** (2006) Experimental validation of a predicted feedback loop in the multi-oscillator clock of *Arabidopsis thaliana*. *Mol. Syst. Biol*, **2**, 1-6

42 **Locke, J.C.W., Millar, A.J. and Turner, M.S.** (2005a) Modelling genetic networks with noisy and varied experimental data: the circadian clock in *Arabidopsis thaliana*. *J. Theor. Biol*, **234**, 383–393.

43 **Locke, J.C.W., Southern, M.M., Kozma-Bognar, L., Hibberd, V., Brown, P.E., Turner, M.S. and Millar, A.J.** (2005b) Extension of a genetic network model by iterative experimentation and mathematical analysis. *Mol. Syst. Biol*, **1**, 13.

44 **Ma, L.G., Li, J.M., Qu, L.J., Hager, J., Chen, Z.L., Zhao, H. and Deng, X.W.** (2001) Light control of *Arabidopsis* development entails coordinated regulation of genome expression and cellular pathways. *Plant Cell*, **13**, 2589-2607.

45 **Martin-Tryon, E.L., Kreps, J.A., Harmer, S.L.** (2007) GIGANTEA Acts in Blue Light Signaling and Has Biochemically Separable Roles in Circadian Clock and Flowering Time Regulation. *Plant Physiol*, **143**, 473–486.

46 **Mas, P., Alabadi, D., Yanovsky, M.J., Oyama, T. and Kay, S.A.** (2003) Dual role of TOC1 in the control of circadian and photomorphogenic responses in *Arabidopsis*. *Plant Cell*, **15**, 223–236.

47 **Mas, P., Devlin, P.F., Panda, S. and Kay, S.A.** (2000) Functional interaction of phytochrome B and cryptochrome 2. *Nature*, **408**, 207-11.

48 **McClung, C.R.** (2006) Plant circadian rhythms. *Plant Cell*, **18**, 792–803.

49 **McWatters, H.G., Bastow, R.M., Hall, A. and Millar, A.J.** (2000) The ELF3 zeitnehmer regulates light signaling to the circadian clock. *Nature*, **408**, 716-720.

50 **Millar, A.J.** (1999) Biological clocks in *Arabidopsis thaliana*. *New Phytol*, **141**, 175-97.

51 **Millar, A.J., Strame, M., Chory, J., Chua, N.H. and Kay, S.A.** (1995) The regulation of circadian period by phototransduction pathways in *Arabidopsis*. *Science*, **267**, 1163-1166.

52 **Mizoguchi, T., Wheatley, K, Hanzawa, Y., Wright, L., Mizoguchi, M., Song, H.-R., Carre´, I.A. and Coupland, G.** (2002) LHY and CCA1 are partially redundant genes required to maintain circadian rhythms in *Arabidopsis*. *Dev. Cell*, **2**, 629–641.

53 **Mizoguchi, T., Wright, L., Fujiwara, S., Cremer, F., Lee, K., Onouchi, H., Mouradov, A., Fowler, S., Kamada, H., Putterill, J. and Coupland, G.** (2005) Distinct roles of GIGANTEA in promoting flowering and regulating circadian rhythms in *Arabidopsis*. *Plant Cell*, **17**, 2255-70.

54 **Neff, M.M., Fankhauser, C. and Chory, J.** (2000) Light: an indicator of time and place. *Genes Dev,* **14**, 257-271.

55 **Nelson, D.C., Lasswell, J., Rogg, L.E., Cohen, M.A. and Bartel, B.** (2000) FKF1, a clock-controlled gene that regulates the transition to flowering in *Arabidopsis*. *Cell*, **101**, 331-340.

56 **Nozue, K., Maloof, J.N.** (2006) Diurnal regulation of plant growth. *Plant Cell Environ*, **29**, 396-408.

57 **Paltiel, J., Amin, R., Gover, A., Ori, N. and Samach, A.** (2006) Novel roles for GIGANTEA revealed under environmental conditions that modify its expression in *Arabidopsis* and *Medicago truncatula*. *Planta*, **224**, 1255-1268.

58 **Park, D.H., Somers, D.E., Kim, Y.S., Choy, Y.H., Lim, H.K., Soh, M.S., Kim, H.J., Kay, S.A. and Nam, H.G.** (1999) Control of circadian rhythms and photoperiodic flowering by the *Arabidopsis GIGANTEA* gene. *Science*, **285**, 1579-1582.

59 **Perrotta, G., Ninu, L., Flamma, F., Weller, J.L., Kendrick, R.E., Nebuloso, E. and Giuliano, G.** (2000) Tomato contains homologues of *Arabidopsis* cryptochrome 1 and 2. *Plant Mol. Biol*, **42**, 765-773.

60 **Perrotta, G., Yahoubian, G., Nebuloso, E., Renzi, L. and Giuliano, G.** (2001) Tomato and barley contain duplicated copies of cryptochrome 1. *Plant Cell Environ*, **24**, 991-997.

61 **Reed, J.W., Nagpal, P., Bastow, R.M., Solomo,n K.S., Dowson-Day, M.J., Elumalai, R.P. and Millar, A.J.** (2000) Independent action of ELF3 and phyB to control hypocotyl elongation and flowering time. *Plant Physiol*, **122**, 1149-1160.

62 **Riechmann, J.L.** (2002) Transcriptional regulation: a genomic overview. *In CR Somerville, EM Meyerwitz, eds, The Arabidopsis Book.* The American Society of Plant Biologists, Rockville, MD. http://www.aspb.org/ publications/arabidopsis/

63 **Sambrook, J., Fritsch, E.F., Maniatis, T.** (1989) *Molecular cloning: A Laboratory Manual*, 2nd edn. Cold Spring Harbor: Cold Spring Harbor Laboratory Press.

64 **Schaffer, R., Landgraf, J., Accerbi, M., Simon, V., Larson, M. and Wisman, E.** (2001) Microarray analysis of diurnal and circadian-regulated genes in *Arabidopsis*. *Plant Cell*, **13**, 113-123.

65 **Schaffer, R., Ramsay, N., Samach, A., Corden, S., Putterill, J., Carre´, I.A. and Coupland, G.** (1998) The late elongated hypocotyl mutation of Arabidopsis disrupts circadian rhythms and the photoperiodic control of flowering. *Cell*, **93**, 1219–1229.

66 **Somers, D.E., Schultz, T.F., Milnamow, M. and Kay, S.A.** (2000) ZEITLUPE encodes a novel clock-associated PAS protein from *Arabidopsis*. *Cell*, **101**, 319-329.

67 **Somers, D.E., Webb, A.A.R., Pearson, M. and Kay, S.A.** (1998) The short-period mutant, toc1-1, alters circadian clock regulation of multiple outputs throughout development in *Arabidopsis thaliana*. *Development*, **125**, 485-494.

68 **Tepperman, J.M., Zhu, T., Chang, H.S., Wang, X. and Quail, P.H.** (2001) Multiple transcription-factor genes are early targets of phytochrome A signaling. *Proc. Natl. Acad. Sci.* U S A, **98**, 9437-9442.

69 **Tòth, R., Kevei, E., Hall, A., Millar, A.J., Nagy, F. and Kozma-Bognàr, L.** (2001) Circadian clock-regulated expression of phytochrome and cryptochrome genes in *Arabidopsis*. *Plant Physiol*, **127**, 1607-1616.

70 **Wang, Z.-Y. and Tobin, E.M.** (1998) Constitutive expression of the CIRCADIAN CLOCK ASSOCIATED1 (CCA1) gene disrupts circadian rhythms and suppresses its own expression. *Cell*, **93**, 1207–1217.

71 **Weller, J.L., Perrotta, G., Schreuder, M.E., Van Tuinen, A., Koornneef, M., Giuliano, G. and Kendrick, R.E.** (2001) Genetic dissection of blue-light sensing in tomato using mutants deficient in cryptochrome 1 and phytochromes A, B1 and B2. *Plant J*, **25**, 427–40.

72 **Yanovsky, M.J., Gazzella, M.A. and Casal, J.J.** (2000) A quadruple photoreceptor mutant still keeps track of time. *Curr. Biol*, **10**, 1013-1015.

73 **Zerr, D.M., Hall, J.C., Rosbash, M. and Siwicki, K.K.** (1990) Circadian fluctuactions of period protein immunoreactivity in the CNS and the visual system of *Drosophila*. **J. Neurosci**, **10**, 2749-2762.

Tables

Table 1

Number of light-regulated TFs genes

GENE FAMILY	zt0	zt8	zt16	zt20	Total
ZINC FINGER	9	18	2	11	40
WRKY	1	12	0	2	15
bHLH	2	4	0	5	11
bZIP	3	1	0	2	6
MYB	6	2	1	3	12
HD TF	1	2	0	5	8
AP2	0	4	0	1	5
GRAS	0	4	1	1	6
MADS	0	1	0	2	3
ERF/DB3	0	7	0	3	10
OTHERS	6	12	3	4	25

Table 2

Carotenoid related transcripts

zt0	zt8	zt16	zt20	Gene_ID	Annotation
1	0.04	0.50	0.98	M84744	Tomato phytoene synthetase (PSY)
1	0.27	0.69	0.63	L23424	phytoene synthase (PSY2)
1	0.08	0.10	0.43	Y14809	beta-carotene hydroxylase (β-CHY;CrtR-b1 gene)
1	0.26	0.54	0.57	sgn-U212844	phytoene synthase [geranylgeranyl-diphosphate geranylgeranyl transferase](PSY)
1	0.09	0.09	0.29	sgn-U215829	beta-carotene hydroxylase (β-CHY)
1	0.10	0.09	0.44	sgn-U233360	beta-carotene hydroxylase (β-CHY)
1	0.29	0.46	0.69	sgn-U234580	lycopene beta-cyclase (β-LCY)
1	0.04	0.58	0.79	sgn-U212843	phytoene synthase [geranylgeranyl-diphosphate geranylgeranyl transferase](PSY)
1	0.03	0.79	1.59	sgn-U212842	phytoene synthase [geranylgeranyl-diphosphate geranylgeranyl transferase](PSY)
1	26.49	5.37	0.85	Z83835	zeaxanthin epoxidase (ZEP)
1	14.34	3.76	0.92	sgn-U221254	zeaxanthin epoxidase precursor (LOS6/ABA1)(ZEP)
1	0.26	1.30	1.12	AF385366	violaxanthin de-epoxidase (VDE)
1	0.35	1.49	1.27	sgn-U222306	violaxanthin de-epoxidase precursor (VDE)

Flavonoid related transcripts

zt0	zt8	zt16	zt20	Gene_ID	Annotation
1	0.09	0.21	0.81	sgn-U217139	UDP-glucose:anthocyanin 5-O-glucosyltransferase [Verbena x hybrida] (FGT)
1	0.32	0.01	0.53	sgn-U242106	Flavonol 3-O-glucosyltransferase 5 (UDP-glucose flavonoid 3-O-glucosyltransferase 5) (FGT)
1	4.01	3.11	1.33	sgn-U217841	flavonol 3-O-glucosyltransferase (anthocyanin rhamnosyl transferase) (FGT)
1	60.38	37.55	6.88	sgn-U215136	putative anthocyanidine rhamnosyl-transferase (FGT)
1	4.95	5.22	2.13	sgn-U215140	putative anthocyanidine rhamnosyl-transferase (FGT)
1	1.73	1.83	5.53	sgn-U215206	2OG-Fe(II) oxygenase family similar to flavanone 3-hydroxylase [Persea americana]
1	18.76	4.31	1.76	sgn-U213371	2OG-Fe(II) oxygenase family similar to IDS3 [Hordeum vulgare]
1	14.11	4.70	3.01	sgn-U213372	2OG-Fe(II) oxygenase family similar to IDS3 [Hordeum vulgare]
1	134.63	51.98	3.79	sgn-U215281	2OG-Fe(II) oxygenase family similar to IDS3 [Hordeum vulgare]
1	4.39	16.96	10.86	sgn-U222641	cytochrome p450 family flavonoid 3',5'-hydroxylase
1	36.64	4.78	10.13	sgn-U215219	cytochrome P450 75A5 / flavonoid 3'-monooxygenase / flavonoid 3'-hydroxylase (F3'H) (F3'5'H)
1	4.64	1.59	1.32	sgn-U219109	cytochrome P450 75A5 / flavonoid 3'-monooxygenase / flavonoid 3'-hydroxylase (F3'H) (F3'5'H)

Flowering-time and photosensory-related transcripts

zt0	zt8	zt16	zt20	Gene_ID	Annotation
1	0.71	14.22	3.98	sgn-U226837	early flowering 4 (ELF4)
1	43.02	123.24	4.99	sgn-U223492	F-box protein FKF1/ADO3 (FKF1)
1	0.09	1.24	0.54	sgn-U221674	bZIP protein HY5 identical to HY5 protein[Arabidopsis thaliana]
1	438.01	536.53	33.21	sgn-U214381	gigantea protein -related strong similarity[Arabidopsis thaliana] (GI)
1	4.27	43.86	12.10	sgn-U218528	gigantea protein -related strong similarity [Arabidopsis thaliana] (GI)
1	0.04	0.11	0.03	sgn-U237511	LHY
1	0.32	0.17	0.01	sgn-U225455	CONSTANS-LIKE 1 (COL1)
1	0.10	0.16	0.26	sgn-U222883	similar to phytochrome A supressor spa1 (GI:4809171) [Arabidopsis thaliana]
1	0.25	0.38	0.61	sgn-U216241	identical to COP1 regulatory protein/FUSCA protein FUS1
1	40.68	37.20	3.88	sgn-U216348	APRR7 (APRR1/TOC1 family) identical to pseudo-response regulator 7 [Arabidopsis thaliana]
1	3.25	1.47	1.01	sgn-U237464	photoregulatory zinc-finger protein COP1
1	3.90	0.83	1.22	sgn-U214668	expressed protein COP1-interacting protein CIP8, Arabidopsis thaliana
1	0.83	1.03	0.89	sgn-U226667	ZTL/LKP1/ADO1, AtFBX2b E3 ubiquitin ligase SCF complex F-box subunit; identical to clock-associated PAS protein
1	0.81	1.56	1.19	sgn-U218780	early flowering 3 [Mesembryanthemum crystallinum] (EF3)
1	2.06	1.62	0.90	sgn-U225214	early flowering 3 [Mesembryanthemum crystallinum] (EF3)
1	4.25	1.51	0.88	sgn-U216278	nonphototropic hypocotyl 1 (NPH1)
1	0.21	0.13	0.14	16M22AY547	early light-induced protein (ELIP)
1	0.27	0.58	0.88	sgn-U213895	early light-induced protein (ELIP)
1	0.34	0.48	0.31	sgn-U225151	type II CPD photolyase PHR1 (PHR1)
1	0.32	1.05	0.73	sgn-U214962	photolyase/blue-light receptor (PHR2)
1	5.59	0.99	1.73	sgn-U214740	putative phytochrome A signal transduction 1 (PAT1)

Figure legends

Figure 1. Summary of the tomato genes with light-regulated expression pattern.
The light-regulated 1372 genes were clustered in four phase groups of peak expression time. 303 genes shown an expression peak in the dawn (ZT0), 546 in the middle of the light phase (ZT8), 202 near dusk (ZT16) and 321 in the night (ZT20).

Figure 2. The impact of the light response on different categories of genes based on Gene Ontology.
The percentages of responsive genes in each class are shown. (A) Classification by cellular compartment. (B) Classification by molecular function. Cross-hatched bars: ZT0. Grey bars: ZT8. White bars: ZT16. Black bars: ZT20. See text for details.

Figure 3. Comparison of different expression patterns.
The 1732 photoregulated genes were clustered. 13 representative patterns, each with an idealized graph representing patterns of expression, are shown. Open and closed bars along the horizontal axis represent light and dark periods, respectively; these are measured in hours from dawn (Zeitgeber Time [ZT]).For the clusters, black represents expression similar to the dawn, ZT0, green represents a down-regulation and red an up-regulation of expression with respect to dawn. See text for details.

Figure 4. Pearson's correlations between gene expression levels determined by qRT-PCR and oligonucleotide microarray for cryptochrome and phytochrome genes assessed in this study.

Figure 5. Abundance of the mRNAs of Cryptochrome and Phytochrome genes analyzed by RT-PCR in wild-type (Wt) tomato plants grown in LD conditions.
Results are presented as a proportion of the highest value after normalization with respect to β-actin expression levels. Open and closed bars along the horizontal axis represent light and dark periods, respectively; these are measured in hours from dawn (zeitgeber Time [ZT]). Each experiment was done at least twice with similar results.

Figure 6. Abundance of the mRNAs of Cryptochrome and Phytochrome genes analyzed by RT-PCR in wild-type (Wt) tomato plants grown in LD conditions and transferred to LL.
Results are presented as a proportion of the highest value after normalization with respect to β-actin expression levels. Open and hatched bars along the horizontal axis represent light and subjective night periods, respectively; these are measured in hours from dawn (zeitgeber Time [ZT]). Each experiment was done at least twice with similar results.

Figure 7. Effect of *CRY1a* mutations and *CRY2* overexpression on light induced expression of tomato cryptochrome genes.
Wild-type (Wt), CRY1a deficient mutant (*cry1a*) and CRY2 overexpressor (*CRY2-OX*) tomato plants were grown under LD conditions. The abundance of the mRNAs of Cryptochrome genes were measured by RT-PCR. Results are presented as a proportion of the highest value after normalization with respect to β-actin expression levels. Open and closed bars along the horizontal axis represent light and dark periods, respectively; these are measured in hours from dawn (zeitgeber Time [ZT]). Each experiment was done at least twice with similar results.

Figure 8. Effect of *CRY1a* mutations and *CRY2* overexpression on light induced expression of tomato phytochrome genes.
Wild-type (Wt), CRY1a deficient mutant (*cry1a*) and CRY2 overexpressor (*CRY2-OX*) tomato plants were grown under LD conditions. The abundance of the mRNAs of phytochrome genes were measured by RT-PCR. Results are presented as a proportion of the highest value after normalization with respect to β-actin expression levels. Open and closed bars along the horizontal axis represent light and dark periods, respectively; these are measured in hours from dawn (zeitgeber Time [ZT]). Each experiment was done at least twice with similar results.

Figure 9. Effect of *CRY1a* mutations and *CRY2* overexpression on light induced expression of tomato cryptochrome genes in LL.
Wild-type (Wt), CRY1a deficient mutant (*cry1a*) and CRY2 overexpressor (*CRY2-OX*) tomato plants were grown under LD cycles and transferred to LL. The abundance of the mRNAs of Cryptochrome genes were measured by RT-PCR. Results are presented as a proportion of the highest value after normalization with respect to β-actin expression levels. Open and closed bars along the horizontal axis represent light and dark periods, respectively; these are measured in hours from dawn (zeitgeber Time [ZT]). Each experiment was done at least twice with similar results.

Figure 10. Effect of *CRY1a* mutations and *CRY2* overexpression on light induced expression of tomato phytochrome genes in LL.
Wild-type (Wt), CRY1a deficient mutant (*cry1a*) and CRY2 overxpressing (*CRY2-OX*) tomato plants were grown under LD cycles and transferred to LL. The abundance of the mRNAs of phytochrome genes were measured by RT-PCR. Results are presented as a proportion of the highest value after normalization with respect to β-actin expression levels. Open and closed bars along the horizontal axis represent light and dark periods, respectively; these are measured in hours from dawn (zeitgeber Time [ZT]). Each experiment was done at least twice with similar results.

Figure 11. Effect of *CRY1a* mutations and *CRY2* overexpression on light induced expression of tomato *GI* and *CAB4* genes.
Wild-type (Wt), CRY1a deficient mutant (*cry1a*) and CRY2 overexpressor (*CRY2-OX*) tomato plants were grown under LD conditions. The abundance of the mRNAs of *GI* and *CAB4* genes were measured by RT-PCR. Results are presented as a proportion of the highest value after normalization with respect to β-actin expression levels. Open and closed bars along the horizontal axis represent light and dark periods, respectively; these are measured in hours from dawn (zeitgeber Time [ZT]). Each experiment was done at least twice with similar results.

Figure 12. Effect of *CRY1a* mutations and *CRY2* overexpression on light induced expression of tomato *GI* and *CAB4* genes in LL.
Wild-type (Wt), CRY1a deficient mutant (*cry1a*) and CRY2 overexpressor (*CRY2-OX*) tomato plants were grown under LD cycles, and transferred to LL. The abundance of the mRNAs of *GI* and *CAB4* genes were measured by RT-PCR. Results are presented as a proportion of the highest value after normalization with respect to β-actin expression levels. Open and closed bars along the horizontal axis represent light and dark periods, respectively; these are measured in hours from dawn (zeitgeber Time [ZT]). Each experiment was done at least twice with similar results.

Figure 13. A model of genetic interactions among tomato CRY1a and CRY2 proteins and tomato photoreceprtor, *CAB4* and *GI* genes.
The arrows represent a stimulatory effect, and the lines terminated with a bar represent an inhibitory effect. Positive and negative effects mediated by circadian machinery are represented by the clock symbol.

Figures

Figure 1

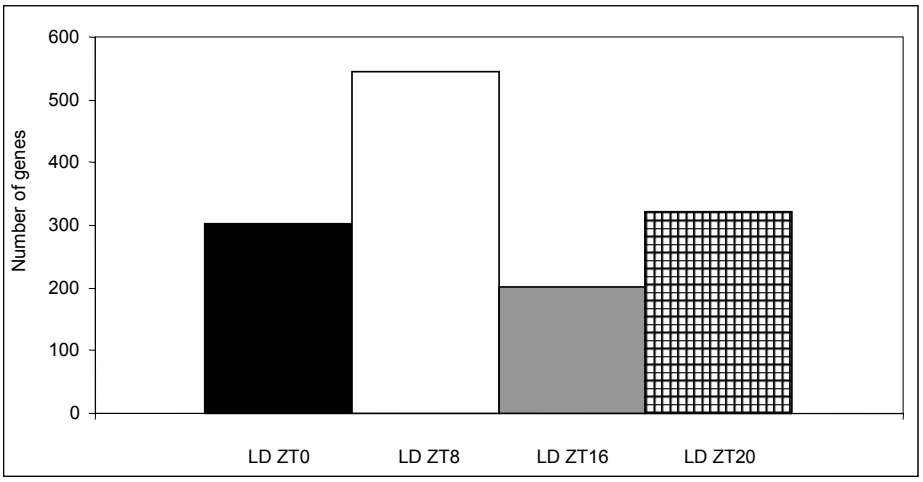

Figure 2

A

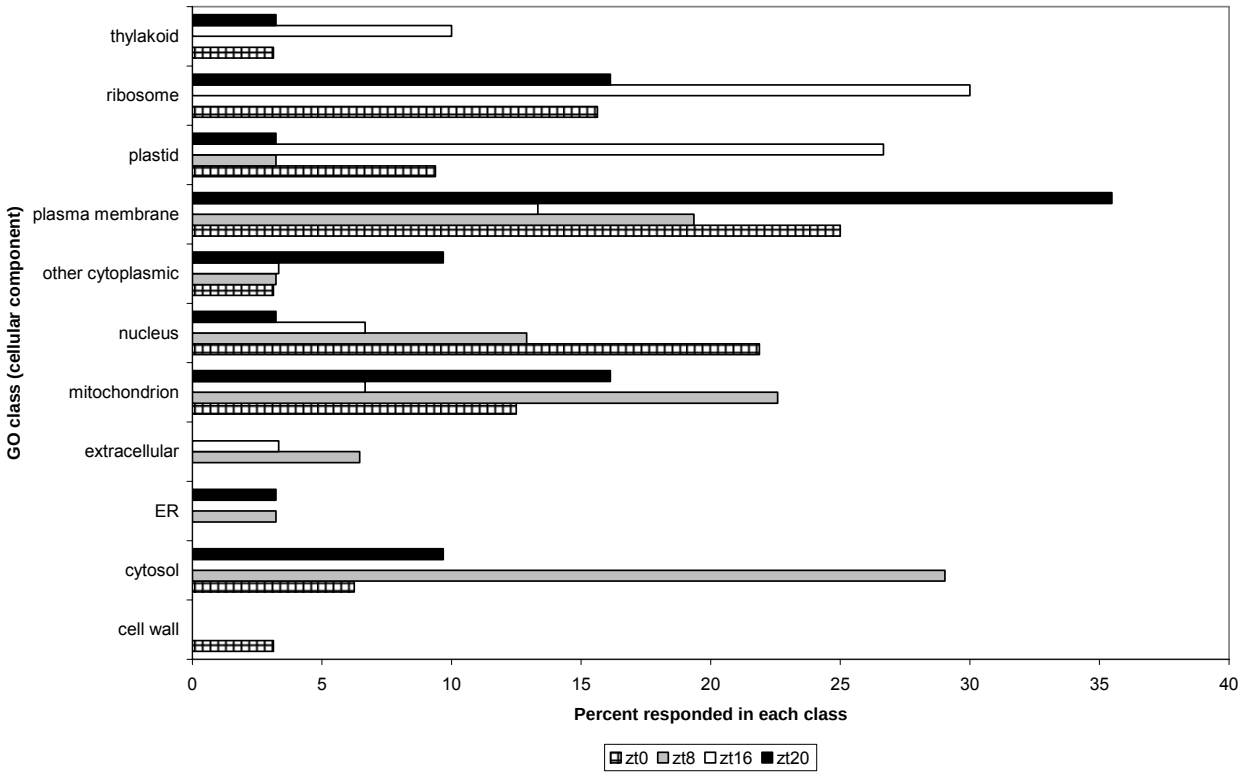
thylakoid
ribosome
plastid
plasma membrane
other cytoplasmic
nucleus
mitochondrion
extracellular
ER
cytosol
cell wall
GO class (cellular component)
0
5
10
15
20
25
30
35
40
Percent responded in each class
zt0 zt8 zt16 zt20

B

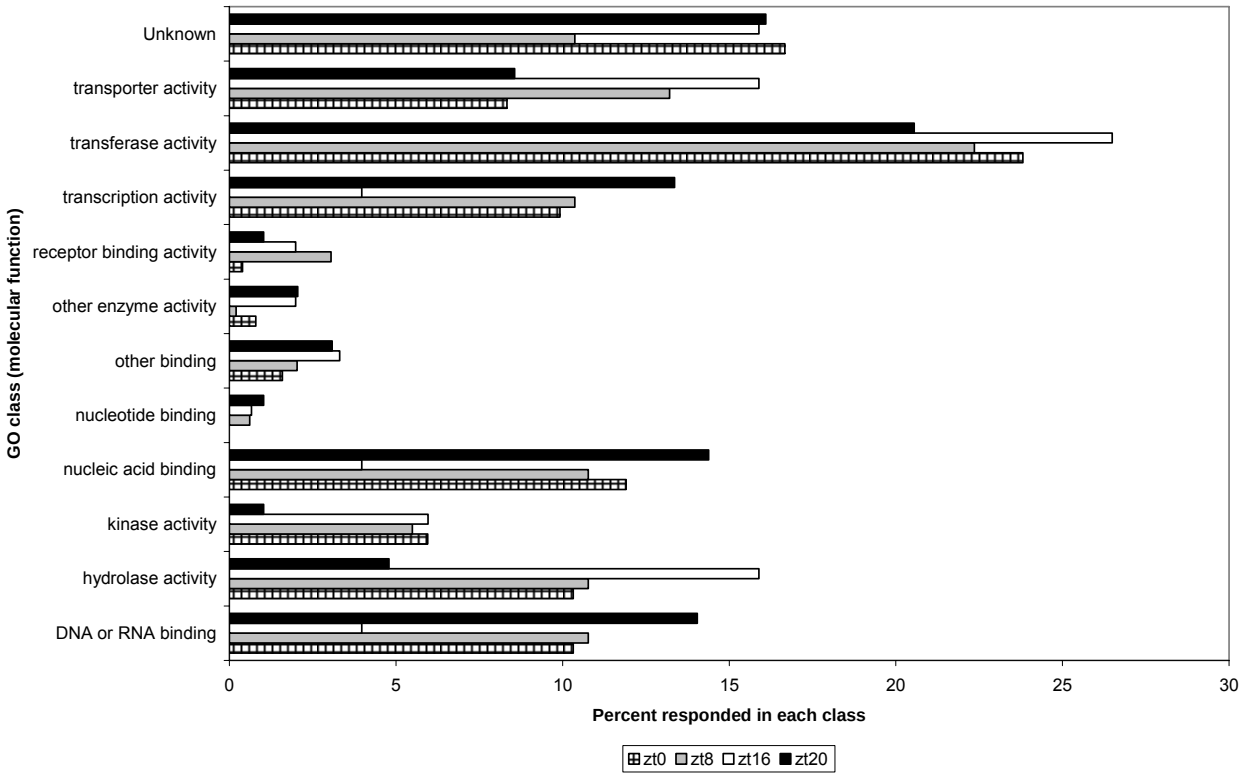
Unknown
transporter activity
transferase activity
transcription activity
receptor binding activity
other enzyme activity
other binding
nucleotide binding
nucleic acid binding
kinase activity
hydrolase activity
DNA or RNA binding
GO class (molecular function)
0
5
10
15
20
25
30
Percent responded in each class
zt0 zt8 zt16 zt20

Figure 3

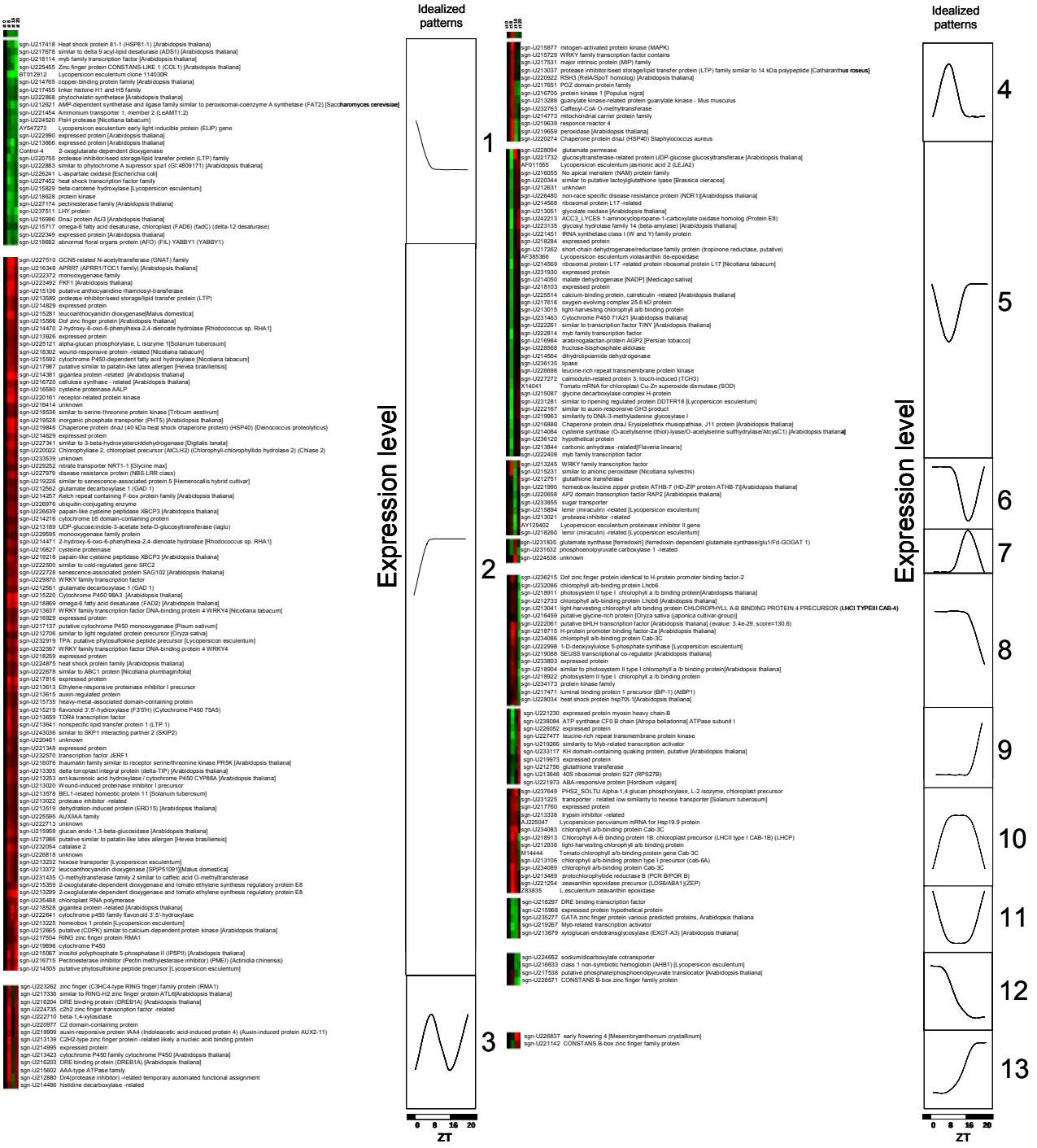
Idealized patterns
Expression level
ZT
0 8 16 20
1
2
3
Idealized patterns
Expression level
ZT
0 8 16 20
4
5
6
7
8
9
10
11
12
13

Figure 4

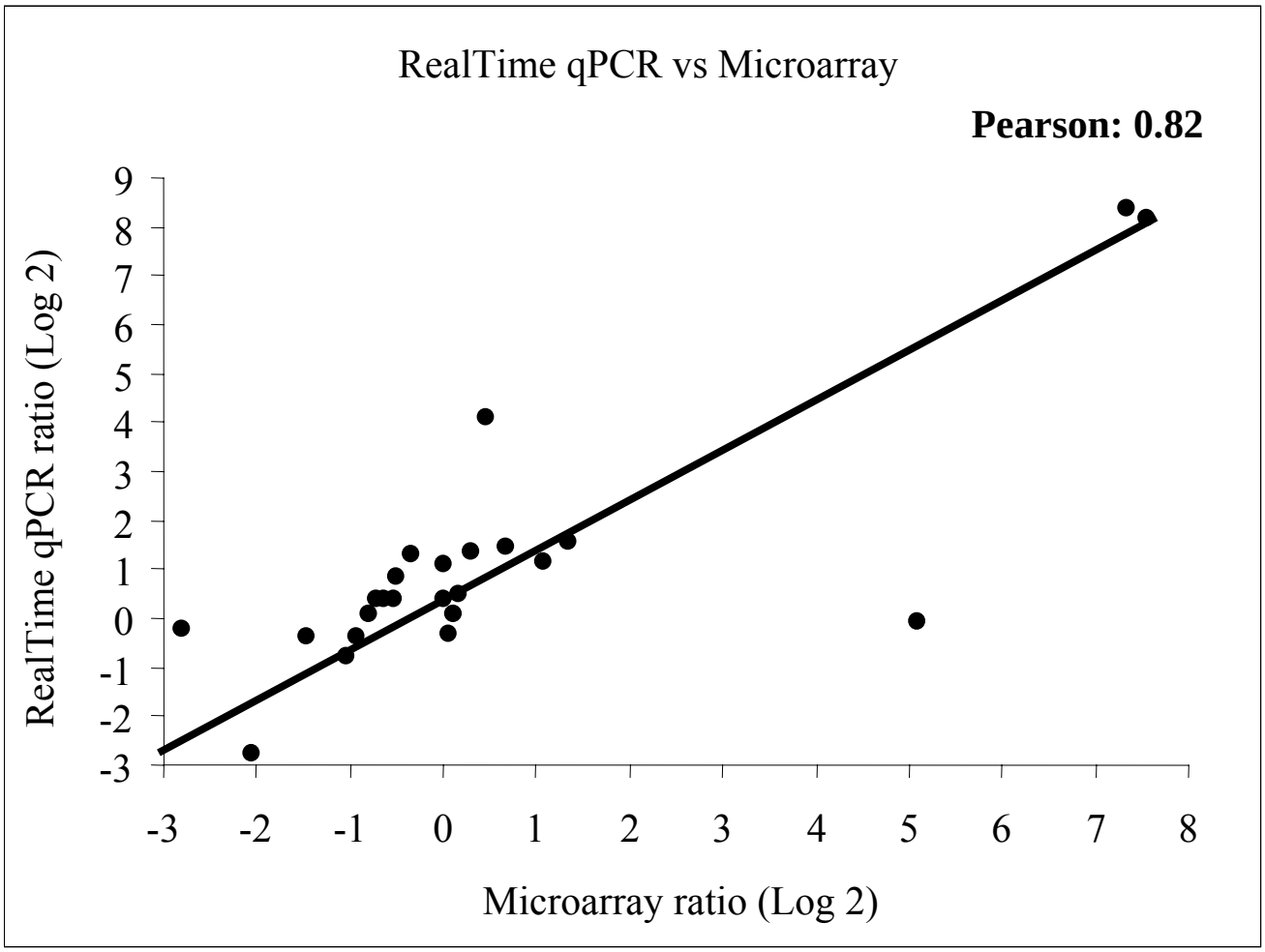
RealTime qPCR vs Microarray
Pearson: 0.82
RealTime qPCR ratio (Log 2)
Microarray ratio (Log 2)
9
8
7
6
5
4
3
2
1
0
-1
-2
-3
-3
-2
-1
0
1
2
3
4
5
6
7
8

Figure 5

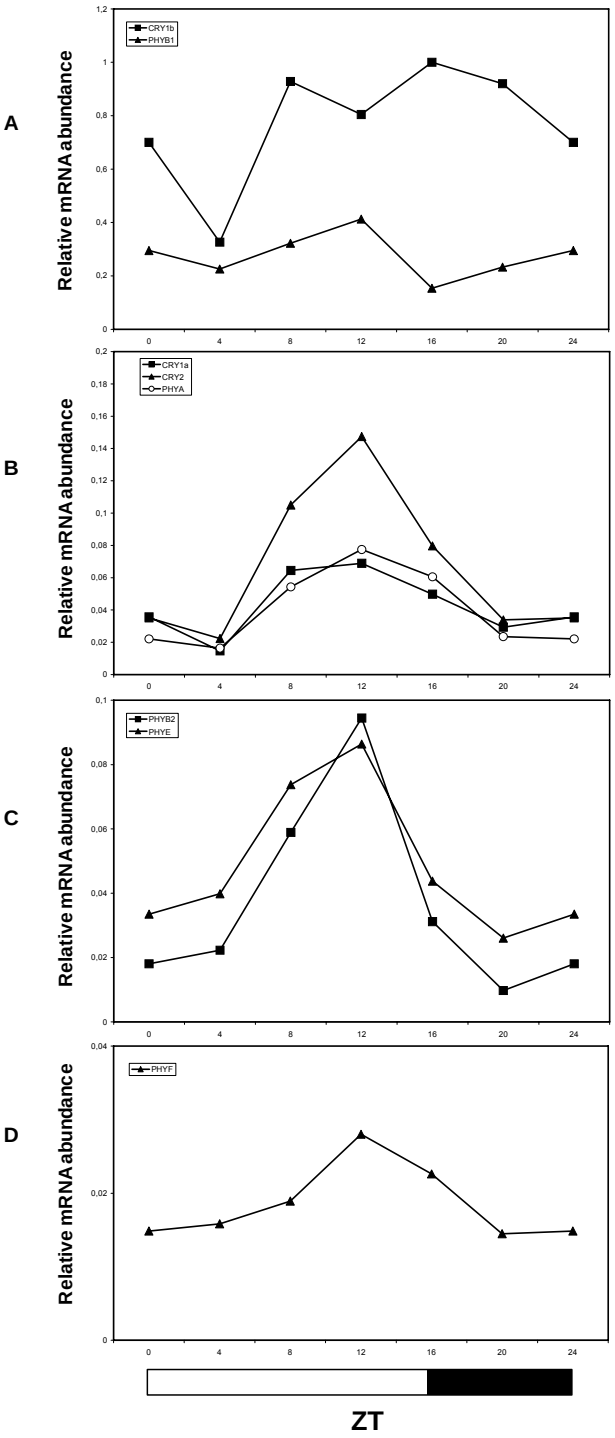
A
CRY1b
PHYB1
Relative mRNA abundance
B
CRY1a
CRY2
PHYA
Relative mRNA abundance
C
PHYB2
PHYE
Relative mRNA abundance
D
PHYF
Relative mRNA abundance
ZT

Figure 6

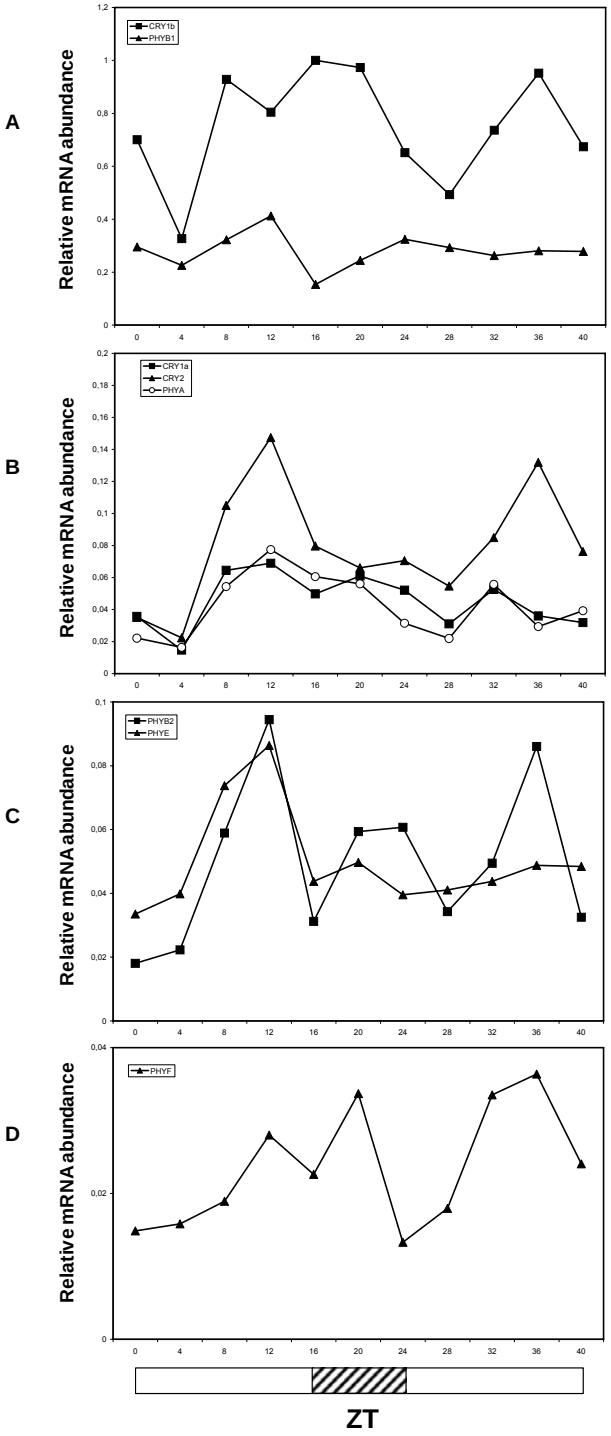
A
CRY1b
PHYB1
Relative mRNA abundance
B
CRY1a
CRY2
PHYA
Relative mRNA abundance
C
PHYB2
PHYE
Relative mRNA abundance
D
PHYF
Relative mRNA abundance
ZT

Figure 7

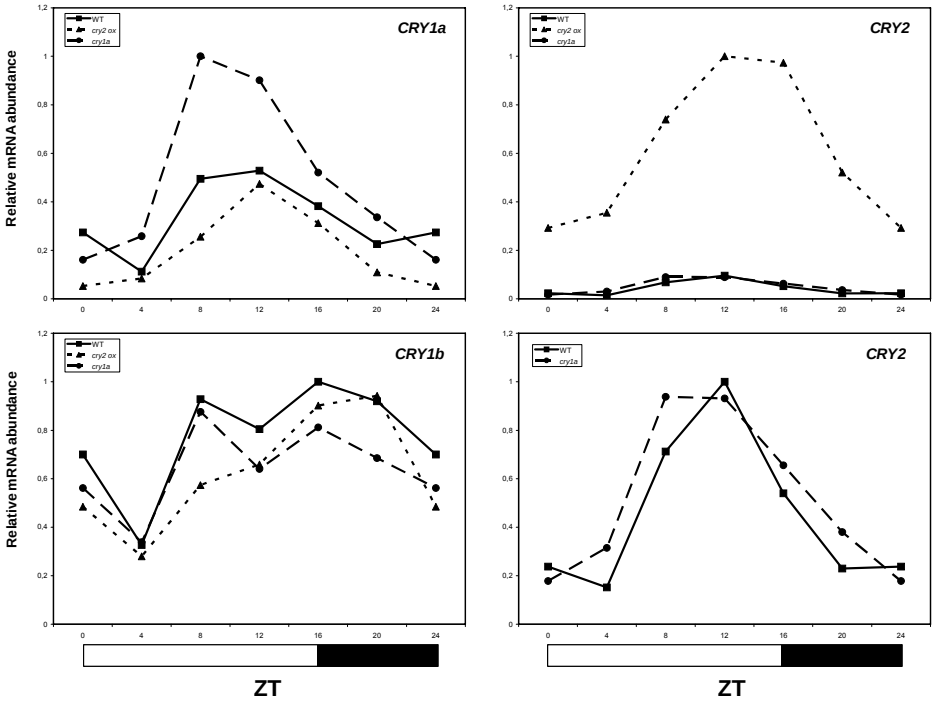

Figure 8

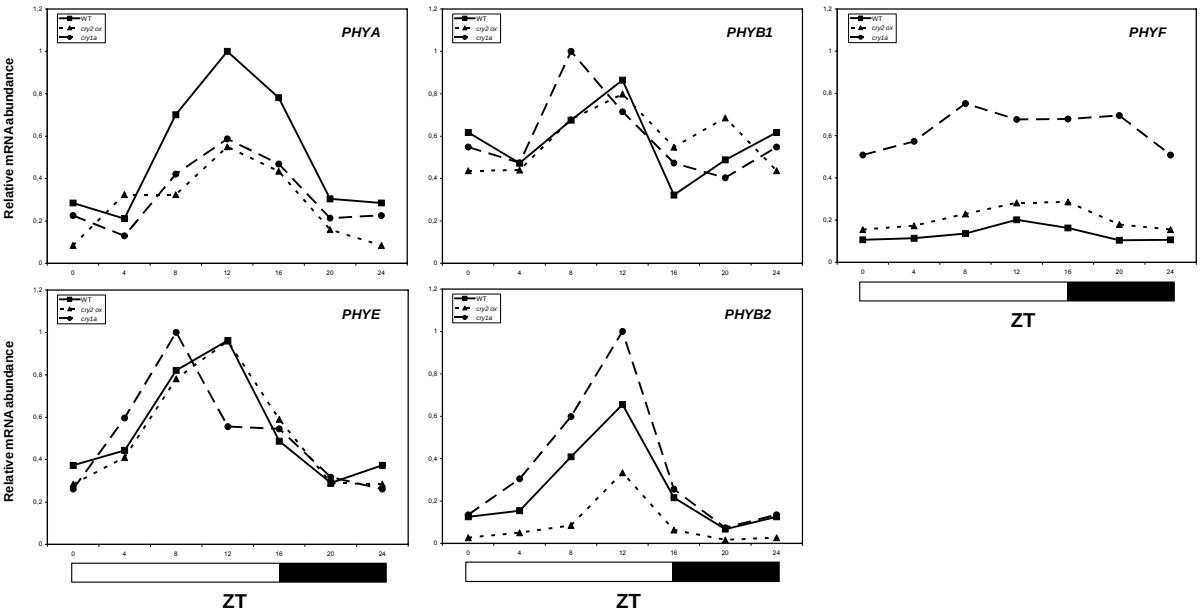

Figure 9

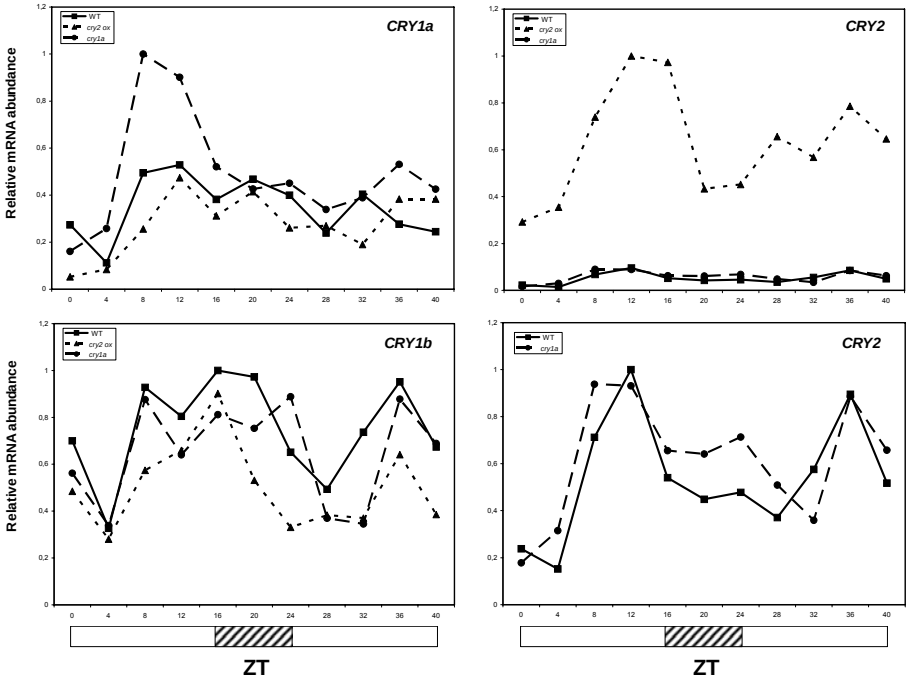

Figure 10

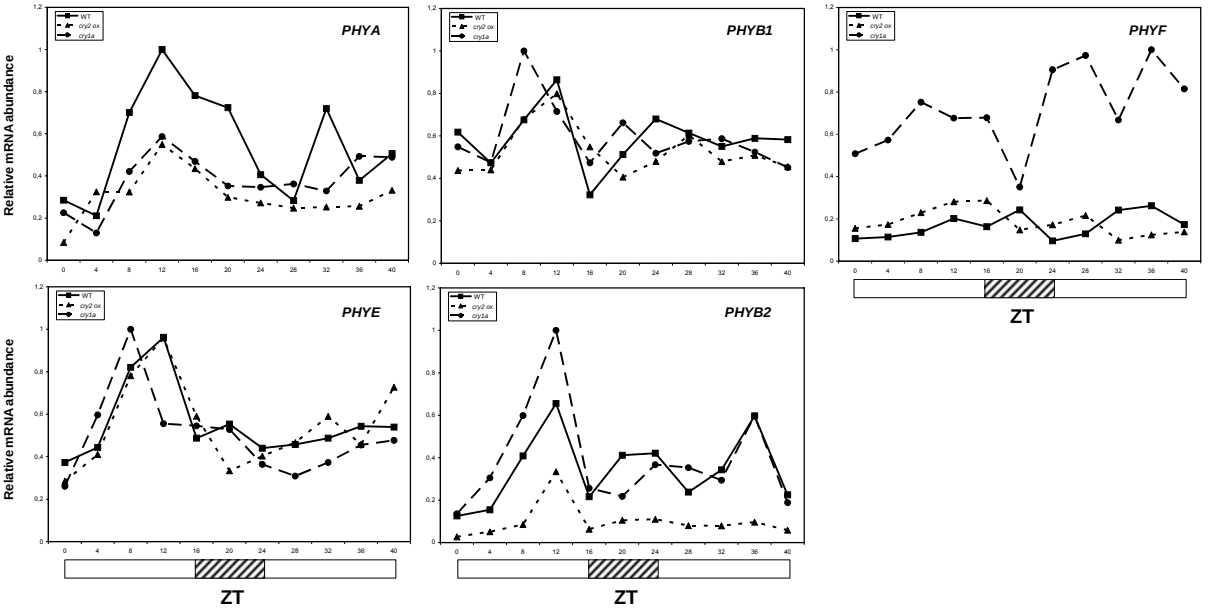

Figure 11

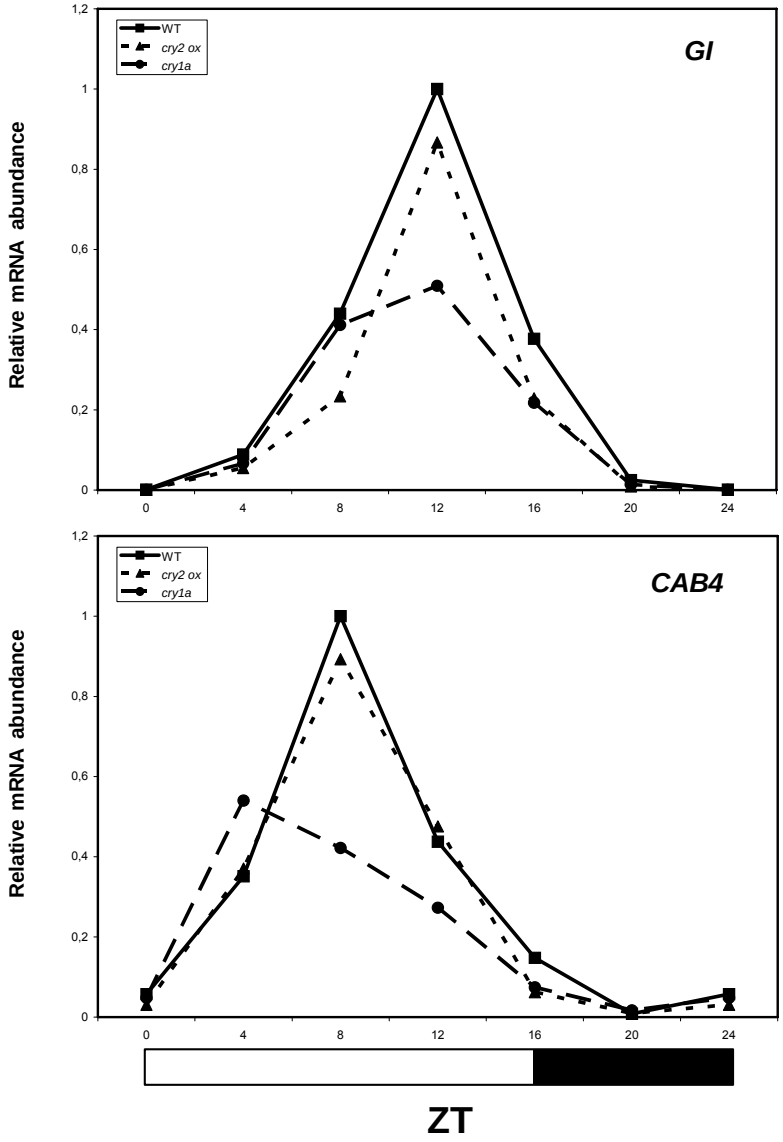
WT
cry2 ox
cry1a
GI
Relative mRNA abundance
1,2
1
0,8
0,6
0,4
0,2
0
0
4
8
12
16
20
24
WT
cry2 ox
cry1a
CAB4
Relative mRNA abundance
ZT

Figure 12

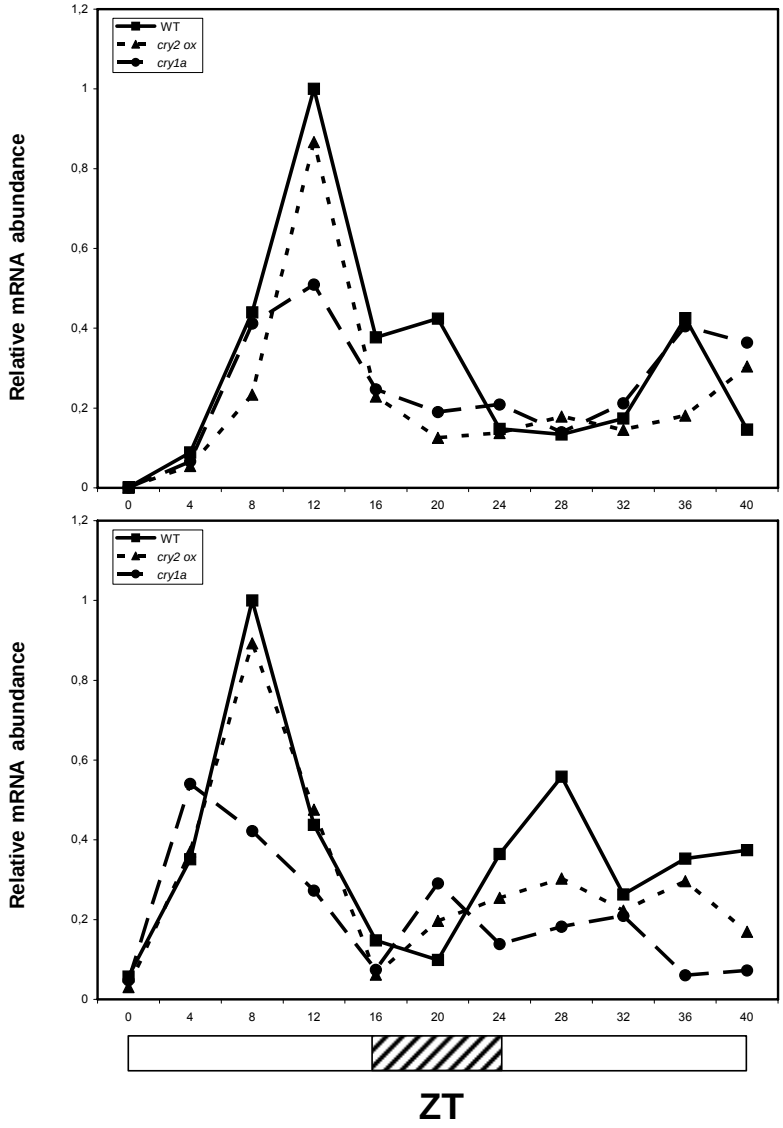
WT
cry2 ox
cry1a
Relative mRNA abundance
1,2
1
0,8
0,6
0,4
0,2
0
0
4
8
12
16
20
24
28
32
36
40
WT
cry2 ox
cry1a
Relative mRNA abundance
ZT

Figure 13

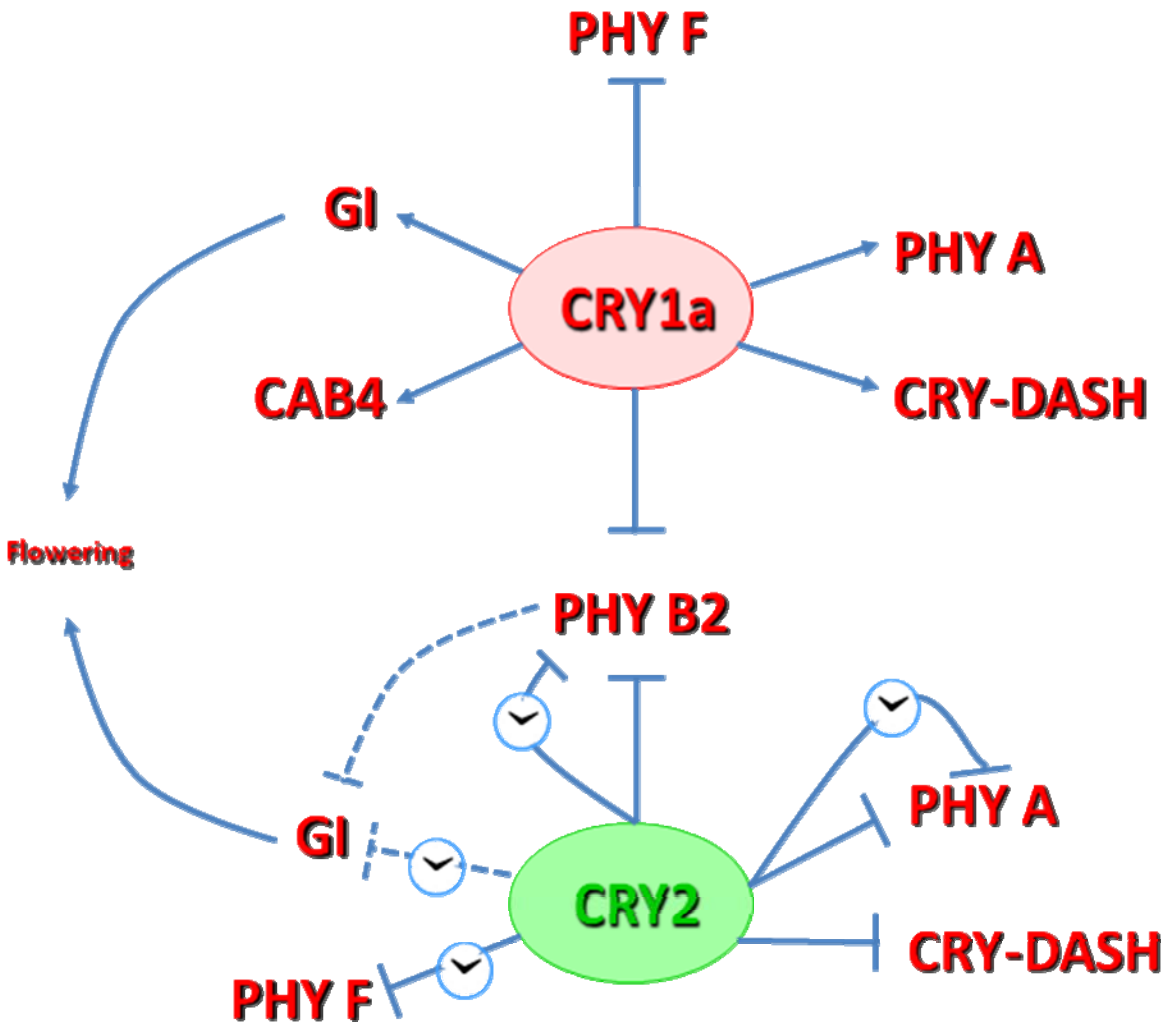
PHY F
GI
PHY A
CRY1a
CAB4
CRY-DASH
Flowering
PHY B2
GI
PHY A
CRY2
CRY-DASH
PHY F

3.7 Microarray Analysis of circadian-regulated genes in tomato leaves.

Plants respond to day/night cycling in a number of physiological ways. At mRNA level, the expression of some genes changes during the 24-hr period (Schaffer et al., 2001). To identify novel genes regulated in this way, we have used microarrays containing 12736 tomato probes, representing an estimated 12008 unique genes, to determine gene expression levels at 8-hr intervals throughout the day. 1373 genes showed a diurnal expression pattern (see attached paper: "Analysis of temporal rhythmic oscillation of tomato mRNAs: cryptochromes can alterate transcription fluctuations of photoreceptor and circadian regulated genes"). To identified genes controlled by a circadian clock, we have transferred plants that had been trained in 16-hr-light/8-hr-dark cycles (long day, LD) to continuous light (LL) and genes expression was monitored for additional 40 h at 8h intervals. Target RNAs were extracted from ZT0 (presumptive dawn), ZT8 (eight hours after dawn), ZT16 (presumptive dusk) grown in LD conditions, and from ZT20 (four hours after transferring in LL conditions), ZT24 (eight hours after transferring in LL conditions), ZT32 (sixteen hours after transferring in LL conditions), and ZT40 (twenty-four hours after transferring in LL conditions). These comparisons have comprehended seven experimental points taking ZT0 as a common reference: ZT8 vs. ZT0, ZT8 vs. ZT0, ZT16 vs. ZT0, ZT20 vs. ZT0, ZT24 vs. ZT0, ZT32 vs. ZT0, and ZT40 vs. ZT0 (fig. 18).

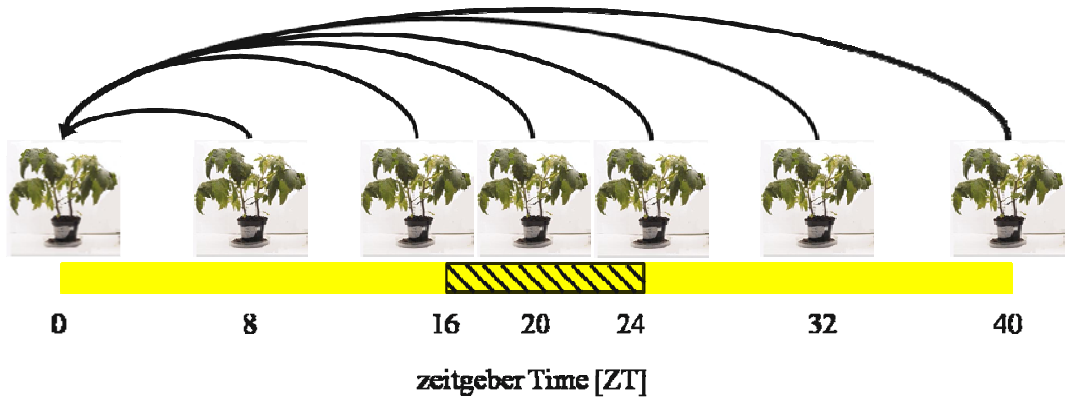

Figure 18: Comparating profiling by oligoarray. The gene expression of tomato leaves harvested for 40 hours at 8h intervals has been analyzed. These comparisons have comprehended seven experimental points taking ZT0 as a common reference: ZT8 vs. ZT0, ZT8 vs. ZT0, ZT16 vs. ZT0, ZT20 vs. ZT0, ZT24 vs. ZT0, ZT32 vs. ZT0, and ZT40 vs. ZT0. Please see text for details.

Raw hybridization signals were filtered by imposing a minimal signal/noise ratio of 2.0 and flagging the non-passed spots. In order to obtain a homogeneous dataset for all hybridized slides we have filtered microarray data imposing good quality spots to be present in at least three out of four hybridized slides (two dye-swap and two biological replicas, respectively) for each experimental point. According to this criterion of 1372 photoregulated genes in LD 1172 genes have passed the quality filters also in LL grown conditions.

To evaluate similar regulations and interactions among different genes and to identify possible gene regulation by circadian clock, we have arranged mathematically this group of genes by cluster analysis according to similarity of gene expression (Eisen et al., 1998) (fig. 19).

In figure 19 are shown four patterns representing genes analyzed in accordance with a possible circadian regulation, each with a idealized patterns of expression. Of the 1172 clustered genes, 20 show a significant peak of expression at ZT24 (24 hours after the dawn presumptive ZT0) (cluster I), 17 genes are more expressed 24 hours after midday (ZT32) (cluster II), 17 show higher transcript levels at ZT40 (24 hours after presumptive dusk ZT16) (cluster III, fig.), and 3 genes are more represented in ZT20 (24 hours after presumptive night) (Cluster IV).

Then, in cluster I were represented genes with an expression peak at ZT0 and showing a oscillation of gene expression also after 24-hr in LL conditions. Of them, mostly have been involved in light signaling and flowering as the Suppressor of Phytochrome A (SPA1) , the Early Light Inducible (ELIP), and a signal transducer of phototropic response genes (Ledger et al., 2001; Ishikawa et al., 2006; Laubinger et al., 2006, Bruno and Wetzel, 2004), three putative MYB-related transcription factor, putative transcription factors (TFs) transcripts of several families, as DRE, bZIP, and BHLH, and finally two transcripts of phenylpropanoids and vitamin C pathway (tab. 1.).

Of the genes peaked at ZT8, 17 genes maintain high transcript levels also after 24 hours in LL conditions. Two flavonoid genes were regrouped in this cluster, with a phenylpropanoid gene, and different TFs (tab. 1).

Of the genes showing a expression peak in the dusk, a flowering-time gene have been found (ELF4) show an expression pattern strictly light-regulated in a

circadian way. In fact, this gene present a recurrence of transcript level alteration 24-hr after the dusk, like as a gene coding phytochrome A signal transduction 1 (PAT1) (tab. 1).

Finally, we have found only three transcripts coding for two TFs and one hypothetical protein up-regulated at night and showing high transcript levels also after 24-hr in LL conditions (tab. 1).

Clearly, the proportion of genes controlled by circadian clock detected in this study it is probably an underestimate of effective number of such genes in tomato. Therefore, our analysis will need additional insights that are at present in progress.

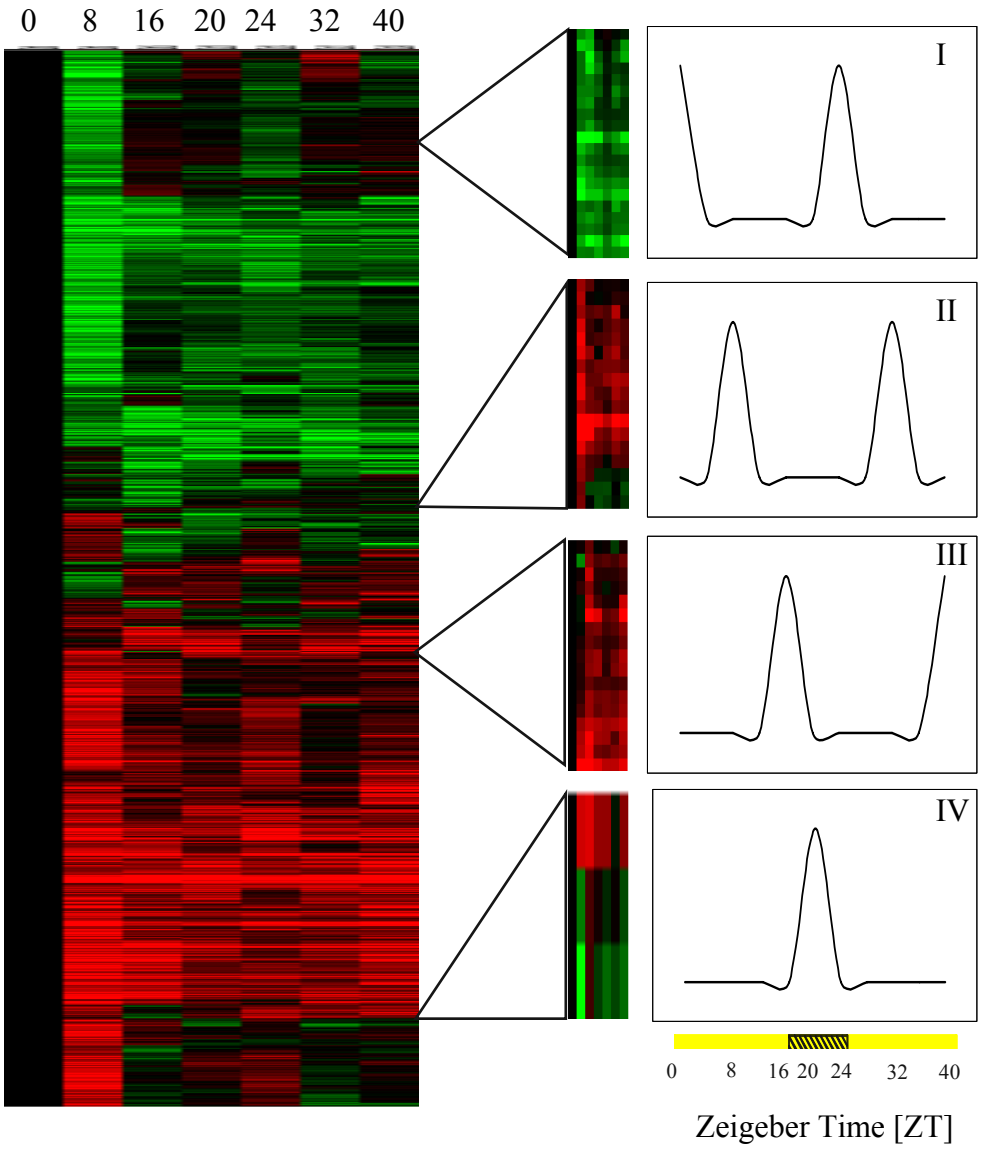

Figure 19: Comparison of different expression patterns.

The 1172 genes that have passed the quality filters also in LL grown conditions photoregulated genes were clustered. 4 representative patterns, each with an idealized graph representing patterns of expression, are shown. Open and closed bars along the horizontal axis represent light and presumptive dark periods, respectively; these are measured in hours from dawn (Zeitgeber Time [ZT]).For the clusters, black represents expression similar to the dawn, ZT0, green represents a down-regulation and red an up-regulation of expression with respect to dawn. See text for details.

Cluster I

zt0	zt8	zt16	zt20	zt24	zt32	zt40	Gene_ID	Annotation
1.00	0.21	0.13	1.01	1.28	0.89	0.71	AY547273	early light inducible protein (ELIP)
1.00	0.08	0.10	0.70	1.10	0.55	0.16	sgn-U217418	heat shock protein 81-1
1.00	0.27	0.20	0.38	0.79	0.36	0.51	sgn-U219607	hypothetical protein predicted proteins [Arabidopsis thaliana]
1.00	0.27	0.05	0.33	0.78	0.32	0.12	sgn-U231437	phototropic response protein putative [Arabidopsis thaliana]
1.00	0.22	0.22	0.31	0.73	0.20	0.40	sgn-U222868	phytochelatin synthetase
1.00	0.27	0.07	0.23	0.71	0.52	0.60	sgn-U218114	myb family transcription factor
1.00	0.20	0.16	0.55	0.69	0.30	0.56	sgn-U217642	DNA binding protein MybSt1
1.00	0.30	0.28	0.59	0.63	0.60	0.55	sgn-U230487	phenylalanine ammonia-lyase (PAL2)
1.00	0.27	0.14	0.35	0.57	0.47	0.48	sgn-U213443	myo-inositol 1-phosphate synthase -related
1.00	0.10	0.18	0.31	0.54	0.25	0.20	sgn-U216986	DnaJ protein AtJ3
1.00	0.17	0.31	0.38	0.52	0.47	0.42	sgn-U218166	protein kinase -related
1.00	0.25	0.31	0.23	0.50	0.13	0.28	sgn-U218297	DRE binding transcription factor putative
1.00	0.27	0.23	0.29	0.45	0.25	0.23	sgn-U225911	bZIP transcription factor -related
1.00	0.10	0.16	0.30	0.40	0.33	0.38	sgn-U222883	phytochrome A supressor spa1
1.00	0.21	0.15	0.22	0.40	0.28	0.27	sgn-U226681	bHLH protein family
1.00	0.22	0.23	0.13	0.25	0.21	0.17	sgn-U215968	hypothetical protein [Arabidopsis thaliana]
1.00	0.03	0.01	0.05	0.25	0.15	0.06	BT012912	Lycopersicon esculentum clone 114030R
1.00	0.05	0.14	0.18	0.24	0.18	0.20	sgn-U226241	L-aspartate oxidase family similar to L-aspartate oxidase
1.00	0.13	0.03	0.07	0.23	0.09	0.04	sgn-U212621	peroxisomal-coenzyme A synthetase (FAT2)
1.00	0.02	0.09	0.09	0.18	0.09	0.09	sgn-U218279	myb family transcription factor

Cluster II

zt0	zt8	zt16	zt20	zt24	zt32	zt40	Gene_ID	Annotation
1.00	14.39	2.12	1.26	2.50	3.90	2.70	sgn-U218715	Dof zinc finger protein identical to H-protein promoter binding factor-2a
1.00	6.74	2.98	1.09	1.23	1.27	1.11	sgn-U222061	bHLH protein family
1.00	6.98	2.76	4.05	4.29	4.44	3.29	sgn-U214101	polyamine oxidase
1.00	6.49	2.81	3.47	2.62	9.26	1.31	sgn-U214842	GT-related trihelix DNA-binding protein
1.00	20.10	1.97	2.49	2.88	4.75	2.70	sgn-U215935	NADPH:quinone oxidoreductase (NQR)
1.00	8.82	1.16	0.90	1.15	1.73	1.54	sgn-U217384	cytochrome p450 family
1.00	3.86	0.45	0.43	0.41	1.00	0.40	sgn-U217651	POZ domain protein family
1.00	5.61	2.60	0.62	0.63	0.79	0.65	sgn-U222803	myb family transcription factor
1.00	17.99	4.32	2.59	2.22	7.44	4.65	sgn-U234089	
1.00	8.74	4.06	3.56	1.67	4.59	3.80	sgn-U213022	protease inhibitor -related
1.00	16.07	6.11	0.94	4.51	7.82	2.44	sgn-U213305	delta tonoplast integral protein (delta-TIP)
1.00	60.38	37.55	4.97	3.42	8.98	6.73	sgn-U215136	UDP-glucoronosyl and UDP-glucosyl transferase
1.00	134.63	51.98	20.00	10.04	47.04	19.78	sgn-U215281	leucoanthocyanidin dioxygenase (ANS)
1.00	17.49	3.40	3.49	6.05	8.95	7.66	sgn-U221348	expressed protein
1.00	17.07	6.31	3.63	2.55	5.10	2.98	sgn-U231435	caffeic acid O-methyltransferase
1.00	6.23	2.46	2.03	0.90	2.77	2.62	AF112368	catalase 2
1.00	4.48	0.95	0.40	0.51	0.88	0.54	sgn-U213319	Ser/Thr protein kinase [Zea mays]

Cluster III

zt0	zt8	zt16	zt20	zt24	zt32	zt40	Gene_ID	Annotation
1.00	0.13	7.66	2.95	3.68	2.75	5.00	sgn-U228094	
1.00	0.73	68.08	28.29	3.84	5.49	54.41	sgn-U218045	expressed protein
1.00	1.52	4.66	3.08	1.96	2.22	5.08	sgn-U221281	short-chain dehydrogenase/reductase family protein
1.00	1.22	4.42	0.93	1.20	0.42	1.36	sgn-U221288	nicotianamine synthase 2 [Hordeum vulgare]
1.00	1.65	4.67	2.76	2.90	2.47	3.16	sgn-U221404	1 4-alpha-glucan branching enzyme (starch branching enzyme class II/sbe2-2)
1.00	1.34	20.93	1.86	1.75	1.84	2.54	sgn-U229667	TCP family transcription factor putative
1.00	2.12	6.91	1.65	0.71	1.41	2.08	sgn-U217919	expressed protein
1.00	2.96	10.05	4.42	6.11	5.25	10.40	sgn-U218630	alternative oxidase putative (IMMUTANS)
1.00	2.07	10.24	5.35	6.00	4.66	8.71	sgn-U226043	Aspartate-glutamate racemase family
1.00	0.71	14.22	2.68	1.55	1.50	21.36	sgn-U226837	early flowering 4 (ELF4)
1.00	0.89	5.28	6.21	2.65	3.58	8.03	sgn-U226936	expressed protein
1.00	1.95	6.83	9.79	2.15	4.94	13.80	sgn-U227196	chloroplast division protein FtsZ (FtsZ2-1)
1.00	1.71	7.80	9.91	1.82	6.15	11.62	sgn-U227709	short-chain dehydrogenase/reductase family protein
1.00	12.79	41.68	11.36	10.01	3.27	14.07	sgn-U215096	peptide transporter -related
1.00	15.58	35.57	5.31	4.35	6.87	10.77	sgn-U221426	phytochrome A signal transduction 1 (PAT1)
1.00	9.63	19.14	14.02	10.24	12.48	18.87	sgn-U214629	expressed protein
1.00	333.96	427.39	29.98	16.11	16.65	31.80	sgn-U227510	GCN5-related N-acetyltransferase (GNAT) family

Cluster IV

zt0	zt8	zt16	zt20	zt24	zt32	zt40	Gene_ID	Annotation
1.00	3.07	3.3	2.23	2.22	0.89	2.08	sgn-U217504	zinc finger (C3HC4-type RING finger) family protein (RMA1)
1.00	0.51	1.49	1.11	0.81	1.05	0.67	sgn-U218925	
1.00	0.15	1.43	0.73	0.57	0.69	0.56	sgn-U222408	myb family transcription factor

Table 1: Using TOM2 oligo-arrays, 57 genes with an expression pattern consistent with a circadian rhythm have been identified and were clustered in 4 representative patterns.

4. DISCUSSIONS

4.1 Comparative profiling of tomato fruits and leaves

We have monitored the fruit at three different ripening stages versus (vs) leaf gene expression profiling in tomato using both cDNA microarray (TOM1, http://bti.cornell.edu/CGEP/CGEP.html) and quantitative real time reverse transcription polymerase chain reaction (RT-qPCR) approaches (see attached paper: Carbone et al., 2005). The extent of transcriptional modulation was confirmed by real time RT-qPCR on selected genes, showing significant levels of regulation during fruit development. Most of the genes involved in energy pathways, hormone responses and protein biosynthesis/degradation are mostly up-regulated in fruits probably correlated to a considerable increase of protein synthesis or turnover during fruit development. Of the fruit up-regulated genes, we have found genes known to play a key role in the biosynthesis of volatile compounds (Schwab et al., 2001). Therefore, the higher transcript levels in the ripening fruits could eventually lead to the synthesis of aroma- and flavor- related compounds in red ripe tomato. We have also detected the up-regulation of genes which is involved in carotenoid and ABA biosynthesis (Giuliano et al., 1993; Isaacson et al., 2002).

To confirm the microarray expression data, we have performed experiments on some differentially expressed genes by microarray experiments. The real time RT-qPCR analysis has widely confirmed the up-regulations found in microarray experiments, suggesting that genes actually up-regulated in all fruit stages vs. leaf could be more than those selected by our criteria.

Besides, in order to better investigate effect of light in tomato fruit development and ripening, comparative profiling RT-qPCR experiments have been carried out to measure the transcript level changes of structural genes of the carotenoid biosynthesis pathway and of genes involved in light signal transduction at different fruit stages. The analysis of genes involved in biosynthesis of carotenoid indicate an up-regulation of the early part of the pathway, leading to the synthesis of the major fruit carotenoid, lycopene, and a downregulation of the later part of the pathway, in agreement with tomato fruit ripening physiology (Giuliano et al.,

1993; Isaacson et al., 2002). Moreover, our results suggest that during tomato fruit development and ripening the transcripts coding for photosensory receptors and light signaling proteins are highly regulated, and that tomato light responsiveness during fruit development may be modulated by these wide fluctuations in transcript abundance (Liu et al., 2004; Giliberto et al., 2005).

4.2 Evaluating strawberry fruit quality traits and selecting improved genotypes by cDNA Microarrays

cDNA microarrays containing ~1800 ESTs were produced and used to characterize fruit quality traits of several strawberry genotypes (*Fragaria x ananassa* Duch.) and reveal differences among genotypes at ripening and post-harvest stages (see attached paper: Carbone et al., 2006). Given its outstanding fruit quality, cultivar (cv.) Queen Elisa was taken as the control genotype in all microarray experiments, and compared with selection (sel.) USB35, cv. Miss, cv. Maya, and cv. Onda. We have found a strong correspondence between the transcription pattern of the reference and test cultivars, with few genes being differentially expressed pathways controlling fruit quality traits. Some of the altered cDNAs encode putative cinnamyl alcohol dehydrogenase (CAD), cinnamoyl CoA reductase (CCR), cellulase (CEL1), galattosidase (beta-GAL1), xylosidase (XYL1) and expansin (EXP) genes, involved in the early steps of lignin biosynthesis and in cell wall structure, respectively. CCR and CAD are involved in early steps of lignin synthesis (Anterola and Lewis, 2002) and are mostly expressed in achenes and vascular tissue of strawberry fruit (Blanco-Portales et al., 2002). Expression of expansin, cellulase and xylosidase genes in strawberry is associated with tissue softening (Civello et al., 1999), and is therefore related to fruit firmness. Interestingly, up-regulation of CCR, EXP4 and CEL1, and down-regulation of CCR, were consistent with the lower firmness of cv. Miss, cv. Onda, cv. Maya and sel. USB35 fruits. Moreover, our results are in agreement with recent results on other genotypes (Salentijn et al., 2003), indicating the major influence of these genes in the control of such an important polygenic trait.

In reference cv. Queen Elisa AAT gene involved in fruit flavor synthesis is up-regulated. The key role of aat in ester production was shown when comparing genotypes with different levels of volatile compound emission. Expression of aat increases during fruit ripening, peaking at full red stage with high levels of transcript (Aharoni et al. 2000). A correlation between the expression of an AAT gene, total AAT activity and the presence of related esters, studied by Proton Transfer Reaction-Mass Spectrometry (PTR-MS), in fruit headspace was found (see attached paper: Carbone et al., 2006).

Microarray data were generally validated by real time RT-qPCR experiments, although the latter method of analysis often magnified differences in gene expression.

All together, our results point out a wide set of candidate genes whose coordinated and differential expression could be related with the variation of fruit firmness, and flavor important quality and quantitative breeding traits.

4.3 Transcriptional characterization of major genes involved in flavonoid biosynthesis in strawberry (*Fragaria x ananassa*)

Real time RT-qPCR experiments were carried out to determine the steady state levels of phenylpropanoid and flavonoid genes in fruits of the reference strawberry genotype Queen Elisa (*Fragaria x ananassa* Duch.) throughout ripening [at early green (G1, 7–10 days after anthesis, daa), intermediate green (G2, 12–14 daa), white (W, ca. 20 daa), turning (T, ca. 25 daa) and ripe red (R, ca. 30 daa) stages] as well as in leaves, petals and roots (see attached paper: Almeida et al., 2007). Remarkable differences in gene expression patterns were found. Phenylpropanoid genes PAL, C4H and 4CL were among the most strongly expressed at all stages. The high transcript levels of these three genes not only meet the demand flavonoid synthesis, but also account for the formation of phenylpropanoid monomers (acids, esters, aldehydes and alcohols) which serve the synthesis of the natural polymer lignin (Anterola and Lewis, 2002) present in vascular tissues and achenes. Transcripts of all members of the CHS family are very strong regulated and peaked at T stage, followed by a decrease in relative transcript abundance at red stage in agreement with the central role of CHS in

flavonoid biosynthesis. A tissue-specific regulation of the expression of the CHS gene family was found: in fruits, CHS1 and CHS2 were consistently more expressed than CHS3 and CHS5; on the other hand, CHS2 and CHS5 were more expressed in petals, while CHS1 and CHS3 transcripts were more abundant in red fruits. CHS are plant polyketide synthases (PKSs) which underwent extensive duplication and evolution events to produce genes with diverse expression patterns and multifunctional enzymes (Helariutta et al., 1996; Durbin et al., 2000). Expression of CHS/PKS members is typically organ-specific and developmentally regulated e.g. in *Petunia*, *Rubus* and *Vitis* (Koes et al., 1990; Wiese et al., 1994; Kumar and Ellis, 2003).

A coordinated up-regulation of flavonoid pathway genes involved in the biosynthesis of anthocyanins was observed at T stage. Transcript abundance of CHI, FHT, DFR, ANS, and FGT either remained constant at T and R stages or slightly increased at R stage, consistent with the metabolite flux demand to maintain high pigment levels in ripe fruits. Only CHI showed a slight down-regulation, in agreement with the pattern of all CHS genes. Finally, FLS, LAR, and ANR genes, involved in the side branches of the flavonoid pathway, have distinct developmental transcription patterns, with a sharp decrease at R stage, which is likely to indicate separate regulation mechanisms by cis-acting factors, in agreement with the decrease of flavonols and flavan-3-ols (Halbwirth et al., 2006). The strongest down-regulation of fls reflects the metabolic competition between flavonols, flavan-3-ols and anthocyanins in the final ripening stages.

Expression levels of all genes were consistently low in leaves, possibly indicating a homeostasis situation. On the other hand, petals and roots showed distinct tissue-specific expression patterns when compared to each other and to fruit red stage. Phenylpropanoid pathway genes PAL, C4H, and 4CL were strongly expressed in petals, consistent with a strong synthesis of phenylpropanoid and flavonoid compounds for pollinator attraction (Dixon and Steele, 1999). Moreover, an up-regulation trend from PAL through 4CL was evident in roots, which is likely to indicate the central role of coumaroyl-CoA in the synthesis of flavonoids but also of lignin precursors (Anterola and Lewis, 2002) in this organ. As for flavonoid pathway genes, their expression pattern in petals clearly

indicated a redirection towards the synthesis of flavonol derivatives: CHI, FHT, and FLS were strongly up-regulated, while DFR and ANS were repressed. The relative strong expression of LAR and ANR should account for the presence of flavan-3-ols, with a prevalence of the latter compounds. A less clear-cut situation was shown in roots: only LAR and ANR genes were clearly up-regulated, with LAR more expressed than ANR.

4.4 Flavonoid content: effect of genotype and environment

Molecular analyses were carried out to characterize the flavonoid pathway in fruits of strawberry élite genotypes. Varietal differences among the strawberry genotypes are observed in Kosar et al. (2004). The levels of phenolic compounds of strawberry fruits are affected from varietal variation, growing site, and degree of ripeness. For this reason, a preliminary screening to determine flavonoid accumulation patterns of about thirty-four different genotypes has been carried out. Then, were selected two genotypes with high anthocyanin content (Camarosa, Candonga), one genotype with high flavan-3-ol + Pas contents (99.163.14), two genotypes with low flavonoid content (Onda, 99.20.1) and QueenElisa (reference genotype). Four of them, Camarosa, Candonga, 99.20.1, and 99.163.14, were sampled in two different grown areas (Northern and Southern location) in order to investigate possible environment influences. Genetic and environmental causes can account for such differences in chemotype. Genetic factors include allelic differences of flavonoid genes (further complicated by the octoploid background), cis-acting regulatory sequences, and transcription factors. Environmental factors as variations in light quality and temperature at different latitudes should be taken into account. In contrast, fruits of several genotypes accumulated low levels of both classes of compounds. In order to get information on the genetic bases underlying the biosynthesis and the accumulation of flavonoids during fruit ripening, we have monitored flavonoid gene expression profiles during fruit development in the selected genotypes. Real time RT-qPCR experiments targeted on flavonoid related genes, showed fine modulations of the transcripts abundance of genes related to flavonoid biosynthesis and fruit quality.

The similar regulation with respect to Queen Elisa (see attached paper: Almeida et al., 2007) was observed among different genotypes of the genes involved in early steps of the flavonoid pathway (CHS, CHI, FHT) is probably related to synthesis of precursors. In fact, our results show that the mRNA levels encoding chs, chi, and fht enzymes in developing strawberries increase in concurrence with the accumulation of anthocyanins but also in the early development steps when proanthocyanidins (Pas) appear to be more synthesized (Halbwirth et al., 2006).

In plants, flavonols have been found to possess a protective role as a UV filter, and they also may function as copigments for anthocyanins in fruit and flowers (Koes et al., 1994; Bohm, 1998). In strawberry, flavonols kaempferol and quercetin are found (Hakkinen and Torronen, 2000). Dihydrokaempferol is also the precursor for dihydroquercitin (F3'H), and flavonol sinthase (FLS) catalyzes the dehydrogenation of these 3-hydroxyflavanones to the corresponding flavonols (Bohm, 1998). At early stages of berry development, flavonols were the major flavonoids, but the levels decreased dramatically during the progress of ripening (Jaakola et al., 2002), which agrees with the results from gene expression analysis (see attached paper: Almeida et al., 2007).

Some differences were observed for the genes involved in the regulation of the key steps that induce anthocyanin and/or flavan-3-ols and Pas synthesis.

The expression of anthocyanin pathway genes (DFR,FGT, and ANS) was specifically up-regulated at the period when anthocyanin accumulation grows most rapidly. The genotypes grown in northern location with high anthocyanin content (Camarosa, Candonga) show higher transcript levels of FGT and DFR at ripe stage, while a up-regulation in the genotype grown in the southern area with higher PAs content (99.163.14) were observed for ANS at turning stage. The results obtained in this study provide additional evidence for the correlation between the expression of structural flavonoid pathway genes and anthocyanin production during fruit development, but induce further investigations especially for role of ANS in PAs and anthocyanins regulation. In fact, its substrate leuconathocyanidin is a precursor to synthesis of anthocyanins such as cyanidine-3-glucoside but also contributes the extension subunits of the PA polymer (Bogs et al., 2005). Recently, the role of ANS have been put into question because the

recombinant enzyme from *Arabidopsis* exhibited primarily fls activity with negligible ans activity (Pourcel et al., 2005). Although, the catalytic activity documented by Wellmann et al. (2006) for ans, that reported for the first time the enzymatic dimerization of catechin monomers, clearly differs from the mode of action proposed for the polymerization of flavonoid in *Arabidopsis* seed coat testa, which relies on a laccase-type enzyme oxidizing epicatechin to the corresponding o-quinone (Pourcel et al., 2005), suggesting a role of ans beyond the oxidation of leucocyanidins.

PAs appear to be synthesized during the first phase of fruit development, and there is a decline in extractable PA after veraison and throughout ripening which is thought to be the result of complexation of the PA polymers with other cellular components (Kennedy et al., 2000, 2001; Downey et al., 2003). Our data show a down-regulation during the development of the principal genes involved in the flavan-3-ols synthesis that can form the unit of the PA polymer (LAR, and ANR). Dramatic differences among genotypes in LAR expression patterns were observed. In particular the gene expression analysis by real time RT-qPCR show higher transcripts levels of LAR gene in the genotype with high flavan-3-ols and PAs content (99.163.14) suggesting a possible key role of this gene in the control of PAs synthesis in strawberry fruit. In grapevine, it appears that both ANR and LAR contribute to PA synthesis in leaves, flowers, and in the skin and seeds of the developing fruit (Bogs et al., 2005). As there are two distinct pathways to the formation of catechin and epicatechin, manipulation of the relative activies of anr and lar may have the potential to modify both the content and composition of PAs in plant tissues (Schijlen et al., 2004).

4.5 Effects of CRY2 overexpression on genome regulation in tomato fruits

Accumulation of lycopene and flavonoids in tomato transgenic CRY2-OX fruits is very interesting considering the nutritional and health benefits of these metabolites (Giliberto et al., 2005). Therefore, in order to identify possible molecular factors related to the role of photoreceptors in the accumulation of fruit carotenoids and flavonoids, we have compared the transcriptional activity of fruit

tissues of two different lines of tomato transgenic CRY2-OX (3C and 8D), and of wild type (Wt) by using TOM2 oligo-arrays.

We have found some differences in the transcription of the two transgenic CRY2OX lines. Indeed we have identified many more genes differentially expressed in CRY2OX-8D vs. Wt with respect to CRY2OX-3C vs. Wt. All these different regulations can be connected with the broad set of biochemical responses associated with the development and followed by transgenic manipulation as already noted by Giliberto et al. (2005).

In tomato transgenic CRY2OX the majority of genes involved in photosynthesis were up-regulated. This could indeed account for the biosynthetic processes correlated to photosynthesis usually driven by light. Moreover, many flavonoid genes are differentially regulated between transgenic lines and Wt, with higher transcripts levels in CRY2OX fruits.

We have observed striking similarities between the tomato gf mutant (Kerr, 1956) and CRY2OX phenotypes. Upon visual inspection, gf as well as CRY2OX fruits show increased pigmentation, resulting in a rusty or dirty red color. The fruit phenotype of gf is due to significant amounts of the chloroplast thylakoid grana along with structures characteristic of tomato chromoplast. The maintenance of chloroplast structures of gf mutant ripe fruit was paralleled on the molecular level by the retention of plastid photosynthetic components that normally decline significantly during ripening like chlorophyll a/b-binding protein (CAB), Photosystem I and II subunit precursor, Photosystem I and II oxygen-evolving system, Photosystem I and II stability/assembly factors, and ribulose bisphosphate carboxylase (RuBisCO) (Cheung et al., 1993). Microarray experiments have pointed out that the same group of photosynthesis related genes were strongly up-regulated in CRY2OX fruit. So it is plausible that also in CRY2OX chloroplast structures are maintained during ripening. This hypothesis is also supported by the higher chlorophyll content of the CRY2OX fruits with respect to Wt (data don't shown). At the molecular level these similarities could thus be the effect of alterations in photoperception possibly induced by cry2.

On the other hand, as previously shown, the impairment of tomato cry1a function reduces anthocyanin levels and increases internode and hypocotyls length (Ninu et

al., 1999; Weller et al., 2001). This suggests that cry2 plays roles partially redundant with those of cry1 in the control of tomato photomorphogenesis (Giliberto et al., 2005). we report an opposite regulation of CRY1a and CRY1b, down- and up-regulated in CRY2OX fruits, respectively. The partial redundancy hypothesized in the functional role of cry1a and cry2 could be partly explained by down-regulation of CRY1a in a CRY2OX background, where a greater expression of the gene CRY2 could inhibit the expression of CRY1. However, the function of CRY1b, which is derived from a recent duplication of CRY1 happened in tomato but not in *Arabidopsis* (Perrotta et al., 2001), is currently under study. Nevertheless, differences in expression of these two cryptochromes observed in other studies (see attached paper: Carbone et., 2005), leads us to foresee a different functional role.

4.6 Analysis of diurnal rhythmic oscillation of tomato mRNAs

In order to identify genes involved in diurnal rhythms in tomato (*Solanum lycopersicum*) leaves we have performed extensive transcription analyses either using TOM2 oligo-arrays (see attached paper: "Analysis of temporal rhythmic oscillation of tomato mRNAs: cryptochromes can alterate transcription fluctuations of photoreceptor and circadian regulated genes"). We have identified 1372 genes that were regulated in a diurnal pattern corresponding to 20% of the genes that passed quality controls.

As it occur in *Arabidopsis* in continuous light (Harmer et al., 2000), when we place light-regulated genes into phase clusters of peak expression time, we observe the highest number of genes in the middle of the light phase (ZT8) (39,7%), whereas very few genes peaked near dusk (ZT16) (14,7%); moreover, it is very interesting to note that 748 transcripts present the maximum level of expression during the light phase of the day (ZT8-ZT16), whereas 624 transcripts are up-regulated during the night (ZT20-ZT0). This result indicates that the global transcriptional activity of tomato (as it happened in *Arabidopsis*, Ma et al., 2001) doesn't present remarkable differences between day and night concerning the number of genes expressed. A large number of the genes coding for structural

proteins of cellular components involved in light-stimulated processes exhibited a peak of expression during the light phase (ZT8-16): plastidial and tylacoidal proteins, involved in photosynthetic light reaction; mitochondrial and ribosomic proteins, involved in photorespiration and proteic synthesis. Several genes coding for cytoplasmatic membrane proteins showed a maximum of expression in the dark phase (ZT20); among these, we have found genes coding for protein implicated in water transport across plasma membrane (sgn-U212566, sgn-U214798 and sgn-U214603) and in extrusion of multidrug and toxic compound (MATE family proteins, Brown et al., 1998) (sgn-U215960, sgn-U231281), indicating that the process of detoxification in tomato is probably down-regulated by light.

Clustering gene expression patterns generated by microarray analysis can greatly enhance our understanding of coordinately expressed genes that are involved in similar processes. The several genes more expressed during daylight encode for protein elements involved in photosynthesis, fatty acid biosynthesis, secondary metabolites with photo-protective properties, light signaling and flowering; while most of the genes repressed during daylight serve to prepare the plant organism to the biochemical processes to be accomplished during dark hours. Among the latter genes we found elements involved in degradation of cell wall and oxidation of fatty acids. Most of these genes are already known to be down-regulated by light in *Arabidopsis* (Ma et al., 2001). Thus, it is conceivable that light temporal regulated genes influence the same diurnal based biochemical processes in *Arabidopsis* and tomato.

As expected, many genes involved in metabolites with antioxidant properties, such as carotenoids and phenolic compounds, were more expressed during light hours in order to protect cells and tissues from the damaging effects of free radicals and singlet oxygen generated by the excess of light. In green tissues, carotenoids prevent the chlorophyll-photosensitized formation of highly destructive singlet oxygen by intercepting the chlorophyll triplet states and may also scavenge additional singlet oxygen present. Furthermore, they perform an antenna function by transferring the energy of absorbed light at the singlet excited state level to the chlorophyll system for the execution of photosynthesis. Thus the

up-regulation of most of the carotenoids related genes over TOM2 microarray in correspondence of the presumptive dawn is perfectly accountable with the predicted function of carotenoids in tomato green tissue. Coincidently, most of the genes involved in phenilpropanoid biosynthetic pathway were coordinately regulated to peak at early hours (ZT0-ZT8). The phenylpropanoid pathway produces many secondary metabolites (Anterola and Lewis, 2002), several of which act as fenolic sunscreen by absorbing light in the visible and ultraviolet (UV) range (Shirley, 1996). The coordinate expression of these genes suggest that they may be controlled by one or more common regulatory factors.

Finally, a large number of genes discussed in this work are totally uncharacterized. These photoregulated genes doubtless play important roles in pathways not discussed here and will provide fertile ground for future experimentation.

4.7 Analysis of circadian rhythmic oscillation of tomato mRNAs

Using TOM2 oligo-arrays, we have identified 57 genes with an expression pattern consistent with a circadian rhythm. Most of the genes that were found to cycle with a circadian rhythm were predicted to encode proteins involved in light signaling and flowering, phenylpropanoids and vitamin C biosynthesis, and transcription factors (TFs).

The analysis of circadian genes in this study is currently in progress. Preliminary and partial data available at present identify a number of transcripts already known to undergo rhythmic oscillation in Arabidopsis (Harmer et al., 2000; Schaffer et al., 2001).

5. CONCLUSIONS

During the Doctorate-Research Program in Plant Biology at the University of Calabria, we have developed molecular tools to investigate genes related to quality and quantity traits in crop plants. In particular, we have applied a large/small scale transcription analyses strategy to identify genes associated with ripening and photoperception of both tomato and strawberry species.

Analysis of gene expression is important in many fields of biological research, since changes in the physiology of an organism or a cell will be accompanied by changes in the pattern of gene expression. We thus have produced databases of quantitative information about the degree to which some genes respond to photoperiod, and other environmental variation and we have obtained a extensive information about which genes respond to changes in developmental processes.

These databases of gene expression information may provide insights into the pathways of genes that control complex responses and could be a first step toward an ecology of the genome in which the genome is viewed as a whole and the relationships of gene products to each other will be considered from at least one perspective (relative level of expression).

The accumulation of gene expression data from many different experiments will create a potentially very powerful opportunity to assign functional information to genes of otherwise unknown function. The conceptual basis of the approach is that genes that contribute to the same biological process will exhibit similar patterns of expression. Thus, by clustering genes based on the similarity of their relative levels of expression in response to diverse stimuli or developmental or environmental conditions, it is possible to assign hypothetical functions to many genes based on the known function of other genes in the cluster. Work with plant microarrays is just beginning but there is every reason to believe that this approach will soon be a standard component of the repertoire of plant biologists.

A number of experiments have compared the extent of transcriptional changes in different stages of fruit development and leaf including studies on the regulation of transcripts encoding photosensory receptors, light signaling proteins and carotenoid biosynthesis genes (Carbone et al., 2005).

Some of our results suggest that during tomato fruit development and ripening, the transcripts coding for photosensory receptors and light signalling proteins are highly regulated, and that tomato light responsiveness during fruit development may be modulated by these wide fluctuations in transcript abundance. Moreover, our investigations on the expression of carotenoid biosynthetic genes indicate an upregulation of the early part of the pathway, leading to the synthesis of the major fruit carotenoid, lycopene.

We have also exploited the availability of the transgenic CRY2OX tomato genotype in order to investigate a possible role of light and photo-perception in the control of fruit pigment accumulation. CRY2 over-expressor show a typical high-pigment phenotype, resulting in overproduction of anthocyanins and chlorophyll in leaves and of flavonoids and lycopene in fruits.

Finally, additional transcriptional characterization of tomato has been extended to genes potentially involved in diurnal and circadian cycles. We have identified a number of genes that was regulated in a diurnal and circadian pattern.

A similar approach has been applied on strawberry. Extended transcriptional profiling experiments were carried out to detect alterations in different genotypes selected by different quality and quantity traits (Carbone et al., 2006). Comparative transcription profiling experiments in selected genotypes pointed out a number of differentially-expressed genes, possibly related to important fruit quality traits as aroma and fruit firmness. Some of the altered cDNAs encode putative cinnamyl alcohol dehydrogenase, cinnamoyl CoA reductase, cellulase and expansin genes, involved in the early steps of lignin biosynthesis and in cell wall structure, respectively. Besides, to advance in the knowledge of gene regulations involved in flavonoid biosynthesis pathway, expression patterns of main structural genes of phenylpropanoids and flavonoid pathways in different organs and during fruit ripening has provided useful information (Almeida et al., 2007).

In our knowledge, these data provide a contribute to the identification of genes directing quality and quantity traits in crop plants and may offer useful informations for breeding programs.

6. REFERENCES

Adams M., Kelley J., Gocayne J. et al. Complementary DNA sequencing: expressed sequence tags and human genome project. Science (1991) 252, 1651–1656.

Adamska I., Scheel B., and Kloppstech K. Circadian oscillations of nuclear-encoded chloroplast proteins in pea (Pisum sativum). Plant Mol Biol. (1991) 17, 1055-1065.

Aharoni A., and O'Connell A. Gene expression analysis of strawberry achene and receptacle maturation using DNA microarrays. J. Exp. Bot. (2002) 53, 2073–2087.

Aharoni A., Leopold C. P. Keizer, Harro J. Bouwmeester, Zhongkui Sun, Mayte Alvarez-Huerta, Harrie A. Verhoeven, Jan Blaas, Adèle M. M. L. van Houwelingen, Ric C. H. De Vos, Hilko van der Voet, Ritsert C. Jansen, Monique Guis, Jos Mol, Ronald W. Davis, Mark Schena, Arjen J. van Tunen, and Ann P. O'Connell. Identification of the SAAT gene involved in strawberry flavor biogenesis by use of DNA microarray. The Plant Cell (2000) 12, 647-661.

Aharoni A., Ric De Vos C. H., Wein M., Sun Z., Greco R., Kroon A., Mol J. N. M., and O'Connell A. P. The strawberry FaMYB1 transcription factor suppresses anthocyanin and flavonol accumulation in transgenic tobacco. The Plant Journal (2001) 28, 319-332.

Ahmad M, Jarillo JA, Smirnova O, Cashmore AR (1998). The CRY1 blue light photoreceptor of Arabidopsis interacts with phytochrome A in vitro. Mol. Cell 1: 939-48.

Akhtar R.A., Reddy A.B., Maywood E.S., Clayton J.D., King V.M., Smith A.G., Gant T.W, Hastings M.H., and Kyriacou C.P. Circadian cycling of the mouse liver transcriptome, as revealed by cDNA microarray, is driven by the suprachiasmatic nucleus. Curr Biol (2002) 12, 540-550.

Akimoto-Tomiyama C. et al. Rice gene expression in response to N-acetylchitooligosaccharide elicitor: comprehensive analysis by DNA microarray with randomly selected ESTs. Plant Mol. Biol. (2003) 52, 537–551.

Alabadi D., Oyama T., Yanovsky M.J., Harmon F.G., Mas P., and Kay S.A. Reciprocal regulation between TOC1 and LHY/CCA1 within the Arabidopsis circadian clock. Science (2001) 293, 880–883.

Alabadi D., Yanovsky M.J., Mas P., Harmer S.L., and Kay S.A. Critical role for CCA1 and LHY in maintaining circadian rhythmicity in arabidopsis. Curr. Biol (2002) 12, 757–761.

Alba R, Fei Z., Payton P., Liu Y., Moore S.L., Debbie P., Cohn J., D'Ascenzo M., Gordon J. S., Rose J.K.C., Martin G., Tanksley S.D., Bouzayen M, Jahn M.M., and Giovannoni J. ESTs, cDNA microarrays, and gene expression profiling: tools for dissecting plant physiology and development. The Plant Journal (2004) 39, 697–714.

Alba R, Payton P, Fei Z, McQuinn R, Debbie P, Martin GB, Tanksley SD, Giovannoni JJ. Transcriptome and selected metabolite analyses reveal multiple points of ethylene control during tomato fruit development. Plant Cell. (2005) 17, 2954–2965.

Alba R., Cordonnier-Pratt M.M., and Pratt L.H. Fruit-localized phytochromes regulate lycopene accumulation independently of ethylene production in tomato. Plant Physiology (2000) 123, 363–370.

Alkharouf N.W., and Matthews B.F. SGMD: the Soybean Genomics and Microarray Database. Nucleic Acids Res. (2004) 32, D398–D400.

Allemeersch J. et al. Benchmarking the CATMA microarray. A novel tool for Arabidopsis transcriptome analysis. Plant Physiol. (2005) 137, 588–601.

Almeida J.R.M., D'Amico E., Preuss A., Carbone F., Ric de Vos C.H., Deiml B., Mourgues F., Perrotta G., Fisher T.C., Bovy A., Martens S. and Rosati C.. Characterization of major enzymes and genes involved in flavonoid and proanthocyanidin biosynthesis during fruit development in strawberry (*Fragaria x ananassa*). Archives of Biochemistry and Biophysics (2007) 465, 61-71.

Alwine J.C., Kemp D.J., and Stark G.R. Method for detection of specific RNAs in agarose gels by transfer to diazobenzyloxymethyl-paper and hybridization with DNA probes. Proc. Natl Acad. Sci. USA(1977) 74, 5350–5354.

Anterola AM, and Lewis NG. Trends in lignin modification: a comprehensive analysis of the effects of genetic manipulations/mutations on lignification and vascular integrity. Phytochemistry (2002) 61, 221–294.

Arumuganathan K., and Earle E. Nuclear DNA content of some important plant species. Plant Mol. Biol. Rep. (1991) 9, 208–218.

Bachem C., Horvath B., Trindade L., Claassens M., Davelaar E., Jordi W., and Visser R. A potato tuber-expressed mRNA with homology to steroid dehydrogenases affects gibberellin levels and plant development. Plant J. (2001) 25, 595–604.

Bachem C., Oomen R., and Visser R. Transcript imaging with cDNA-AFLP: a step-by-step protocol. Plant Mol. Biol. Rep. (1998) 16, 157–173.

Bachem C., van der Hoeven R., de Bruijn S., Vreugdenhil D., Zabeau M., and Visser, R. Visualisation of differential gene expression using a novel method of RNA finger-printing based on AFLP: analysis of gene expression during potato tuber development. Plant J. (1996) 9, 745–753.

Bauer A. Progress in breeding decaploid *Fragaria* × *vescana*. Acta Hort. (1993) 348, 60-64.

Baxter C.J. et al. Comparison of changes in fruit gene expression in tomato introgression lines provides evidence of genome-wide transcriptional changes and reveals links to mapped QTLs and described traits. J. Exp. Bot. (2005) 56, 1591–1604.

Becker A., Reith A., Napiwotzki J., and Kadembach B. A quantitative method of determining initial amounts of DNA by polymerase chain reaction cycle titration using digital imaging and a novel DNA stain. Anal. Biochem. (1996) 237, 204-207.

Beekwilder J., Alvarez-Huerta M., Neef E., Verstappen F.W.A., Bouwmeester H.J., and Aharoni A. Functional characterization of enzymes forming volatile esters from strawberry and banana . Plant Physiology (2004) 135, 1865-1878.

Benoit V., Steel A. B. Torres M. P., Yu, Y.-Y., Yang H., and Cooper J. Anal Chem (2001) 73, 2412–2420.

Berk A.J. and Sharp, P.A. Sizing and mapping of early adenovirus mRNAs by gel electrophoresis of S1 endonuclease-digested hybrids. Cell (1977)12, 721–732.

Bernard P.S., Lay M.J., and Wittwer C.T. Integrated amplification and detection of the C677T point mutation in the methylenetetrahydrofolate reductase gene by fluorescence resonance energy transfer and probe melting curves. Anal. Biochem. (1998) 255, 101-107.

Birnbaum K. et al. A gene expression map of the Arabidopsis root. Science (2003) 302, 1956–1960.

Blanco-Portales R, Medina-Escobar N, Lopez-Raez JA, Gonzalez-Reyes JA, Villalba JM, Moyano E, Caballero JL, and Munoz-Blanco J. Cloning, expression and immunolocalization pattern of a cinnamyl alcohol dehydrogenase gene from strawberry (*Fragaria x ananassa* cv. Chandler). J Exp Bot (2002) 53:1723–1734.

Bogorad L. Possibilities for intergenomic integration: regulatory crosscurrents between the plastid and nuclear cytoplasmic compartments. In L Bogorad, LK Vasil, eds, The Photosynthetic Apparatus. Molecular Biology and Operation. Academic Press, New York, (1991) 447-466.

Bogs J., Downey M.O., Harvey J.S., Ashton A.R., Tanner G.J., and Robinson S.P. Proanthocyanidin synthesis and expression of genes encoding leucoanthocyanidin reductase and anthocyanidin reductase in developing grape berries and grapevine leaves. Plant Physiol (2005) 139, 652-663.

Bohm B (1998) Introduction of Flavonoids. Harwood Academic Publishers,Singapore.

Bourdon V., Naef F., Rao P., Reuter V., Mok S., Bosl G., Koul S., Murty V., Kucherlapati R., and Chaganti R. Genomic and expression analysis of the 12p11-p12 amplicon using EST arrays identifies two novel amplified and over expressed genes. Cancer Res. (2002) 62, 6218–6223.

Boylan M.T., and Quail P.H. Oat phytochrome is biologically active in transgenic tomatoes. Plant Cell (1989) 1, 765–773.

Brady C.J. Fruit ripening. Annu Rev Plant Physiol (1987) 38, 155-178.

Bramley P.M. Regulation of carotenoid formation during tomato fruit ripening and development. J. Exp. Bot. (2002) 53, 2107–2113.

Bramley PM, Bird C, Schuch W. Carotenoid biosynthesis and manipulation. In: Grierson D, ed. Biosynthesis and manipulation of plant products. London: Chapman & Hall, (1993) 139-177.

Bramley PM. Isoprenoid metabolism. In: Dey PM, Harbone JB, eds. Plant biochemistry. San Diego: Academic Press, (1997) 417-437.

Briggs WR, Christie JM. 2002. Phototropins 1 and 2: versatile plant blue-light receptors. Trends Plant Sci. 7, 204–210.

Bringhurst R.S., and Voth V. Breeding octoploid strawberries. Iowa State Journal of Research (1984) 58, 371-381.

Bringhurst, R. Cytogenetics and evolution in American *Fragaria*. HortScience (1990) 25, 879-881.

Brown M.H., Paulsen I.T., and Skurray R.A. The multidrug efflux protein NorM is a prototype of a new family of transporters. Mol. Microbiol. (1998) 31, 393–395.

Brummell D., and Harpster M. Cell wall metabolism in fruit softening and quality and its manipulation in transgenic plants. Plant Mol. Biol. (2001) 47, 311–340.

Brummell D.A., Hall B.D., and Bennett A.B. Antisense suppression of tomato endo-beta-1,4-glucanase Cel2 mRNA accumulation increases the force required to break fruit abscission zones but does not affect fruit softening. Plant Mol. Biol. (1999a) 40, 615–622.

Brummell D.A., Harpster M.H., Civello P.M., Palys J.M., Bennett A.B., and Dunsmuir P. Modification of expansin protein abundance in tomato fruit alters softening and cell wall polymer metabolism during ripening. Plant Cell (1999b) 11, 2203–2216.

Bruno A.K., and Wetzel C.M. The early light-inducible protein (ELIP) gene is expressed during the chloroplast-to-chromoplast transition in ripening tomato fruit. J. Exp. Bot (2004) 55, 2541-2548.

Callow M., Dudoit S., Gong E., Speed T., and Rubin, E. Microarray expression profiling identifies genes with altered expression in HDL-deficient mice. Genome Res. (2000) 10, 2022–2029.

Carbone F., Mourgues F., Biasioli F., Gasperi F., Mark T.D., Rosati C., Perrotta G. Development of molecular and biochemical tools to investigate fruit quality traits in strawberry elite genotypes. Molecular Breeding (2006) 18, 127-142.

Carbone, F., Pizzichini, D., Giuliano, G., Rosati, C., Perrotta, G. Comparative profiling of tomato fruits and leaves evidences a complex modulation of global transcript profiles. Plant Science (2005) 169 , 165-175.

Carol P, Kuntz M. A plastid terminal oxidase comes to light: implications for carotenoid biosynthesis and chlororespiration. Trends in Plant Science (2001) 6, 31-36.

Caruthers M. H. Acc Chem Res (1991) 24, 278–284.

Casazza A.P., Rossini S., Rosso M.G., and Soave C. Mutational and expression analysis of ELIP1 and ELIP2 in Arabidopsis thaliana Plant Molecular Biology (2005) 58, 41-51.

Case-Green S., Mir K. U., Pritchard C. E., and Southern E. M. Curr Opin Chem Biol (1998) 2, 404–410.

Ceriani M.F., Hogenesch J.B., Yanovsky M., Panda S., Straume M, and Kay S.A. Genome-wide expression analysis in Drosophila reveals genes controlling circadian behavior. The Journal of Neuroscience (2002) 22, 9305–9319.

Chee M., Yang R., Hubbell E., Berno A., Huang X.C., Stern D., et al. Science (1996) 274, 610.

Cheek B. J., Steel A. B., Torres M. P., Yu, Y.-Y., Yang H. Anal Chem (2001) 73, 5777–5783.

Chen J., Wu R., Yang P.-C. et al. Profiling expression patterns and isolating differentially expressed genes by cDNA microarray system with colorimetry detection. Genomics (1998) 51, 313–324.

Chen C. Y., and Shyu A. B. Mol. Cell. Biol. (1994) 14, 8471–8482.

Chen G., Alexander L., and Grierson D. Constitutive expression of EIL-like transcription factor partially restores ripening in the ethylene-insensitive Nr tomato mutant. J Exp Bot (2004a) 55, 1491–1497.

Chen GP, Hackett R, Walker D, Taylor A, Lin ZF, Grierson D.. Identification of a specific isoform of tomato lipoxygenase (TomloxC) involved in the generation of fatty acidderived flavor compounds. Plant Physiol (2004b) 136, 2641–2651.

Cheng G.W., andBreen P.J. Activity Of Phenylalanine Ammonia-Lyase (Pal) And Concentrations Of Anthocyanins And Phenolics In Developing Strawberry Fruit. Journal Of The American Society For Horticultural Science (1991) 116, 865-869.

Cheung A.Y., McNellis T., and Piekos B. Maintenance of chloroplast components during chromoplast differentiation in the tomato mutant green flesh. Plant Physiology (1993) 101, 1223-1229.

Cho Y. et al. Gene-expression profile comparisons distinguish seven organs of maize. Genome Biol. (2002) 3.

Chrisey L. A., Lee G. U., and O'Ferrall C. E. Nucleic Acids Res (1996) 24, 3031–3039.

Churchill G. Fundamentals of experimental design for cDNA microarrays. Nat. Genet. (2002) 32 (Suppl. 2), 490–495.

Civello PM, Powell ALT, Sabehat A, Bennett AB. An expansin gene expressed in ripening strawberry fruit. Plant Physiology (1999) 121, 1273-1279.

Claridge-Chang A., Wijnen H., Naef F., Boothroyd C., Rajewsky N., and Young M.W. Circadian regulation of gene expression systems in the Drosophila head. Neuron. (2001) 32, 657-671.

Clarke B., and Rahman S. A microarray analysis of wheat grain hardness. Theor. Appl. Genet. (2005)110, 1259–1267.

Cleveland W.S. Robust locally weighted regression and smoothing scatterplots. J. Amer. Statist. Assoc. (1979) 74, 829-836.

Cleveland W.S., and Devlin S.J. Locally weighted regression: an approach to regression analysis by local fitting. J. of Am. Stat. Assoc. (1998) 83, 596-610.

Close T.J. et al. A new resource for cereal genomics: 22K barley GeneChip comes of age. Plant Physiol. (2004) 134, 960–968.

Cochran W., and Cox G. Experimental Designs, 2nd edn. New York: Wiley & Sons Inc., (1992) 95–182.

Covington M.F., Panda S., Liu X.L., Strayer C.A., Wagner D.R., and Kay S.A. ELF3 Modulates Resetting of the Circadian Clock in Arabidopsis. Plant Cell (2001) 13, 1305–1316.

Craigon, D.J. et al. NASCArrays: a repository for microarray data generated by NASC's transcriptomics service. Nucleic Acids Res. (2004) 32, D575–D577.

Cunningham F.X., Gantt E. Genes and enzymes of carotenoid biosynthesis in plants. Annual Review of Plant Physiology and Plant Molecular Biology (1998) 49, 557-583.

de Hoon M., Imoto S., Kobayashi K., Ogasawara N., and Miyano S. Inferring gene regulatory networks from time-ordered gene expression data of Bacillus subtilis using differential equations. Pac. Sym. Biocomp. (2003) 8, 17–28.

de la Fuente A., Brazhnik P., and Mendes P. Linking the genes: inferring quantitative gene networks from microarray data. Trends Genet. (2002) 18, 395–398.

de Saizieu A., Certa U., Warrington J., Gray C., Keck W., and Mous J. Nature Biotechnol. (1998) 16, 45.

DellaPenna D., Alexander D.C., and Bennett A.B. Molecular cloning of tomato fruit polygalacturonase: analysis of polygalacturonase mRNA levels during ripening. Proc Natl Acad Sci USA (1986) 83, 6420-6424.

DellaPenna D., Lincoln J.E., Fischer R.L., and Bennett A.B. Transcriptional analysis of polygalacturonase and other ripening associated genes in Rutgers, rin, nor, and Nr tomato fruit. Plant Physiol. (1989) 90, 1372–1377.

Dellaqi A., Birch P., Heilbronn J., Lyon G., and Toth, I. cDNA-AFLP analysis of differential gene expression in the prokaryotic plant pathogen Erwinia carotovora. Microbiology (2000) 146, 165–171.

Demmig-Adams B, Adams WW. The role of xanthophyll cycle carotenoids in the protection of photosynthesis. Trends in Plant Science (1996) 1, 21-26.

DeRisi J., Penland L., Brown P., Bittner M., Meltzer P., Ray M., Chen Y., Su Y., and Trent J. Use of a cDNA microarray to analyze gene expression patterns in human cancer. Nat. Genet. (1996) 14, 457–460.

DeRisi J., Iyer V., and Brown P. Exploring the metabolic and genetic control of gene expression on a genomic scale. Science (1997) 278, 680–686.

Deroles S.C., Bradley J.M., Schwinn K.E., Markham K.R., Bloor S., Manson D.G., and Davies K.M. An antisense chalcone synthase cDNA leads to novel colour patterns in lisianthus (Eustoma grandiflorum) flowers. Mol. Breeding (1998) 4, 59–66.

Devlin P.F., and Kay S.A. Circadian photoreception. Annu. Rev. Physiol. (2001) 63, 677-694.

Dixon R.A., and Paiva N.L. Stress-induced phenylpropanoid metabolism. Plant Cell. (1995) 7, 1085–1097.

Dixon R.A., and Steele C.L. Trends Plant Sci. (1999) 4, 394–400.

Dobbin K., and Simon R. Comparison of microarray designs for class comparison and class discovery. Bioinformatics (2002) 18, 1438–1445.

Dobbin K., Shih J., and Simon R. Questions and answers on design of dual-label microarrays for identifying differentially expressed genes. J. Natl Cancer Inst. (2003) 95, 1362–1369.

Dong Y., Glasner J., Blattner F., and Triplett E. Genomic interspecies microarray hybridization: Rapid discovery of three thousand genes in the maize endophyte, Klebsiella pneumonia 342, by microarray hybridization with Escherichia coli K-12 open reading frames. Appl. Environ. Microbiol. (2001) 67, 1911–1921.

Dooner H.K., Robbins T.P., Jorgensen R.A., Genetic and developmental control of anthocyanin biosynthesis. Annu. Rev. Genet. (1991) 25, 173–199.

Downey M.O., Harvey J.S., and Robinson S.P. Analysis of tannins in seeds and skins of Shiraz grapes throughout berry development. Aust J Grape Wine Res (2003) 9, 15–27.

Doyle M.R., Davis S.J., Bastow R.M., McWatters H.G., Kozma-Bognar L., Nagy F., Millar A.J., and Amasino R.M. The ELF4 gene controls circadian rhythms and flowering time in Arabidopsis thaliana. Nature (2002) 419, 74-77.

Ducreux L.J.M. et al. Metabolic engineering of high carotenoid potato tubers containing enhanced levels of b-carotene and lutein. J. Exp. Bot. (2005) 56, 81–89.

Duffield, 2003

Duggan D.J., Bittner M., Chen Y., Meltzer P., and Trent J.M. Expression profiling using cDNA microarrays. Nature Genetics Supplement (1999) 21, 10-14.

Dunlap JC. Molecular bases for circadian clocks. Cell (1999) 96, 271-290.

Durbin M.L., McCaig B., and Clegg M.T. Molecular evolution of the chalcone synthase multigene family in the morning glory genome. Plant Mol Biol (2000) 42, 79-92.

Durrant W., Rowland O., Piedras P., Hammond-Kosack K., and Jones, J. cDNA-AFLP reveals a striking overlap in racespecific resistance and wound response gene expression profiles. Plant Cell (2000) 12, 963–977.

Eisen M.B., Spellman P.T., Brown P.O., and Botstein D. Cluster analysis and display of genome-wide expression patterns. Proc. Natl. Acad. Sci. USA (1998) 95, 14863–14868.

Eriksson E.M. et al. Effect of the colorless non-ripening mutation on cell wall biochemistry and gene expression during tomato fruit development and ripening. Plant Physiol. (2004) 136, 4184–4197.

Ewing R., Kahla A., Poirot O., Lopez F., Audic S., and Claverie, J. Large-scale statistical analyses of rice ESTs reveal correlated patterns of gene expression. Genome Res. (1999) 9, 950–959.

Fan XT, Mattheis JP, Fellman JK. A role for jasmonates in climacteric fruit ripening. Planta (1998) 204, 444–449.

Farré E.M., Harmer S.L., Harmon F.G., Yanovsky M.J., and Kay S.A. Overlapping and distinct roles of PRR7 and PRR9 in the Arabidopsis circadian clock. Current Biology (2005) 15, 47-54.

Fei ZJ, Tang XM, Alba R, Giovannoni J. Tomato Expression Database (TED): a suite of data presentation and analysis tools. Nucleic Acids Res (2006) 34, D766–D770.

Ferea T. L., and Brown P. O. Curr Opin Genet Dev (1999) 9, 715–722.

Fernandes J. et al. Comparison of RNA expression profiles based on maize expressed sequence tag frequency analysis and microarray hybridization. Plant Physiol. (2002) 128, 896–910.

Ferrandiz C., Liljegren S.J., and Yanofsky M.F. Negative regulation of the SHATTERPROOF genes by FRUITFULL during Arabidopsis fruit development. Science (2000) 289, 436–438.

Fodor S. P., Leighton P. A. J., Pirrung M. C., Stryer L., and Solas, D. Science (1991) 251, 767–773.

Forkmann G., and Heller W., Biosynthesis of flavonoids. In: Comprehensive Natural Products Chemistry. Amsterdam, Elsevier (1999) 713–748.

Forkmann G., and Martens S. Metabolic engineering and applications of flavonoids. Current Opinion in Biotechnology (2001) 12, 155–160.

Fowler S., and Thomashow M. Arabidopsis transcriptome profiling indicates that multiple regulatory pathways are activated during cold acclimation in addition to the CBF cold response pathway. Plant Cell (2002) 14, 1675–1690.

Fowler S, Lee K, Onouchi H, Samach A, Richardson K, Morris B, Coupland G, and Putteril J. GIGANTEA: a circadian clock-controlled gene that regulates photoperiodic flowering in Arabidopsis and encodes a protein with several membrane-spanning domains. EMBO J. (1999) 18, 4679-4688.

Fray R.G., and Grierson D. Identification and genetic analysis of normal and mutant phytoene synthase genes of tomato by sequencing, complementation and co-suppression. Plant Mol. Biol. (1993) 22, 589–602.

Freeman W.M., Walker S.J., and Vrana K.E. Quantitative RT-PCR: Pitfalls and potential. BioTechiniques (1999) 26, 112-125.

Fridman E, Carrari F, Liu YS, Fernie AR, Zamir D.. Zooming in on a quantitative trait for tomato yield using interspecific introgressions. Science (2004) 305, 1786–1789.

Fujii T., Nagasawa N., Iwamatsu A., Bogaki T., Tamai Y., and Hamachi M. Molecular cloning, sequence analysis, and expression of the yeast alcohol acetyltransferase gene. Appl. Environ. Microbiol. (1994) 60, 2786–2792.

Fujii T., Yoshimoto H., Nagasawa N., Bogaki T., Tamai Y., and Hamachi M. Nucleotide sequences of alcohol acetyltransferase genes from lager brewing yeast, Saccharomyces carlsbergensis. Yeast (1996) 12, 593–598.

Gao X., Gulari E., and Zhou X. In situ synthesis of oligonucleotide microarrays. Biopolymers (2004) 73, 579–596.

Gardiner J. et al. Design, production and utilization of long oligonucleotide microarrays for expression analysis in maize. Maydica (2006)(in press)

Gibson U.E., Heid C.A., and Williams P.M. A novel method for real time quantitative RT-PCR. Genome Res. (1996) 6, 995-1001.

Giliberto L., Perrotta G., Pallara P., Weller J.L., Fraser P.D., Bramley P.M., Fiore A., Tavazza M., and Giuliano, G., Manipulation of the blue light photoreceptor cryptochrome 2 in tomato affects vegetative development, flowering time, and fruit antioxidant content. Plant Physiology (2005) 137, 199-208.

Gill R., Katsoulakis E., Schmitt W., Taroncher-Oldenburg G., Misra J., and Stephanopoulos G. Genome-wide dynamic transcriptional profiling of the light-to-dark transition in Synechocystis sp. strain PCC 6803. J. Bacteriol. (2002) 184, 3671–3681.

Giovannoni J. Genetic Regulation of Fruit Development and Ripening The Plant Cell (2004) 16, S170–S180.

Giovannoni J., DellaPenna D., Bennett A., and Fischer R. Expression of a chimeric polygalacturonase gene in transgenic rin (ripening inhibitor) tomato fruit results in polyuronide degradation but not fruit softening. Plant Cell (1989) 1, 53–63.

Giovannucci E, Ascherio A, Rimm EB, Stampfer MJ, Colditz GA, Willett WC (1995) Intake of carotenoids and retinol in relation to risk of prostate cancer. J Natl Cancer Inst 87: 1767–1776.

Giuliano G., G.E. Bartley, P.A. Scolnik, Regulation of carotenoid biosynthesis during tomato development. Plant Cell (1993) 5, 379–387.

Given N.K., Venis M.A., Grierson D. Phenylalanine ammonia-lyase activity and anthocyanin synthesis in ripening strawberry fruit. Journal of Plant Physiology (1988) 133, 25–30.

Given NK, Venis MA, Grierson D. Hormonal regulation of ripening in the strawberry a non-climacteric fruit. Planta (1988) 174, 402–406.

Grierson D., and Kader A.A. Fruit ripening and quality. In The Tomato Crop. A Scientific Basis for ImproVement; Atherton, J. G., Rudich, J., Eds.; Chapman and Hall: New York, (1986) 242-280.

Häkkinen S.H., and Törrönen A.R. Content of flavonols and selected phenolic acids in strawberry and Vaccinium species: influence of cultivar, cultivation site and technique. Food Res Int (2000) 33, 517-524.

Halbwirth H., Puhl I., Haas U., Jesik K., Treutter D., and Stich K. J. Agric. Food Chem. (2006) 54, 1479–1485.

Hancock J.F., Dale A., and Luby J.J. Should we reconstitute the strawberry? Acta Hort. (1993) 348, 86–93.

Harada M., Ueda Y., and Iwata T. Purification and some properties of alcohol acetyltransferase from banana fruit. Plant Cell Physiol. (1985) 26, 1067–1074.

Harmer S.L., Hogenesch J.B., Straume M., Chang H.S., Han B., Zhu T., Wang X., Kreps J.A., and Kay S.A. Orchestrated transcription of key pathways in Arabidopsis by the circadian clock. Science (2000) 290, 2110-2113.

Harpster MH, Brummell DA, Dunsmuir P. Expression analysis of a ripening-specific, auxin-repressed endo-1,4-betaglucanase gene in strawberry. Plant Physiology (1998) 118, 1307-1316.

Harris W.M., and Spurr A.R. Chromoplasts of tomato fruits. The red tomato. Am J Bot (1969b) 56, 380-389.

Harris W.M., and Spurr A.R. Chromoplasts of tomato fruits. I. Ultrastructure of low-pigment and high-beta mutants. Carotene analyses. Am J Bot (1969a) 56, 369-379.

Harrison EP, McQueen Mason SJ, Manning K. Expression of six expansin genes in relation to extension activity in developing strawberry fruit. Journal of Experimental Botany (2001) 52, 1437-1446.

Hashimoto R., Kim S., Shmulevich I., Zhang W., Bittner M., and Dougherty E. Growing genetic regulatory networks from seed genes. Bioinformatics (2004) 20, 1241–1247.

Hauser B., Pratt L., and Cordonnier-Prat, M.-M. Absolute quantification of five phytochrome transcripts in seedlings and mature plants of tomato (*Solanum lycopersicum* L.). Planta (1997) 201, 379–387.

Hauser BA, Cordonnier-Pratt MM, Daniel-Vedele F, Pratt LH. The phytochrome gene family in tomato includes a novel subfamily. Plant Mol. Biol. (1995) 29, 1143-1155.

Hayama R and Coupland G. The molecular basis of diversity in the photoperiodic flowering responses of Arabidopsis and Rice. Plant Physiol. (2004) 135, 677-684.

Hazen S.P. et al. Expression profiling of rice segregating for drought tolerance QTLs using a rice genome array. Funct. Integr. Genomics (2005) 5, 104–116.

Hegde P., Qi R., Abernathy K., Gay C., Dharap S., Gaspard R., Earle-Hughes J., Snesrud E., Lee N., and Quackenbush, J. A concise guide to cDNA microarray analysis. Biotechniques (2000) 29, 548–562.

Heid C.A., Stevens J., Livak K.J., and Williams P.M. Real time quantitative PCR. Genom Res. (1996) 6, 986-994.

Heinonen M. et al. J.Agr. Food Chem (1998) 46, 4107.

Helariutta Y., Kotilainen M, Elomaa P., Kalkkinen N., Bremer K., Teeri T.H., and Albert V.A. Duplication and functional divergence in the chalcone synthase gene family of Asteraceae: evolution with substrate change and catalytic simplification. Proc Natl Acad Sci USA (1996) 93, 9033-9038.

Heller R.A., Schena M., Chai A., Shalon D., Bedilion D., Gilmore J., et al. Proc. Natl. Acad. Sci. USA (1997) 94, 2150.

Hennig L. et al. Arabidopsis transcript profiling on Affymetrix GeneChip arrays. Plant Mol. Biol. (2003) 53, 457–465.

Higuchi R., Dollinger G., Walsh P.S., and Griffith R. Simultaneous amplification and detection of specific DNA sequences. Bio/Technology (1992) 10, 413-417.

Higuchi R., Fockler C., Dollinger G., and Watson R. Kinetic PCR analysis: Real-time monitoring of DNA amplification reactions. Bio/Technology (1993) 11, 1026-1030.

Hirschberg J. Carotenoid biosynthesis in flowering plants. Curr Opin Plant Biol (2001) 4, 210–218.

Hirschberg J. Production of high-value compounds: carotenoids and vitamin E. Current Opinion in Biotechnology (1999) 10, 186-192.

Hobson GE, Nichols R, Davies JN, Atkey PT. The inhibition of tomato lycopersicon-esculentum fruit ripening by silver. J Plant Physiol (1984)116, 21–30.

Hoecker U., and Quail P.H. The phytochrome A-specific signaling intermediate SPA1 interacts directly with COP1, a constitutive repressor of light signaling in Arabidopsis. J. Biol. Chem. (2001) 276, 38173 -38178.

Hoecker U., Xu Y., and Quail P. H. SPA1: a new genetic locus involved in phytochrome A-specific signal transduction. Plant Cell (1998). 10, 19-33.

Holland P.M., Abramson R.D., Watson R., and Gelfand D.H. Detection of specific polymerase chain reaction product by utilizing the 5'-3' exonuclease activity of Thermus aquaticus DNA polymerase. Proc. Natl. Acad. Sci. (1991) 88, 7276-7280.

Horikoshi T., et al. Cancer Res. (1992) 52, 108–116.

Horvath D., Schaffer R., West M., and Wisman E. Arabidopsis microarrays identify conserved and differentially expressed genes involved in shoot growth and development from distantly related plant species. Plant J. (2003) 34, 125–134.

Hrazdina G., and Wagner G. Metabolic pathways as enzyme complexes: Evidence for the synthesis of phenylpropanoids and flavonoids in membrane-associated enzyme complexes. Archives Of Biochemistry And Biophysics (1985) 237, 88–100.

Huber DJ. Strawberry fruit softening: the potential roles of polyuronides and hemicelluloses. Journal of Food Science (1984) 49, 1310-1315.

Isaacson T, Ronen G, Zamir D, Hirschberg J. Cloning of tangerine from tomato reveals a carotenoid isomerase essential for the production of betacarotene and xanthophylls in plants. Plant Cell (2002) 14, 333-342.

Ishiguro T., Saitoh J., Yawata H., Yamagishi H., Iwasaki S., and Mitoma Y. Homogeneous quantitative assay of hepatitis C virus RNA by polymerase chain reaction in the presence of a fluorescent intercalator. Anal. Biochem. (1995) 229, 207-213.

Ishikawa M., Kiba T., and Chua N.H. The Arabidopsis SPA1 gene is required for circadian clock function and photoperiodic flowering. Plant J (2006) 46, 736–746.

Iyer V. R., et al. Science (1999) 283, 83–87.

Jaakola L., Maatta-Riihinen K., Kärenlampi S., and Hohtola A. Activation of flavonoid biosynthesis by solar radiation in bilberry (Vaccinium myrtillus L.) leaves. Planta (2004) 218, 721–728.

Jarrillo JA, Capel J, Tang RH, Yang HQ, Alonso JM, Ecker JR and Cashmore AR. An Arabidopsis circadian clock component interacts with both CRY1 and phyB. Nature (2001) 410, 487-490.

Jen JJ, Watada AE Red light advances respiration and ethylene evolution in ripening tomatoes. Hortic Sci (1977) 12: 459–460.

Jiang M., Ryu J., Kiraly M., Duke K., Reinke V., and Kim S. Genome-wide analysis of developmental and sex-regulated gene expression profiles in Caenorhabditis elegans. Proc. Natl Acad. Sci. USA (2001) 98, 218–223.

Jimenez-Bermudez S., Redondo-Nevado J., Munoz-Blanco J., Caballero J.L., Lopez-Aranda J.M., Valpuesta V., Pliego-Alfaro F., Quesada M.A., and Mercado J.A. Manipulation of strawberry fruit softening by antisense expression of a pectate lyase gene. Plant Physiol (2002) 128, 751–775.

Jin H., and Martin C., Multifunctionality and diversity within the plant MYB-gene family. Plant Molecular Biology (1999) 41, 577-585.

Jorgensen R.A., Cluster P.D., English J., Que Q., Napoli C.A.. Chalcone synthase cosuppression phenotypes in petunia flowers: comparison of sense vs. antisense constructs and single-copy vs. complex T-DNA sequences. Plant Mol. Biol. (1996) 31, 957–973.

Kanwischer M., Porfirova S., Bergmuller E., and Dormann P. Alterations in tocopherol cyclase activity in transgenic and mutant plants of Arabidopsis affect tocopherol content, tocopherol composition, and oxidative stress. Plant Physiol. (2005) 137, 713-723.

Kawasaki S. et al. Gene expression profiles during the initial phase of salt stress in rice. Plant Cell (2001) 13, 889–905.

Kendrick RE, Kronenberg GHM. (1994). Photomorphogenesis in plants. 2nd edn. Dordrecht, The Netherlands: Kluwer Academic Publishers.

Kennedy J.A., Hayasaka Y., Vidal S., Waters E.J., and Jones G.P. Composition of grape skin proanthocyanidins at different stages of berry development. J Agric Food Chem (2001) 49, 5348–5355.

Kennedy J.A., Matthews M.A., and Waterhouse A.L. Changes in grape seed polyphenols during ripening. Phytochemistry (2000) 55, 77–85.

Kerr E.A. Green flesh, gf. Tomato Gen Corp (1956) 6, 17 .

Kerr M., Afshari C., Bennett L., Bushel P., Martinez J., Walker N., and Churchill, G. Statistical analysis of gene expression microarray experiment with replication. Statistica Sinica, (2000a) 12, 2003–2118.

Kerr M., and Churchill G. Experimental design for gene expression microarrays. Biostatistics (2001) 2, 183–201.

Kerr M., Martin M., and Churchill G. Analysis of variance for gene expression microarray data. J. Comp. Biol. (2000b) 7, 819–837.

Khudairi AK, Arboleda OP. Phytochrome-mediated carotenoid biosynthesis and its influence by plant hormones. Physiol Plant (1971) 24, 18–22.

Kirk J.T.O., and Tilney-Bassett R.A.E. (1978) The Plastids. Elsevier/North Holland Biomedical Press, New York.

Kiyosue T and Wada M (2000). LKP1 (LOV kelch protein 1): a factor involved in the regulation of flowering time in Arabidopsis. Plant J. 23: 807-15.

Klee HJ, Hayford MB, Kretzmer KA, Barry GF, Kishore GM. Control of ethylene synthesis by expression of a bacterial enzyme in transgenic tomato plants. Plant Cell (1991) 3, 1187–1194.

Kobayashi H. Differentiation of amyloplasts and chromoplasts. In L Bogorad, IK Vasil, eds, The Photosynthetic Apparatus. Molecular Biology and Operation. Academic Press, New York, (1991), 395-415.

Koes R.E., Quattrocchio F., Mol J.N.M., The flavonoid biosynthetic pathway in plants: function and evolution. BioEssays (1994) 16, 123–132.

Koes R.E., van Blokland R., Quattrocchio F., van Tunen A.J., and Mol J.N.M. Plant Cell (1990) 2, 379–392.

Kosar M., Kafkas E., Paydas S., and Can Baser K.H. Phenolic composition of strawberry genotypes at different maturation stages. J. Agric. Food Chem. (2004) 52, 1586-1589.

Kreps J. A., and Kay S. A. Plant Cell (1997) 9, 1235.

Kumar A., and Ellis B.E. Phytochemistry (2003) 62, 513–526.

Lan, L. et al. Monitoring of gene expression profiles and isolation of candidate genes involved in pollination and fertilization in rice (Oryza sativa L.) with a 10K cDNA microarray. Plant Mol. Biol. (2004) 54, 471–487.

Lanahan MB, Yen H-C, Giovannoni JJ, Klee HJ. The never ripe mutation blocks ethylene perception in tomato. Plant Cell (1994) 6, 521–530.

Langmead C.J., McClung C.R., and Donald B.R. A maximum entropy algorithm for rhythmic analysis of genome-wide expression patterns. Proc. IEEE Comput. Soc. Bioinform. Conf. (2002) 1, 237–245.

Lanshkari D.A., DeRisi J.L., McCusker J.H., Namath A.F., Gentile C., Hwang S.Y., et al. Proc. Natl. Acad. Sci. USA (1997) 94, 13057.

Lashbrook C., Giovannoni J., Hall B., Fischer R., and Bennett A. Transgenic analysis of tomato endo-beta-1,4-glucanase gene function: Role of CEL1 in floral abscission. Plant J. (1998) 13, 303–310.

Laubinger S., Marchal V., Le Gourrierec J., Wenkel S., Adrian J., Jang S., Kulajta C., Braun H., Coupland G., and Hoecker U. Arabidopsis SPA proteins regulate photoperiodic flowering and interact with the floral inducer CONSTANS to regulate its stability. Development (2006) 133, 3213-3222.

Laubinger S., Marchal V., Le Gourrierec J., Wenkel S., Adrian J., Jang S., Kulajta C., Braun H., Coupland G., and Hoecker U. Arabidopsis SPA proteins regulate photoperiodic flowering and interact with the floral inducer CONSTANS to regulate its stability. Development (2006) 133, 3213-3222.

Lay M.J., and Wittwer C.T. Real-time fluorescence genotyping of factor V Leiden during rapid-cycle PCR. Clin. Chem. (1997) 43, 2262-2267.

Le Gall G., DuPont M.S., Mellon F.A., Davis A.L., Collins G.J., Verhoeyen M.E., Colquhoun I.J. Characterization and content of flavonoid glycosides in genetically modified tomato (Lycopersicon esculentum) fruits. J. Agric. Food. Chem. (2003) 51, 2438–2446.

Ledger S., Strayer C., Ashton F., Kay S.A., and Putterill J. Analysis of the function of two circadian-regulated CONSTANS-LIKE genes. Plant J (2001) 26, 15-22.

Lee M.-L., Kuo F., Whitmore G., and Sklar, J. Importance of replication in microarray gene expression studies: statistical methods and evidence from repetitive cDNA hybridizations. Proc. Natl Acad. Sci. USA, (2000) 97, 9834–9839.

Lelievre J.M., Latche A., Jones B., Bouzayen M., and Pech J.C. Ethylene and fruit ripening. Physiol. Plant. (1997) 101, 727–739.

Lemieux B., Aharoni A., and Schena M. Mol. Breeding (1998) 4, 277.

Leproust E., Zhang H., Yu P., Zhou X., and Gao X. Nucleic Acids Res (2001) 29, 2171–2180.

Liang P. and Pardee A.B. Differential display of eukaryotic messenger RNA by means of the polymerase chain reaction. Science (1992) 257, 967–971.

Lin CT. Blue light receptors and signal transduction. Plant Cell (2002) 14, S207–25.

Lipshutz R. J., Fodor S. P. A., Gingeras T. R., and Lockhart D. J. Nat Genet (1999) 21, 20–24.

Liu X.L., Covington M.F., Fankhauser C., Chory J., and Wagner D.R. ELF3 encodes a circadian clock-regulated nuclear protein that functions in an Arabidopsis PHYB signal transduction pathway. Plant Cell (2001) 13, 1293-1304.

Liu Y., Roof S., Ye Z., Barry C., van Tuinen A., Vrebalov J., Bowler C., Giovannoni J. Manipulation of light signal transduction as a means of modifying fruit nutritional quality in tomato, Proc. Natl. Acad. Sci. USA (2004) 101, 9897–9902.

Livak K. J., and Schmittgen T.D. Analysis of relative gene expression data using real-time quantitative PCR and the 2ΔΔCT method. Methods (2001) 25, 402–408.

Livak K.J., Flood S.J, Marmaro J., Giusti W., and Deetz K. Oligonucleotides with fluorescent dyes at opposite ends provide a quenched probe system useful for detecting PCR product and nucleic acid hybridization. PCR Methods Appl. (1996) 4, 357-362.

Llop Tous I, Dominguez Puigjaner E, Palomer X, Vendrell M. Characterization of two divergent endo-beta-1,4-glucanase cDNA clones highly expressed in the non-climacteric strawberry fruit. Plant Physiology (1999) 119, 1415-1421.

Locke J.C.W., Millar A.J., and Turner M.S. Modelling genetic networks with noisy and varied experimental data: the circadian clock in Arabidopsis thaliana. J. Theor. Biol (2005a) 234, 383–393.

Locke J.C.W., Southern M.M., Kozma-Bognar L., Hibberd V., Brown P.E., Turner M.S., and Millar A.J. Extension of a genetic network model by iterative experimentation and mathematical analysis. Mol. Syst. Biol (2005b) 1, 13.

Lockhart D., Dong H., Byrne M. et al. Expression monitoring by hybridization to high-density oligonucleotide arrays. Nature Biotech. (1996) 14, 1675–1680.

Lockhart D.J., Dong H., Byrne M.C., Follettie M.T., Gallo M.V., Chee M.S., et al. Nature Biotechnol. (1996) 14, 1675.

Lois L., Rodriguez C., Gallego F., Campos N., and Boronat A. Carotenoid biosynthesis during tomato fruit development: Regulatory role of 1-deoxy-D-xylulose 5-phosphate synthase. Plant J. (2000) 22, 503–513.

Lopez-Gomez R., Gomez-Lim M.A. A method for extracting intact RNA from fruits rich in polysaccharides using ripe mango mesocarp, Hort. Sci. 27 (1992) 440-442.

Ma L.G., Li J.M., Qu L.J., Hager J., Chen Z.L., Zhao H., and Deng X.W. Light control of Arabidopsis development entails coordinated regulation of genome expression and cellular pathways. Plant Cell (2001) 13, 2589-2607.

Maarse H. (1991). Volatile Compounds in Foods and Beverages. (New York: Marcel Dekker).

Malcorps P., and Dufour J.P. Short-chain and mediumchain aliphatic-ester synthesis in Saccharomyces cerevisiae. Eur. J. Biochem. (1992) 210, 1015–1022.

Manning K, Seymour GB, Taylor JE, and Tucker GA, eds, Biochemistry of Fruit Ripening. Chapmann and Hall, Cambridge, UK, (1993) 347–373.

Manning K, Tor M, Poole M, Hong Y, Thompson AJ, King GJ, Giovannoni JJ, Seymour GB. A naturally occurring epigenetic mutation in a gene encoding an SBP-box transcription factor inhibits tomato fruit ripening. Nat Genet (2006) 38, 948–952.

Manning K. Isolation of a set of ripening-related genes from strawberry: Their identification and possible relationship to fruit quality traits. Planta (1998) 205, 622–631.

Marin E, Nussaume L, Quesada A, Gonneau M, Sotta B, Hugueney P , Frey A, Marion-Poll A. Molecular identification of zeaxanthin epoxidase of Nicotiana plumbaginifolia, a gene involved in abscisic acid biosynthesis and corresponding to the ABA locus of Arabidopsis thaliana. EMBO Journal (1996) 15, 2331-2342.

Marshall A., and Hodgson, J. DNA chips: an array of possibilities. Nature Biotech. (1998) 16, 27–31.

Martin-Tryon E.L., Kreps J.A., and Harmer S.L. GIGANTEA Acts in Blue Light Signaling and Has Biochemically Separable Roles in Circadian Clock and Flowering Time Regulation. Plant Physiol (2007) 143, 473–486.

Mas P., Alabadi D., Yanovsky M.J., Oyama T., and Kay S.A. Dual role of TOC1 in the control of circadian and photomorphogenic responses in Arabidopsis. Plant Cell (2003) 15, 223–236.

Maskos U., and Southern E. M. Nucleic Acids Res (1992) 20, 1675–1678.

Mayne ST. Beta-carotene, carotenoids, and disease prevention in humans. FASEB Journal (1996) 10, 690-701.

McBride L. J., and Caruthers M. H. Tetrahedron Lett (1983) 24, 245–248.

McDonald M.J., and Rosbash M. Microarray analysis and organization of circadian gene expression in Drosophila. Cell (2001) 107, 567-578.

McWatters H.G., Bastow R.M., Hall A., and Millar A.J. The ELF3 zeitnehmer regulates light signaling to the circadian clock. Nature (2000) 408, 716-720.

Medina Escobar N, Cardenas J, Valpuesta V, Munoz Blanco J, Caballero JL. Cloning and characterization of cDNAs from genes differentially expressed during the strawberry fruit ripening process by a MAST-PCR-SBDS method. Analytical Biochemistry (1997) 248, 288-296.

Mendes P. Modeling large scale biological systems from functional genomic data: parameter estimation. In Foundations of Systems Biology (Kitano, H., ed.), Boston: MIT Press (2001) pp. 163–186.

Milborrow BV. The pathway of biosynthesis of abscisic acid in vascular plants: a review of the present state of knowledge of ABA biosynthesis. Journal of Experimental Botany (2001) 52, 1145-1164.

Millar AJ, Strame M, Chory J, Chua NH and Kay SA. The regulation of circadian period by phototransduction pathways in Arabidopsis. Science (1995) 267, 1163-1166

Mol J. N. M., Grotewold E., and Kohchi T., Trends Plant Sci. (1998) 3, 212.

Moreau C. et al. A genomic approach to investigate developmental cell death in woody tissues of Populus trees. Genome Biol. (2005) 6, R34.

Moy P. et al. Patterns of gene expression upon infection of soybean plants by Phytophthora sojae. Mol. Plant–Microbe Interact. (2004) 17, 1051–1062.

Moyano E., Portero-Robles I., Medina-Escobar N., Valpuesta V., Munoz-Blanco J., and Caballero J. L. A Fruit-Specific Putative Dihydroflavonol 4-Reductase

Gene Is Differentially Expressed in Strawberry during the Ripening Process. Plant Physiology (1998) 117, 711–716.

Murphy L. D., Herzog C. E., Rudick J. B., Fojo A. T., and Bates S. E. Biochemistry (1990) 29, 10351–10356.

Mustilli A.C., Fenzi F., Ciliento, R., Alfano F., and Bowler C. Phenotype of the tomato high pigment-2 mutant is caused by a mutation in the tomato homolog of DEETIOLATED1. Plant Cell (1999). 11, 145–157.

Napoli C.A., Fahy D., Wang H.-Y., Taylor L.P. White anther: a Petunia mutant that abolishes pollen flavonol accumulation, induces male sterility, and is complemented by a chalcone synthase transgene. Plant Physiol. (1999) 120, 615–622.

Nelson DC, Lasswell J, Rogg LE, Cohen MA and Bartel B. FKF1, a clock-controlled gene that regulates the transition to flowering in Arabidopsis. Cell (2000) 101, 331-340.

Ninu L, Ahmad M, Miarelli C, Cashmore AR, Giuliano G. Cryptochrome 1 controls tomato development in response to blue light. Plant J. (1999) 18, 551–556.

Nishiyama T., Fujita T., Shin-I T. et al. Comparative genomics of Physcomitrella patens gametophytic transcriptome and Arabidopsis thaliana: implication for land plant evolution. Proc. Natl Acad. Sci. USA (2003) 100, 8007–8012.

Nogata Y., Ohta H., and Voragen A.G.J. Polygalacturonase in strawberry fruit. Phytochemistry (1996) 34, 617-620.

Noonan K. E., Beck C., Holzmayer T. A., Chin J. E., Wunder J. S., Andrulis I. L., Gazdar A. F., Willman C. L., Griffith B., Von-Hoff D. D., and Robinson I. B. Proc. Natl. Acad. Sci. USA (1990) 87, 7160–7164.

Norris SR, Barrette TR, DellaPenna D. Genetic dissection of carotenoid synthesis in Arabidopsis defines plastoquinone as an essential component of phytoene desaturation. Plant Cell (1995) 7, 2139-2149.

Oeller PW, Min Wong L, Taylor LP, Pike DA, Theologis A. Reversible inhibition of tomato fruit senescence by antisense RNA. Science (1991) 254, 437–439.

Ogihara Y., Mochida K., Nemoto Y., Murai K., Yamazaki Y., Shin-I T., and Kohara Y. Correlated clustering and virtual display of gene expression patterns in

the wheat life cycle by large-scale statistical analyses of expressed sequence tags. Plant J. (2003) 33, 1001–1011.

Okamoto T., Suzuki T., and Yamamoto N. Nat Biotech (2000) 18, 438–441.

Okubo K. et al. Large-scale cDNA sequencing for analysis of quantitative and qualitative aspects of gene expression. Nature Genet. (1992) 2, 173–179.

Olias J.M., Sanz C., Rios J.J., and Perez A.G. Substrate specificity of alcohol acyltransferase from strawberry and banana fruits. In Fruit Flavors: Biogenesis, Characterization and Authentication, R.L. Rouseff and M.M. Leahy, eds (Washington, DC: American Chemical Society), (1995) 134–141.

Olsen JA. Provitamin A function of carotenoid. The conversion of betacarotene into vitamin A. Journal of Nutrition (1989) 119, 105-108.

Orfila C., Seymour G.B., Willats W.G., Huxham I.M., Jarvis M.C., Dover C.J., Thompson A.J., and Knox J.P. Altered middle lamella homogalacturonan and disrupted deposition of (1!5)-alpha- L-arabinan in the pericarp of Cnr, a ripening mutant of tomato. Plant Physiol. (2001) 126, 210–221.

Otto B., Grimm B., Ottersbach P., and Kloppstech K. Circadian Control of the Accumulation of mRNAs for Light- and Heat-Inducible Chloroplast Proteins in Pea (Pisum sativum L.). Plant Physiol (1988) 88, 21-25.

Oztur Z.N. et al. Monitoring large-scale changes in transcript abundance in drought- and salt-stressed barley. Plant Mol. Biol. (2002) 48, 551–573.

Panda S., Antoch M.P., Miller B.H, Su A.I., Schook A.B., Straume M., Schultz P.G., Kay S.A., Takahanshi J.S., and Hogenesch J.B. Coordinated Transcription of Key Pathways in the Mouse by the Circadian Clock. Cell (2002) 109, 307–320.

Park D.H., Somers D.E., Kim Y.S., Choy Y.H., Lim H.K., Soh M.S., Kim H.J., Kay S.A., and Nam H.G. Control of circadian rhythms and photoperiodic flowering by the Arabidopsis GIGANTEA gene. Science (1999) 285, 1579-1582.

Parkinson H. et al. ArrayExpress – a public repository for microarray gene expression data at the EBI. Nucleic Acids Res. (2005) 33, D553–D555.

Parr A.J., Bowell G.P. Phenols in the plant and in man. The potential of possible nutritional enhancement of the diet by modifying the phenol content or profile. J. Sci. Food Agric. (2000) 80, 985–1012.

Paterson A., Bowers J., Burow M. et al. Comparative genomics of plant chromosomes. Plant Cell (2000) 12, 1523–1540.

Payton P., Alba R., and Moore S. Gene expression profiling. In Handbook of Plant Biotechnology (Christou, P. and Klee, H., eds). New York: John Wiley & Sons Ltd (2003).

Peirson S.N., Butler J.N., and Foster R.G. Experimental validation of novel and conventional approaches to quantitative real-time PCR data analysis. Nucleic Acids Res (2003) 31, e73.

Peng X., Wood C., Blalock E., Chen K.-C., Landfield P., and Stromberg A. Statistical implications of pooling RNA samples for microarray experiments. BMC Bioinformatics (2003) 4, 26–35.

Perez A.G., Sanz C., and Olias J.M. Partial purification and some properties of alcohol acyltransferase from strawberry fruits. J. Agric. Food Chem. (1993) 41, 1462–1466.

Perez A.G., Sanz C., Olias R., Rios J.J., and Olias J.M. Evolution of strawberry alcohol acyltransferase activity during fruit development and storage. J. Agric. Food Chem. (1996) 44, 3286–3290.

Perin C., Gomez J., Hagen L., Dogimont C., Pech J., Latche A., Pitrat M., and Lelievre J. Molecular and genetic characterization of a non-climacteric phenotype in melon reveals two loci conferring altered ethylene response in fruit. Plant Physiol. (2002) 129, 300–309.

Perkin-Veazie P. Growth and ripening of strawberry fruit. Horticultural Reviews (1995)17, 267–297.

Perrotta G., Ninu L., Flamma F.,Weller J.L., Kendrick R.E., et al. Tomato contains homologues of Arabidopsis cryptochromes 1 and 2. Plant Mol. Biol. (2000) 42, 765–773.

Perrotta G., Yahoubyan G., Nebuloso E., Renzi L., Giuliano G. Tomato and barley contains duplicated copies of cryptochrome 1. Plant Cell Environ. (2001) 24, 991–997.

Peters J.L., van Tuinen A., Adamse P., Kendrick R.E., and Koornneef M. High pigment mutants of tomato exhibit high sensitivity for phytochrome action. Plant Physiol. (1989) 134, 661–666.

Pfaffl M.W. A new mathematical model for relative quantification in real-time RT-PCR. Nucleic Acids Res (2001) 29, e45.

Phillips J., and Eberwine, J. Antisense RNA amplifications: a linear amplification method for analyzing the mRNA population from single living cells. Methods (1996) 10, 283–288.

Picton S, Barton SL, Bouzayen M, Hamilton AJ, Grierson D. Altered fruit ripening and leaf senescence in tomatoes expressing an antisense ethylene-forming enzyme transgene. Plant J (1993a) 3, 469–481.

Picton S, Barton SL, Bouzayen M, Hamilton AJ, Grierson D. Altered fruit ripening and leaf senescence in tomatoes expressing an antisense ethylene-forming enzyme transgene. Plant J (1993a) 3, 469–481.

Picton S, Gray J, Barton S, Abubakar U, Lowe A, Grierson D. CDNA cloning and characterisation of novel ripeningrelated mRNAs with altered patterns of accumulation in the ripening inhibitor (rin) tomato ripening mutant. Plant Mol Biol (1993b) 23, 193–207.

Pinyopich A., Ditta G.S., Savidge B., Liljegren S.J., Baumann E., Wisman E., and Yanofsky M.F. Assessing the redundancy of MADS-box genes during carpel and ovule development. Nature(2003) 424, 85–88.

Piringer AA, Heinze PH Effect of light on the formation of a pigment in the tomato fruit cuticle. Plant Physiol (1954) 29, 467–472.

Potter E., and Kloppstech K. Effects of light stress on the expression of early light-inducible proteins in barley. European Journal of Biochemistry (1993) 214, 779–786.

Pourcel L., Routaboul J.M., Kerhoas L., Caboche M., Lepiniec L., and Debeaujon I. TRANSPARENT TESTA10 Encodes a Laccase-Like Enzyme Involved in Oxidative Polymerization of Flavonoids in Arabidopsis Seed Coat. The Plant Cell (2005) 17, 2966–2980.

Pratt LH, Cordonnier-Pratt MM, Hauser B, Caboche M. Tomato contains two differentially expressed genes encoding B-type phytochromes, neither of which can be considered an ortholog of Arabidopsis phytochrome B. Planta (1995) 197, 203-206.

Pritchard C.C., Hsu L., Delrow J., and Nelsen P.S. Project normal: defining normal variance in mouse gene expression. Proc Natl Acad Sci USA (2001) 98, 13266-13271.

Putterill J., Robson F., Lee K., Simon R., and Coupland G. The CONSTANS gene of Arabidopsis promotes flowering and encodes a protein showing similarities to zinc finger transcription factors. Cell. (1995) 24, 847-857.

Qin L., Overmars H., Helder J., Popeijus H., van der Voort J., Groenink W., van Koert P., Schots A., Bakker J., and Smant G. An efficient cDNA-AFLP-based strategy for the identification of putative pathogenicity factors from the potato cystnematode Globodera rostochiensis. Mol. Plant Microbe Interact. (2000) 13, 830–836.

Ramakers C., Ruijter J.M., Deprez R.H., and Moorman A.F. Assumption-free analysis of quantitative real-time polymerase chain reaction (PCR) data. Neurosci Lett (2003) 339, 62–66.

Ramakrishnan R. Nucleic Acids Res (2002) 30, e30.

Ramirez D.A., and Tomes M.L. Relationship between chlorophyll and carotenoid biosynthesis in dirty-red (green-flesh) mutant in tomato. Bot Gaz (1964) 125, 221-226.

Rampal J.B. DNA Arrays: methods and protocols. Humana press, Totowa, New Jersey (2001).

Redgwell R.J., MacRae E., Hallett I., Fischer M., Perry J., Harker R. In vivo and in vitro swelling of cell walls during fruit ripening. Planta (1997) 203, 162-173.

Redman J.C. et al. Development and evaluation of an Arabidopsis whole genome Affymetrix probe array. Plant J. (2004) 38, 545–561.

Redondo Nevado J, Moyano E, Medina Escobar N, Caballero JL, Munoz Blanco J. A fruit-specific and developmentally regulated endopolygalacturonase gene from strawberry (*Fragaria x ananassa* cv. Chandler). Journal of Experimental Botany (2001) 52, 1941-1945.

Rensink W.A. et al. Gene expression profiling of potato responses to cold, heat, and salt stress. Funct. Integr. Genomics (2005) 5, 201–207.

Restrepo S. et al. Gene profiling of a compatible interaction between Phytophthora infestans and Solanum tuberosum suggests a role for carbonic anhydrase. Mol. Plant–Microbe Interact. (2005) 18, 913–922.

Rhee S.Y. et al. The Arabidopsis Information Resource (TAIR): a model organism database providing a centralized, curated gateway to Arabidopsis biology, research materials and community. Nucleic Acids Res. (2003) 31, 224–228.

Rice-Evans C.A., Millier N.J., Paganga G., Structure–antioxidant activity relationships of flavonoids and phenolic acids. Free Radical Biol. Medicine (1995) 20, 933–956.

Ririe K.M., Rasmussen R.P., and Wittwer C.T. Product differentiation by analysis of DNA melting curves during the polymerase chain reaction. Anal. Biochem. (1997) 245, 154-160.

Roeder A.H., Ferrandiz C., and Yanofsky M.F. The role of the REPLUMLESS homeodomain protein in patterning the Arabidopsis fruit. Curr. Biol. (2003) 13, 1630–1635.

Rogaev E., Sherrington R., Rogaeva E. et al. Familial Alzheimer's disease in kindreds with missense mutations in a gene on chromosome 1 related to Alzheimer's disease type 3 gene. Nature, (1995) 376, 775–778.

Ronen G., Carmel-Goren L., Zamir D., and Hirschberg J. An alternative pathway to -carotene formation in plant chromoplasts discovered by map-based cloning of Beta and oldgold color mutations in tomato. Proc. Natl. Acad. Sci. USA(2000) 97, 11102–11107.

Ronen G., Cohen M., Zamir D., and Hirschberg J. Regulation of carotenoid biosynthesis during tomato fruit development: Expression of the gene for lycopene epsilon-cyclase is down-regulated during ripening and is elevated in the mutant delta. Plant J. (1999) 17, 341–351.

Ronning C., Stegalkina S., Ascenzi R. et al. Comparative analyses of potato expressed sequence tag libraries. Plant Physiol. (2003) 131, 419–429.

Rose J.K.C., and Bennett A.B. Cooperative disassembly of the cellulose-xyloglucan network of plant cell walls: parallels between cell expansion and fruit ripening. Trends Plant Sci (1999) 4, 176–183.

Rose J.K.C., Lee H.H., and Bennett A.B. Expression of a divergent expansin gene is fruit-specific and ripening-regulated. Proc. Natl. Acad. Sci. USA (1997) 94, 5955–5960.

Ross J.A., and Kasum C.M. Dietary flavonoids: bioavailability, metabolic effects, and safety. Annu. Rev. Nutrition (2002) 22, 19–34.

Rosso S.W. The ultrastructure of chromoplast development in red tomato. J Ultrastructure Res (1968) 25, 307-322.

Rottmann WH, Peter GF, Oeller PW, Keller JA, Shen NF, Nagy BP, Taylor LP, Campbell AD, Theologus A. 1-Aminocyclopropane-1-carboxylate synthase in tomato is encoded by a multigene family whose transcription is induced during fruit and floral senescence. J Mol Biol (1991) 222, 937-961.

Ruuska S., Girke T., Benning C., and Ohlrogge J. Contrapuntal networks of gene expression during Arabidopsis seed filling. Plant Cell (2002) 14, 1191–1206.

Salentijn E.M.J., Aharoni A., Schaart J.G., Boone M.J. and Krens F.A. Differential gene expression analysis of strawberry cultivars that differ in fruit-firmness. Physiologia Plantarum (2003) 118, 571-578.

Salomé P.A., and McClung C.R. Pseudo-response Regulator 7 and 9 are partially redundant genes essential for the temperature responsiveness of the Arabidopsis circadian clock. Plant Cell (2005) 17, 791-803.

Samach A., and Coupland G. Bioessays (2000) 22, 38.

Sambrook J., Fritsch E.F., and Maniatis T. (1989) Molecular cloning: A Laboratory Manual, 2nd edn. Cold Spring Harbor: Cold Spring Harbor Laboratory Press.

Sandmann G. Carotenoid biosynthesis and biotechnological application. Archives of Biochemistry and Biophysics (2001) 385, 4-12.

Schaffer R., Landgraf J., Accerbi M., Simon V., Larson M., and Wisman E. Microarray analysis of diurnal and circadian-regulated genes in Arabidopsis. Plant Cell (2001) 13, 113-123.

Schena M. Bioessays (1996) 18, 427.

Schena M. DNA Microarrays: a practical approach. (The practical approach series, Ed. Hames B.D.), Oxford University Press. New York (1999).

Schena M. Microarray analysis. John Wiley & Sons, Inc., Hoboken, New Jersey (2003).

Schena M. Microarray biochip technology. Eaton Publishing, Sunnyvale, CA (2000).

Schena M., and Davis R.W. In PCR methods manual (ed. Innis M., Gelfand D., and Sninsky J.). Accademic Press, San Diego. (1998) 445-455.

Schena M., Heller R.A., Theriault T.P., Konrad K., Lachenmeier E., and Davis R.W. Trends Biotechnol. (1998) 16, 301.

Schena M., Shalon D., Davis R., and Brown P. Quantitative monitoring of gene expression patterns with a complimentary DNA microarray. Science (1995) 270, 467–470.

Schena M., Shalon D., Heller R., Chai A., Brown P.O., and Davis R.W. Proc. Natl. Acad. Sci. USA (1996) 93, 10614.

Schijlen E.G.W.M., Ric de Vos C.H., van Tunen A. J, Bovy A.G. Modification of flavonoid biosynthesis in crop plants. Phytochemistry (2004) 65, 2631–2648.

Schmid M. et al. A gene expression map of Arabidopsis thaliana development. Nat. Genet. (2005) 37, 501–506.

Schmittgen T. D., and Zakrajsek B. A. J. Biochem. Biophys. Methods (2000) 46, 69–81.

Schmittgen T. D., Zakrajsek B. A., Mills A. G., Gorn V., Singer J., and Reed, M. W. Anal. Biochem. (2000) 285, 194–204.

Schröder J. A family of plant-specific polyketide synthases: facts and predictions. Trends in Plant Science (1997) 2, 373–378.

Schwab W., Aharoni A., Raab T., Garcia Perez A., Sanz C. Citosolic aldolase is a ripening related enzyme in strawberry fruits (*Fragaria x ananassa*). Phytochem (2001) 56, 407–415.

Schwartz SH, Tan BC, Gage DA, Zeevaart JA, McCarty DR. Specific oxidative cleavage of carotenoids by VP14 of maize. Science (1997) 276, 1872-1874.

Seymour G., Taylor J., and Tucker G. Biochemistry of Fruit Ripening. (London: Chapman and Hall) eds (1993).

Sgherri C. L. M., and Navari-Izzo F. Sunflower seedlings subjected to increasing water deficit stress: Oxidative stress and defense mechanisms. Physiol. Plant (1995) 93, 25-30.

Sgherri C., Navari-Izzo F., Pardossi A., Soressi G.P, and Rizzo A. The Influence of diluted seawater and ripening stage on the content of antioxidants in fruits of different tomato genotypes. J. Agric. Food Chem. (2007) 55, 2452-2458.

Shalon D., Smith S., and Brown P. A DNA microarray system for analyzing complex DNA samples using two-color fluorescent probe hybridization. Genome Res. (1996) 6, 639–645.

Sharrock RA and Quail PH Novel phytochrome sequences in Arabidopsis thaliana: structure, evolution, and differential expression of a plant regulatory photoreceptor family. Genes Dev. (1989) 3, 1745-1757.

Shen L. et al. BarleyBase – an expression profiling database for plant genomics. Nucleic Acids Res. (2005) 33, D614–D618.

Shibata D. Genome sequencing and functional genomics approaches in tomato. Journal of General Plant Pathology (2005) 71, 1-7.

Shirley B.W. Trends Plant Sci. (1996) 1, 377.

Shmulevich I., Gluhovsky I., Hashimoto R., Dougherty E., and Zhang W. Steady-state analysis of genetic regulatory networks modeled by probabilistic Boolean networks. Comp. Funct. Gen. (2003) 4, 601–608.

Slater A, Maunders MJ, Edwards K, Schuch W, Grierson D. Isolation and characterization of complementary DNA clones for tomato Lycopersicon-esculentum cultivar Ailsa-Craig polygalacturonase and other ripening-related proteins. Plant Mol Biol (1985) 5, 137–148.

Smith C., Watson C., Ray J., Bird C., Morris P., Schuch W., and Gierson D. Antisense RNA inhibition of polygalacturonase gene expression in transgenic tomatoes. Nature (1988) 334, 724–726.

Smith H. Light quality, photoperception and plant strategy. Annu. Rev. Plant Physiol. (1982) 33, 481–518.

Smyth G., Yang Y., and Speed T. Statistical issues in cDNA microarray data analysis. In Functional Genomics – Methods and Protocols (Brownstein, M. and

Khodursky, A., eds). Methods in Molecular Biology Series. New Jersey: Humana Press (2002) 111–136.

Somers DE, Schultz TF, Milnamow M and Kay SA. ZEITLUPE encodes a novel clock-associated PAS protein from Arabidopsis. Cell (2000) 101, 319-329.

Somers DE, Webb AAR, Pearson M and Kay SA. The short-period mutant, toc1-1, alters circadian clock regulation of multiple outputs throughout development in Arabidopsis thaliana. Development. (1998) 125, 485-494.

Steel A. B., Torres M., Hartwell J., Yu Y., Ting N., Hoke G., and Yang H. In Microarray Biochip Technology; Schena, M., Ed.; Biotechniques Books: Natick, MA (1999).

Straume M. DNA microarray time series analysis: Automated statistical assessment of circadian rhythms in gene expression patterning. Methods Enzymol. (2004) 383, 149–166.

Tanksley S., et al. High density molecular maps of the tomato and potato genomes. Genetics (1992) 132, 1141–1160.

Tanner G.J., Francki K.T., Abrahams S., Watson J.M., Larkin P.J., and Ashton A.R. J. Biol. Chem. (2003) 278, 31647–31656.

Taylor IB, Burbidge A, and Thompson AJ. Control of abscisic acid synthesis. Journal of Experimental Botany 51, (2000) 1563-1574.

Taylor W.C. Regulatory interactions between nuclear and plastid genomes. Annu Rev Plant Physiol (1989) 40, 211-233.

Thibaud-Nissen F. et al. Clustering of microarray data reveals transcript patterns associated with somatic embryogenesis in soybean. Plant Physiol. (2003) 132, 118–136.

Thomas RL, Jen JJ. Phytochrome-mediated carotenoid biosynthesis in ripening tomatoes. Plant Physiol (1975) 56, 452–453.

Thomson W.W., and Whatley J.M. Development of nongreen plastids. Annu Rev Plant Physiol (1980) 31, 375-394.

Thorp H. Cutting out the middleman: DNA biosensors base on electrochemical oxidation. Trends Biotech. (1998) 16, 117–121.

Tieman D.M., Harriman R.W., Ramamohan G., and Handa A.K. An antisense pectin methylesterase gene alters pectin chemistry and soluble solids in tomato fruit. Plant Cell (1992) 4, 667–679.

Tieman DM, Klee HJ. Differential expression of two novel members of the tomato ethylene-receptor family. Plant Physiol (1999)120, 165–172.

Tòth R., Kevei E., Hall A., Millar A.J., Nagy F., and Kozma-Bognàr, L. Circadian clock-regulated expression of phytochrome and cryptochrome genes in Arabidopsis. Plant Physiol (2001) 127, 1607-1616.

Trainotti L, Spinello R, Piovan A, Spolaore S, Casadoro G. beta-galactosidases with a lectin-like domain are expressed in strawberry. Journal of Experimental Botany (2001) 52, 1635-1645.

Treutter D. J Chromatogr (1989) 467, 185.

Tseng G., Oh M., Rohlin L., Liao J., and Wong W. Issues in cDNA microarray analysis: quality filtering, channel normalization, models of variations and assessment of gene effects. Nucleic Acids Res. 29, 2549–2557.

Ueda Y., Tsuda A., Bai J.H., Fujishita N., and Chachin K. Characteristic pattern of aroma ester formation from banana, melon, and strawberry with reference to the substrate specificity of ester synthetase and alcohol contents in pulp. J. Jpn. Soc. Food Sci. Technol. (1992) 39, 183–187.

Valverde F, Mouradov A, Soppe W, Ravenscroft D, Samach A and Coupland G. Photoreceptor regulation of CONSTANS protein in photoperiodic flowering. Science (2004) 303, 1003-1006.

van der Hoeven R., Ronning C., Giovannoni J., Martin G., and Tanksley, S. Deductions about the number, organization and evolution of genes in the tomato genome based on analysis of a large EST collection and selective genomic sequencing. Plant Cell (2002) 14, 1441–1456.

Van der Meer I.M., Stam M.E., Van Tunen A.J., Mol J.N., Stuitje A.R. Antisense inhibition of flavonoid biosynthesis in petunia anthers results in male sterility. Plant Cell. (1992) 4, 253–262.

Vardhini BV, Rao SSR. Acceleration of ripening of tomato pericarp discs by brassinosteroids. Phytochemistry (2002) 61, 843–847.

Velculescu V.E., Zhang L., Vogelstein B., and Kinzler, K.W. Serial analysis of gene expression. Science (1995) 270, 484–487.

Ventelon-Debout M., Nguyen T., Wissocq A., Berger C., Laudie M., Piegu B., Cooke R., Ghesquiere A., Delseny M., and Brugidou C. Analysis of the transcriptional response to Rice Yellow Mottle Virus infection in Oryza sativa indica and japonica cultivars. Mol. Genet. Gen. (2003) 270, 253–262.

Vodkin L. et al. Microarrays for global expression constructed with a low redundancy set of 27,500 sequenced cDNAs representing an array of developmental stages and physiological conditions of the soybean plant. BMC Genomics (2004) 5, 73.

Vrebalov J, Ruezinsky D, Padmanabhan V, White R, Medrano D, Drake R, Schuch W, Giovannoni J. A MADS-box genenecessary for fruit ripening at the tomato ripening-inhibitor (rin) locus. Science (2002) 296, 343–346.

Walt D. R. Science (2000) 287, 451–452.

Wang H. et al. Temporal progression of gene expression responses to salt shock in maize roots. Plant Mol. Biol. (2003) 52, 873–891.

Wang R., Okamoto M., Xing X., and Crawford N. Microarray analysis of the nitrate response in Arabidopsis roots and shoots reveals over 1,000 rapidly responding genes and new linkages to glucose, trehalose-6-phosphate, iron, and sulfate metabolism. Plant Physiol. (2003) 132, 556–567.

Waters D.L.E. et al. cDNA microarray analysis of developing grape (Vitis vinifera cv. Shiraz) berry skin. Funct. Integr. Genomics (2005) 5, 40–58.

Watkinson J.I. et al. Photosynthetic acclimation is reflected in specific patterns of gene expression in drought-stressed loblolly pine. Plant Physiol. (2003) 133, 1702–1716.

Weller JL, Perrotta G, Schreuder ME, Van Tuinen A, Koornneef M, et al. Genetic dissection of blue-light sensing in tomato using mutants deficient in cryptochrome 1 and phytochromes A, B1 and B2. Plant J. (2001) 25, 427–440.

Wellmann F., Griesser M., Schwab W., Martens S., Eisenreich W., Matern U., and Lukačin R. Anthocyanidin synthase from Gerbera hybrida catalyzes the conversion of (+)-catechin to cyanidin and a novel procyanidin. FEBS Lett (2006) 580, 1642-1648.

Wiese W., Vornam B., Krause E., and Kindl H. Plant Mol. Biol. (1994) 26, 667–677.

Wilkinson J.Q., Lanahan M.B., Conner T.W., and Klee H.J. Identification of mRNAs with enhanced expression in ripening strawberry fruit using polymerase chain reaction differential display. Plant Mol. Biol. (1995b) 27, 1097–1108.

Winer J., Jung C. K., Shackel I., and Williams P. M. Anal. Biochem. (1999)270, 41–9.

Wittwer C.T., Herrmann M.G., Moss A.A., and Rasmussen R.P. Continuous fluorescence monitoring of rapide cycle DNA amplification. BioTechinques (1997a) 22, 130-138.

Wittwer C.T., Ririe K.M., Andrew R.V., David D.A., Gundry R.A., and Balis U.J. The LightCycler: A microvolume multisample fluorimeter with rapid temperature control. BioTechniques (1997b) 22, 176-181.

Wodicka L., Dong H., Mittmann M., Ho M.-H, and Lockhart D.J. Nature Biotechnol. (1998) 15, 1359.

Wong M.L., and Medrano J.F. Real-time PCR for mRNA quantitation. Biotechniques (2005) 39, 75–85.

Woolley L.C., James D.J., and Manning K. Purification and properties of an endo-beta-1,4-glucanase from strawberry and downregulation of the corresponding gene cel1. Planta(2001) 214, 11–21.

Yamakawa Y., Goto S., and Yokotsuka I. Fractionation and some properties of acetic-ester synthesizing enzyme from Cladosporium cladosporioides Agric. Biol. Chem. (1978) 42, 269–274.

Yamauchi H., Hasuo T., Amachi T., Akita O., Hara S., and Yoshizawa K. Purification and characterization of acyl coenzyme A: Alcohol acyltransferase of Neurospora sp. Agric. Biol. Chem. (1989). 53, 1551–1556.

Yan O. Y., Andersson C. R., Kondo T., Golden S. S., and Johnson C. H. Proc. Natl. Acad. Sci. U.S.A. (1998) 95, 8660.

Yang SF, Hoffman NE. Ethylene biosynthesis and its regulation in higher plants. Annu Rev Plant Physiol (1984) 35, 155–190.

Yang Y., and Speed T. Design issues for cDNA microarray experiments. Nat. Rev. Genet. (2002a) 3, 579–588.

Yang Y., and Speed T. Design of microarray expression experiments. In DNA Microarrays – A Molecular Cloning Manual (Bowtell, D. and Sambrook, J., eds). New York: Cold Spring Harbor Laboratory Press, (2003) 517–518.

Yang Y., Dudoit S., Luu P., and Speed T. Normalization for cDNA microarrays. Microarrays: optical technologies and informatics. SPIE (2001) 4266, 141–152.

Yang Y., Dudoit S., Luu P., Lin D., Peng V., Ngai J., and Speed T. Normalization for cDNA microarray data: a robust composite method addressing single and multiple slide systematic variation. Nucleic Acids Res. (2002b) 30, e15.

Yanovsky MJ, Gazzella MA and Casal JJ. A quadruple photoreceptor mutant still keeps track of time. Curr. Biol. (2000) 10, 1013-1015.

Yeakley J. M. Nat Biotechnol (2002) 20, 353–358.

Ylstra B., Busscher J., Franken J., Hollman P.C.H., Mol J.N.M., van Tunen.. Flavonols and fertilization in Petunia hybrida: localization and mode of action during pollen tube growth. Plant J. (1994) 6, 201–212.

Yoshioka K., and Hashimoto N. Ester formation by brewers' yeast during sugar fermentation. Agric. Biol. Chem. (1984) 45, 333–340.

Yu L.X., and Setter, T.L. Comparative transcriptional profiling of placenta and endosperm in developing maize kernels in response to water deficit. Plant Physiol. (2003) 131, 568–582.

Zabetakis I., and Holden M.A. Strawberry flavour: Analysis and biosynthesis. J. Sci. Food Agric. (1997) 74, 421–434.

Zegzouti H, Jones B, Frasse P, Marty C, Maitre B, Latche A, Pech J-C, Bouzayen M. Ethylene-regulated gene expression in tomato fruit: Characterization of novel ethylene-responsive and ripening-related genes isolated by differential display. Plant J (1999) 18, 589–600.

Zhu T. et al. Transcriptional control of nutrient partitioning during rice grain filling. Plant Biotechnol. J. (2003) 1, 59–70.

Zhu T., and Wang, X. Large-scale profiling of the Arabidopsis transcriptome. Plant Physiol. (2000) 124, 1472–1476.

7. PUBBLICATIONS

Published papers

Carbone F., Pizzichinini D., Giuliano G., Perrotta G., Rosati C., 2005. Comparative profiling of tomato fruits and leaves evidences a complex modulation of global transcript profiles. Plant Science 169, 165-175.

Carbone F., Mourgues F., Biasioli F., Gasperi F., Maerk T. D., Rosati C., Perrotta G., 2006. Development of molecular and biochemical tools to investigate fruit quality traits in strawberry élite genotypes. Molecular Breeding 18, 127-142.

Almeida J.R.M., D'Amico E., Preuss A., Carbone F., Ric de Vos C.H., Deiml B., Mourgues F., Perrotta G., Fisher T.C., Bovy A., Martens S. and Rosati C., 2007. Characterization of major enzymes and genes involved in flavonoid and proanthocyanidin biosynthesis during fruit development in strawberry (Fragaria x ananassa). Archives of Biochemistry and Biophysics 465, 61-71.

Paper in preparation

Analysis of temporal rhythmic oscillation of tomato mRNAs: cryptochromes can alterate transcription fluctuations of photoreceptor and circadian regulated genes. Authors (presently strictly alphabetic order) Carbone F., Facella P., Giuliano G., Lopez L., Perrotta G.

Oral Communications and Posters

Carbone F., D'Amico E., Bovy A., de Vos C.H.R., Rosati C., Perrotta G.. 2005. Flavonoids accumulation in strawberry genotypes is related to specific gene expression pattern. Proc. XLIX SIGA (Italian Society of Agriculture Genetics) Annual Congress, Potenza, Italy, September 12-15, poster B32.

Carbone F., Rosati C., Bianco L., Di Carli M., Desiderio A., Benvenuto E., Perrotta G.. 2006. Characterization of strawberry genotypes through a combined transcriptomics and proteomics approach. Proc. 1st ItPA (The Italian Proteomic Association) Annual National Congress, Pisa, Italy, July 2-4, oral communication OP23.

Carbone F., D'Amico E., Bovy A., de Vos C.H.R., Rosati C., Perrotta G., 2006 Different accumulation of flavonoid compounds among strawberry genotypes is related to specific gene expression pattern. Proc. XXIII Internetional Conference on Polyphenols, Winnipeg, Manitoba, Canada, August 22-25.

D'Amico E., De Almeida J.R.M., Carbone F., Mourgues F., Martens S., Preuss A., Fisher T., Deiml B., Bovy A., Rosati C., Perrotta G., 2006. Characterization of strawberry flavonoid pathway

by molecular and biochemical approaches. Proc. L SIGA (Italian Society of Agriculture Genetics) Annual Congress, Ischia, Italy, September 10-14, oral communication 2.03.

D'Amico E., Carbone F., Bovy A., de Vos C.H.R., Martens S., Perrotta G., Rosati C., 2006. Unravelling strawberry flavonoid metabolism during fruit development by molecular and biochemical approaches. Proc. I Joint Meeting of WG1 and WG4 (Genetic bases for bioactive compounds affecting human health in berry fruits) Cost 863 Euroberry, Barcelona, September 28-30.

D'Amico E., Carbone F., Rosati C., Perrotta G., 2007. Molecular characterization of flavonoid genes in strawberry. Proc. FLAVO meeting, Murcia, Spain, April 18-20, oral communication.

Carbone F., Saud G., Caligari P.D.S., Perrotta G., 2007. Comparative gene expression analysis between the chilean native strawberry, Fragaria chiloensis, and its world-wide cultivated relative, Fragaria x ananassa. Proc. Trans-COST ARRAY meeting, Sant Feliu de Guixols, Girona, Spain, May 23-24, oral communication.

D'Amico E., Carbone F., Rosati C., Perrotta G. 2007. Analysis of the genetic diversity in promoter sequences of genes encoding flavonoid related enzymes in strawberry. Proc. 51st SIGA (Italian Society of Agriculture Genetics) Annual Congress, Riva del Garda, Italy, September 23-26, poster B.13.

Facella P., Lopez L., Carbone F., Giuliano G., Perrotta G., 2007. Cryptochromes can alterarate transcription fluctuations of photoreceptor and circadian regulated genes. Proc. 51st SIGA (Italian Society of Agriculture Genetics) Annual Congress, Riva del Garda, Italy, September 23-26, oral communication 5.03.

Partecipation to Meeting, Congress and Workshops

Workshop of Gene Expression Analysis (Lev. I & II), Casalecchio di Reno (BO), Italy, January 27-28 2005.

International Microarray Workshop, Tucson (Arizona), USA, May 8-13 2005

XLIX SIGA (Italian Society of Agriculture Genetics) Annual Congress, Potenza, Italy, September 12-15 2005.

Course of Bioinformatics applied to plant breeding, Salsomaggiore Terme (PR), Italy, November 28-30 2005.

2nd FLAVO Meeting, Avignon, France, December 12-13 2005.

FLAVO meeting, Murcia, Spain, April 18-20 2007.

Trans-COST ARRAY meeting, Sant Feliu de Guixols, Girona, Spain, May 23-24 2007.

Relazione finale del Collegio dei docenti
sull'attività svolta dal dott.re Fabrizio CARBONE

Nel corso del dottorato il dott. Fabrizio Carbone ha condotto attività relative allo sviluppo di metodologie molecolari per lo studio di caratteri qualitativi in piante di interesse agronomico.

Durante il corso degli studi il dottorando ha progressivamente acquisito una notevole autonomia sviluppando buona capacità propositiva in parte dovuta ad una approfondita conoscenza della letteratura scientifica del settore.

L'approccio metodologico ha principalmente riguardato una analisi comparativa dell'espressione genica a livello trascrizionale sia su larga scala che incentrata su alcune classi di geni scelti in maniera oculata. Tra i risultati più interessanti della ricerca è da menzionare l'identificazione di geni coinvolti nei processi di maturazione, biosintesi di metaboliti secondari e fotopercezione, in fragola e pomodoro.

Il dott. Carbone ha svolto il lavoro sperimentale presso l'ENEA CR Trisaia e alcuni risultati della sua ricerca sono stati oggetto di pubblicazioni su riviste scientifiche internazionali e di numerose presentazioni a convegni scientifici nazionali ed internazionali.

Si esprime dunque parere ampiamente positivo e piena soddisfazione per il lavoro svolto al dottorando.

A nome del Collegio dei docenti
Il Coordinatore del Corso di Dottorato
Prof. Aldo Musacchio

INFO: Dipartimento di Ecologia, Cubo 4A/4B/6B,
Coordinatore del Dottorato di Ricerca in Biologia Vegetale: Prof. A Musacchio
Via Ponte P. Bucci, 87036, Arcavacata di Rende, (CS), Italia
Tel.: +39 0984 492959 Fax: +39 0984 492986 E-mail: aldo.musacchio@unical.it